

CHANGING THE PANCREATIC CANCER TREATMENT PARADIGM: DEVELOPING  
*CLOSTRIDIUM NOVYI* AS AN INTRAVENOUSLY INJECTABLE SOLID-STATE TUMOR  
THERAPEUTIC

A Dissertation  
Submitted to the Graduate Faculty  
of the  
North Dakota State University  
of Agriculture and Applied Science

By

Kaitlin Marie Dailey

In Partial Fulfillment of the Requirements  
for the Degree of  
DOCTOR OF PHILOSOPHY

Major Program:  
Cellular and Molecular Biology

November 2020

Fargo, North Dakota

North Dakota State University  
Graduate School

---

**Title**

CHANGING THE PANCREATIC CANCER TREATMENT PARADIGM:  
DEVELOPING *CLOSTRIDIUM NOVYI* AS AN INTRAVENOUSLY  
INJECTABLE SOLID-STATE TUMOR THERAPEUTIC

---

**By**

Kaitlin Marie Dailey

---

The Supervisory Committee certifies that this *disquisition* complies with North Dakota  
State University's regulations and meets the accepted standards for the degree of

**DOCTOR OF PHILOSOPHY**

SUPERVISORY COMMITTEE:

Sanku Mallik

---

Chair

Amanda Brooks

---

Penelope Gibbs

---

Jane Schuh

---

Approved:

11/23/2020

---

Date

Katie Reindl

---

Department Chair

## ABSTRACT

The development of a drug able to distinguish between tumor and host cells has been long sought, but the solid tumor microenvironment (TME) confounds many current therapeutics. Solid tumors present several challenges for oncotherapeutics, primarily, (1) aberrant vascularization, resulting in hypoxia, necrosis, abnormally high pH, and (2) tumor immune suppression. Oncolytic microbes are drawn to this microenvironment by an innate ability to selectively penetrate, colonize, and eradicate solid tumors as well as reactivate tumor associated immune components. To consider oncolytic bacteria deployment into this microenvironment, Chapter 1 dives into the background of oncolytic microbes. A discussion of the oncolytic bacterial field state, identifying *Clostridium novyi*, as a promising species, and details genetic engineering techniques to develop customized bacteria. Despite the promise of *C.novyi* in preclinical/clinical trials when administered intratumorally, the genetic and biochemical uniqueness of *C.novyi* necessitated the development of new methodologies to facilitate more widespread acceptance. Chapter 2 reports the development of methods that facilitate experimental work and therapeutic translation of *C.novyi*, including the ability to work with this obligate micro-anaerobe aerobically on the benchtop. While methods development is a necessary step in the clinical translation of *C.novyi* so too is choosing the correct model of the TME within which to test a potential anti-cancer therapy. While the typical solid TME includes both phenotypic and genotypic heterogeneity, the methods used to model this disease state often do not reflect this complexity. This simplistic approach may have contributed to stagnant five-year survival rates over the past four decades. Nevertheless, simplistic models are a necessary first step in clinical translation. Chapter 3 explores the impact of cancer cell lines co-cultured with *C. novyi* to establish the efficacy of this oncolytic bacteria in a monolayer culture. Chapter 4

extends this analysis adding not only a level of complexity by using an in vivo model, but also using CRISPR/Cas9 to modify the genome of *C.novyi* to encode a tumor targeting peptide, RGD, for expression within the spore coat. The combination of these studies indicates that *C. novyi* is uniquely poised to accomplish the long sought after selective tumor localization via intravenous delivery.



## ACKNOWLEDGMENTS

Where to even begin – it took a village to reach this point, I could never say thank you enough. I will forever be grateful to the mentors I’ve had along this path, but especially to Dr. Amanda Brooks. I am so proud to be a product of your training – as a scientist, a woman in STEM, an educator, a leader, and as a person in general. Thank you for believing in me when I was the most broken, and for teaching me to believe in myself again. You saved more than my career. And to Dr. Ben Brooks, who also believed I had untapped potential and never held back as he helped me to see that for myself. To Jessica, Austin, Owen, Oliver, and all the four legged family members, being adopted into your family has been one of the biggest honors of my life. Thank you to Dr. Sanku Mallik for fostering me without hesitation and helping me with the last push to complete this body of work.

To my wonderful boyfriend, Matt, who put up with me through the absolute rollercoaster this last year has been, I owe such a debt of gratitude I don’t know how I could ever repay it. To Watson and Oche, the loves of my life, we finally did it and I promise to take even better care of you. Soon I’ll get you the best quality treats and comfiest beds you’ve ever known. To Steve and Kambri, I’ve always dreamed of having friends like you. I will forever cherish your love and encouragement through this. And to my family for always being there for me and for continuing to believe and pray for me even when they had no idea what I was going through.

To my tribe, near and far, related or not, professional and personal – thank you.

And now, onward.

## **DEDICATION**

To the bright eyed child with a fire in her heart who never stopped dreaming, and to all the bulls  
that bucked her off.

## PREFACE

“Learn how to see. Realize that everything connects to everything else.”

-Leonardo da Vinci

## TABLE OF CONTENTS

ABSTRACT.....	iii
ACKNOWLEDGMENTS .....	v
DEDICATION.....	vi
PREFACE.....	vii
LIST OF TABLES.....	xiv
LIST OF FIGURES .....	xv
LIST OF ABBREVIATIONS.....	xix
LIST OF SYMBOLS .....	xxvi
LIST OF APPENDIX TABLES.....	xxvii
LIST OF APPENDIX FIGURES .....	xxix
CHAPTER 1: THE NEXT FRONTIER OF ONCOTHERAPEUTICS: ACCOMPLISHING CLINICAL TRANSLATION OF ONCOLYTIC BACTERIA THROUGH GENETIC ENGINEERING.....	1
Abstract .....	1
Introduction .....	2
Current Treatments.....	5
Chemotherapeutics .....	5
Microbe Treatments.....	6
Oncolytic Viruses .....	7
Challenges of Current Cancer Therapeutics.....	9
Tumor Microenvironment .....	9
Survey of Oncolytic Bacteria Currently Under Development .....	17
Indirect Oncolytic Activity: <i>Mycobacterium</i> , <i>Listeria</i> , <i>Klebsiella</i> , <i>Serratia</i> , <i>Streptococcus</i> , <i>Proteus</i> , <i>Caulobacter</i> , <i>Lactobacillus</i> , <i>Bifidobacteria</i> .....	18
Direct Oncolytic Action: <i>Salmonella</i> , <i>Clostridia</i> .....	24

Techniques to Engineer Oncolytic Bacteria.....	27
Meganucleases/Homing Endonucleases.....	28
Zinc Finger Nucleases (ZFNs) .....	30
Transcription Activator Like Effector Nucleases (TALENs) .....	32
CRISPR/Cas .....	33
Group II Intron Based Methods.....	36
Attenuation/Auxotrophy.....	37
Bacterial Transformation.....	38
Challenges of Oncolytic Bacteria Development .....	40
Systemic Toxicity and Off-Target Colonization .....	40
Pro-Oncogenic Bacteria.....	40
Model Systems .....	41
Conclusion.....	43
Acknowledgments .....	45
Author Contributions.....	45
Funding.....	45
Conflicts of Interest.....	45
References .....	46
 CHAPTER 2: METHODS AND TECHNIQUES TO FACILITATE THE DEVELOPMENT OF <i>CLOSTRIDIUM NOVI</i> -NT AS AN EFFECTIVE, THERAPEUTIC ONCOLYTIC BACTERIA .....	 61
Abstract .....	61
Introduction .....	62
Materials and Methods .....	65
Vegetative <i>C. novyi</i> Growth .....	65
Growth Curve .....	66

Sporulation of <i>C. novyi</i> : Atmospheric Chamber .....	66
Spore Isolation.....	67
Spore Activation.....	70
Spore Enumeration .....	70
Alpha-toxin Knock-Out.....	70
Colony PCR Screening.....	71
<i>C. novyi</i> Cell Staining.....	72
Comparison of <i>C. novyi</i> to <i>C. difficile</i> and <i>E. coli</i> .....	73
CRISPR/Cas Plasmid Design .....	73
CRISPR/Cas Plasmid Construction.....	76
Preparation of Calcium Competent <i>C. novyi</i> .....	78
Transformation of Calcium Competent <i>C. novyi</i> .....	79
Verifying Plasmid Transformation.....	80
Verifying Genomic Modification .....	80
Determining Off-Target Effects .....	81
Results .....	82
Establishing Growth of <i>C. novyi</i> (Fig 2.1) : <i>C. novyi</i> Cell Images.....	82
$\alpha$ -Toxin Removal .....	84
Comparison of Growth Techniques (Fig 2.2).....	84
Addition of Tch .....	84
CRISPR/Cas9n Plasmid Design (Fig 2.3).....	85
Discussion .....	90
Comparison to Other Bacterial Species and Techniques .....	92
CRISPR/Cas Gene Modification in <i>C. novyi</i> .....	93
Off-Target Effects .....	95

Conclusion.....	95
Acknowledgments.....	97
Author Contributions.....	97
Funding.....	97
Conflicts of Interest.....	97
References.....	98
CHAPTER 3: PROBING CLINICAL RELEVANCE: ESTABLISHING THE EFFICACY OF <i>C. NOVI</i> AGAINST A PANEL OF 2D CULTURED PANCREATIC CANCER CELLS.....	101
Abstract.....	101
Introduction.....	102
Materials and Methods.....	106
Tissue Cell Culture.....	106
Bacterial Culture.....	107
Lysis Assay.....	107
Results.....	108
BxPC-3.....	108
HPAF-II.....	108
MIA PaCa-2.....	108
PANC-1.....	109
KPC.....	109
Discussion and Conclusions.....	110
Acknowledgments.....	112
Author Contributions.....	112
Funding.....	113
Conflicts of Interest.....	113

References .....	113
CHAPTER 4: EFFICACY OF RGD-MODIFIED CLOSTRIDIUM NOVYI-NT AS AN INTRAVENOUS THERAPY FOR PANCREATIC CANCER .....	116
Abstract .....	116
Introduction .....	117
Materials and Methods .....	120
Generation and Preparation of RGD-Modified <i>C. novyi</i> Spores .....	120
Characterization of RGD-modified <i>C. novyi</i> Spores .....	123
Immunocompetent Mouse Model Establishment .....	125
Characterization of RGD-modified <i>C. novyi</i> Spores <i>In Vivo</i> .....	127
Results .....	129
RGD Peptide Encoding Gene Genomic Insertion Confirmation .....	129
Characterization of RGD-Modified <i>C. novyi</i> Spores .....	129
<i>In Vivo</i> Modeling of Intravenously Injected <i>C. novyi</i> Spores .....	133
Discussion .....	139
Characterization of RGD-modified <i>C. novyi</i> Spores .....	139
<i>In Vivo</i> Biodistribution of Intravenously Injected <i>C. novyi</i> Spores .....	141
Conclusions .....	144
Supplementary Figures .....	146
References .....	165
CHAPTER 5: CONCLUSION .....	168
References .....	174
APPENDIX A: CLONING SEQUENCES FOR SPORE COAT GENE INSERTION IN <i>C. NOVYI</i> .....	176
APPENDIX B: CLONING SEQUENCES FOR INSERTION GENE .....	181
APPENDIX C: CLONING SCHEMATIC FOR INSERTION GENE .....	182



APPENDIX D: EXPECTED RESULTS OF RESTRICTION DIGESTS IN THE GENERATION OF CRISPR PLASMIDS .....	183
APPENDIX E: GENE SEQUENCES USED TO COMPARE <i>C. NOVYI</i> , <i>E. COLI</i> , AND <i>C. DIFFICILE</i> .....	189
APPENDIX F: PUTATIVE CODON BIAS UTILIZED TO TRANSLATE SEQUENCES FOR <i>C. NOVYI</i> CLONING .....	202

## LIST OF TABLES

<u>Table</u>	<u>Page</u>
3.1. Characteristics of the original tissue sample for each pancreatic cancer cell line. ....	105
3.2. Genotypic information regarding the four most commonly mutated genes in tumorigenic pancreatic cancer cell lines. (WT – wild type, HD – homologous deletion).....	105
4.1. Representative table of the number and sex of mice in each cohort.....	134
4.2. Biodistribution of <i>C. novyi</i> spores after IV injection. Primers designed specifically for 16s rRNA of <i>C. novyi</i> were used to conduct PCR to determine the biodistribution of spores twenty-four hours after injection. Each ‘+’ indicates the presence of an amplicon representing the presence of <i>C. novyi</i> in a single animal.....	137
4.3. Assessing the $\alpha_v\beta_3$ coated surface designed for an adhesion assay. X-ray photoelectron spectroscopy was conducted to assess the elements present on a borosilicate sild cover after corona plasma treatment and subsequent coating with integrin. Adequate presence of integrin was determined when silicate was no longer detec and nitrogen content had reached its maximum.....	152
4.4. Key to the samples run in Supplementary Figures 4.17. ....	161

## LIST OF FIGURES

<u>Figure</u>	<u>Page</u>
1.1. Comparison of current solid state tumor therapeutics. ....	5
1.2. Oncolytic virotherapy. ....	7
1.3. Solid-state tumor microenvironment. ....	11
1.4. Summary of literature reported medians for %O <sub>2</sub> <sup>48</sup> .....	11
1.5. Attributes to consider for genetic modification of oncolytic bacterial under investigation. ....	17
1.6. Brief explanation of important gene modification methods' characteristics for implementation. ....	27
1.7. Comparison of bacterial gene modification techniques. ....	38
1.8. Isikawa (fishbone) Diagram of the compounding factors inhibiting clinical translation for oncolytic bacteria. ....	39
2.1. Demonstrating ability to grow <i>C.novyi</i> . A) Schematic representation of <i>Clostridium novyi</i> life cycle. B) Brightfield images captured under oil-immersion at 40X. From left to right: a) Gram stain of vegetative <i>C. novyi</i> , b) Gram stain of <i>C. novyi</i> post –sporulation, c) Malachite green spore stain of post-sporulation <i>C. novyi</i> . C) PCR amplicons primers designed with specificity to <i>C. novyi</i> 16s rRNA and a-toxin. D) PCR amplification with <i>C. novyi</i> a-toxin primers after a-toxin knockout was performed. ....	69
2.2. Comparison of growth techniques. A) Growth curves from observing OD <sub>600</sub> of <i>Costridium novyi</i> under glovebag conditions versus with oxyrase enzyme. No statistical difference was found at any time point as determined by a Student's standard t-test (n=3 samples per time point). B) Growth curves from observing OD <sub>600</sub> of <i>Costridium novyi</i> under in oxyrase versus oxyrase with the addition of taurocholate. No statistical difference was found at any time point as determined by a Student's standard t-test (n=3 samples per time point). C) Spore enumeration of <i>Clostridium novyi</i> wild type and non-toxic strains with and without the addition of tauocholate. No statistical difference was found at any time point as determined by a Holms-Sidak test. (n=3 samples per enumeration). ....	71

- 2.3. Designing the plasmid. A and B) The resulting codon adaptation index (CAI) values for orthologous genes in *C. difficile* or *E. coli* were plotted against those of *C. novyi* to ascertain a correlation. C-D) Upon the comparison of the primary sequences of *C. novyi* genes with the orthologs found in *C. difficile* and *E. coli*, the GC skew (C) was determined as was the percent purines for each sequence (D). E) The literature was mined for expression data and the putative molecular percent was obtained for each gene and its ortholog. F) Table indicating the chosen *C. novyi* genes to target CRISPR mediated gene insertion and a few of the important characteristics considered when selecting these targets. .... 75
- 2.4. Building the CRISPR/Cas9n plasmid. A) Schematic representation of stepwise cloning method. B) DNA domain map of CRISPR cloning cassette build and utilized within pNICKclos1.0 to generated plasmid (pKMD002) used in this study. C) Verification restriction digests confirming the insert of sgrNA002 targeting NT01CX0401. Singlet is negative for insertion of desired sgrNA after digest with BglIII, doublet indicates positive insertion. D) Verification restriction digests confirming the insert of HDR cassette corresponding sgrNA002 to gene target NT01CX0401. Singlet is negative for insertion of desired sgrNA after digest with KpnI, doublet indicates positive insertion..... 83
- 2.5. Calcium competent *C. novyi* transformations A) Schematic representation of experimental flow. B ) Resulting CFUs after *C. novyi* cells underwent calcium competent transformation with pUC19. Statistical significance was determined to be  $p < 0.001$  through the application of the Holms-Sidak test ( $n=3$  experiments) C) After calcium competent *C. novyi* were transformed with pKMD002, five candidates (A-E) underwent plasmid isolation, and restriction digest to confirm plasmid present in cultures. Singlet is negative for presence, doublet is positive due to the presence of a *EcoRV* site designed in the insert. D) After calcium competent *C. novyi* were transformed with pKMD002, five candidates (A-E) underwent genomic DNA isolation, and subsequent restriction digestion to confirm plasmid present in cultures. Singlet is negative for genomic insertion, doublet is positive due to the presence of a *EcoRV* site designed within the insert. .... 86
- 2.6. Determining off-target effects of CRISPR/Cas9 mediated gene editing. A) Growth curves were determined by observing candidates A-E were for 72 hours collecting OD600 at significant time points. No statistical difference was determined at any time point ( $n=3$  for each time point, Holms-Sidak test,  $p=0.056$ ). B) Spore enumeration was conducted for genetically modified candidates and compared to non-modified wild-type and non-toxin *C. novyi* strains. No statistical difference was determined at any time point ( $n=3$  for each strain, Holms-Sidak test,  $p=0.058$ ) C) Cell lysis was determined under both anaerobic and aerobic conditions by applying vegetative *C. novyi* wild-type, non-toxic, candidate a, and non-toxic candidate a to PANC-1 cells. (No statistical significance was determined by Holms-Sidak test  $n=3$  for each group). .... 89

3.1.	Pictorial summation of phenotypical characteristics of pancreatic cancer cell lines as correlated to clinical tumorigenicity.....	106
3.2.	Lytic capacity of wild-type and non-toxic <i>C. novyi</i> . <i>C. novyi</i> vegetative or sporulated cells (5000/well) were added to cultures of pancreatic cancer cell lines A) BxPC-3, B) HPAF-II, C) KPC, D) MIA PaCa-2, and E) PANC-1 to assess the lytic capacity in anaerobic and aerobic conditions .....	110
4.1.	CRISPR-mediated genomic insertion of RGD peptide encoding gene. A) Schematic representation of the CRISPR cloning cassette utilized in pKMD002 for gene insertion. B) DNA sequences relevant to the cloning and confirmation of the pKMD002 plasmid. C) The results of CRISPR/Cas9n mediated genomic insertion of the RGD peptide into <i>C. novyi</i> candidates A-E and controls. ....	121
4.2.	Pictorial description of the $\alpha_v\beta_3$ adhesion assay methodology. ....	130
4.3.	Physical characterization of the inserted RGD peptide A) Fold change observed in crystal violet (CV) absorbance at a wavelength of 570 for wild type (WT), non-toxic (NT) <i>C. novyi</i> as well as the putative RGD-modified candidates ( A and B) after exposure to the $\alpha_v\beta_3$ coated surface of the adhesion assay. B) Average CV pixel count for candidates A and B as well as wild-type (WT) and non-toxic (NT) <i>C. novyi</i> that remain on the $\alpha_v\beta_3$ coated surface. C) Transmission electron microscopy images of wild type and RGD-modified candidate A <i>C. novyi</i> spores. (Co – core, Cx- cortex, Ct – coat, G – granular layer).....	131
4.4.	Pictorial representation of the surgical procedure utilized to produce the orthotopic pancreatic tumor model in C57/Bl6 immunocompetent mice. ....	133
4.5.	The effect of RGD-modified <i>C. novyi</i> spores intravenously injected in an <i>in vivo</i> orthotopic tumor model. A) The average percent weight of tumors harvested from murine models. C) Phase contrast confocal microscopy images of representative blood smears from each cohort. Scale bar in bottom right is 30uM. ....	135
4.6.	Quantifying <i>C. novyi</i> spores after IV injection. After tissue harvest and homogenization, bacterial burden was assessed for tissues that indicated a presence of <i>C. novyi</i> . 16s rRNA PCR was conducted with the template concentration normalized across tissues. A) The combined bioburden of all major organs within each cohort (WT – wild type <i>C. novyi</i> spore tail vein injection, RGD-mod - RGD-modified <i>C. novyi</i> tail vein injection) and Each major organ within a cohort when B) mock tumor implantation surgery occurred versus when C) tumor implantation with KPC cells was conducted. (Sp – spleen, P – pancreas, P&Pt – pancreas and pancreatic tumor, Lv- liver, Kd- kidney, Lu – lung, Hr – heart, Br – brain.).....	138
4.7.	TEM images of unmodified <i>C. novyi</i> NT spores. ....	146
4.8.	TEM images of RGD-modified <i>C. novyi</i> NT spores. ....	149

4.9.	Generation of a non-toxic RGD-modified <i>C. novyi</i> spore. In order to accomplish <i>in vivo</i> introduction without substantial toxicity, the $\alpha$ -toxin encoded phage DNA had to be knocked out in <i>C. novyi</i> that had already undergone successful genetic modification with RGD-encoding DNA. Upon knockout, PCR was conducted with primers specific to the $\alpha$ -toxin so that a lack of a band around 500bp represents a-toxin removal. ....	153
4.10.	Representative images used to generate the CV pixel count quantification of the adhesion assay. ....	154
4.11.	16s rRNA PCR amplicons used to establish the biodistribution for the mock tumor (PBS) implant cohort treated with PBS via tail vein injection. (Sp – spleen, P – pancreas, Lv- liver, Kd- kidney, Lu- lung, Ht- heart, Br- brain, (-) no template control, <i>E. coli</i> DNA control) .....	155
4.12.	16s rRNA PCR amplicons used to establish the biodistribution for the mock tumor (PBS) implant cohort treated with <i>C. novyi</i> NT spores (100,000) via tail vein injection. (Sp – spleen, P – pancreas, Lv- liver, Kd- kidney, Lu- lung, Ht- heart, Br- brain, (-) no template control, <i>E. coli</i> DNA control) .....	156
4.13.	16s rRNA PCR amplicons used to establish the biodistribution for the mock tumor (PBS) implant cohort treated with RGD-modified <i>C. novyi</i> NT spores (100,000) via tail vein injection. (Sp – spleen, P – pancreas, Lv- liver, Kd- kidney, Lu- lung, Ht- heart, Br- brain, (-) no template control, <i>E. coli</i> DNA control).....	157
4.14.	16s rRNA PCR amplicons used to establish the biodistribution for the tumor (KPC) implant cohort treated with PBS via tail vein injection. (Sp – spleen, P – pancreas, Pt – pancreatic tumor, Lv- liver, Kd- kidney, Lu- lung, Ht- heart, Br- brain, (-) no template control, <i>E. coli</i> DNA control). ....	158
4.15.	16s rRNA PCR amplicons used to establish the biodistribution for the tumor (KPC) implant cohort treated with <i>C. novyi</i> NT spores (100,000) via tail vein injection. (Sp – spleen, P – pancreas, Pt – pancreatic tumor, Lv- liver, Kd- kidney, Lu- lung, Ht- heart, Br- brain, (-) no template control, <i>E. coli</i> DNA control).....	159
4.16.	16s rRNA PCR amplicons used to establish the biodistribution for the tumor (KPC) implant cohort treated with RGD-modified <i>C. novyi</i> NT spores (100,000) via tail vein injection. (Sp – spleen, P – pancreas, Pt – pancreatic tumor, Lv- liver, Kd- kidney, Lu- lung, Ht- heart, Br- brain, (-) no template control, <i>E. coli</i> DNA control).....	160
4.17.	16s rRNA PCR amplicons from normalized genomic DNA isolates used to establish the bacterial burden in ng/amplicon in Figure 4.6. A sample legend can be found in Sup. Table 4.4. ....	163

## LIST OF ABBREVIATIONS

% mol	Molecular fraction
%O <sub>2</sub>	Percent oxygenation
%R	Percent purine
°C	Degrees Celsius
16s rRNA	Ribosomal RNA component
2D	Two-dimensional
3D	Three-dimensional
Abs <sub>570</sub>	Absorbance at 570 nanometers
ACS	American Chemical Society
AdV	Adenovirus
B cell	Bone marrow derived lymphocyte
BCG	Bacille Calmette-Guerin
BLASTn	Basic local alignment search tool, nucleotide version
Bp	Base pair (nucleotide)
CAI	Codon adaption index
Cas	CRISPR-associated protein
Casn	CRISPR-associated nickase protein
cDNA	Complementary DNA
CFUs	Colony forming units
Co	Spore Core
CO <sub>2</sub>	Carbon dioxide
COX-2	Cylco-oxygenase 2
CPT	Camptothecin

CPT-11 .....	Irinotecan
CreI .....	<i>Chlamydomonas reinhardtii</i> homing nuclease
CRISPR .....	Clustered regularly interspaced short palindromic repeats
crRNA .....	CRISPR RNA
Ct.....	Spore Coat
CTCC .....	Corrected total cell blue/violet color
CV.....	Crystal Violet
Cx.....	Spore Cortex
Cys .....	Cystine
DMEM .....	Dubelco's Modified Minimum Media
DNA.....	Deoxyribonucleic acid
dsDNA .....	Double stranded DNA
dtLLO .....	Detoxified listeriolysis O
e.g. ....	"For example"
ECM .....	Extra cellular matrix
EDTA .....	Ethylenediaminetetraacetic acid
EMEM.....	Essential Modified Minimum Media
EPR .....	Enhanced permeability and retention
Eq .....	Equation
Et al .....	Et alia, "and others"
Etc .....	Et cetera, "and so on"
FBS .....	Fetal bovine serum
FDA .....	Federal Drug Administration
Fig.....	Figure
g.....	Gram



G.....Spore Granular layer

GC .....Guanine and Cytosine

GGA.....Glycine-Glycine-Alanine peptide

GMP .....General manufacturing protocol

H<sup>+</sup> .....Hydrogen

HDR .....Homologous domain repair

HF .....High fidelity

HIF-1 .....Hypoxia-inducible factor 1

His .....Histidine

HNSCC .....Head and neck squamous cell carcinoma

HO.....Homing endonuclease

Hr .....Hours

HSV .....Herpes simplex virus

i.e. ....Id est, “in other words”

IDT.....Integrated DNA Technologies

IEP .....Intron-encoded protein

IFN $\gamma$  .....Interferon gamma

IgA .....Immunoglobulin A

IgG .....Immunoglobulin G

IL-1 .....Interleukin 1

IL-2 .....Interleukin 2

IL-6 .....Interleukin 6

*In vitro*.....Performed in a test tube

*In vivo*.....Performed in a biological system

IV .....Intravenous

kbp.....Kilobase pair  
 kg.....Kilogram  
 L .....Liter  
 LHE .....LAGLIDADG homing endonucleases  
 LLO .....Listeriolysis O  
 LPS .....Lipopolysaccharide  
 M.....Molar  
 mDNA.....Mitochondrial DNA  
 Min.....Minute  
 mL.....Milliliter  
 Mm.....Millimeter  
 MMP .....Matrix metalloproteinase  
 MN .....Meganuclease  
 MPS .....Mononuclear phagocyte system  
 mRNA .....Messenger RNA  
 NCBI.....National Center for Biotechnology Information  
 ng.....Nanogram  
 NHEJ .....Non-homologous end joining  
 NK .....Natural killer  
 NLS.....Nuclear localization sequence  
 nm .....Nanometer  
 NSG .....NOD skid gamma  
 NT .....Non-Toxic  
 OA .....Oxyrase for Agar  
 OB .....Oxyrase for Broth

OD .....	Optical density
OD <sub>600</sub> .....	Optical density at 600nm
OV .....	Oncolytic virus
p .....	p-Value, observed results of a stastical hypothesis test
PAD .....	Peptidyl arginine deaminase
PAM.....	Protospacer adjacent motif
PAMPs .....	Pathogen associated molecular patterns
PBS .....	Phosphate buffered saline
PCR .....	Polymerase chain reaction
PD-1 .....	Programed cell death protein 1
PDX .....	Patient derived xenograph
PEG.....	Polyethylene glycol
pH.....	A measure of the acidity or alkalinity of a solution
Pro-MMP .....	Pro-matrix metalloproteinase
PSF .....	Penicillin Streptomycin Fugisome
RAM .....	Retrotransporition-activated markers
RCM .....	Reinforced Clostridial Media
RGD .....	Arginylglycylaspartic acid
RNA .....	Ribonucleic acid
rpm .....	Revolutions per minute
RPMI.....	Roswell Park Memorial Institute Media
rRNA.....	Ribsomal RNA
RT .....	Reverse transcriptase
RVD .....	Repeat variable di-residue
s .....	Seconds

SC.....	Sub-cutaneous
sgRNA .....	Short guide RNA
SOC .....	Super optimal brother medium
Sp .....	Species
SpCas9n .....	<i>Streptococcus pyrogens</i> Cas9 nickase
Sup fig.....	Supplementary Figures
T cells .....	Thymus derived lymphocyte
TALE .....	Transcription activator like effector
TALEN .....	Transcription activator like effector nuclease
TAM.....	Tumor-associated macrophages
TAN .....	Tumor associated neutrophils
tch.....	Taurocholate
TEM .....	Transmission electron microscopy
TIME .....	Tumor immune microenvironment
TLR4 .....	Toll-like receptor 4
TNF $\alpha$ .....	Tumor necrosis factor alpha
TPRT .....	Targeted DNA-primed reverse transcription
TPT .....	Topotecan
tracrRNA.....	Trans-activating CRISPR RNA
Treg.....	Regulatory T-cell
TV .....	Tail vein injection
ug .....	Microgram
uL .....	Microliter
uM.....	Micromolar
V .....	Volts

v/v .....Volume per volume  
VACV .....Vaccinia virus  
Vs .....Versus  
VSV .....Vesicular stomatitis virus  
w/v.....Weight per volume  
WT .....Wild type  
ZF .....Zinc Finger  
ZFN .....Zinc finger nuclease  
 $\alpha\upsilon\beta 3$  .....Alpha five Beta three integrin

## LIST OF SYMBOLS

/	.....	Per, division
#	.....	Number
%	.....	Percent
°	.....	Degree
<	.....	Less than
=	.....	Equal
>	.....	Greater than
\$	.....	Dollar
\$	.....	Dollar
C	.....	Celsius
V	.....	Five
$\alpha$	.....	Alpha
$\beta$	.....	Beta

## LIST OF APPENDIX TABLES

<u>Table</u>	<u>Page</u>
A.1. Gene sequences of insertion target. Sequences of the four genes identified as targets for spore coat protein insertion. sgRNA sequences are within brackets (targets [1] and {2}) and underlined and bold. ....	177
A.2. Sequences of designed sgRNA. Sequences of the four sgRNA sequences designed to targets [1] and {2} in Sup Table 1. These sequences include necessary restriction digest sequences for cloning as well as additional nucleotides to allow for digestion. Bold underlined sequence – <i>SpeI</i> cloning site, bold text crRNA sequence, <i>bold underlined italics</i> – <i>BglIII</i> verification site, <i>bold italics</i> – <i>NotI</i> cloning site. Codon bias for <i>Clostridium novyi</i> is accounted for in every synthetic sequence. ....	178
A.3. Sequences of designed homologous domain repair arms. Sequences of the four correlating homologous domain repair (HDR) sequences designed to repair targeted DNA breaks at the sites in Supplemental table 1. These sequences include necessary restriction digest sequences for cloning as well as cloning verification. Bold italics text – <i>NotI</i> cloning site; bold – <i>EcoRV</i> verification site, bold italic underlined - <i>KpnI</i> cloning site, bold underlined – <i>SacI</i> cloning site, bold – <i>XhoI</i> cloning site. ....	179
B.1. Sequences of RGD gene inserts designed. Sequences of the three genes designed to be inserted into the <i>C. novyi</i> genome. Due to the surface characteristics of the spore coat, a triple and novemiple repeated insert was also designed. A Start Codon, Shine-Delgarno sequence, TATA box and stop codon were all included as well. <i>Bold italic underlined</i> - <i>KpnI</i> cloning site, ALL CAPS BOLD - RDG sequence, ALL CAPS ITALICS - GGA spacer, <i>italics</i> - <i>ClaI</i> verification site, bold underlined – <i>SacI</i> cloning site. ....	181
E.1. Ten most expressed genes in <i>C. novyi</i> . Genes that were considered the most expressed <i>C. novyi</i> genes from previously published data were utilized to draw comparisons with <i>E. coli</i> and <i>C. difficile</i> . ....	189
E.2. Ten least expressed genes in <i>C. novyi</i> . Genes that were considered the least expressed <i>C. novyi</i> genes from previously published data were utilized to draw comparisons with <i>E. coli</i> and <i>C. difficile</i> . ....	192
E.3. <i>E. coli</i> genes that were considered orthologs to the most expressed <i>C. novyi</i> genes from previously published data utilized to draw comparisons with <i>C. novyi</i> and <i>C. difficile</i> . ....	194
E.4. <i>E. coli</i> orthologs for the ten most expressed genes in <i>C. novyi</i> . <i>E. coli</i> genes that were considered orthologs to the least expressed <i>C. novyi</i> genes from previously published data utilized to draw comparisons with <i>C. novyi</i> and <i>C. difficile</i> . ....	196

E.5.	<i>C. difficile</i> orthologs for the ten most expressed genes in <i>C. novyi</i> . <i>C. Difficile</i> genes that were considered orthologs to the most expressed <i>C. novyi</i> genes from previously published data utilized to draw comparisons with <i>C. novyi</i> and <i>E. coli</i> . .....	198
E.6.	<i>C. difficile</i> orthologs for the ten least expressed genes in <i>C. novyi</i> . <i>C. difficile</i> genes that were considered orthologs to the least expressed <i>C. novyi</i> genes from previously published data utilized to draw comparisons with <i>C. novyi</i> and <i>E. coli</i> . .....	200
F.1.	Putative codon bias for <i>C. novyi</i> . Codon bias was probed using the genes selected for insertion. SerialCloner software was used to accomplish the annotation of the gene sequence's open reading frame into amino acids. ....	202



## LIST OF APPENDIX FIGURES

<u>Figure</u>	<u>Page</u>
C.1. Schematic representation of cloning scheme. Schematic map of the cloning elements incorporated to generate a CRISPR/Cas plasmid for gene insertion in <i>C. novyi</i> . Restriction digest enzyme cleavage sites: <i>SpeI</i> , <i>NotI</i> , <i>XhoI</i> , <i>KpnI</i> , <i>SacI</i> and <i>EcoRI</i> , <i>BglIII</i> , <i>ClaI</i> ; sgRNA= single guide ribonucleic acid; HDR = homologous domain repair .....	182
D.1. Verification of insertion of desired sgRNA <i>BglIII</i> digest. Insertion of desired sgRNA can be determined by <i>BglIII</i> restriction digest. A digest with <i>BglIII</i> of candidate plasmids will result in either 1) a single 11kb band, which would confirm that insertion did not occur, or 2) two bands at 10.1kb and 973bp, which would confirm that insertion took place. ....	183
D.2. Verification of insertion of desired HDR <i>KpnI</i> digest. Desired HDR can be determined by <i>KpnI</i> restriction digest. A digest of candidate plasmids with <i>KpnI</i> will result in either 1) a single 11kb band, which would indicate that insertion did not occur, or 2) two bands at 8.14kb and 3.0kb, confirming that insertion took place. ....	184
D.3. Verification of insertion of desired HDR by alternative <i>SacI</i> digest. The desired HDR can be determined by <i>SacI</i> restriction digest. Digesting candidate plasmids with <i>SacI</i> will result in either 1) the presence of bands at 8.0kb and 3.1kb, which will indicate a negative plasmid or 2) the presence of three bands at 5.1kb, 3.1kb and 2.9kb, confirming a positive on a 3% agarose gel. ....	185
D.4. Verification of insertion of desired RGD by <i>SacI</i> and <i>KpnI</i> digest. Insertion of a single RGD sequence can be determined by a double digest with <i>SacI</i> and <i>KpnI</i> . A digest with both <i>SacI</i> and <i>KpnI</i> of candidate plasmids will result in either 1) confirmation of negative result for desired sequence by the presence of 2 visible bands at 3.0kb, 2.2kb, and 54bp, or 2) confirmation of positive clone for desired cloning event will generate three bands at 5.8kb, 3.1kb, and 2.2kb. ....	186
D.5. Verification of insertion of desired 3xRGD by <i>ClaI</i> digest. Insertion of the single RGD sequence can be distinguished from the insertion of the 3xRGD repeat by a digest with <i>ClaI</i> . A digest with <i>ClaI</i> of candidate plasmids will result in either 1) the presence of a single band at 11.1kb indicating a clone with 1xRGD, or 2) two bands at 9.0kb and 2.1kb, indicating the presence of 3xRGD. ....	187
D.6. Verification of insertion of desired 9xRGD by <i>BamHI</i> digest. The insertion of the single RGD sequence can be distinguished from the insertion of the 9x RGD repeat by a digest with <i>BamHI</i> . A digest with <i>BamHI</i> of candidate plasmids will result in either 1) a single band at 11.1kb for 1xRGD, or 2) two bands at 6.7kb and 4.5kb indicating the insertion of 9xRGD. ....	188

**CHAPTER 1: THE NEXT FRONTIER OF ONCOTHERAPEUTICS:  
ACCOMPLISHING CLINICAL TRANSLATION OF ONCOLYTIC BACTERIA  
THROUGH GENETIC ENGINEERING<sup>1</sup>**

**Abstract**

The development of a “smart” drug able to distinguish between tumor cells and host cells has been sought after for centuries, but the microenvironment of solid tumors continues to confound current therapeutics and throw up roadblocks in this pursuit. Solid tumors present several challenges for current oncotherapeutics including aberrant vascularization, which results in hypoxia, necrosis, and an abnormally high pH. In addition to these physical and biochemical barriers, irregular vascularization also contributes to overall tumor immune suppression. While most non-cancer cells are inhibited by the tumor micro-environment, oncolytic microbes are drawn to it, having an innate ability to selectively infect, colonize, and irradiate solid tumors. They may also restore the immune balance, reactivating tumor associated immune components. To harness the advantages of these oncolytic species and achieve their domestication, several modern genetic engineering techniques could be implemented to develop customized “Frankenstein” bacteria with advantageous characteristics from several distinct species. The development and clinical translation of an oncolytic species as a chemotherapeutic would represent a shift in the paradigm for cancer therapeutics and would have ramifications that reach from the medical into the realm of socio-economics. This review seeks to marry the current field

---

<sup>1</sup> The material in this chapter was co-authored by Dailey, K. M.; Allgood, J. E; Johnson, P. R., Ostelie, K.; Brooks, B. D.; Brooks, A. E. Dailey, K. M. had primary responsibility for designing all experiments, collecting all data, analyzing all data, and generating subsequent figures and tables. Dailey, K. M. was the primary developer of the conclusions that are advanced here. Dailey K.M. also drafted and revised all versions of this chapter. Brooks, A. E. served as proofreader and checked the math in the statistical analysis conducted by Dailey, K. M.

of oncolytic bacteria with the expanding field of modern bacterial genetic engineering techniques in prospect of such a therapeutic.

## **Introduction**

Historically, the maintenance of human health has been an arms race between bacteria and biomedical technology; however, reexamining the presence of bacteria in the human host has led to recognition of the symbiotic relationship between microbes and their human hosts. Recently, the research community has begun untangling the complex bidirectional communication<sup>1,2</sup> not only between host cells and organ systems but also between these commensal microorganisms, leading to an appreciation of the etiological consequences of dysbiosis. It is now clear that changes in the human microbial community can mediate cellular transformation, genetic instability, somatic mutations, and microenvironmental shifts associated with malignancy<sup>3,4</sup>. Manipulation of the resident microbiota through both probiotics and antibiotics, a revolutionary and now indispensable part of healthcare, to restore balance has prompted researchers to re-examine the role of bacteria in human health, reclassifying certain species from healthcare foe to indispensable friend. Bacteria have become a powerful tool when it comes to tackling some of our most challenging modern health crises such as obesity and cancer.

Despite the renewed interest in bacteria as a tool in the fight against cancer, anecdotes dating back as far as 1500 BC describe beneficial bacterial infections within tumors<sup>5</sup>. In an attempt to legitimize such anecdotes, clinical trials to probe the efficacy of bacteria as a method to treat cancer were conducted in the 1990s but generated mixed results, leaving the field unable to clearly interpret the results and wary to continue the investigation. Nevertheless, a growing body of work has elucidated that specific microbes are not only good for aspects of human health

such as digestion and infection response<sup>4</sup>, but also have an innate ability to rectify disease states such as through selective infection of solid tumors. Unfortunately, mobilizing these species for use as a therapeutic is not without stumbling blocks. With the discovery and advancement of new gene modification technologies, efforts have been renewed to ‘domesticate’ bacterial species by harnessing their natural infection capabilities to seek and lyse solid tumors. These bacteria have been collectively termed oncolytic, or cancer lysing, bacteria for their ability to actively localize to tumors and lyse the tumorigenic cells.

Several genera, including *Bifidobacterium*<sup>6</sup>, *Caulobacter*<sup>7,8</sup>, *Clostridium*<sup>9,10</sup>, *Escherichia*<sup>11</sup>, *Klebsiella*<sup>12</sup>, *Lactobacillus*<sup>13</sup>, *Listeria*<sup>14</sup>, *Mycobacterium*<sup>15,16</sup>, *Proteus*<sup>17,18</sup>, *Salmonella*<sup>19</sup>, and *Streptococcus*<sup>20</sup>, include species currently classified as oncolytic bacteria. The idea of using bacteria as a tumor targeting therapy may be considered ‘ancient’, but a thorough understanding of what makes these species particularly skilled at targeting tumors at the molecular level has lagged far behind, hindering its implementation at the clinical level. Several gaps in knowledge still exist in the current literature. For species that have been studied (i.e. *Clostridium* sp.) much of the experimental design relies on assumptions gathered from studies of loosely related cousin species. When the fundamental understanding of oncolytic bacteria’s innate ability for tumor localization and destruction has been established in more detail, that knowledge will pave the way for innovative therapies relevant not only for cancer, but also potentially for insect-borne pathogens (i.e. utilizing *Wolbachia* as a mosquito pathogen to control malaria transmission<sup>21</sup>). Furthermore, it will provide crucial insight to improve site-specific delivery of drug payloads<sup>22</sup> and gene therapies<sup>23</sup> in a vast range of disease states, as well as for immunomodulation and vaccine adjuvants<sup>24</sup>.

Bacteria classified as oncolytic have several common characteristics, but perhaps the most important is their ability to sense and process biomolecule gradients as an impetus for chemotactic mobility. The ability to actively seek out and respond to a physio-chemical environment has been widely sought after in pharmaceuticals, particularly in chemotherapeutics. Developing “smart” drugs that can distinguish between tumor cells and normal cells - selectively effecting only malignant cells while sparing normal cells may be the holy grail of chemotherapeutics. To harness the advantages of these oncolytic species, biomedical technology could take a page from the biofuel industry, which through genetic engineering has developed customized bacteria to produce 1) biodiesel as an alternative to petroleum-based diesel<sup>25,26</sup>, 2) fuel-precursor producing microorganisms<sup>27</sup>, and 3) bacteria to mitigate polymeric waste<sup>28</sup>. The discovery of new gene manipulation techniques such as CRISPR, has accomplished the reprogramming of bacterial gene expression in a predictable way yet with unforeseen potential. The adaptation of bacteria as drugs, perpetual micro-bioincubator producers of drugs, or drug vehicles has been thrust into the realm of immediate possibility, making genetic manipulation of bacteria the next frontier of biomedical engineering. However, these concepts have yet to achieve significant clinical translation. In order to translate the field of genetic engineering into the clinic, several challenges need to be addressed. In an effort to move the field of bacterial therapeutics forward, this manuscript will provide not only an accurate accounting and assessment of the bacterial genetic engineering toolbox, but also the optimal context of each available method.

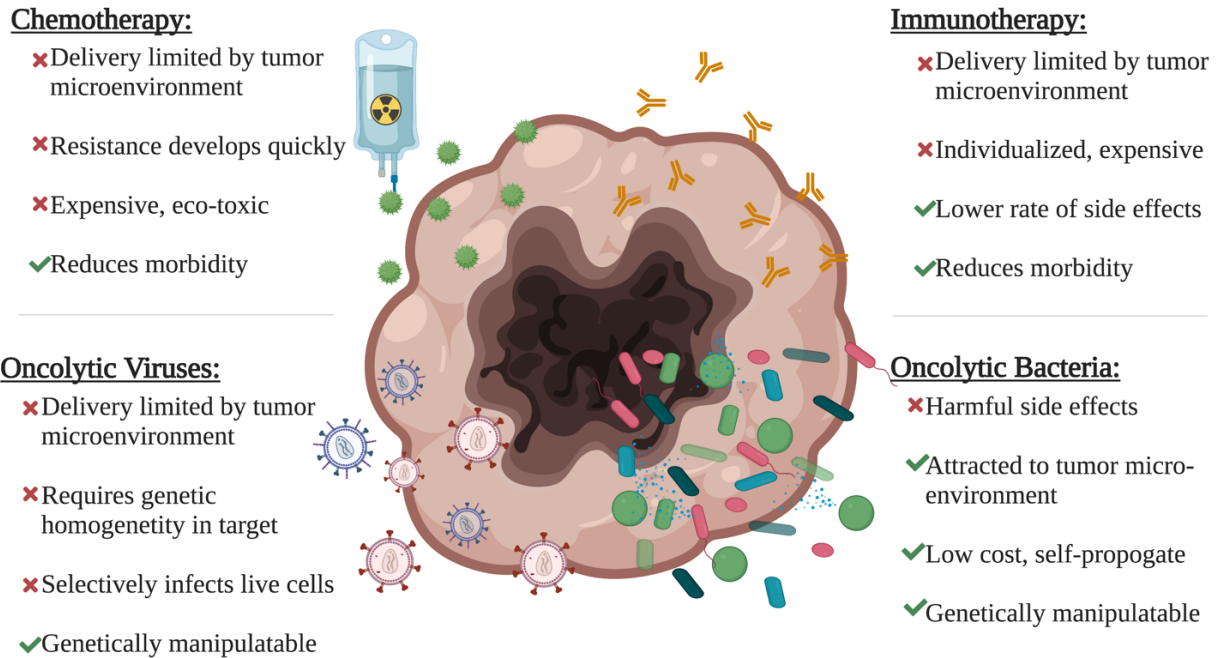


**Figure 1.1.** Comparison of current solid state tumor therapeutics.

## Current Treatments

### Chemotherapeutics

While chemotherapeutics, a standard of care for many if not most solid tumors, have shown great efficacy and potency for mitigating tumors, research in the last five years has revealed a treatment paradigm wherein drug resistance has not only led to decreased effectiveness, but some evidence suggests that certain chemotherapies may make tumorigenic cells more resistant, aggressive, and metastatic (Fig 1.1). While single tumor cell resistance may not initially seem like a major hurdle to successful treatment, the persistence of these cells throughout the treatment regimen can confer resistance to other tumor cells, creating entire tumors resistant to available therapeutics<sup>29,30</sup>. Drug resistance is a common limitation of chemotherapeutics. Two types of resistance have been observed: when the drug works upon initial treatment but resistance arises due to adaptation (acquired resistance), and when existing tumor cells are resistant to the drug prior to any exposure (intrinsic)<sup>29</sup>. While some of the issues

surrounding drug resistance have been eased using an evidence based medicine approach and screening for novel biomarkers of therapeutic efficacy, these pre-therapies are costly in both time and money, leaving lower socio-economic groups behind in the cancer survival rates.

### **Microbe Treatments**

The use of viruses and bacteria have been explored as oncolytics with both accumulating anecdotal and rigorous scientific evidence to back their use (Fig 1.1). While records of oncolytic bacteria far out date oncolytic viruses, oncolytic viruses also have a robust body of literature with their use dating back to the late nineteenth century<sup>31</sup>; furthermore, they seem to have been more well accepted as a potential oncotherapy. The ability to scientifically understand the oncolytic use of viruses was greatly aided in the 1950s-60s by the advancement of cell and tissue culture systems, allowing *in vitro* viral propagations<sup>31</sup>. In the subsequent years, the structure, biochemical mechanisms, and ‘life’ cycle have been intensely studied, generating a robust foundation of knowledge that rivals any other organism<sup>31</sup>. The first hints at the ability to use viruses as a disease state therapy occurred in the early 1900s with other sporadic attempts at clinical testing occurring (notably below modern ethical standards) for the next fifty years in a desperate attempt to mitigate cancer<sup>31</sup>. The current radical advances of twenty-first century technological capacity (*e.g.* gene editing and disease modeling) have returned both oncolytic viral and oncolytic bacterial therapies to the realm of possibility. Given the large body of foundational knowledge detailing all aspects of viruses, the study and development of oncolytic viruses serve as an important beginning for the field of bacterial therapeutics.

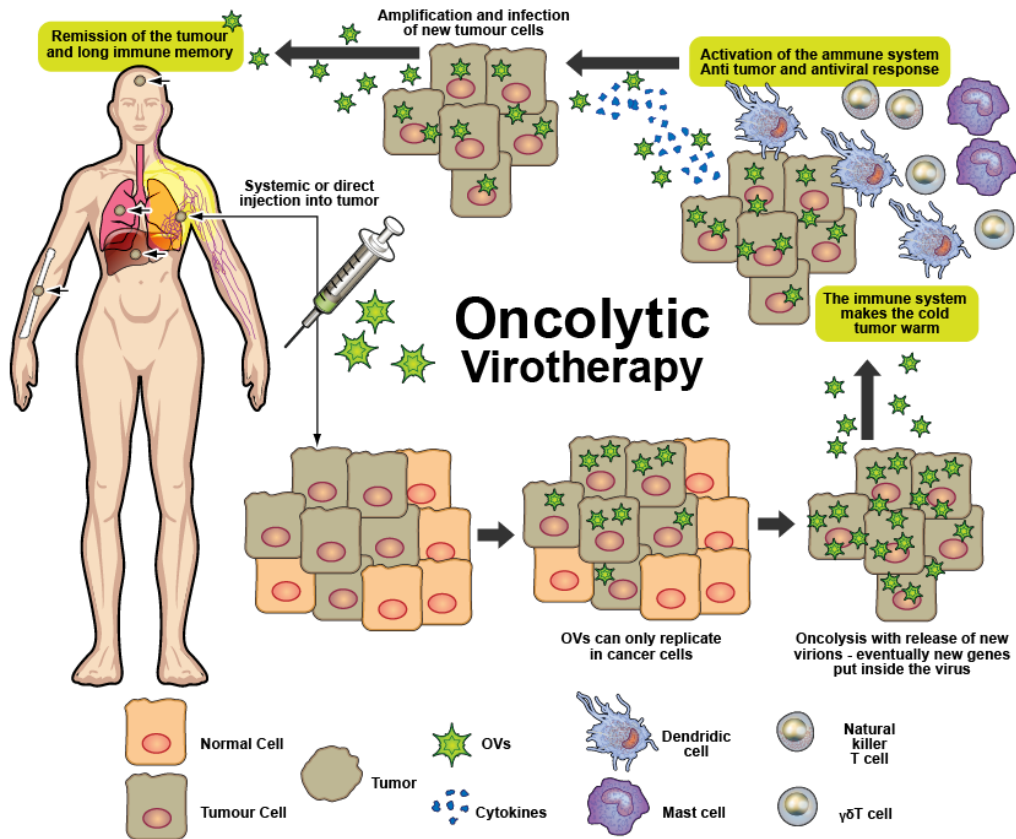


**Figure 1.2.** Oncolytic virotherapy.

### Oncolytic Viruses

The use of oncolytic virus (OV) therapy and combination OV and immunotherapy, immune modulators in particular, is rapidly expanding<sup>32</sup>. OV viral platforms, which are designed to selectively bind and kill cancer cells, include adenovirus (AdV)<sup>32</sup>, herpes simplex virus (HSV)<sup>33,34</sup>, measles virus<sup>35,36</sup>, parvovirus<sup>37</sup>, vaccinia virus (VACV)<sup>38</sup>, and vesicular stomatitis virus (VSV)<sup>39</sup>. OVs can facilitate anti-tumor responses either directly or indirectly by viral oncolysis or induction of host immunity respectively<sup>40</sup>. OVs hold great promise, often being heralded as the “ultimate” cancer-targeted therapeutic due to their ability to selectively amplify themselves, thereby increasing the therapeutic dose within the tumor microenvironment (Fig 1.2). However, oncolytic bacteria possess this intrinsic multiplication ability as well. OV possess



several unique mechanisms when compared to traditional and emerging oncotherapies (Fig 1.1). First, numerous highly specific killing mechanisms for OV's exist. These include cancer-specific cell-membrane receptors, selective replication in tumor cells (thymidine kinase-deleted mutant)<sup>41</sup>, transcriptional control of expression of viral genes by cancer cells<sup>42</sup>, as well as numerous others beyond the scope of this article<sup>32,33,41,43-45</sup>. Next, OV's efficacy extends beyond the tumor microenvironment<sup>46</sup> into vascular environments and into the immune system<sup>32</sup>. As noted by Martin et al., "Each of these points of interaction provides an opportunity for combining orthogonal therapeutics to complement or even synergistically kill OV's and improve outcomes for cancer patients"<sup>32</sup>. Moreover, this dual mechanism provides the opportunity to not only increase efficacy, but also reduce resistance to the therapy - a classic problem facing many current cancer therapeutics. Lastly, several OV platforms have the potential to be engineered to express therapeutic payloads<sup>32</sup>. Modern technology allows for engineering of a virus much like a bacteria to encode transgenes within the virus backbone or to be coupled to another stand-alone therapeutic (*e.g.*, drugs, antibodies, cells)<sup>40</sup>. The coupling of other anti-cancer therapeutics for additive or synergistic effects is potentially available as well. Furthermore, OV's are routinely genetically modified to decrease pathogenicity, increase lytic potential and enhance immunogenicity, improving the risk-benefit ratio for clinical development<sup>40</sup>.

For all of the advantages of oncolytic viruses, they are not a panacea, in fact several key challenges persist. First, cancers can be either genetically or phenotypically heterogeneous - often both<sup>32</sup>. Moreover, the tumor microenvironment is composed of mixtures of normal and cancerous cells with a unique, complex extracellular matrix (ECM), making it challenging for the virus to find, access, infect, and then completely eradicate the tumorigenic cells while not infecting healthy cells or evoking a neutralizing host immune response. OV's face significant

challenges in the development phase, especially in clinical trials. Challenges include limited target indication opportunities due to unique biosafety concerns, alternative regulatory requirements, public perceptions, challenging trial designs and end point assessments, as well as viral manufacturing at a GMP level<sup>40</sup>. Beyond the challenges these approaches present, delivery of the OV is likely the most cumbersome. Several approaches exist for delivering a therapeutic payload to the tumor. The two most common ways of administering the virus are through intratumoral or intravenous injections<sup>40</sup>. The OV may be inefficacious if a sustained or dosed therapy is necessary<sup>40</sup>. A more detailed review of OV delivery advantages and disadvantages is available<sup>32,40</sup>. Most of these challenges will also translate to oncolytic bacterial therapy. With OV development already in the later stages, such technologies are likely to blaze the trail for other microbial treatments.

## **Challenges of Current Cancer Therapeutics**

### **Tumor Microenvironment**

#### ***Vascularization***

When discussing drug delivery methods, aberrant tumor vascularization is arguably the foremost challenge to overcome for cancer therapeutics (Fig 1.3). Typically, this vascularization is a meticulously organized network where cells are only a few micrometers away from a vessel. This intricate yet dynamic organization of vascularization breaks down in the solid tumor environment, largely because tumorigenic cells tend to out-proliferate the epithelial cells responsible for capillary formation<sup>47</sup>. Proliferation such as this causes disruption in the nutrient and oxygen delivery where cells are now more than one hundred times further away from vasculature than normally observed<sup>47</sup>. Furthermore, exacerbation of this dysfunction occurs due to ‘leaky’ blood vessels that are characterized by poorly organized epithelial cells and

compression from physical infringement of tumor cells causing inconsistent blood flow<sup>47</sup>. In addition to aberrant vasculature, solid state tumors almost ubiquitously lack functioning lymphatics - ultimately resulting in increased interstitial fluid pressure<sup>47</sup>. Subsequently, the blood vessels necessary to consistently deliver nutrient macromolecules have to be manufactured or commandeered to accommodate the tumor's expedited growth rate and size<sup>20</sup>. As a result of the continued, unchecked growth of solid tumor cells, vasculature from the middle of the tumor is frequently relocated in order to encourage new cell proliferation, giving rise to a relatively avascular core. Consequently, these masses have a relatively nutrient starved core, with both hypoxic and acidic characteristics almost ubiquitous to all solid tumors regardless of size<sup>48</sup>. This harsh tumor microenvironment poses a significant challenge not only for traditional chemotherapy delivery vehicles but also for drug efficacy. It is widely accepted that tumor cells consume more oxygen than is available<sup>21</sup>, leading to both poor oxygen saturation in the tumor tissue and localized acidosis because metabolites are cleared at subnormal rates. However, defining decreased oxygen saturation as 'hypoxia' has been somewhat elusive. A concrete characterization of tumor hypoxia will likely prove necessary for developing an effective oncolytic bacterial therapy as this will more clearly indicate which anaerobic bacteria can be delivered to the tumors as well as the method of introduction (*e.g.* intratumoral vs intravenous injections).

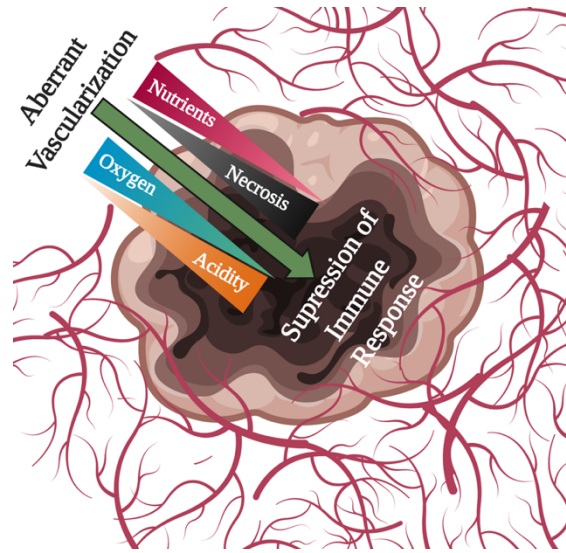


**Figure 1.3.** Solid-state tumor microenvironment.

**Median Reported Tumor Hypoxia vs Physoxia (%O<sub>2</sub>)**

Tissue	Tumor
3.4	Brain 1.7
5.9	Head/Neck 1.7
5.6	Lung 2.0
6.8	Breast 1.3
6.8	Pancreas 1.02
3.9	Liver 0.8
4.9	Renal 1.3
5.5	Cervical 1.2
NR	Vulval 1.5
3.9	Prostate 0.6
6.8	Rectal 3.4
6.7	Sarcoma 1.8
5.3	Melanoma 1.5
4.6	<b>Overall 1.4</b>

**Figure 1.4.** Summary of literature reported medians for %O<sub>2</sub> <sup>48</sup>

## *Hypoxia*

Despite widely implemented 'normal' oxygen levels of 20% (normoxia) in tissue culture, physiological levels of oxygenation, or physoxia, is dynamic and not recapitulated in these artificial tissue culture conditions. In lung alveola the reported oxygen level is around 15%, which drops to 3.4-6.8% as diffusion to peripheral tissues occurs<sup>49</sup>. It is worth noting that each tissue has its own physoxia level, which is homeostatically regulated by the metabolic biases occurring within those particular tissues. It is reasonable then to assume that hypoxia tolerance of each cell is a characteristic of its originating tissue<sup>48</sup>. Therefore, physoxia is perhaps better defined by the transitory 3-6% oxygen levels tissues maintain through a number of means, including the upregulation of hypoxia regulating genes such as, hypoxia-inducible factor 1 (HIF-1)<sup>50</sup>. Establishing a clinically relevant baseline for oxygenation is crucial for characterizing the hypoxia brought about by aberrant vascularization in solid state tumors.

Pathological hypoxia can therefore be better described as a situation where the homeostatic mechanisms to maintain oxygen saturation levels do not respond effectively to extracellular and environmental signaling<sup>48</sup>. The hypoxia levels characteristic of solid state tumors are particularly intriguing as they differ from those of other pathologic hypoxia inducing conditions such as ischemic disease states (diabetes, heart attack, concussion, etc.)(Fig 1.3). It is thought that the hypoxia of ischemic events, both chronic and acute, is caused by a physical blockage or reduction of blood flow, making the return to physoxia (around 4.6% oxygen<sup>48</sup>) all but impossible until the blockage is removed. Solid tumors in contrast have characteristically enhanced angiogenesis and HIF-1 upregulation<sup>51,52</sup>, yet fail to maintain physoxia, with levels falling between 0.3-4%<sup>48</sup>. These extremely low levels of oxygen are therefore unique to the tumor microenvironment. Indeed, there are several lines of investigation attempting to use this

characteristic as a method for targeted drug delivery<sup>53,54</sup>. However, current methods of hypoxia-induced drug delivery have encountered issues with off-target effects where drugs are offloaded in other areas of low oxygenation in the body, often with dangerous side effects. Hence, it would seem that hypoxia alone may not be enough to selectively target tumorigenic cells with traditional and perhaps even novel synthetic drug delivery vehicles (*e.g.*, liposomes, polymerosomes, nanoparticles, etc.).

### ***Acidity***

Due to inadequate vascularization among other factors, solid state tumors often have low extracellular pH in addition to hypoxia (Fig 1.3). These two characteristics are intricately entwined and have been proven to impact tumor aggression and metastatic capacity both synergistically and individually. Typically, interstitial pH is maintained between 7.3 and 7.4. Under physiological conditions with normal perfusion, this can be considered equivalent to the pH of blood with a few notable instances of pH variance for tissues such as the pancreas or colon, or due to acid/base secretion (*i.e.* skeletal muscle). Low extracellular pH in solid tumors is thought to be largely caused by an accumulation of metabolites such as lactic acid due to upregulated anaerobic glycolysis (*i.e.* Warburg Effect) and a decreased ability to clear these deleterious metabolites through vasculature. Alternatively, or perhaps synergistically, an excess of carbonic anhydrase catalyzes the formation of free H<sup>+</sup> and excess CO<sub>2</sub> through the pentose phosphate pathway, potentially impacting tumoral pH<sup>55</sup>. The molecular pathways that detail these influences have been thoroughly reviewed elsewhere<sup>55,56,57</sup>; but within the context of developing an oncolytic therapy, some key pathways warrant a brief discussion here.

The acidic characteristic of tumor cells initiates the activation of intracellular lysosomal enzymes, which contributes to accelerated degradation of many anti-cancer therapies.

Furthermore, some proteinases are activated by an acidic pH<sup>55</sup>. In normal physiological processes, matrix metalloproteinase (MMP) family members are largely responsible for the breakdown of extracellular matrices<sup>58</sup>. Host-sourced inactive pro-matrix metalloproteinase-9 (proMMP-9), proMMP-2 and proMMP-8 were found in saliva and could be activated by acid<sup>58</sup>. While this study was done in the context of tooth dentin demineralization, the results have implications for the aberrant activation of MMPs as well as other proteins found in solid tumors. Acid-activation of proMMP-9 has also been demonstrated in a human melanoma model, where this activation impacted the invasiveness of tumorigenic cells<sup>59</sup>. Tumor acidity has not only been indicated as a central regulator of cancer immunity, but has proven to be a significant compounding challenge for drug delivery. Much like hypoxia, while ubiquitous to almost all solid tumors, the quantifiable levels of tumor acidity vary greatly depending upon size, progression, tissue of origin, and gene expression among other factors (Fig 1.4).

This acidic environment can be used as a trigger for drug release, providing a measure of selective targeting. Both topotecan (TPT) and irinotecan (CPT-11), analogues of camptothecin (CPT), have demonstrated clinical efficacy. These drugs function through the formation of an inactive hydroxyl group derived from the CPT E ring lactone at a pH 7.4. However, at acidic pH, this reaction is reversible, giving rise to marginal selectivity for solid tumors since while the extracellular pH changes, the intracellular pH largely remains within normal levels<sup>60</sup>. Though this selectivity allows for intravenous administration of TPT, more than 40% of the administered dose is cleared by the kidneys with a half-life of 3hrs<sup>61</sup>. Mitoxantrone and topotecan cellular uptake and subsequent clearance is inhibited by acidic pH, enhancing the half-life and therefore the efficacy of these drugs<sup>60</sup>. However, this efficacy often has only a short-lived impact on the tumor as cells distal to blood vessels quickly resume proliferation<sup>62,63</sup>. While these therapies are

evidence of significant advancement in the development of anti-cancer therapies, they also clearly demonstrate room for improvement and challenges that could be overcome by an active biological system, *i.e.*, oncolytic bacteria.

### ***Suppressed immune environment***

The acidic characteristic of solid tumors has a variety of impacts but ultimately seems to play a key role in immune suppression and consequently cancer progression and metastasis<sup>64,55,65</sup> (Fig 1.3). The acidity of solid tumors not only confers an immediate level of protection from the immune system, but also contributes to – if not orchestrates – exquisitely tailored molecular mechanisms that both mitigate anti-tumor action and accomplish the pro-tumor conversion of the immune cells immediately surrounding the tumor<sup>65</sup>. Tumor-derived lactate itself can have a direct effect on inflammatory pathways occurring in and around the tumor<sup>65</sup>. Myeloid and regulatory T cells have demonstrated a proclivity to engage tumor acidity to support tumor growth and block immune responses with anti-tumor effects<sup>56</sup>. Other tumor effector cells such as NK and T cells have been shown to lose function, and in some circumstances enter an irreversible anergic state due to the acidic environment of a solid tumor<sup>56</sup>.

With more than 25% of cancers displaying some kind of association to aberrant immune reactions<sup>66</sup>, chronic inflammation is a critical aspect to be considered while designing therapeutics and their delivery strategies, especially those that rely on particles - both inorganic (*e.g.*, polymericosomes) or organic (*e.g.*, bacteria or viruses). The role of the immune system in tumor development has long confounded the field because of the tumor's apparent ability to evade immune destruction. Within the last decade, studies have demonstrated, perhaps unsurprisingly, the unique microenvironment created within a solid-state tumor also gives rise to a unique immune system profile. While it is widely accepted that the immune system



malfunctions in a tumor environment, the possible source of these aberrant immune reactions can range from bacterial or parasitic infections to autoimmune conditions due to genetic mutations or dysregulation of governing cell signaling pathways.

In large part, the immune response is hypothesized to contribute to tumor generation through selecting aggressive clones, thereby giving rise to immunosuppression and subsequent cell proliferation and metastasis<sup>66</sup>. During early stages of tumor development, natural killer (NK) cells and CD8+ cells identify and destroy cells with higher immunogenicities - thereby inadvertently selecting for tumorigenic cells adapted with lower immunogenicity to evade the host immune response<sup>66</sup>. The less immunogenic cells can subsequently escape T cell immune control and survive through a process termed cancer immune editing. In addition to cancer immune editing, these cells develop mechanisms to mimic peripheral tolerance<sup>67</sup>. Tumorigenic cells are therefore able to mitigate and, in some circumstances, prevent the cytotoxic response of effector T cells, tumor-associated macrophages (TAMs), natural killer cells (NKs), and tumor-associated neutrophils (TANs)<sup>68</sup>. Several murine studies have clearly demonstrated T cell dysfunction in cancer as characterized by high levels of inhibitory receptors such as CTLA-4, PD-1, and TIM-3 on T cell surfaces, as well as through loss of cytokine IFN $\gamma$ , IL-2, and TNF $\alpha$  production<sup>66</sup>. Furthermore, select populations of immune cells have a directly suppressive action against the tumor immune microenvironment (TIME) such as neutrophils<sup>67</sup> and T<sub>reg</sub> cells<sup>68</sup>. Inflammatory cell distribution throughout the tumor microenvironment and the evolution of the tumor have been thoroughly detailed elsewhere in the literature<sup>66,68,67</sup> and are beyond the scope of this review. While the non-immunogenic characteristic of solid tumors represents a hurdle for current therapeutics, it provides a conducive niche for oncolytic bacteria colonization – potentially even allowing for a stronger mechanism of tumor lysis as the majority of oncolytic

bacterial treatments can successfully recruit the immune system in a way that current therapeutics cannot.

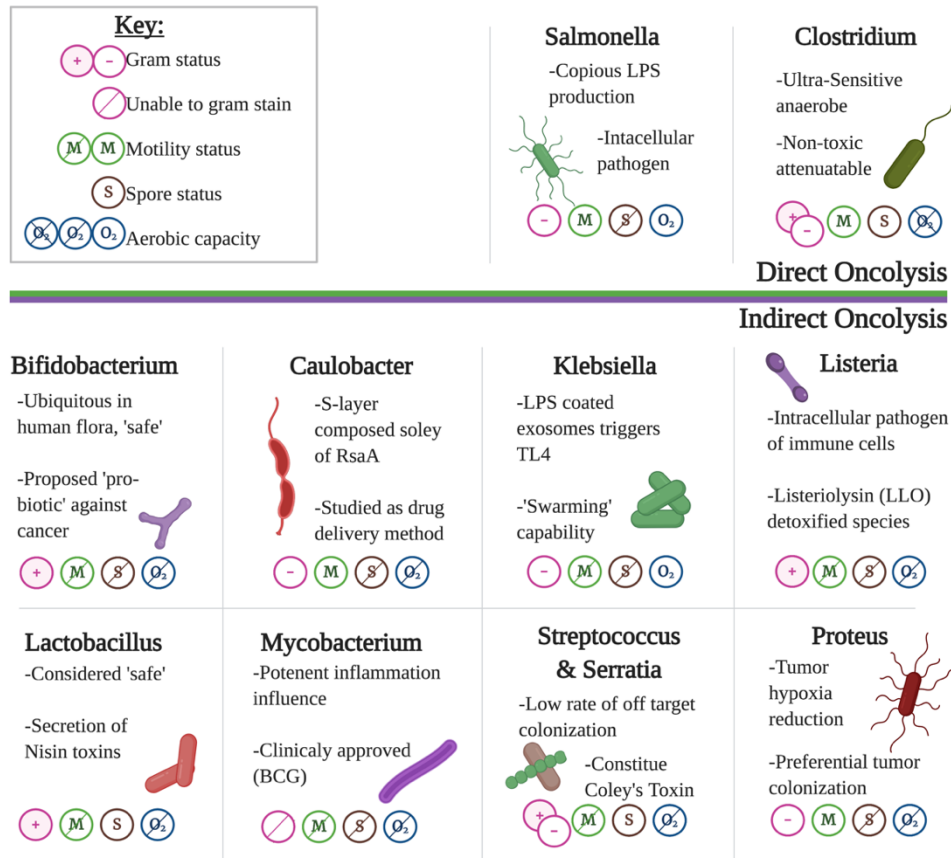


**Figure 1.5.** Attributes to consider for genetic modification of oncolytic bacterial under investigation.

### Survey of Oncolytic Bacteria Currently Under Development

While oncolytic bacteria will face some of the same challenges as oncolytic viruses, there will also be novel challenges due to their more complex physiology. However, it is worth noting the main advantage oncolytic bacteria have over oncolytic viruses: they do not require a living cell to replicate and proliferate. The oncolytic bacteria species under consideration for development as a cancer therapeutics have been thoroughly reviewed elsewhere<sup>5,11,69,70</sup>, but a brief description of several species of interest and where they currently lie in development has been included as a contextual reference (Fig 1.5). A fundamental lack of knowledge about the

biochemical basis for the characteristics that classify a bacterial species as oncolytic can be seen for most species, complicating clinical development severely. While studies have elucidated the biochemical basis for some oncolytic species, this knowledge has been extended, perhaps too widely, to other members of the family, inadvertently complicating clinical translation.

**Indirect Oncolytic Activity: *Mycobacterium*, *Listeria*, *Klebsiella*, *Serratia*, *Streptococcus*, *Proteus*, *Caulobacter*, *Lactobacillus*, *Bifidobacteria***

***Mycobacterium: An Acid Fast, Non-Motile, Non-Sporulating, Obligate Aerobe***

The oldest FDA approved oncolytic bacterial therapy consists of an attenuated strain of *Mycobacterium bovis* Bacille Calmette-Guerin (BCG) - this bacteria has been a clinically approved therapy to treat bladder cancer for more than thirty years<sup>15</sup> and has been the only licensed vaccine known to control tuberculosis<sup>71</sup>. Despite the well-established history of efficacy, the biochemical mechanisms of BCG have yet to be fully understood. However, it is known that while BCG has minimal direct cytolytic effects, it is a potent inducer of local inflammation in the mucosal lining of the bladder<sup>16</sup>. Repeated exposure to BCG escalates the inflammation, likely based upon BCG attachment and penetration into urothelial cells<sup>16</sup>. While eliciting localized inflammation, the presence of BCG cells also provokes a macrophage response. Macrophages, which are considered central regulators of the immune response, trigger the influx of other inflammatory cells and elicit the production of a cytokine storm, further coordinating the activation of neutrophils, natural killer cells, and reactive lymphocytes<sup>15</sup>. While BCG therapy has limitations in terms of direct anti-tumorigenic effects, there are many lessons to be learned from this particular species about harnessing host/microbe interactions. The as yet uncharacterized molecules that make BCG such a potent immune system stimulant could perhaps be inserted into

the genome of other oncolytic bacterial species in order harness the inflammatory immune response, ultimately decreasing tumor refractoriness rates.

***Listeria: A Gram-Positive, Physiologically Non-Motile<sup>72</sup>, Non-Sporulating, Facultative Anaerobe***

The *Listeria* species, in particular *L. monocytogenes*, is known for its ability to invade and colonize not only the tumor, but also the host's own monocytes, macrophages, and polymorphonuclear leukocytes<sup>70</sup>. *L. monocytogenes* has evolved the capacity to escape the typical mechanisms of phagocytosis by disrupting the phagosome lipid membrane with lipases and the virulence factor listeriolysin O (LLO)<sup>70</sup>. In fact, the main method through which *L. monocytogenes* exerts its oncolytic capacity relies on its ability to colonize macrophages and induce the activation of antigen presentation mechanisms, recruiting and activating destructive T cells. When *Listeria* is injected intratumorally, it strongly stimulated the production of proinflammatory signals, including reactive oxygen species<sup>73</sup>. It has also demonstrated a direct capacity for inhibiting the immune suppressive environment common for solid state tumors. Several studies have modified *Listeria sp.* to remove virulence factors ('detoxified', dtLLO) but retain the ability to activate the TLR4 (Toll Like Receptor 4) pathway<sup>74,75</sup>. Surprisingly, these modified bacteria were still able to induce the production of inflammatory-related cytokines and lyse tumor cells<sup>74</sup>. The ability to detoxify *Listeria* but retain the potent immune-recruiting capacity is very intriguing and should be considered an example for the power of genetic modification.

***Klebsiella: A Gram-Negative, Non-Motile, Non-Sporulating, Facultative Anaerobe***

Similar to other members of the *Enterobacteria* family, *Klebsiella* is notable because the lipopolysaccharide (LPS) contained on its outer membrane can trigger TLR4, a key regulator in

the in the inflammatory pathway<sup>76</sup>. Furthermore, this particular bacterium can produce outer membrane vesicles coated in LPS, thereby triggering proinflammatory cytokine expression<sup>70</sup>.

*Klebsiella pneumoniae* has been studied because of its selective targeting of lung cells, making it potentially useful in treating small cell lung carcinoma<sup>77</sup>. The use of genetic engineering gives rise to the ability to harness and utilize the produced outer membrane vesicles apart from the live bacteria itself, potentially overcoming the clinical hesitancy to use a live oncotherapeutic.

***Serratia and Streptococcus: Gram-Negative and Gram-Positive Mixture, Non-Motile, Sporulating, Facultative Anaerobe***

*Serratia marcescens* and *Streptococcus pyogenes*, also known as Coley's toxin – named for William B. Coley, the first to study this bacterial mixture in 1946, constitutes another of the first oncolytic bacteria treatments<sup>70</sup>. *Serratia marcescens*, like *Clostridium novyi*, is a potent potential oncolytic bacterium because, while being naturally ubiquitous, it is rarely the cause of human disease<sup>78</sup>. *Streptococcus pyogenes*, however, has several virulence factors displayed on its outer membrane, giving rise to the ability to attach to host tissues and evade the immune system; therefore *S. pyogenes* is frequently responsible for pharyngitis, skin damage and septic shock<sup>5</sup>. It is worth noting that *S. pyogenes* has also been detected as an asymptomatic pharyngeal bacteria in some circumstances<sup>5</sup>. Coley accomplished one of the earliest genetic modifications of bacteria, removing the pathogenic characteristics while retaining its oncolytic capacity<sup>79</sup>. After heat treating the bacterial mixture, Coley administered a cocktail of what was later found to be mainly composed of endotoxins, not live bacteria<sup>80</sup>. The main active components were prodigiosin produced by *S. marcescens*<sup>81</sup> and SpeA, SpeB, and SpeC produced by *S. pyogenes*<sup>80</sup>. While these particular bacterial species may not be considered fully oncolytic in and of themselves, the Coley combination inadvertently probed the underlying biochemistry of oncolytic bacteria and

provided a potential mechanism for future oncolytic bacterial treatment. Additionally, Coley's success highlighted two key principles for the field. First, the bacteria themselves need not be whole to elicit tumor lysis. Aspects of different bacterial species such as *S. marcesens*' prodigiosin could be implemented in other ways to accomplish tumor mitigation - perhaps even through genetic incorporation into another oncolytic bacterial species. Second, Coley's toxin largely failed to gain general acceptance by the clinical field because of the inability to consistently prepare the bacterial mixture – up to 16 different toxin cocktails have been utilized<sup>80</sup>. This potential for inconsistency is a hurdle that still looms large over the field of oncolytic bacteria today.

***Proteus: A Gram-Negative, Motile, Non-Sporulating, Facultative Anaerobe***

*Proteus mirabilis* was reported to have been isolated from pus resulting from tumor lysis. Subsequent studies in 1965 indicated Ehrlich solid carcinoma, sarcoma 180, C3H spontaneous mammary cancer and AH49 solid sarcoma tumors were completely necrotized after administration of whole bacterial cells, regardless of the delivery route (*i.e.* intratumor, intraperitoneal or intravenous injection)<sup>17,18</sup>. Furthermore, within three to five weeks the tumors showed a complete cure rate with no off target colonization or toxicity reported<sup>17,18</sup>. More recent studies conducted in 2017 indicated a continuation of the oncolytic effect of *Proteus mirabilis* in a murine breast cancer model<sup>82</sup>. These results suggest *Proteus mirabilis* preferentially colonized tumor tissues and suppressed primary breast cancer and pulmonary metastatic growth in the 4T1 murine model<sup>82</sup>. The study went on to probe the mechanistic basis for such an effect, concluding that *P. mirabilis* likely exerts oncolytic capacity by (1) lowering the expression of carbonic anhydrase IX and hypoxia inducible factor-1 $\alpha$  (HIF-1 $\alpha$ ) – proteins that are indicative of hypoxia, and (2) elevating the levels of NKp46 and CD11c – proteins responsible for priming the immune

system<sup>82</sup>. Based on its ability to activate the immune system and reduce tumor hypoxia, *Proteus mirabilis* may prove to be a powerful oncolytic bacterial strain against breast tissue primary tumor growth and subsequent pulmonary metastasis. Despite this promise, more studies should be carried out to validate these substantial results. The selective colonization characteristic of this species certainly should not be ignored when trying to create better oncolytic bacterial species.

***Caulobacter: a Gram-Negative, Motile, Non-Sporulating, Aerobe***

*Caulobacter crescentus* has been studied largely because of the unique protein surface layer characteristic of this particular species. The surface layer, or S-layer, of *C. crescentus* is composed of a single protein, RsaA, that organizes as a self-assembled crystalline array<sup>8</sup>. Several studies have focused on this rare, homogenous surface as a canvas to insert cancer associated peptides in an effort to better prime the immune system to target and destroy tumors<sup>8</sup>. A single study in 2006 noted anti-tumor activity against three transplantable murine tumor models (Lewis lung carcinoma cells transfected with the MUC1 gene in C57BL/6, mammary carcinoma (EMT-6) in BALB/c, and leukemia cells (L1210) in DBA2)<sup>7</sup>. All three models demonstrated prolonged survival, reduced tumor mass or reduced number of lung nodules when treated with *C. crescentus* compared to saline controls<sup>7</sup>. Most importantly, this study directly compared treatment of heat or formalin fixed cells with intact, live cells and concluded that the later were significantly more effective<sup>7</sup>. These results indicate that *C. crescentus* has potential as both an indirect oncolytic bacteria and a potent vehicle for drug delivery and immune modification.

***Lactobacillus: A Gram-Positive, Non-Motile, Sporulating, Aerotolerant Anaerobe***

Though members of this family of bacteria are more well known for their ability to convert sugars to lactic acid in the agricultural industry, *Lactobacillus crispatus* has demonstrated efficacy against mammary carcinoma in the murine BALB/c 4T1 model<sup>83</sup>. Study

authors concluded that both tumor size was decreased and survival rates were increased<sup>83</sup>.

Experiments to probe the underlying mechanism of the effect led the authors to hypothesize that it was due to marked increases in the level of COX-2 expression in tumor tissues<sup>84</sup>. COX-2 is a cyclo-oxygenase that catalyzes the formation of prostaglandin and modulates cellular proliferation and apoptosis<sup>85</sup>. The up-regulation of COX-2 would presumably re-regulate the aberrant control pathways that allow tumor cell unchecked proliferation. Earlier studies conducted in the 1970s discovered that *Lactobacillus lactis* produces toxins that elicited a cytotoxic effect on the MCF-7 human breast adenocarcinoma cell line, HepG2 liver hepatocellular carcinoma cell line, and HNSCC (head and neck squamous cell carcinoma) cell lines, both *in vitro* and *in vivo*<sup>83</sup>. Despite this oncolytic capacity, these toxins – collectively termed Nisin, are approved for human consumption and demonstrate no known toxicity, somewhat contradicting the potential of the Coley toxin to inspire future oncolytic bacteria derived formulations<sup>86</sup>. The public acceptance and ‘safeness’ of consuming *Lactobacillus* could open the door for further clinical translation of bacterial therapeutics.

***Bifidobacterium: gram-positive, non-motile, non-sporulating, anaerobe***

*Bifidobacterium* is commonly known due to its nearly ubiquitous presence in human flora and recent rise as a commercial probiotic<sup>86</sup>. This family of bacteria has been harnessed for the creation of dairy products for decades, earning the designation of “safe” from both the clinical field and consumers at large. Several studies have been conducted on the efficacy of this family of bacteria against several disease states, but particularly against gastrointestinal issues such as colonic adenomas and irritable bowel syndrome. Current oncolytic bacteria studies have focused efforts on three species: *Bifidobacterium longum*, *Bifidobacterium infantis*, and *Bifidobacterium adolescentis*. A landmark study conducted in 1980 established that Ehrlich ascites tumors



implanted in mice could be colonized selectively by *Bifidobacteria* through intravenous injection<sup>87</sup>. While this study demonstrated impressively selective tumor colonization with negligible off target localization, there were no significant antitumor effects – limiting this family’s effectiveness as an oncolytic bacterium<sup>87</sup>. Surprisingly, other studies focused specifically on *B. adolescentis* noted the prevention of colorectal carcinoma development, and modern studies have shifted to focus on using *Bifidobacterium* as a drug delivery vehicle rather than as an oncolytic itself<sup>86,84</sup>. However, several of the genetic modification techniques detailed in this article could be utilized to enhance its oncolytic capacity as the characteristic selective colonization of tumors is quite an advance over current therapeutics.

#### **Direct Oncolytic Action: *Salmonella*, *Clostridia***

##### ***Salmonella: A Gram Negative, Motile, Non-Sporulating, Facultative Anaerobe***

Both *Salmonella typhimurium* and *Salmonella choleraesuis* have shown great potential as oncolytic bacteria and have been widely studied since its tumor-targeting attributes were first discovered in the early 1950s<sup>70</sup>. As a gram-negative, facultative anaerobe, the off-target colonization potential of this species is relatively low. *Salmonella sp.*, like *Listeria sp.*, are intracellular pathogens. However, unlike *Listeria*, intracellular infiltration of *Salmonella* provides a direct oncolytic effect as it subsequently kills tumor cells with its ability to proliferate inside the cell, causing cell lysis and releasing progeny bacterial cells to infect neighboring cells<sup>88</sup>. Unfortunately, despite their efficient lytic ability, most *Salmonella* species provoke strong adverse immune activation due to the copious amounts of lipopolysaccharide and other virulence factors they produce<sup>70</sup>. Several attenuated and genetically modified strains have been developed in order to mitigate the toxicity of *Salmonella* injections and have been largely successful<sup>19,89,90,91</sup>. Many strains have also been successfully engineered as auxotrophs, further

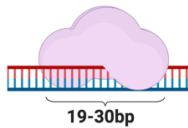
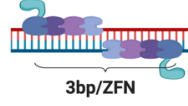
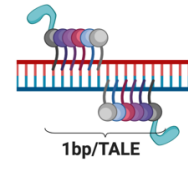
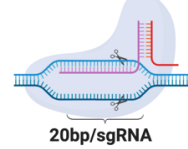
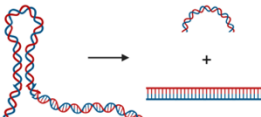
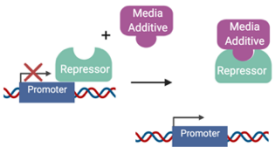
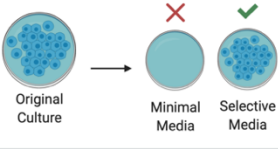
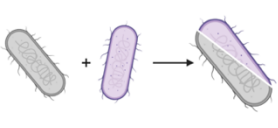
mitigating off-target colonization by removing the bacteria's ability to produce necessary nutrients and thereby rendering the bacteria reliant on its environment to supplement its deficiency<sup>92,93</sup>. Further studies have also described expression of exogenous therapeutic proteins to promote tumor regression<sup>94</sup>. While the genetic modifications of *Salmonella* provide powerful examples of harnessing oncolytic bacteria, both clinical trials initiated with attenuated *Salmonella sp.* have failed to demonstrate significant tumor regression with very few patients even showing significant tumor colonization<sup>70,94,95</sup>. These failures highlight the intricate balance between mitigating toxicity while still capitalizing on the bacteria's innate cell lytic capacity.

### ***Clostridium: A Gram-Variable, Motile, Sporulating, Obligate Anaerobe***

The *Clostridium* family includes a diverse spread of eighty species and counting<sup>70</sup>. Among these species, at least five have been specifically studied within the context of a cancer tumor (*C. histolyticum*, *C. tetani*, *C. sporogenes*, *C. acetobutylicum*, and *C. novyi*)<sup>5</sup>. While typically gram-positive bacteria, several species have been noted to be gram-variable when cultured in the lab – alternating from gram-positive in early passages to gram-negative for more mature cultures with no current explanation for the alteration<sup>5</sup>. Furthermore, these bacteria are motile through the use of a flagellated outer membrane and can quite elegantly chemotax to hypoxic areas for subsequent proliferation<sup>96</sup>. While members of this genus can substantially differ genetically and physiologically, the one characteristic these species share is the necessity for an anerobic environment to proliferate - though even the sensitivity to this requirement varies from the ultra-sensitive, strictly anaerobic *Clostridium novyi*<sup>97</sup> to the facultative anaerobe *Clostridium tetani*<sup>96</sup>. Perhaps the characteristic that confers the greatest commercial oncolytic potential upon this family is the ability to form spores tolerant of aerobic environments<sup>98</sup>. Not only are these spores able to mitigate aerobic environments, the micro anaerobic *C. novyi* species

will not germinate to the active, lytic bacterial form in virtually any level of oxygen (*e.g.* blood stream)<sup>97,99</sup>. Furthermore, these spores are relatively easy to produce and store long-term for commercial application while mitigating off-target effects through the dependence on an anaerobic environment for colonization and subsequent cell lysis<sup>9</sup>. Finally, *Clostridium novyi* spores have indicated levels of metabolic activity above that considered normal for other species that generate dormant spores<sup>99</sup>. Counter to the prevailing hypothesis of dormant, inactive spores, studies of *C. novyi* have noted that spores of this species possess the capacity for sensing and migrating out of the blood stream towards a hypoxic environment at the center of a tumor<sup>99,100</sup>.

Several animal model studies have demonstrated the excellent capacity for *Clostridium sp.*, and in particular *Clostridium novyi*, as a potent cancer therapeutic<sup>9,97,99</sup>. An early attenuation of *C. novyi*, produced by the knockout of a phage-DNA encoded toxin, mitigated much of the septic toxicity that previously complicated the development of this oncolytic bacteria<sup>97</sup>. However, unlike the *Salmonella* modifications, knockout of *C.novyi* toxin did not compromise the innate chemotaxic or lytic abilities of the species<sup>97,99</sup>. Clinical trials for this particular species are currently underway with largely positive preliminary patient results<sup>101</sup>. It is worth noting that several early studies encountered further complications with *C. novyi*'s ultra-sensitivity to oxygen, prohibiting the clearance of the tumor margins fully<sup>99</sup>. Subsequent studies have focused on combination therapies, such as a co-administration of *C. novyi* with a common chemotherapeutic to address both the hypoxic tumor core and the more oxygenated tumor margins<sup>102</sup>.

Genetic Modification Method	Important Characteristics for Implementation
Meganuclease	 <ul style="list-style-type: none"> <li>-Endo-deoxynucleases (ISce-I, ICre-I)</li> <li>-Leaves unique 4bp 3' overhang</li> <li>-Difficult to achieve active state</li> </ul>
ZFN	 <ul style="list-style-type: none"> <li>-Uncoupled binding vs cleavage domains</li> <li>-Modularity, customize ZFNs to targets</li> <li>-Dimerization <i>and</i> specificity to cleave</li> </ul>
TALEN	 <ul style="list-style-type: none"> <li>-No reliance on cell DNA repair pathways</li> <li>-Effector domains commercially available</li> <li>-Difficult to achieve the modular repeats</li> </ul>
CRISPR	 <ul style="list-style-type: none"> <li>-Extremely customizable, easily</li> <li>-PAMs are necessary to cleave</li> <li>-Naturally occurs in bacteria</li> </ul>
Group II Intron	 <ul style="list-style-type: none"> <li>-Self-catalyzed ribozymes</li> <li>-High efficiency retro-homing</li> <li>-No reliance on host factors</li> </ul>
Attenuation	 <ul style="list-style-type: none"> <li>-Reduction of virulence</li> <li>-Level of targeting control</li> <li>-May impact oncolytic activity</li> </ul>
Auxotropy	 <ul style="list-style-type: none"> <li>-Increased control of colonization</li> <li>-'Kill' switch for clinical therapy</li> <li>-May impact oncolytic ability</li> </ul>
Chimeras	 <ul style="list-style-type: none"> <li>-Combination of two species</li> <li>-Insert desirable functions from other oncolytic bacteria</li> </ul>

**Figure 1.6.** Brief explanation of important gene modification methods' characteristics for implementation.

### Techniques to Engineer Oncolytic Bacteria

Within the toolbox for developing cancer fighting bacteria, there are two categories of gene-specific manipulations: targeted and untargeted (random); although it is important to note

that genetic modification of oncolytic bacteria is a rather unexplored area. Untargeted, or random, mutations such as those generated by ultra violet light or manganese chloride have long been used in plant<sup>103,104</sup> as well as yeast<sup>105,106</sup> experimentation to determine gene functionality. However, the advent of targeted manipulations, especially the ease and simplicity of the latest technological advances (*e.g.* CRISPR/Cas) have changed the field. Targeted manipulations are used to make localized sequence changes, allowing several distinct alterations with different functional consequences to be made within a specific sequence. While a relatively simple concept, the creation and implementation of these types of techniques is much more nuanced. The majority of engineering techniques start with an ability to elicit cleavage at a particular DNA site, thus triggering DNA repair pathways (Fig .16). The two major DNA repair pathways are homologous recombination and non-homologous end joining, with bacteria strongly favoring homologous recombination<sup>107,108</sup> – making them very well suited for knocking-in desirable genes to better confer oncolytic activity<sup>109</sup>. The nucleases ScaI and HO are largely considered the prototypes for stimulating double stranded DNA breaks, thereby initiating repair processes that could be manipulated<sup>109</sup>. These enzymes have characteristically long recognition sites, conveying a modest amount of specificity<sup>109</sup>. However, it is crucial to note that most bacteria have an adverse reaction to double stranded DNA breaks (*i.e.* notably higher rates of death<sup>110</sup>) that must be considered when designing these studies<sup>110</sup>. Ultimately, using these techniques has proved difficult to accomplish the modification of the DNA recognition sites without negatively impacting the protein structure and thus endonuclease function<sup>111</sup>.

### **Meganucleases/Homing Endonucleases**

Meganucleases were identified in the early 1990s for their potential to accomplish early attempts at genetic engineering<sup>111</sup>. As endodeoxy-ribonucleases, these enzymes occur naturally

and are present in all biological super-kingdom organisms<sup>112</sup>. Two classes of these enzymes exist: intron endonucleases (intervening sequences removed at the RNA level) and intein endonucleases (intervening sequences removed at the protein level)<sup>112</sup> – both encoded by the relative mobile elements of intron and inteins<sup>109</sup>. There are at least four families of homing endonucleases: LAGLIDADG, GIY-YIG, HNH, and His-Cys Box - all classified by the characteristic highly conserved amino acid sequences as identified in their respective names<sup>112</sup>. The most characterized class is the LAGLIDADG homing endonucleases (LHEs) which includes the well-known and utilized ICre-I and ISce-I enzymes<sup>111</sup>. As the core of the structural interface between the endonuclease domains, the LAGLIDADG motif contributes acidic residues to the active site<sup>112</sup>. The active site of the LHE nuclease has long DNA recognition sites of 19-30 base pairs, and uniquely leaves a four base pair 3' overhang<sup>112</sup>. This recognition site confers a level of target specificity since the possibility of finding another identical 18bp sequence is statistically unlikely and would take a genome about twenty times larger than the human genome<sup>111</sup>. Enzymes with a single LAGLIDADG motif typically recognize palindromic target DNA due to their homodimeric nature, but it is notable that these enzymes will also recognize pseudopalindromic sequences as well, leading to a level of off-target, non-specificity intrinsic to meganucleases<sup>111</sup>.

The creation of engineered meganucleases brought about the ability to recognize custom, specific target sites and has been detailed in several studies<sup>109</sup>. By recombining different complete LHE domains, a fully active chimeric enzyme can be created. However, extensive restructuring of the tertiary and quaternary structure of these complexes to recreate a competent active site can be quite a challenge to overcome<sup>111</sup>. When this modularity was paired with the relatively straightforward natural method of DNA recognition in the 1990s and 2000s, it created

a powerful gene engineering tool<sup>111</sup>. However, these customized enzymes were discovered to have several drawbacks. Perhaps the drawback most responsible for the fading popularity of meganuclease engineering is the difficulty of repacking the chimeric enzyme domains to elicit function. This pitfall is likely due to a largely unknown method of discrimination between cognate and non-cognate target sites, and future studies may illuminate this method and lead to a re-emergence of the meganuclease technique.

### **Zinc Finger Nucleases (ZFNs)**

Zinc finger nucleases (ZFNs) represent another early genetic manipulation tool that allowed specific DNA sequences to be targeted for double stranded breaks, thus initiating repair pathways that could be further manipulated<sup>113</sup>. This technique offered an advantage over the earlier *SceI* and HO endonucleases methods because while modification of those recognition sites negatively affected the cleavage sites, ZFNs have a DNA-binding domain fully separated from the DNA-cleavage domain, preserving the cleavage domain regardless of any alterations to the targeting domain<sup>111</sup>. ZFNs were originally discovered through studies examining the type IIS restriction enzyme *FokI* from *Flavobacterium okeanokoites*, which was of interest because of this enzyme's physical separation between its binding and cleavage activities, making it an excellent candidate for fusion to other recognition domains<sup>111</sup>. Early experiments demonstrated due to this domain separation, the nuclease activity could be redirected with relative ease through substitution of the DNA recognition domain<sup>113</sup>.

Original studies indicated the cleavage domain had no intrinsic sequence specificity, but rather was governed by physical proximity to the target site due to a linked DNA-binding domain, differentiating this technique from meganuclease<sup>113</sup>. Later studies of the crystal structure elucidated that *FokI* must achieve dimerization in order for DNA cleavage to occur<sup>114</sup>. This

dimerization interface is notably weak, and therefore not adept at recognizing sites that are not contiguous, making it necessary to design recognition sites that are on neighboring strand locations and joined to a single, monomeric cleavage domain<sup>114</sup>. Cleavage subsequently occurs when the ZFN concentration bound to a specific DNA locale reaches a concentration conducive to dimerization, initiating cleavage of the phosphodiester backbone<sup>113</sup>. This necessity to dimerize before cleavage occurs confers a significant experimental advantage because the monomer itself is not active and therefore will not elicit the DNA breakage<sup>114</sup>. The physical separation of the binding and cleavage domains in conjunction with the need to dimerize prior to cleavage, allows ZFN-based gene modifications to achieve a range of specificity that provides functional utility<sup>113</sup>.

Discovery of the ZFN crystal structure indicated that each finger unit contains about thirty amino acids bound to a zinc atom, knowledge that made this technique even more attractive<sup>113</sup>. A single ZFN two-finger domain recognizes six DNA base pair units, and each ZFN unit can be designed to consist of two, three-finger motifs, translating into about an eighteen base pair recognition site that is considered specific enough to accomplish selective gene targeting even in an entire genome<sup>113</sup>. The crystal structure also demonstrated that each zinc finger molecule contacts three base pairs modularly, suggesting that novel assemblies could be created and give rise to DNA site recognition specificity<sup>113</sup>. In order to constitute a specific DNA-binding domain, a customizable combination of two-finger molecules can be linked together to create a larger, successive ZFN molecule that recognizes longer, more unique sequences of DNA, thereby limiting off target effects<sup>113</sup>. Two-finger molecules are fused to the DNA-cleavage domain and act as the guide to target the site at which genomic cleavage occurs. Cleavage domains usually have a high percent identity to the *FokI* protein<sup>111</sup>. ZF domains have been



developed correlating to almost every one of the possible codons, enabling a “plug and chug” system for linking modules in tandem to create specific DNA target sequences, and subsequently systems using this approach have been commercialized and are available on demand from retailers<sup>111</sup>. Notably, several studies have indicated that not all ZF DNA identification motifs contribute equally to identify the target DNA, thereby increasing significantly the propensity of this method to elicit off target effects<sup>111</sup>. Furthermore, it has been demonstrated by the literature that, as with most molecular processes, context is crucial to success, and subtle changes to that context can subsequently mitigate the modular approach of ZFNs<sup>111</sup>.

### **Transcription Activator Like Effector Nucleases (TALENs)**

As programmable chimeric nucleases, transcription activator like effector nucleases, or TALENS, make up a subsequent evolution in gene modification techniques. This particular class differentiates from those previously discussed as they were produced via recombination.

TALENs are intensely unique because the mechanism of action does not rely on cellular DNA repair pathways such as HDR or NHEJ<sup>111</sup>. As a family of virulence factors produced by plant pathogens, transcription activator like effectors (TALEs) serve to bind specific host promoter sequences, leading to both positive and negative gene regulation<sup>115</sup>. TALEs are composed of a nuclear localization sequence (NLS), a central variable number (though typically 34) of amino acid repeats, and the transcriptional activation domain made up of acidic residues<sup>114</sup>. Within the central domain, the specificity of each TALE is determined largely, but not exclusively, by the hypervariable repeat amino acids at positions 12 and 13; which have been termed the repeat-variable di-residue, or RVD<sup>115</sup>. The number and order of amino acid repeats within this domain have also been shown to influence specificity<sup>114</sup>. This characteristic gives TALEs the ability to link repeats together contiguously, allowing for the custom targeting of a particular DNA

sequence<sup>111</sup>. The basis of the TALEN technique lies in the fusion of TALEs to the cleavage domain of a nuclease such as Fok-I<sup>111</sup>. Once recombinantly linked to the TALE module, the nuclease domain can serve as a guide for creating double-stranded DNA (dsDNA) breaks<sup>115</sup>. Alternatively, TALEs can often be found fused to meganucleases as well, conferring added specificity due to their longer DNA recognition sites as discussed previously<sup>111</sup>.

TALENs represent a slight advantage over ZFNs because the linkage between the individual DNA recognition modules did not have to be re-engineered in order to create effective, longer modules<sup>115</sup>. Currently, there are several effector domains commercially available for fusion to customizable TALE repeats<sup>115</sup>. Recent advancements have expanded fusion domains to include transcription activation and recombinases with site-specificity in addition to the original nuclease abilities<sup>111,115</sup>. While TALEN technology represents progress compared to zinc fingers - and remains a viable modern technique - several notable challenges cannot be ignored when implementing this technique. The ability for the DNA-binding domains of TALE modules to recognize single base pairs allowed for extended flexibility in sequence target design, but this also made cloning to create the modular repeats necessary for specificity within the host genome difficult. TALENs take a significant amount of resources to create the individualized enzymes needed for modern genetic engineering. While this does not preclude the use of this technique, it is a significant disadvantage.

### **CRISPR/Cas**

Perhaps the most popular technique currently available for gene modification is the CRISPR/Cas system. While the advent of this system has had an exponential impact on eukaryotic cell research - particularly on human disease model creation and manipulation, there are several reasons bacterial gene modification has been hesitant to adopt this method. Bacteria

contain a naturally occurring, constitutively active CRISPR-Cas system – it is this system that forms the foundation for the modified technique in use today<sup>116</sup>. CRISPR, or clustered regularly interspaced short palindromic repeats, describes a family of short DNA fragments commonly found in the genomes of archaea and bacterial species<sup>116</sup>. These fragments were discovered to provide what is considered the equivalent of an adaptive immune system in prokaryotes because CRISPR DNA sequences are thought to have evolved from attempts by bacteriophages to insert DNA as part of an infection event<sup>117</sup>. Briefly, a family of enzymes termed CRISPR-associated, or Cas, proteins evolved with the ability to seek out and excise DNA sequences from subsequent exposures to pathogens through the use of complementary short guide RNA sequences (sgRNA)<sup>117</sup>. While these ~20 nucleotide sgRNAs confer a level of specificity to the CRISPR method, the necessity of protospacer adjacent motifs, or PAMs, add another crucial level of additional specificity to significantly reduce off target effects. Together, CRISPR sequences, engineered target sgRNA, and Cas enzyme constitute a system for genetic engineering with unprecedented specificity while still remaining easily customizable and subsequently lending itself to usefulness in a vast array of research projects<sup>117</sup>.

Since the discovery of CRISPR/Cas systems in 2012<sup>116</sup>, several different variants have been subsequently discovered - all with their own potential applications for modifying oncolytic bacteria. A wide range of CRISPR system variations exist: double stranded DNA editing (Cas9)<sup>117</sup>, single-stranded DNA ‘nicks’ (Cas9nickase)<sup>118</sup>, and RNA targeting (Cas13)<sup>119</sup>. The Cas12a variant has the ability to create staggered dsDNA breaks and to process its own guide RNAs allowing for increased multiplexing with a longer, and therefore, more unique guide length<sup>120</sup>. Cas enzymes have also been modified to selectively target genes and subsequently recruit the required activation or repression mechanisms, creating a ‘tuneable’ expression system

where specific levels of known-down or up-regulation are achievable<sup>121</sup>. Ultra-specific base editors were created through the fusion of a Cas9nickase to a deaminase, allowing for point mutations in the genome without any cleavage of the backbone. Through this enzymatic engineering both cytosine<sup>122</sup> and adenosine<sup>123</sup> deaminating Cas enzymes have been developed. Eukaryotic experiments have recently demonstrated success using these targeted point mutations to reactivate entire genes that have been dormant since fetal development<sup>124</sup>. Further Cas enzymes have been fused to methylation enzymes to probe the epigenetic regulation of gene expression as well<sup>125</sup>. Pooled target RNA sequences with target loci occurring within the same regions (often termed ‘tiling’) can be utilized to confer added selectivity and decrease off target DNA modification<sup>126</sup>. The specificities of this multitude of resources and technological advances have been thoroughly reviewed elsewhere in the literature<sup>117,127,128,129</sup>, but in the context of this review it is important to note that not every CRISPR variant can be used in bacteria.

Though CRISPR/Cas genetic engineering is just beginning to be fully characterized in bacteria - nonetheless oncolytic bacteria - its ability to target specific DNA sequences in order to affect gene expression makes it a powerful tool, particularly for harnessing oncolytic bacteria. A handful of examples of successful utilization of CRISPR in bacterial species do exist in the literature<sup>130-132</sup>. While the possibility remains for complications due to the naturally occurring CRISPR recognition systems present in oncolytic bacteria, most of these complications can theoretically be avoided by choosing Cas9 proteins from species with alternate promoter spacer-adjacent motifs (PAMs) than that of the host species. One can imagine a customized bacterial species - retaining its innate tumor targeting and lysing abilities but modified through CRISPR/Cas9 to abdicate virulence factors causing systemic toxicity or to gain functions found in other species furthering their oncolytic capacity.

## Group II Intron Based Methods

As a whole, group II introns are a family of self-catalyzed ribozymes and mobile genetic elements conserved from bacteria to higher order organisms<sup>133,134</sup>. Group II introns are unique from group I introns because the excision of the intron does not require the input of energy, but instead forms a lariat with high structural similarity to other lariats formed during pre-mRNA splicing<sup>133</sup>. This excised DNA then inserts itself directly into one strand of a double-stranded DNA target site through a reverse splicing reaction. Concurrently, the intron-encoded protein (IEP) for reverse transcriptase (RT) cleaves the correlating opposite strand of DNA and uses the 3' end for insertion of the intron RNA through targeted DNA-primed reverse transcription (TPRT)<sup>134</sup>. This genetic mobility process has been collectively termed “retrohoming”, which has extremely high efficiency – often approaching 100%, making it a particularly attractive genetic manipulation method<sup>134</sup>. Furthermore, this method does not rely entirely on host factors like several other available techniques – TPRT requires only the IEP, excised intron, and cDNA copy of the intron to accomplish genomic integration through either DNA repair or recombination<sup>134</sup>. The culmination of these characteristics is an effective, targetable system for gene insertion into almost any desired DNA loci. To harness this naturally occurring process for desired research outcomes, it is crucial to understand how group II introns recognize target DNA sites. A group II intron based system was patented and commercialized as ‘Targetron’ by Sigma-Aldrich<sup>135</sup>.

As a genus, *Clostridium* has shown great promise as not only an oncolytic bacteria species, but also as a single cell bioreactor to create biofuels and pharmaceutical compounds<sup>136</sup>. While the full genome sequences are established for most of the major species in the family, the ability to fully utilize and manipulate this data has lagged behind. Clostridial species have quite the potential as tumor-targeting organisms, causing an increased focus on developing new

techniques for genetic manipulation specifically in this genus<sup>137</sup>. As a specialized group II intron based technique for *Clostridia*, ClosTron was first reported in 2007 as an adaptation to the group II intron recombination and Targetron methods previously used in gram negative bacteria<sup>136–138</sup>. These methods had to be adapted for several reasons - including a natural propensity for *Clostridia* to be resistant to the common selectable markers kanamycin and trimethoprim<sup>137</sup>. Additionally, a species mismatched non-functional promoter made the original published methods for retrotransposition-activated markers (RAM) irreproducible<sup>138</sup>. Despite the benefit of the large amount of information gathered by the implementation of this technique, there are several drawbacks to remain cognizant of when choosing. Perhaps the most limiting aspect of this the ClosTron technique is that sites can be difficult to locate when coding genes are less than four hundred base pairs, limiting the possibilities for gene insertion<sup>138</sup>.

### **Attenuation/Auxotrophy**

Attenuation artificially weakens bacterial species and is commonly used for both bacteria and viruses to produce vaccines. This method of decreasing virulence is proving to be an absolutely crucial step in the development of a viable oncolytic bacteria therapeutic in order to prevent colonization and often subsequent sepsis of the patient. Several species of oncolytic bacteria have been attenuated<sup>5,70</sup>, successfully reducing virulence and systemic toxicity while retaining the innate characteristics that make these species desirable candidates for cancer therapeutics. *Clostridium novyi* was successfully attenuated through a heat shock protocol that accomplish the knockout of a phage DNA encoding alpha toxin, creating a non-toxic species – *Clostridium novyi* NT<sup>97</sup>. *Listeria monocytogenes* was de-toxified through the removal of the listeriolysin O (LLO) protein, which is primarily responsible for this species' ability to lyse lymphocytes, giving rise to the dtLLO *L. monogenes* species, which no longer causes the lysis of

lymphocytes but it still demonstrates a strong ability to activate IL-1, IL-6, TNF $\alpha$ , and IL-2 among other proinflammatory cytokines - ultimately resulting in the characteristic *L. monogenes* immune system instigated tumor destruction<sup>70,74</sup>.



**Figure 1.7.** Comparison of bacterial gene modification techniques.

### Bacterial Transformation

Not only are there a plethora of possible genetic engineering techniques available for bacteria, but perhaps one of the strongest arguments for implementing genetically engineered bacteria is the ease through which any of the aforementioned techniques can be introduced to bacterial cells. Many species of bacteria have evolved innate abilities to acquire advantageous plasmid DNA such as through conjugation and transduction<sup>139</sup>. These characteristics have been

expanded upon and harnessed to accomplish targeted DNA uptake for decades but have returned to the forefront of importance within the context of genetic engineering. Several reviews thoroughly detail the many ways to transform bacteria including heat shock, electroporation, lentiviral or bacteriophage infection, ultrasound, and gene guns<sup>139-141</sup>. The method of transformation must be taken into account when designing a genetic engineering plan for modifying oncolytic bacteria to harness their innate therapeutic potential.

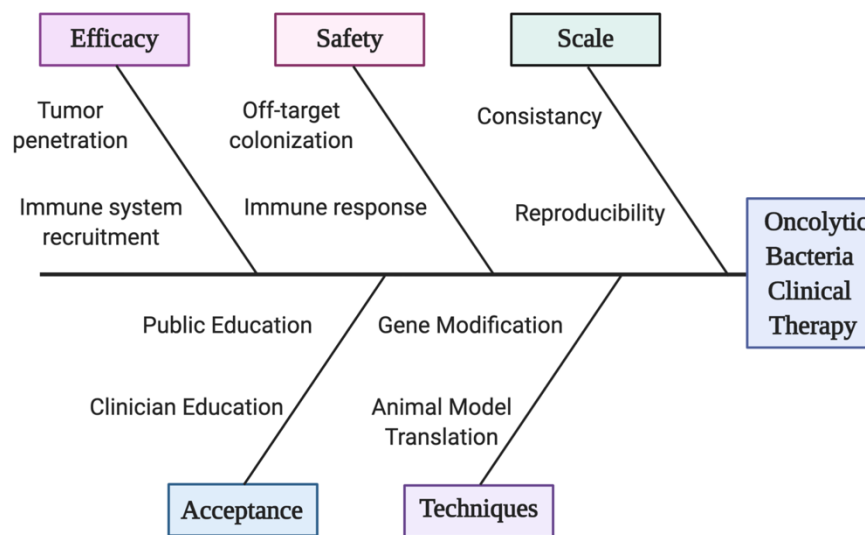


**Figure 1.8.** Isikawa (fishbone) Diagram of the compounding factors inhibiting clinical translation for oncolytic bacteria.

A further argument for bacterial genetic modifications is the comparative ease with which a post-modification selection strategy can be created and implemented. Unlike multicellular organisms, the utilization of a selectable marker can be easily included with little to no side effects. Often times the most difficult aspect of genetic engineering is confirming that the genetic modification event occurred with the desired effect while avoiding any off-target effects. Furthermore, the majority of bacterial species being developed and tested as oncolytic bacteria have full genome sequences published and readily available, lending incredible ease to designing conformational assays such as PCR and sequencing. This also means that several commercial



plasmids have been designed with viable promoters and accessible cloning sites to facilitate genetic engineering for a very reasonable cost (Fig 1.7).

## **Challenges of Oncolytic Bacteria Development**

### **Systemic Toxicity and Off-Target Colonization**

Perhaps the largest hurdle to overcome for effective clinical translation is the perceived potential for off target colonization of non-tumor tissues and subsequent adverse immune stimulation leading to sepsis (Fig 1.8). Indeed, the presence of pathogen associated molecular patterns (PAMPs) on the cell surface of bacteria and correlating host pattern recognition receptors presents quite the challenge to overcome. Oncolytic bacteria themselves may offer the solution. Oncolytic bacteria have the capacity to overcome tumor-induced immune suppression by using PAMPs and damage-associated molecular patterns to instigate immune activity that had been previously down regulated. However, the question of balance remains: when is provoking the immune system beneficial and not harmful?

### **Pro-Oncogenic Bacteria**

Several species of bacteria have demonstrated a capacity for promoting tumorigenesis, both directly through the secretion of toxins that disrupt cell signaling and subsequently cause the mis-regulation and dysregulation of cell growth mechanisms as well as indirectly through the initiation inflammatory pathways<sup>11</sup>. *Helicobacter pylori* is perhaps the most well-known pro-oncogenic bacteria due to its strong association with gastric cancers; however, several other species have also been associated with tumorigenesis<sup>11</sup>. Studies have also demonstrated that peptides secreted from bacteria species (*i.e.* quorum sensing peptide PhrG secreted by *Bacillus subtilis*) promote the invasion of tumor cells and further dysregulate angiogenesis, influencing the metastatic capability of tumors<sup>11</sup>. Furthermore, several bacterial enzymes, such as the

secretion of peptidyl arginine deaminase (PAD) by several oral bacteria, which has established a strong correlation with pancreatic cancer, are currently being studied to establish the extent of their carcinogenic capability<sup>11</sup>. In light of these well publicized pro-oncogenic bacteria, it is no surprise that the public, and arguably the scientific community as well, has strong reservations about developing and implementing the use of bacteria as an oncotherapy. However, research in the last decade has established that current cancer therapeutics in clinical use demonstrate as much if not more capability for enhancing the aggressive and metastatic capacity of tumors<sup>142,143</sup>. Again, anecdotes of quite successful bacterial mediated tumor therapy have existed for centuries, but the delicate balance of adverse side effects from such treatment cannot be ignored and must be properly balanced with the demonstrated anti-cancer characteristics in order to successfully accomplish clinical translation.

### **Model Systems**

Despite the promise and advancements in the commercialization potential of oncolytic bacteria, their clinical potential has yet to be realized. A common theme throughout the previous survey of bacteria in current development is that these bacteria show great efficacy in murine models. However, improper use of murine model systems or out of context analysis of the data generated within these systems may significantly complicate the clinical translation of oncolytic bacterial therapy. Mouse preclinical models are an essential, well-established method for ascertaining the viability of oncotherapies. However, each murine model has its own characteristic immune system bias - making choosing the appropriate murine strain absolutely critical, especially when probing the capacity of intravenous oncolytic bacteria and the subsequent initial immune response. Many of the challenges that apply to the clinical translation of nanoparticles<sup>144</sup> also apply to oncolytic bacteria. Until more data is generated about oncolytic

bacteria immune clearance specifically, nanoparticle studies are the literature basis to formulate experimental models.

Immune deficient murine models are a very powerful tool when studying various types of tumor development and other disease states. A NOD Skid Gamma (NSG) mouse model is commonly used due to its ease in tumor formation. NSG mice are commonly chosen due to the well-characterized Patient Derived Xenograph (PDX) models in which direct xenograft from human tissue allows for powerful mimicry of the tumor diversity found in clinical tumors including tumor microenvironment, gene expression and mutations, inflammation and subsequent histopathology<sup>145</sup>. While this is an extremely powerful tool, it must be used within the appropriate context. NSG models are susceptible to xenograph tumor implantations because they have a physiologically compromised immune system, and this deficiency will have an effect on oncolytic bacterial clearance – regardless of the administration route. The lack of immune system to mount a response to infection will especially bias studies that require repeated administration of the oncotherapy as NSG mice have virtually no adaptive immunity<sup>146,147</sup>. Nude mice, like NSG mice, are T cell deficient, but nude mice have been reported to develop mature T cells as they age – typically around six months or older<sup>148</sup>. Lack of T cells decreases the concentration of opsonizing IgG and IgA in circulation, significantly biasing results for oncolytic bacteria clearance in both these murine models. A study of nanoparticle clearance using various animal models found that this model system bias can at least be partially mitigated when the nanoparticles were pre-incubated in plasma from the intended model species<sup>149</sup>. Data generated from these model systems is not without merit and should not be ignored; however, the context within which oncolytic bacterial are tested is critical for accomplishing clinical translation.

Several immune-competent mouse models also exist, and while these models are certainly a more relevant model when determining immune clearance of oncolytic bacteria, it is important to note not all immune-competent mice have the same immune components. BALB/c and DBA/2 mice have been noted to clear nanoparticles at a higher rate than the Th1-biased C57BL/6 or B10D2<sup>150</sup>. Healthy humans with a robust immune system produce a balanced Th1 and Th2 response<sup>151</sup>, and therefore both Th1 and Th2 biased murine strains should be considered to generate complete clearance data for oncolytic bacteria administration, especially when intravenous delivery is intended. However, Th2 biased strains are considered the most stringent to determine *in vivo* clearance due to the presence of mature T and B cells and therefore IgG and IgA as well as effective macrophages<sup>144</sup>.

### **Conclusion**

The number of cancer diagnoses in the United States for the next decade is expected to increase by more than 60% (2.3 million new diagnoses) from that reported in the 2010 census – despite the advances of current oncotherapeutics in the past decade<sup>152</sup>. In fact, a significant percentage of patients who survive will experience relapses or serious, delayed complications due to treatment<sup>153</sup>. In spite of the advent of new therapeutics, the survival rate of certain solid state cancers (*e.g.*, pancreatic and glioblastoma) have remained relatively unaffected, demanding a new approach and an exploration of other potential oncotherapeutic options. Anecdotes of the efficacy of oncolytic bacteria-mediated tumor lysis date back centuries, and these current cancer projections demand a thorough re-examination of such alternative treatments, especially given that oncolytic bacteria represent a wide-array of novel therapeutic options with very different mechanisms of action (penetrating to the tumor core and lysing to the margins) than that of current therapies (attempting to passively diffuse into the center of the tumor from the

surrounding abnormal vasculature). Many of the stumbling blocks that initially prevented the widespread implementation of oncolytic bacterial therapy have since been overcome by advances in research technologies and techniques that can now clarify much of the confounding work of previous researchers.

While the broad range of bacteria that can be classified as oncolytic has been a significant confounder and hurdle to clinical translation, as a classification, oncolytic bacteria based therapeutics represent a promising, low cost, perpetually regenerating strategy to mitigate cancerous tumors. Sporulating oncolytic bacteria such as *Clostridia* and *Lactobacillus* are extremely stable for both transport and storage, with *Lactobacillus* and *Bifidobacterium* species already being widely accepted by the general public as probiotic, beneficial species. The potential advantages of oncolytic bacteria not only decrease the ever-growing overall costs of healthcare associated with treating cancer, but also advance the ability to treat patients that are low-income or underserved, thus helping to breach the socio-economical access barrier to healthcare. These minority populations in the United States are projected to experience a staggering 99% of the increase in cancer diagnoses by 2030<sup>152</sup>.

Furthering the translation of oncolytic bacterial therapeutics recent advances in gene editing techniques could easily be applied to these microorganisms to ‘customize’ an oncolytic bacteria - subsequently enhancing, generating or ablating innate tumor targeting and lysing characteristics at will. Bacteria with the capacity to seek and destroy solid tumors could become the highly sought after ‘smart’ cancer therapeutic uniquely able to distinguish tumorigenic cells from normal cells. Not only do these bacterial species actively seek out the environment at the center of solid tumors, it is extremely likely that they will do so regardless of the tissue of origin, giving this therapy an unprecedented level of translation between cancer types. Moreover, since

the characteristics attracting oncolytic bacterial are universal to solid tumors and not dependent on genotype, it is thus entirely feasible that a single dose may be able to target not only the primary tumor, but any metastases as well - regardless of size or progression. Indeed, it is reasonable to assume even a late-stage diagnosed tumor could be adequately mitigated by administering the correct oncolytic bacteria. Though there is no question that several knowledge gaps remain to be addressed, there should also be no question that oncolytic bacteria are a viable route forward for treatment of solid tumors.

### **Acknowledgments**

The authors would like to acknowledge the use of Biorender for the creation of all figures contained within. The authors also acknowledge funding support from the Center for Diagnostic and Therapeutic Strategies in Pancreatic Cancer at North Dakota State University.

### **Author Contributions**

Conceptualization: KMD, AEB.; writing—original draft preparation: KMD, JEA, BDB, AEB; writing—review and editing: KMD, AEB, PRJ, MO, BDB, JEA; figure creation and editing KMD, AEB, BDB, PRJ, MO; supervision AEB.

### **Funding**

This research was funded in part by a pilot project award to AEB from NIH COBRE award 1P20 GM109024 (SM) and by a NDSU Graduate School Dissertation Fellowship to KMD.

### **Conflicts of Interest**

The authors declare no conflict of interest. The funders had no role in the design of the reveiw; in the collection, analyses, or interpretation of data; in the writing of the manuscript, or in the decision to publish the results.

## References

- (1) Secombe, K. R.; Collier, J. K.; Gibson, R. J.; Wardill, H. R.; Bowen, J. M. The Bidirectional Interaction of the Gut Microbiome and the Innate Immune System: Implications for Chemotherapy-Induced Gastrointestinal Toxicity. *Int. J. Cancer* **2019**, *144* (10), 2365–2376. <https://doi.org/10.1002/ijc.31836>.
- (2) Burns, M. B.; Montassier, E.; Abrahante, J.; Priya, S.; Niccum, D. E.; Khoruts, A.; Starr, T. K.; Knights, D.; Blekhman, R. Colorectal Cancer Mutational Profiles Correlate with Defined Microbial Communities in the Tumor Microenvironment. *PLOS Genet.* **2018**, *14* (6), e1007376. <https://doi.org/10.1371/journal.pgen.1007376>.
- (3) Whisner, C. M.; Athena Aktipis, C. The Role of the Microbiome in Cancer Initiation and Progression: How Microbes and Cancer Cells Utilize Excess Energy and Promote One Another's Growth. *Curr. Nutr. Rep.* **2019**, *8* (1), 42–51. <https://doi.org/10.1007/s13668-019-0257-2>.
- (4) Wang, X.; Yang, Y.; Huycke, M. M. Microbiome-Driven Carcinogenesis in Colorectal Cancer: Models and Mechanisms. *Free Radic. Biol. Med.* **2017**, *105*, 3–15. <https://doi.org/10.1016/j.freeradbiomed.2016.10.504>.
- (5) Wei, M. Q.; Mengesha, A.; Good, D.; Anné, J. Bacterial Targeted Tumour Therapy-Dawn of a New Era. *Cancer Lett.* **2008**, *259* (1), 16–27. <https://doi.org/10.1016/j.canlet.2007.10.034>.
- (6) Ngo, N.; Choucair, K.; Creeden, J. F.; Qaqish, H.; Bhavsar, K.; Murphy, C.; Lian, K.; Albrethsen, M. T.; Stanbery, L.; Phinney, R. C.; Brunnicardi, F. C.; Dworkin, L.; Nemunaitis, J. Bifidobacterium Spp: The Promising Trojan Horse in the Era of Precision Oncology. *Future Oncol.* **2019**, *15* (33), 3861–3876. <https://doi.org/10.2217/fon-2019-0374>.
- (7) Bhatnagar, P. K.; Awasthi, A.; Nomellini, J. F.; Smit, J.; Suresh, M. R. Anti-Tumor Effects of the Bacterium *Caulobacter Crescentus* in Murine Tumor Models. *Cancer Biol. Ther.* **2006**, *5* (5), 485–491. <https://doi.org/10.4161/cbt.5.5.2553>.
- (8) Nomellini, J. F.; Duncan, G.; Dorocicz, I. R.; Smit, J. S-Layer-Mediated Display of the Immunoglobulin G-Binding Domain of Streptococcal Protein G on the Surface of *Caulobacter Crescentus*: Development of an Immunoactive Reagent. *Appl. Environ. Microbiol.* **2007**, *73* (10), 3245–3253. <https://doi.org/10.1128/AEM.02900-06>.
- (9) Staedtke, V.; Roberts, N. J.; Bai, R.-Y.; Zhou, S. Clostridium Novyi-NT in Cancer Therapy. *Genes Dis.* **2016**, *3* (2), 144–152. <https://doi.org/10.1016/j.gendis.2016.01.003>.
- (10) Wang, L.; Smith, J.; Breton, C.; Clark, P.; Zhang, J.; Ying, L.; Che, Y.; Lape, J.; Bell, P.; Calcedo, R.; Buza, E. L.; Saveliev, A.; Bartsevich, V. V.; He, Z.; White, J.; Li, M.; Jantz, D.; Wilson, J. M. Meganuclease Targeting of PCSK9 in Macaque Liver Leads to Stable Reduction in Serum Cholesterol. *Nat. Biotechnol.* **2018**, *36* (8), 717–725. <https://doi.org/10.1038/nbt.4182>.

- (11) Song, S.; Vuai, M. S.; Zhong, M. The Role of Bacteria in Cancer Therapy – Enemies in the Past, but Allies at Present. *Infect. Agent. Cancer* **2018**, *13*.  
<https://doi.org/10.1186/s13027-018-0180-y>.
- (12) Hetz, C.; Bono, M. R.; Barros, L. F.; Lagos, R. Microcin E492, a Channel-Forming Bacteriocin from *Klebsiella Pneumoniae*, Induces Apoptosis in Some Human Cell Lines. *Proc. Natl. Acad. Sci. U. S. A.* **2002**, *99* (5), 2696–2701.  
<https://doi.org/10.1073/pnas.052709699>.
- (13) Motevaseli, E.; Khorramizadeh, M. R.; Hadjati, J.; Bonab, S. F.; Eslami, S.; Ghafouri-Fard, S. Investigation of Antitumor Effects of *Lactobacillus Crispatus* in Experimental Model of Breast Cancer in BALB/c Mice. *Immunotherapy* **2018**, *10* (2), 119–129.  
<https://doi.org/10.2217/imt-2017-0088>.
- (14) Kim, S. H.; Castro, F.; Paterson, Y.; Gravekamp, C. High Efficacy of a *Listeria*-Based Vaccine against Metastatic Breast Cancer Reveals a Dual Mode of Action. *Cancer Res.* **2009**, *69* (14), 5860–5866. <https://doi.org/10.1158/0008-5472.CAN-08-4855>.
- (15) Morales, A. BCG: A Throwback from the Stone Age of Vaccines Opened the Path for Bladder Cancer Immunotherapy. *Can. J. Urol.* **2017**, *24* (3), 8788–8793.
- (16) Shintani, Y.; Sawada, Y.; Inagaki, T.; Kohjimoto, Y.; Uekado, Y.; Shinka, T. Intravesical Instillation Therapy with *Bacillus Calmette-Guérin* for Superficial Bladder Cancer: Study of the Mechanism of *Bacillus Calmette-Guérin* Immunotherapy. *Int. J. Urol.* **2007**, *14* (2), 140–146. <https://doi.org/10.1111/j.1442-2042.2007.01696.x>.
- (17) Arakawa, M.; Sugiura, K.; Reilly, H. C.; Stock, C. C. Oncolytic Effect of *Proteus Mirabilis* upon Tumor-Bearing Animals. II. Effect on Transplantable Mouse and Rat Tumors. *Gan* **1968**, *59* (2), 117–122.
- (18) Murata, T.; Arakawa, M.; Sugiya, Y.; Inazu, Y.; Hattori, Z.; Suzuki, Y.; Minakami, H.; Nakahara, M.; Okazaki, H. Oncolytic Effect of *Proteus Mirabilis* upon Tumor Bearing Animal. *Life Sci.* **1965**, *4* (10), 1055–1067. [https://doi.org/10.1016/0024-3205\(65\)90225-0](https://doi.org/10.1016/0024-3205(65)90225-0).
- (19) Pawelek, J. M.; Low, K. B.; Bermudes, D. Tumor-Targeted *Salmonella* as a Novel Anticancer Vector. *Cancer Res.* **1997**, *57* (20), 4537–4544.
- (20) Maletzki, C.; Linnebacher, M.; Kreikemeyer, B.; Emmrich, J. Pancreatic Cancer Regression by Intratumoural Injection of Live *Streptococcus Pyogenes* in a Syngeneic Mouse Model. *Gut* **2008**, *57* (4), 483–491. <https://doi.org/10.1136/gut.2007.125419>.
- (21) Gomes, F. M.; Barillas-Mury, C. Infection of Anopheline Mosquitoes with *Wolbachia*: Implications for Malaria Control. *PLoS Pathog.* **2018**, *14* (11).  
<https://doi.org/10.1371/journal.ppat.1007333>.



- (22) Hosseinidoust, Z.; Mostaghaci, B.; Yasa, O.; Park, B.-W.; Singh, A. V.; Sitti, M. Bioengineered and Biohybrid Bacteria-Based Systems for Drug Delivery. *Adv. Drug Deliv. Rev.* **2016**, *106* (Pt A), 27–44. <https://doi.org/10.1016/j.addr.2016.09.007>.
- (23) Baban, C. K.; Cronin, M.; O’Hanlon, D.; O’Sullivan, G. C.; Tangney, M. Bacteria as Vectors for Gene Therapy of Cancer. *Bioeng. Bugs* **2010**, *1* (6), 385–394. <https://doi.org/10.4161/bbug.1.6.13146>.
- (24) Gnopo, Y. M. D.; Watkins, H. C.; Stevenson, T. C.; DeLisa, M. P.; Putnam, D. Designer Outer Membrane Vesicles as Immunomodulatory Systems – Reprogramming Bacteria for Vaccine Delivery. *Adv. Drug Deliv. Rev.* **2017**, *114*, 132–142. <https://doi.org/10.1016/j.addr.2017.05.003>.
- (25) Cho, S.; Shin, J.; Cho, B.-K. Applications of CRISPR/Cas System to Bacterial Metabolic Engineering. *Int. J. Mol. Sci.* **2018**, *19* (4). <https://doi.org/10.3390/ijms19041089>.
- (26) Genetic Engineering of Algae for Enhanced Biofuel Production | Eukaryotic Cell <https://ec.asm.org/content/9/4/486> (accessed Jan 23, 2020).
- (27) Lin, H.; Wang, Q.; Shen, Q.; Zhan, J.; Zhao, Y. Genetic Engineering of Microorganisms for Biodiesel Production. *Bioengineered* **2013**, *4* (5), 292–304. <https://doi.org/10.4161/bioe.23114>.
- (28) Liu, L.; Bilal, M.; Duan, X.; Iqbal, H. M. N. Mitigation of Environmental Pollution by Genetically Engineered Bacteria — Current Challenges and Future Perspectives. *Sci. Total Environ.* **2019**, *667*, 444–454. <https://doi.org/10.1016/j.scitotenv.2019.02.390>.
- (29) Redmond, K. M.; Wilson, T. R.; Johnston, P. G.; Longley, D. B. Resistance Mechanisms to Cancer Chemotherapy. *Front. Biosci. J. Virtual Libr.* **2008**, *13*, 5138–5154. <https://doi.org/10.2741/3070>.
- (30) Mansoori, B.; Mohammadi, A.; Davudian, S.; Shirjang, S.; Baradaran, B. The Different Mechanisms of Cancer Drug Resistance: A Brief Review. *Adv. Pharm. Bull.* **2017**, *7* (3), 339–348. <https://doi.org/10.15171/apb.2017.041>.
- (31) Kelly, E.; Russell, S. J. History of Oncolytic Viruses: Genesis to Genetic Engineering. *Mol. Ther.* **2007**, *15* (4), 651–659. <https://doi.org/10.1038/sj.mt.6300108>.
- (32) Martin, N. T.; Bell, J. C. Oncolytic Virus Combination Therapy: Killing One Bird with Two Stones. *Mol. Ther.* **2018**, *26* (6), 1414–1422. <https://doi.org/10.1016/j.ymthe.2018.04.001>.
- (33) Sanchala, D. S.; Bhatt, L. K.; Prabhavalkar, K. S. Oncolytic Herpes Simplex Viral Therapy: A Stride toward Selective Targeting of Cancer Cells. *Front. Pharmacol.* **2017**, *8*. <https://doi.org/10.3389/fphar.2017.00270>.

- (34) Schvartsman, G.; Perez, K.; Flynn, J. E.; Myers, J. N.; Tawbi, H. Safe and Effective Administration of T-VEC in a Patient with Heart Transplantation and Recurrent Locally Advanced Melanoma. *J. Immunother. Cancer* **2017**, *5*, 45. <https://doi.org/10.1186/s40425-017-0250-5>.
- (35) Aref, S.; Bailey, K.; Fielding, A. Measles to the Rescue: A Review of Oncolytic Measles Virus. *Viruses* **2016**, *8* (10), 294. <https://doi.org/10.3390/v8100294>.
- (36) Robinson, S.; Galanis, E. Potential and Clinical Translation of Oncolytic Measles Viruses. *Expert Opin. Biol. Ther.* **2017**, *17* (3), 353–363. <https://doi.org/10.1080/14712598.2017.1288713>.
- (37) Angelova, A. L.; Geletneky, K.; Nüesch, J. P. F.; Rommelaere, J. Tumor Selectivity of Oncolytic Parvoviruses: From in Vitro and Animal Models to Cancer Patients. *Front. Bioeng. Biotechnol.* **2015**, *3*. <https://doi.org/10.3389/fbioe.2015.00055>.
- (38) Sharp, D. W.; Lattime, E. C. Recombinant Poxvirus and the Tumor Microenvironment: Oncolysis, Immune Regulation and Immunization. *Biomedicines* **2016**, *4* (3), 19. <https://doi.org/10.3390/biomedicines4030019>.
- (39) Melzer, M. K.; Lopez-Martinez, A.; Altomonte, J. Oncolytic Vesicular Stomatitis Virus as a Viro-Immunotherapy: Defeating Cancer with a “Hammer” and “Anvil.” *Biomedicines* **2017**, *5* (1), 8. <https://doi.org/10.3390/biomedicines5010008>.
- (40) Kaufman, H. L.; Kohlhapp, F. J.; Zloza, A. Oncolytic Viruses: A New Class of Immunotherapy Drugs. *Nat. Rev. Drug Discov.* **2015**, *14* (9), 642–662. <https://doi.org/10.1038/nrd4663>.
- (41) Thymidine Kinase-Deleted Vaccinia Virus Expressing Purine Nucleoside Phosphorylase as a Vector for Tumor-Directed Gene Therapy | Human Gene Therapy <https://www.liebertpub.com/doi/abs/10.1089/10430349950018724> (accessed Jan 12, 2020).
- (42) Mitsui, K.; Ide, K.; Takahashi, T.; Kosai, K.-I. Viral Vector-Based Innovative Approaches to Directly Abolishing Tumorigenic Pluripotent Stem Cells for Safer Regenerative Medicine. *Mol. Ther. Methods Clin. Dev.* **2017**, *5*, 51–58. <https://doi.org/10.1016/j.omtm.2017.03.002>.
- (43) Goins, W. F.; Huang, S.; Hall, B.; Marzulli, M.; Cohen, J. B.; Glorioso, J. C. Engineering HSV-1 Vectors for Gene Therapy. In *Herpes Simplex Virus : Methods and Protocols*; Diefenbach, R. J., Fraefel, C., Eds.; Methods in Molecular Biology; Springer: New York, NY, 2020; pp 73–90. [https://doi.org/10.1007/978-1-4939-9814-2\\_4](https://doi.org/10.1007/978-1-4939-9814-2_4).
- (44) Lin, L.-T.; Richardson, C. D. The Host Cell Receptors for Measles Virus and Their Interaction with the Viral Hemagglutinin (H) Protein. *Viruses* **2016**, *8* (9). <https://doi.org/10.3390/v8090250>.

- (45) Campadelli-Fiume, G.; De Giovanni, C.; Gatta, V.; Nanni, P.; Lollini, P.-L.; Menotti, L. Rethinking Herpes Simplex Virus: The Way to Oncolytic Agents. *Rev. Med. Virol.* **2011**, *21* (4), 213–226. <https://doi.org/10.1002/rmv.691>.
- (46) Ilkow, C. S.; Marguerie, M.; Batenchuk, C.; Mayer, J.; Ben Neriah, D.; Cousineau, S.; Falls, T.; Jennings, V. A.; Boileau, M.; Bellamy, D.; Bastin, D.; de Souza, C. T.; Alkayyal, A.; Zhang, J.; Le Boeuf, F.; Arulanandam, R.; Stubbert, L.; Sampath, P.; Thorne, S. H.; Paramanthan, P.; Chatterjee, A.; Strieter, R. M.; Burdick, M.; Addison, C. L.; Stojdl, D. F.; Atkins, H. L.; Auer, R. C.; Diallo, J.-S.; Lichty, B. D.; Bell, J. C. Reciprocal Cellular Cross-Talk within the Tumor Microenvironment Promotes Oncolytic Virus Activity. *Nat. Med.* **2015**, *21* (5), 530–536. <https://doi.org/10.1038/nm.3848>.
- (47) Minchinton, A. I.; Tannock, I. F. Drug Penetration in Solid Tumours. *Nat. Rev. Cancer* **2006**, *6* (8), 583–592. <https://doi.org/10.1038/nrc1893>.
- (48) McKeown, S. R. Defining Normoxia, Physoxia and Hypoxia in Tumours—Implications for Treatment Response. *Br. J. Radiol.* **2014**, *87* (1035). <https://doi.org/10.1259/bjr.20130676>.
- (49) Carreau, A.; Hafny-Rahbi, B. E.; Matejuk, A.; Grillon, C.; Kieda, C. Why Is the Partial Oxygen Pressure of Human Tissues a Crucial Parameter? Small Molecules and Hypoxia. *J. Cell. Mol. Med.* **2011**, *15* (6), 1239–1253. <https://doi.org/10.1111/j.1582-4934.2011.01258.x>.
- (50) Cassavaugh, J.; Lounsbury, K. M. Hypoxia-Mediated Biological Control. *J. Cell. Biochem.* **2011**, *112* (3), 735–744. <https://doi.org/10.1002/jcb.22956>.
- (51) Jun, J. C.; Rathore, A.; Younas, H.; Gilkes, D.; Polotsky, V. Y. Hypoxia-Inducible Factors and Cancer. *Curr. Sleep Med. Rep.* **2017**, *3* (1), 1–10. <https://doi.org/10.1007/s40675-017-0062-7>.
- (52) Laitala, A.; Epler, J. T. Hypoxic Signalling in Tumour Stroma. *Front. Oncol.* **2018**, *8*. <https://doi.org/10.3389/fonc.2018.00189>.
- (53) Sharma, A.; Arambula, J. F.; Koo, S.; Kumar, R.; Singh, H.; Sessler, J. L.; Kim, J. S. Hypoxia-Targeted Drug Delivery. *Chem. Soc. Rev.* **2019**, *48* (3), 771–813. <https://doi.org/10.1039/C8CS00304A>.
- (54) Kulkarni, P.; Haldar, M. K.; You, S.; Choi, Y.; Mallik, S. Hypoxia-Responsive Polymersomes for Drug Delivery to Hypoxic Pancreatic Cancer Cells. *Biomacromolecules* **2016**, *17* (8), 2507–2513. <https://doi.org/10.1021/acs.biomac.6b00350>.
- (55) Kato, Y.; Ozawa, S.; Miyamoto, C.; Maehata, Y.; Suzuki, A.; Maeda, T.; Baba, Y. Acidic Extracellular Microenvironment and Cancer. *Cancer Cell Int.* **2013**, *13*, 89. <https://doi.org/10.1186/1475-2867-13-89>.
- (56) Huber, V.; Camisaschi, C.; Berzi, A.; Ferro, S.; Lugini, L.; Triulzi, T.; Tuccitto, A.; Tagliabue, E.; Castelli, C.; Rivoltini, L. Cancer Acidity: An Ultimate Frontier of Tumor

- Immune Escape and a Novel Target of Immunomodulation. *Semin. Cancer Biol.* **2017**, *43*, 74–89. <https://doi.org/10.1016/j.semcancer.2017.03.001>.
- (57) Tunggal, J. K.; Cowan, D. S.; Shaikh, H.; Tannock, I. F. Penetration of Anticancer Drugs through Solid Tissue: A Factor That Limits the Effectiveness of Chemotherapy for Solid Tumors. *Clin. Cancer Res. Off. J. Am. Assoc. Cancer Res.* **1999**, *5* (6), 1583–1586.
- (58) Tjäderhane, L.; Larjava, H.; Sorsa, T.; Uitto, V. J.; Larmas, M.; Salo, T. The Activation and Function of Host Matrix Metalloproteinases in Dentin Matrix Breakdown in Caries Lesions. *J. Dent. Res.* **1998**, *77* (8), 1622–1629. <https://doi.org/10.1177/00220345980770081001>.
- (59) Martínez-Zaguilán, R.; Seftor, E. A.; Seftor, R. E.; Chu, Y. W.; Gillies, R. J.; Hendrix, M. J. Acidic PH Enhances the Invasive Behavior of Human Melanoma Cells. *Clin. Exp. Metastasis* **1996**, *14* (2), 176–186. <https://doi.org/10.1007/bf00121214>.
- (60) Adams, D. J.; Dewhirst, M. W.; Flowers, J. L.; Gamcsik, M. P.; Colvin, O. M.; Manikumar, G.; Wani, M. C.; Wall, M. E. Camptothecin Analogues with Enhanced Antitumor Activity at Acidic PH. *Cancer Chemother. Pharmacol.* **2000**, *46* (4), 263–271. <https://doi.org/10.1007/s002800000157>.
- (61) Herben, V. M.; ten Bokkel Huinink, W. W.; Beijnen, J. H. Clinical Pharmacokinetics of Topotecan. *Clin. Pharmacokinet.* **1996**, *31* (2), 85–102. <https://doi.org/10.2165/00003088-199631020-00001>.
- (62) Kyle, A. H.; Huxham, L. A.; Chiam, A. S. J.; Sim, D. H.; Minchinton, A. I. Direct Assessment of Drug Penetration into Tissue Using a Novel Application of Three-Dimensional Cell Culture. *Cancer Res.* **2004**, *64* (17), 6304–6309. <https://doi.org/10.1158/0008-5472.CAN-04-1099>.
- (63) Huxham, L. A.; Kyle, A. H.; Baker, J. H. E.; Nykilchuk, L. K.; Minchinton, A. I. Microregional Effects of Gemcitabine in HCT-116 Xenografts. *Cancer Res.* **2004**, *64* (18), 6537–6541. <https://doi.org/10.1158/0008-5472.CAN-04-0986>.
- (64) Kleeff, J.; Beckhove, P.; Esposito, I.; Herzig, S.; Huber, P. E.; Löhr, J. M.; Friess, H. Pancreatic Cancer Microenvironment. *Int. J. Cancer* **2007**, *121* (4), 699–705. <https://doi.org/10.1002/ijc.22871>.
- (65) Boedtkjer, E.; Pedersen, S. F. The Acidic Tumor Microenvironment as a Driver of Cancer. *Annu. Rev. Physiol.* **2020**, *82* (1), 103–126. <https://doi.org/10.1146/annurev-physiol-021119-034627>.
- (66) Gonzalez, H.; Hagerling, C.; Werb, Z. Roles of the Immune System in Cancer: From Tumor Initiation to Metastatic Progression. *Genes Dev.* **2018**, *32* (19–20), 1267–1284. <https://doi.org/10.1101/gad.314617.118>.

- (67) Shimizu, K.; Iyoda, T.; Okada, M.; Yamasaki, S.; Fujii, S. Immune Suppression and Reversal of the Suppressive Tumor Microenvironment. *Int. Immunol.* **2018**, *30* (10), 445–455. <https://doi.org/10.1093/intimm/dxy042>.
- (68) Binnewies, M.; Roberts, E. W.; Kersten, K.; Chan, V.; Fearon, D. F.; Merad, M.; Coussens, L. M.; Gaborilovich, D. I.; Ostrand-Rosenberg, S.; Hedrick, C. C.; Vonderheide, R. H.; Pittet, M. J.; Jain, R. K.; Zou, W.; Howcroft, T. K.; Woodhouse, E. C.; Weinberg, R. A.; Krummel, M. F. Understanding the Tumor Immune Microenvironment (TIME) for Effective Therapy. *Nat. Med.* **2018**, *24* (5), 541–550. <https://doi.org/10.1038/s41591-018-0014-x>.
- (69) Wang, Y.; Guo, W.; Wu, X.; Zhang, Y.; Mannion, C.; Brouchkov, A.; Man, Y.-G.; Chen, T. Oncolytic Bacteria and Their Potential Role in Bacterium-Mediated Tumour Therapy: A Conceptual Analysis. *J. Cancer* **2019**, *10* (19), 4442–4454. <https://doi.org/10.7150/jca.35648>.
- (70) Rius-Rocabert, S.; Llinares Pinel, F.; Pozuelo, M. J.; García, A.; Nistal-Villan, E. Oncolytic Bacteria: Past, Present and Future. *FEMS Microbiol. Lett.* **2019**, *366* (12). <https://doi.org/10.1093/femsle/fnz136>.
- (71) Matsuo, K.; Yasutomi, Y. Mycobacterium Bovis Bacille Calmette-Guérin as a Vaccine Vector for Global Infectious Disease Control. *Tuberc. Res. Treat.* **2011**, *2011*. <https://doi.org/10.1155/2011/574591>.
- (72) Gründling, A.; Burrack, L. S.; Bouwer, H. G. A.; Higgins, D. E. Listeria Monocytogenes Regulates Flagellar Motility Gene Expression through MogR, a Transcriptional Repressor Required for Virulence. *Proc. Natl. Acad. Sci.* **2004**, *101* (33), 12318–12323. <https://doi.org/10.1073/pnas.0404924101>.
- (73) Involvement of Reactive Oxygen Intermediate in the Enhanced Expression of Virulence-Associated Genes of Listeria monocytogenes inside Activated Macrophages - Makino - 2005 - Microbiology and Immunology - Wiley Online Library <https://onlinelibrary-wiley-com.ezproxy.lib.ndsu.nodak.edu/doi/full/10.1111/j.1348-0421.2005.tb03661.x> (accessed Aug 24, 2020).
- (74) Michel, E.; Reich, K. A.; Favier, R.; Berche, P.; Cossart, P. Attenuated Mutants of the Intracellular Bacterium Listeria Monocytogenes Obtained by Single Amino Acid Substitutions in Listeriolysin O. *Mol. Microbiol.* **1990**, *4* (12), 2167–2178. <https://doi.org/10.1111/j.1365-2958.1990.tb00578.x>.
- (75) Park, J. M.; Ng, V. H.; Maeda, S.; Rest, R. F.; Karin, M. Anthrolysin O and Other Gram-Positive Cytolysins Are Toll-like Receptor 4 Agonists. *J. Exp. Med.* **2004**, *200* (12), 1647–1655. <https://doi.org/10.1084/jem.20041215>.
- (76) Wieland, C. W.; van Lieshout, M. H. P.; Hoogendijk, A. J.; van der Poll, T. Host Defence during Klebsiella Pneumonia Relies on Haematopoietic-Expressed Toll-like Receptors 4 and 2. *Eur. Respir. J.* **2011**, *37* (4), 848–857. <https://doi.org/10.1183/09031936.00076510>.

- (77) Qu Biologics Inc. *Open Label, Single Arm, Exploratory Study to Evaluate the Safety, Tolerability, Compliance and MOA, of QBKPN SSI in Subjects With 2 or More Second Primary Pre-Invasive/Invasive Adenocarcinoma Following Surgical Resection of Stage I NSCLC*; Clinical trial registration NCT02256852; clinicaltrials.gov, 2016.
- (78) Khanna, A.; Khanna, M.; Aggarwal, A. *Serratia Marcescens- a Rare Opportunistic Nosocomial Pathogen and Measures to Limit Its Spread in Hospitalized Patients. J. Clin. Diagn. Res. JCDR* **2013**, *7* (2), 243–246. <https://doi.org/10.7860/JCDR/2013/5010.2737>.
- (79) Coley, W. B. The Treatment of Inoperable Sarcoma by Bacterial Toxins (the Mixed Toxins of the Streptococcus Erysipelas and the Bacillus Prodigiosus). *Proc. R. Soc. Med.* **1910**, *3* (Surg Sect), 1–48.
- (80) Kramer, M. G.; Masner, M.; Ferreira, F. A.; Hoffman, R. M. Bacterial Therapy of Cancer: Promises, Limitations, and Insights for Future Directions. *Front. Microbiol.* **2018**, *9*, 16. <https://doi.org/10.3389/fmicb.2018.00016>.
- (81) Hong, B.; Prabhu, V. V.; Zhang, S.; van den Heuvel, A. P. J.; Dicker, D. T.; Kopelovich, L.; El-Deiry, W. S. Prodigiosin Rescues Deficient P53 Signaling and Antitumor Effects via Upregulating P73 and Disrupting Its Interaction with Mutant P53. *Cancer Res.* **2014**, *74* (4), 1153–1165. <https://doi.org/10.1158/0008-5472.CAN-13-0955>.
- (82) Zhang, H.; Diao, H.; Jia, L.; Yuan, Y.; Thamm, D. H.; Wang, H.; Jin, Y.; Pei, S.; Zhou, B.; Yu, F.; Zhao, L.; Cheng, N.; Du, H.; Huang, Y.; Zhang, D.; Lin, D. *Proteus Mirabilis* Inhibits Cancer Growth and Pulmonary Metastasis in a Mouse Breast Cancer Model. *PLoS ONE* **2017**, *12* (12). <https://doi.org/10.1371/journal.pone.0188960>.
- (83) Motevaseli, E.; Khorramizadeh, M. R.; Hadjati, J.; Bonab, S. F.; Eslami, S.; Ghafouri-Fard, S. Investigation of antitumor effects of *Lactobacillus crispatus* in experimental model of breast cancer in BALB/c mice <https://www.futuremedicine.com/doi/abs/10.2217/imt-2017-0088> (accessed Feb 12, 2020). <https://doi.org/10.2217/imt-2017-0088>.
- (84) Kucerova, P.; Cervinkova, M. Spontaneous Regression of Tumour and the Role of Microbial Infection – Possibilities for Cancer Treatment. *Anticancer. Drugs* **2016**, *27* (4), 269–277. <https://doi.org/10.1097/CAD.0000000000000337>.
- (85) Sobolewski, C.; Cerella, C.; Dicato, M.; Ghibelli, L.; Diederich, M. The Role of Cyclooxygenase-2 in Cell Proliferation and Cell Death in Human Malignancies <https://www.hindawi.com/journals/ijcb/2010/215158/> (accessed Aug 25, 2020). <https://doi.org/10.1155/2010/215158>.
- (86) Motevaseli, E.; Dianatpour, A.; Ghafouri-Fard, S. The Role of Probiotics in Cancer Treatment: Emphasis on Their In Vivo and In Vitro Anti-Metastatic Effects. *Int. J. Mol. Cell. Med.* **2017**, *6* (2), 66–76. <https://doi.org/10.22088/acadpub.BUMS.6.2.1>.

- (87) (PDF) Selective localization and growth of *Bifidobacterium bifidum* in mouse tumors following intravenous administration [https://www.researchgate.net/publication/16208534\\_Selective\\_localization\\_and\\_growth\\_of\\_Bifidobacterium\\_bifidum\\_in\\_mouse\\_tumors\\_following\\_intravenous\\_administration](https://www.researchgate.net/publication/16208534_Selective_localization_and_growth_of_Bifidobacterium_bifidum_in_mouse_tumors_following_intravenous_administration) (accessed Feb 7, 2020).
- (88) Imaging the Different Mechanisms of Prostate Cancer Cell-killing by Tumor-targeting *Salmonella typhimurium* A1-R <http://ar.iiarjournals.org/content/35/10/5225.long> (accessed Aug 24, 2020).
- (89) Wall, D. M.; Srikanth, C. V.; McCormick, B. A. Targeting Tumors with *Salmonella Typhimurium* - Potential for Therapy. *Oncotarget* **2011**, *1* (8), 721–728.
- (90) Clairmont, C.; Lee, K. C.; Pike, J.; Ittensohn, M.; Low, K. B.; Pawelek, J.; Bermudes, D.; Brecher, S. M.; Margitich, D.; Turnier, J.; Li, Z.; Luo, X.; King, I.; Zheng, L. M. Biodistribution and Genetic Stability of the Novel Antitumor Agent VNP20009, a Genetically Modified Strain of *Salmonella Typhimurium*. *J. Infect. Dis.* **2000**, *181* (6), 1996–2002. <https://doi.org/10.1086/315497>.
- (91) Palmitoylation State Impacts Induction of Innate and Acquired Immunity by the *Salmonella enterica* Serovar *Typhimurium* msbB Mutant | *Infection and Immunity* <https://iai-asm-org.ezproxy.lib.ndsu.nodak.edu/content/79/12/5027.long> (accessed Aug 24, 2020).
- (92) Hiroshima, Y.; Zhao, M.; Zhang, Y.; Zhang, N.; Maawy, A.; Murakami, T.; Mii, S.; Uehara, F.; Yamamoto, M.; Miwa, S.; Yano, S.; Momiyama, M.; Mori, R.; Matsuyama, R.; Chishima, T.; Tanaka, K.; Ichikawa, Y.; Bouvet, M.; Endo, I.; Hoffman, R. M. Tumor-Targeting *Salmonella Typhimurium* A1-R Arrests a Chemo-Resistant Patient Soft-Tissue Sarcoma in Nude Mice. *PLOS ONE* **2015**, *10* (8), e0134324. <https://doi.org/10.1371/journal.pone.0134324>.
- (93) Zhao, M.; Yang, M.; Ma, H.; Li, X.; Tan, X.; Li, S.; Yang, Z.; Hoffman, R. M. Targeted Therapy with a *Salmonella Typhimurium* Leucine-Arginine Auxotroph Cures Orthotopic Human Breast Tumors in Nude Mice. *Cancer Res.* **2006**, *66* (15), 7647–7652. <https://doi.org/10.1158/0008-5472.CAN-06-0716>.
- (94) Nallar, S. C.; Xu, D.-Q.; Kalvakolanu, D. V. Bacteria and Genetically Modified Bacteria as Cancer Therapeutics: Current Advances and Challenges. *Cytokine* **2017**, *89*, 160–172. <https://doi.org/10.1016/j.cyto.2016.01.002>.
- (95) Toso, J. F.; Gill, V. J.; Hwu, P.; Marincola, F. M.; Restifo, N. P.; Schwartzentruber, D. J.; Sherry, R. M.; Topalian, S. L.; Yang, J. C.; Stock, F.; Freezer, L. J.; Morton, K. E.; Seipp, C.; Haworth, L.; Mavroukakis, S.; White, D.; MacDonald, S.; Mao, J.; Sznol, M.; Rosenberg, S. A. Phase I Study of the Intravenous Administration of Attenuated *Salmonella Typhimurium* to Patients With Metastatic Melanoma. *J. Clin. Oncol. Off. J. Am. Soc. Clin. Oncol.* **2002**, *20* (1), 142–152.

- (96) Malmgren, R. A.; Flanigan, C. C. Localization of the Vegetative Form of Clostridium Tetani in Mouse Tumors Following Intravenous Spore Administration. *Cancer Res.* **1955**, *15* (7), 473–478.
- (97) Dang, L. H.; Bettgowda, C.; Huso, D. L.; Kinzler, K. W.; Vogelstein, B. Combination Bacteriolytic Therapy for the Treatment of Experimental Tumors. *Proc. Natl. Acad. Sci. U. S. A.* **2001**, *98* (26), 15155–15160. <https://doi.org/10.1073/pnas.251543698>.
- (98) MacLennan, J. D. THE HISTOTOXIC CLOSTRIDIAL INFECTIONS OF MAN 12. *Bacteriol. Rev.* **1962**, *26* (2 Pt 1-2), 177–274.
- (99) Diaz, L. A.; Cheong, I.; Foss, C. A.; Zhang, X.; Peters, B. A.; Agrawal, N.; Bettgowda, C.; Karim, B.; Liu, G.; Khan, K.; Huang, X.; Kohli, M.; Dang, L. H.; Hwang, P.; Vogelstein, A.; Garrett-Mayer, E.; Kobrin, B.; Pomper, M.; Zhou, S.; Kinzler, K. W.; Vogelstein, B.; Huso, D. L. Pharmacologic and Toxicologic Evaluation of C. Novyi-NT Spores. *Toxicol. Sci.* **2005**, *88* (2), 562–575. <https://doi.org/10.1093/toxsci/kfi316>.
- (100) Staedtke, V.; Bai, R.-Y.; Sun, W.; Huang, J.; Kibler, K. K.; Tyler, B. M.; Gallia, G. L.; Kinzler, K.; Vogelstein, B.; Zhou, S.; Riggins, G. J. Clostridium Novyi-NT Can Cause Regression of Orthotopically Implanted Glioblastomas in Rats. *Oncotarget* **2015**, *6* (8), 5536–5546.
- (101) Safety Study of Intratumoral Injection of Clostridium Novyi-NT Spores to Treat Patients With Solid Tumors That Have Not Responded to Standard Therapies - Full Text View - ClinicalTrials.gov <https://clinicaltrials.gov/ct2/show/NCT01924689> (accessed Apr 24, 2019).
- (102) Pembrolizumab With Intratumoral Injection of Clostridium Novyi-NT - Full Text View - ClinicalTrials.gov <https://clinicaltrials.gov/ct2/show/NCT03435952> (accessed Aug 24, 2020).
- (103) Christ, B.; Pluskal, T.; Aubry, S.; Weng, J.-K. Contribution of Untargeted Metabolomics for Future Assessment of Biotech Crops. *Trends Plant Sci.* **2018**, *23* (12), 1047–1056. <https://doi.org/10.1016/j.tplants.2018.09.011>.
- (104) Mosquera, T.; Alvarez, M. F.; Jiménez-Gómez, J. M.; Muktar, M. S.; Paulo, M. J.; Steinemann, S.; Li, J.; Draffehn, A.; Hofmann, A.; Lübeck, J.; Strahwald, J.; Tacke, E.; Hofferbert, H.-R.; Walkemeier, B.; Gebhardt, C. Targeted and Untargeted Approaches Unravel Novel Candidate Genes and Diagnostic SNPs for Quantitative Resistance of the Potato (*Solanum Tuberosum* L.) to Phytophthora Infestans Causing the Late Blight Disease. *PLOS ONE* **2016**, *11* (6), e0156254. <https://doi.org/10.1371/journal.pone.0156254>.
- (105) Scherens, B.; Goffeau, A. The Uses of Genome-Wide Yeast Mutant Collections. *Genome Biol.* **2004**, *5* (7), 229. <https://doi.org/10.1186/gb-2004-5-7-229>.



- (106) Lawrence, C. W.; Christensen, R. B. The Mechanism of Untargeted Mutagenesis in UV-Irradiated Yeast. *Mol. Gen. Genet. MGG* **1982**, *186* (1), 1–9. <https://doi.org/10.1007/BF00422904>.
- (107) Ayora, S.; Carrasco, B.; Cárdenas, P. P.; César, C. E.; Cañas, C.; Yadav, T.; Marchisone, C.; Alonso, J. C. Double-Strand Break Repair in Bacteria: A View from *Bacillus Subtilis*. *FEMS Microbiol. Rev.* **2011**, *35* (6), 1055–1081. <https://doi.org/10.1111/j.1574-6976.2011.00272.x>.
- (108) González-Torres, P.; Rodríguez-Mateos, F.; Antón, J.; Gabaldón, T. Impact of Homologous Recombination on the Evolution of Prokaryotic Core Genomes. *mBio* **2019**, *10* (1). <https://doi.org/10.1128/mBio.02494-18>.
- (109) Plessis, A.; Perrin, A.; Haber, J. E.; Dujon, B. Site-Specific Recombination Determined by I-SceI, a Mitochondrial Group I Intron-Encoded Endonuclease Expressed in the Yeast Nucleus. *Genetics* **1992**, *130* (3), 451–460.
- (110) Recent Developments of the Synthetic Biology Toolkit for *Clostridium* <https://www.ncbi.nlm.nih.gov/pmc/articles/PMC5816073/> (accessed Jul 15, 2019).
- (111) Khan, S. H. Genome-Editing Technologies: Concept, Pros, and Cons of Various Genome-Editing Techniques and Bioethical Concerns for Clinical Application. *Mol. Ther. Nucleic Acids* **2019**, *16*, 326–334. <https://doi.org/10.1016/j.omtn.2019.02.027>.
- (112) Prieto, J.; Redondo, P.; López-Méndez, B.; D'Abramo, M.; Merino, N.; Blanco, F. J.; Duchateau, P.; Montoya, G.; Molina, R. Understanding the Indirect DNA Read-out Specificity of I-CreI Meganuclease. *Sci. Rep.* **2018**, *8*. <https://doi.org/10.1038/s41598-018-28599-0>.
- (113) Carroll, D. Genome Engineering With Zinc-Finger Nucleases. *Genetics* **2011**, *188* (4), 773–782. <https://doi.org/10.1534/genetics.111.131433>.
- (114) Gaj, T.; Gersbach, C. A.; Barbas, C. F. ZFN, TALEN, and CRISPR/Cas-Based Methods for Genome Engineering. *Trends Biotechnol.* **2013**, *31* (7), 397–405. <https://doi.org/10.1016/j.tibtech.2013.04.004>.
- (115) Cermak, T.; Doyle, E. L.; Christian, M.; Wang, L.; Zhang, Y.; Schmidt, C.; Baller, J. A.; Somia, N. V.; Bogdanove, A. J.; Voytas, D. F. Efficient Design and Assembly of Custom TALEN and Other TAL Effector-Based Constructs for DNA Targeting. *Nucleic Acids Res.* **2011**, *39* (12), e82–e82. <https://doi.org/10.1093/nar/gkr218>.
- (116) Jinek, M.; Chylinski, K.; Fonfara, I.; Hauer, M.; Doudna, J. A.; Charpentier, E. A Programmable Dual RNA-Guided DNA Endonuclease in Adaptive Bacterial Immunity. *Science* **2012**, *337* (6096), 816–821. <https://doi.org/10.1126/science.1225829>.
- (117) Jiang, F.; Doudna, J. A. CRISPR–Cas9 Structures and Mechanisms. *Annu. Rev. Biophys.* **2017**, *46* (1), 505–529. <https://doi.org/10.1146/annurev-biophys-062215-010822>.

- (118) Cong, L.; Ran, F. A.; Cox, D.; Lin, S.; Barretto, R.; Habib, N.; Hsu, P. D.; Wu, X.; Jiang, W.; Marraffini, L. A.; Zhang, F. Multiplex Genome Engineering Using CRISPR/Cas Systems. *Science* **2013**, *339* (6121), 819–823. <https://doi.org/10.1126/science.1231143>.
- (119) Abudayyeh, O. O.; Gootenberg, J. S.; Essletzbichler, P.; Han, S.; Joung, J.; Belanto, J. J.; Verdine, V.; Cox, D. B. T.; Kellner, M. J.; Regev, A.; Lander, E. S.; Voytas, D. F.; Ting, A. Y.; Zhang, F. RNA Targeting with CRISPR–Cas13. *Nature* **2017**, *550* (7675), 280–284. <https://doi.org/10.1038/nature24049>.
- (120) Paul, B.; Montoya, G. CRISPR-Cas12a: Functional Overview and Applications. *Biomed. J.* **2020**, *43* (1), 8–17. <https://doi.org/10.1016/j.bj.2019.10.005>.
- (121) Bin Moon, S.; Lee, J. M.; Kang, J. G.; Lee, N.-E.; Ha, D.-I.; Kim, D. Y.; Kim, S. H.; Yoo, K.; Kim, D.; Ko, J.-H.; Kim, Y.-S. Highly Efficient Genome Editing by CRISPR-Cpf1 Using CRISPR RNA with a Uridinylate-Rich 3'-Overhang. *Nat. Commun.* **2018**, *9* (1), 3651. <https://doi.org/10.1038/s41467-018-06129-w>.
- (122) Komor, A. C.; Kim, Y. B.; Packer, M. S.; Zuris, J. A.; Liu, D. R. Programmable Editing of a Target Base in Genomic DNA without Double-Stranded DNA Cleavage. *Nature* **2016**, *533* (7603), 420–424. <https://doi.org/10.1038/nature17946>.
- (123) Gaudelli, N. M.; Komor, A. C.; Rees, H. A.; Packer, M. S.; Badran, A. H.; Bryson, D. I.; Liu, D. R. Programmable Base Editing of A•T to G•C in Genomic DNA without DNA Cleavage. *Nature* **2017**, *551* (7681), 464–471. <https://doi.org/10.1038/nature24644>.
- (124) Martyn, G. E.; Wienert, B.; Kurita, R.; Nakamura, Y.; Quinlan, K. G. R.; Crossley, M. A. Natural Regulatory Mutation in the Proximal Promoter Elevates Fetal Globin Expression by Creating a de Novo GATA1 Site. *Blood* **2019**, *133* (8), 852–856. <https://doi.org/10.1182/blood-2018-07-863951>.
- (125) Liu, X. S.; Wu, H.; Ji, X.; Stelzer, Y.; Wu, X.; Czauderna, S.; Shu, J.; Dadon, D.; Young, R. A.; Jaenisch, R. Editing DNA Methylation in the Mammalian Genome. *Cell* **2016**, *167* (1), 233–247.e17. <https://doi.org/10.1016/j.cell.2016.08.056>.
- (126) He, W.; Zhang, L.; Villarreal, O. D.; Fu, R.; Bedford, E.; Dou, J.; Patel, A. Y.; Bedford, M. T.; Shi, X.; Chen, T.; Bartholomew, B.; Xu, H. De Novo Identification of Essential Protein Domains from CRISPR-Cas9 Tiling-SgRNA Knockout Screens. *Nat. Commun.* **2019**, *10* (1), 4541. <https://doi.org/10.1038/s41467-019-12489-8>.
- (127) Addgene: CRISPR Guide <https://www.addgene.org/guides/crispr/> (accessed Aug 23, 2020).
- (128) Adli, M. The CRISPR Tool Kit for Genome Editing and Beyond. *Nat. Commun.* **2018**, *9* (1), 1911. <https://doi.org/10.1038/s41467-018-04252-2>.
- (129) Jiang, W.; Marraffini, L. A. CRISPR-Cas: New Tools for Genetic Manipulations from Bacterial Immunity Systems. *Annu. Rev. Microbiol.* **2015**, *69* (1), 209–228. <https://doi.org/10.1146/annurev-micro-091014-104441>.

- (130) Peters, J. M.; Silvis, M. R.; Zhao, D.; Hawkins, J. S.; Gross, C. A.; Qi, L. S. Bacterial CRISPR: Accomplishments and Prospects. *Curr. Opin. Microbiol.* **2015**, *27*, 121–126. <https://doi.org/10.1016/j.mib.2015.08.007>.
- (131) Dong, C.; Fontana, J.; Patel, A.; Carothers, J. M.; Zalatan, J. G. Synthetic CRISPR-Cas Gene Activators for Transcriptional Reprogramming in Bacteria. *Nat. Commun.* **2018**, *9* (1), 2489. <https://doi.org/10.1038/s41467-018-04901-6>.
- (132) Bikard, D.; Jiang, W.; Samai, P.; Hochschild, A.; Zhang, F.; Marraffini, L. A. Programmable Repression and Activation of Bacterial Gene Expression Using an Engineered CRISPR-Cas System. *Nucleic Acids Res.* **2013**, *41* (15), 7429–7437. <https://doi.org/10.1093/nar/gkt520>.
- (133) Karberg, M.; Guo, H.; Zhong, J.; Coon, R.; Perutka, J.; Lambowitz, A. M. Group II Introns as Controllable Gene Targeting Vectors for Genetic Manipulation of Bacteria. *Nat. Biotechnol. N. Y.* **2001**, *19* (12), 1162–1167. <http://dx.doi.org.ezproxy.lib.ndsu.nodak.edu/10.1038/nbt1201-1162>.
- (134) Lambowitz, A. M.; Zimmerly, S. Group II Introns: Mobile Ribozymes That Invade DNA. *Cold Spring Harb. Perspect. Biol.* **2011**, *3* (8). <https://doi.org/10.1101/cshperspect.a003616>.
- (135) TargeTron™ Gene Knockout System Bacterial Gene Knockout | Sigma-Aldrich [https://www.sigmaaldrich.com/catalog/product/sigma/ta0100?lang=en&region=US&gclid=Cj0KCQjws536BRDTARIsANeUZ59xzG58-cWWLPDsxECwZQeXPEuD3rs5Fg53keh8U4w6Yxnp2URBh78aApF6EALw\\_wcB](https://www.sigmaaldrich.com/catalog/product/sigma/ta0100?lang=en&region=US&gclid=Cj0KCQjws536BRDTARIsANeUZ59xzG58-cWWLPDsxECwZQeXPEuD3rs5Fg53keh8U4w6Yxnp2URBh78aApF6EALw_wcB) (accessed Aug 27, 2020).
- (136) Kuehne, S. A.; Minton, N. P. ClosTron-Mediated Engineering of Clostridium. *Bioengineered* **2012**, *3* (4), 247–254. <https://doi.org/10.4161/bioe.21004>.
- (137) Heap, J. T.; Pennington, O. J.; Cartman, S. T.; Carter, G. P.; Minton, N. P. The ClosTron: A Universal Gene Knock-out System for the Genus Clostridium. *J. Microbiol. Methods* **2007**, *70* (3), 452–464. <https://doi.org/10.1016/j.mimet.2007.05.021>.
- (138) Heap, J. T.; Kuehne, S. A.; Ehsaan, M.; Cartman, S. T.; Cooksley, C. M.; Scott, J. C.; Minton, N. P. The ClosTron: Mutagenesis in Clostridium Refined and Streamlined. *J. Microbiol. Methods* **2010**, *80* (1), 49–55. <https://doi.org/10.1016/j.mimet.2009.10.018>.
- (139) Johnston, C.; Martin, B.; Fichant, G.; Polard, P.; Claverys, J. Bacterial Transformation: Distribution, Shared Mechanisms and Divergent Control. *Nat. Rev. Microbiol. Lond.* **2014**, *12* (3), 181–196. <http://dx.doi.org/10.1038/nrmicro3199>.
- (140) Das, M.; Raythata, H.; Chatterjee, S. Bacterial Transformation: What? Why? How? And When? *Annu. Res. Rev. Biol.* **2017**, 1–11. <https://doi.org/10.9734/ARRB/2017/35872>.

- (141) Mercenier, A.; Chassy, B. M. Strategies for the Development of Bacterial Transformation Systems. *Biochimie* **1988**, *70* (4), 503–517. [https://doi.org/10.1016/0300-9084\(88\)90086-7](https://doi.org/10.1016/0300-9084(88)90086-7).
- (142) Longley, D. B.; Johnston, P. G. Molecular Mechanisms of Drug Resistance. *J. Pathol.* **2005**, *205* (2), 275–292. <https://doi.org/10.1002/path.1706>.
- (143) Holohan, C.; Van Schaeybroeck, S.; Longley, D. B.; Johnston, P. G. Cancer Drug Resistance: An Evolving Paradigm. *Nat. Rev. Cancer* **2013**, *13* (10), 714–726. <https://doi.org/10.1038/nrc3599>.
- (144) Shreffler, J. W.; Pullan, J. E.; Dailey, K. M.; Mallik, S.; Brooks, A. E. Overcoming Hurdles in Nanoparticle Clinical Translation: The Influence of Experimental Design and Surface Modification. *Int. J. Mol. Sci.* **2019**, *20* (23). <https://doi.org/10.3390/ijms20236056>.
- (145) Maletzki, C.; Bock, S.; Fruh, P.; Macius, K.; Witt, A.; Prall, F.; Linnebacher, M. NSG Mice as Hosts for Oncological Precision Medicine. *Lab. Invest.* **2020**, *100* (1), 27–37. <https://doi.org/10.1038/s41374-019-0298-6>.
- (146) Moghimi, S. M.; Simberg, D. Translational Gaps in Animal Models of Human Infusion Reactions to Nanomedicines. *Nanomed.* **2018**, *13* (9), 973–975. <https://doi.org/10.2217/nnm-2018-0064>.
- (147) Moghimi, S. M.; Farhangrazi, Z. S. Just so Stories: The Random Acts of Anti-Cancer Nanomedicine Performance. *Nanomedicine Nanotechnol. Biol. Med.* **2014**, *10* (8), 1661–1666. <https://doi.org/10.1016/j.nano.2014.04.011>.
- (148) Mink, J. G.; Radl, J.; van den Berg, P.; Haaijman, J. J.; van Zwieten, M. J.; Benner, R. Serum Immunoglobulins in Nude Mice and Their Heterozygous Littermates during Ageing. *Immunology* **1980**, *40* (4), 539–545.
- (149) Hare, J. I.; Lammers, T.; Ashford, M. B.; Puri, S.; Storm, G.; Barry, S. T. Challenges and Strategies in Anti-Cancer Nanomedicine Development: An Industry Perspective. *Adv. Drug Deliv. Rev.* **2017**, *108*, 25–38. <https://doi.org/10.1016/j.addr.2016.04.025>.
- (150) Jones, S. W.; Roberts, R. A.; Robbins, G. R.; Perry, J. L.; Kai, M. P.; Chen, K.; Bo, T.; Napier, M. E.; Ting, J. P. Y.; DeSimone, J. M.; Bear, J. E. Nanoparticle Clearance Is Governed by Th1/Th2 Immunity and Strain Background. *J. Clin. Invest.* **2013**, *123* (7), 3061–3073. <https://doi.org/10.1172/JCI66895>.
- (151) Tran, S.; DeGiovanni, P.-J.; Piel, B.; Rai, P. Cancer Nanomedicine: A Review of Recent Success in Drug Delivery. *Clin. Transl. Med.* **2017**, *6*. <https://doi.org/10.1186/s40169-017-0175-0>.
- (152) Smith, B. D.; Smith, G. L.; Hurria, A.; Hortobagyi, G. N.; Buchholz, T. A. Future of Cancer Incidence in the United States: Burdens Upon an Aging, Changing Nation. *J. Clin. Oncol.* **2009**, *27* (17), 2758–2765. <https://doi.org/10.1200/JCO.2008.20.8983>.

- (153) Miller, K. D.; Nogueira, L.; Mariotto, A. B.; Rowland, J. H.; Yabroff, K. R.; Alfano, C. M.; Jemal, A.; Kramer, J. L.; Siegel, R. L. Cancer Treatment and Survivorship Statistics, 2019. *CA. Cancer J. Clin.* **2019**, *69* (5), 363–385. <https://doi.org/10.3322/caac.21565>.
- (154) Cancer Prevalence and Cost of Care Projections <https://costprojections.cancer.gov/> (accessed Sep 25, 2020).

## CHAPTER 2: METHODS AND TECHNIQUES TO FACILITATE THE DEVELOPMENT OF *CLOSTRIDIUM NOVYI*-NT AS AN EFFECTIVE, THERAPEUTIC ONCOLYTIC BACTERIA<sup>2</sup>

### Abstract

The tumor microenvironment is characterized by anomalous vascularization, hypoxia, and acidity at the core of solid tumors that culminates in concentrated necrosis and immune system dysregulation among other effects. While this environment presents several challenges for the development of oncotherapeutics that deliver their activity via the enhanced permeability and retention (EPR) effect of the leaky blood vessels around a tumor, oncolytic bacteria, or a class of bacteria with a noted capacity to lyse solid tumors, are attracted to the very environment found at the center of solid tumors that confounds other therapeutics. It is this capacity that allows for a potent, active penetration from the tumor margins into the core, and subsequent colonization to facilitate lysis and immune reactivation. *Clostridium novyi* in particular has recently shown great promise in preclinical and clinical trials when administered directly to the tumor. These studies indicate that *C. novyi* is uniquely poised to effectively accomplish the long sought after ‘holy grail’ of oncotherapeutics: selective tumor localization via intravenous delivery. This study reports the development of efficient methods that facilitate experimental work and therapeutic translation of *C. novyi* including the ability to work with this obligate micro-anaerobe aerobically on the benchtop. Additionally, this study seeks to utilize this

---

<sup>2</sup> The material in this chapter was co-authored by Dailey, K. M.; Jacobson, R.I.; Johnson, P. R.; Woolery, T. J.; Kim, J.; Mallik, S.; Jansen, R; Brooks, A. E. Dailey, K. M. had primary responsibility for designing all experiments, collecting all data, analyzing all data, and generating subsequent figures and tables. Dailey, K. M. was the primary developer of the conclusions that are advanced here. Dailey K.M. also drafted and revised all versions of this chapter. Brooks, A. E. served as proofreader and checked the math in the statistical analysis conducted by Dailey, K. M.

newfound experimental flexibility to address several gaps in the current knowledge regarding the efficacy of CRIPSR/Cas9 gene insertion in this species to further develop this oncolytic bacteria and the genetic customization of bacteria in general.

### **Introduction**

Typically, the microenvironment of a solid tumor is considered a challenge for chemotherapeutic delivery. Characteristically poor vascularization of solid-state tumors is arguably the most difficult aspect of the microenvironment that limits the development of effective therapeutics. The disorganization of the intricate network of blood vessels caused by uncontrolled cellular growth leads to cells abnormally distant from local vessels, ultimately limiting oxygen diffusion as well as severely restricting other necessary nutrients<sup>1,2</sup>. Furthermore, this aberrant vascularization is responsible for a build-up of metabolic byproducts carbonic and lactic acid - resulting in both hypoxic and acidic gradients, with highly concentrated conditions in the center of the solid tumor<sup>3,1</sup>. Additionally, these characteristics have a variety of impacts upon the environment surrounding the tumor, including suppressing the local immune system<sup>4,5</sup>. Recent literature reports have also indicated that this local tumor environment may intrinsically promote further tumor development and subsequent metastases<sup>4</sup>. Despite these challenging conditions under which the majority of oncotherapeutics attempt to passively diffuse into the tumor with assistance from the enhanced permeability and retention (EPR) effect<sup>2</sup>, chemotherapeutics have been the standard of care for solid tumors for decades, and shown great efficacy<sup>6</sup>. However, recent evidence has suggested certain chemotherapies may be responsible for inducing greater resistance and furthering aggressive metastases of the solid tumor<sup>7,8</sup>. A re-examination of oncolytic bacteria may circumvent some of these current challenges.

In direct contrast to the EPR mechanism of action, certain species of bacteria - collectively termed oncolytic bacteria - have an innate attraction to the type of environment found at the center of solid tumors, allowing for a potent, *active* migration to the hypoxic/acidic tumor core<sup>9</sup>. Once the oncolytic bacteria have localized to the center of the tumor, they are able to successfully propagate and ultimately colonize and effectively influence the tumor<sup>10</sup>. Some select oncolytic bacterial species are able to directly lyse tumorigenic cells up to the normoxic margins of the tumor. Once they have migrated near the normoxic margin of the tumor, they can then effectively re-activate and recruit the previously suppressed immune response to complete the tumor irradiation<sup>11</sup>. In order for current pharmaceutical therapeutics to accomplish both tumor lysis and immune system activation, typically more than one drug must be used, further complicating the development of effective therapeutics. While oncolytic bacteria are not a new discovery<sup>12</sup>, due to several advantageous characteristics, it is unsurprising that they are reemerging on the therapeutic landscape<sup>13,14</sup>.

In particular, the motile, gram-variable *Clostridium novyi* has demonstrated several beneficial innate characteristics that lend itself to development as an oncotherapeutic. This oncolytic bacterial species is one of the few capable of both direct and indirect oncolysis, as well as potent recruitment of the immune system due to its gram variability<sup>15</sup>. *C. novyi* has the capacity to sporulate, resulting in a biphasic life cycle including: a proliferative, lytically capable vegetative form, and a more ‘dormant’ sporulated form<sup>16</sup>(Fig 2.1A). While the vegetative form is classified as an ultra-sensitive obligate anaerobe – and thus cannot survive in virtually any level of oxygen, the spore form does not show the same sensitivity. In fact, sporulated *C. novyi* are able to survive atmospheric oxygen; however, the sporulated form of *C. novyi* cannot accomplish germination to the lytic vegetative form until an adequately hypoxic environment (such as the



center of a solid tumor) has been located<sup>10,15,17</sup>. Unlike typical bacterial spores, *C. novyi* spores are thought to have some level of metabolic activity as they are able to sense and chemotax towards hypoxic/acidic gradients<sup>10</sup>, though the mechanism by which this occurs has yet to be elucidated. The culmination of these characteristics lends this particular oncolytic bacterial species to development as a potent therapeutic, which, at least in theory, has the capacity to treat not only a primary solid tumor, but also any metastases regardless of tissue location.

Indeed, *Clostridium novyi* has recently shown promise in mouse studies and preclinical trials<sup>9,13</sup>. Initial challenges of systemic toxicity encountered with *C. novyi* introduction to the bloodstream have been largely mitigated by the ability to create a non-toxic strain (*Clostridium novyi* NT) through a simple heat treatment causing the loss of the phage DNA encoded  $\alpha$ -toxin responsible<sup>15</sup>. Further studies detailing *C. novyi* NT introduction within murine models have suggested minimal toxicity and have observed no behavioral or histological signs of sepsis that were unable to be mitigated with the administration of fluids<sup>10</sup>. This landmark study also found that when *C. novyi* NT spores were intravenously delivered, 95% of murine subjects demonstrated some level of mitigation of subcutaneous tumors<sup>10</sup>. While this statistic is staggering in and of itself, upon examining the biodistribution of spores post-injection, it was shown that the vast majority of spores are quickly and innocuously cleared from subjects, with only around 1% of the initial dose localizing to the tumor<sup>10</sup>. Furthermore, as a testament to the exquisite specificity of this tumor-targeting effect, when other models of physiological hypoxia (*i.e.* ischemia) were tested, *C. novyi* NT colonization was not observed<sup>10</sup>. It is therefore reasonable to suggest that *C. novyi* NT spores could be modified for intravenous delivery to increase tumor localization.

In order to address these challenges and ultimately achieve clinical translation, a molecular toolkit must be developed through which to accomplish the modification of *C. novyi* NT spores, allowing them to “home” to a tumor upon intravenous injection. This study reports the development of efficient methods to facilitate experimental work and therapeutic translation of *C. novyi*. Additionally, it addresses several gaps in the current knowledge, and expands on the data regarding the efficacy of CRIPSR/Cas9 gene insertion in this particular species<sup>18</sup>.

## **Materials and Methods**

### **Vegetative *C. novyi* Growth**

Two different methods were used for anaerobic growth: an atmospheric chamber and an oxygen-fixing enzyme.

#### ***Atmospheric Chamber***

*Clostridium novyi* used in this study were purchased from ATCC (19402) as a lyophilized powder. Cells were cultured at 37°C in reinforced clostridial media (RCM) liquid cultures prepared per manufacturer’s instructions (Difco). Anaerobic conditions were achieved by using a carbon dioxide purged bench top atmospheric chamber (Spilfyter Hands-in-Bag 2-Hand Chamber) and seam tape (Tyvek). Additionally, an oxygen indicator was used to maintain anaerobicity (OxyBlue Indicator, Oxyrase Inc.). Furthermore, adequate biosafety was accomplished by purging the exhaust port through dual exposures to a sanitizer capable of mitigating spores (Spor-Klenz). Cultures were removed from the atmospheric chamber after being placed in airtight containers (BD GasPak EX container system) with adequate oxygen gas conversion sachets (BD GasPakEZ sachets). Solid media cultures were created by adding 3% w/v agar (Sigma Aldrich) to liquid RCM (as previously described). Once solidified, plates were degassed for 48hr prior to use by placing them in anaerobic conditions.

### ***Oxygen-Fixing Enzyme***

In order to work with *C. novyi* outside of the atmospheric chamber, an enzyme capable of producing anaerobic conditions in bacterial broths was used. RCM broth was prepared per the manufacturer's (Difco) protocol and Oxyrase for Broth (OB, Oxyrase Inc) was added to a final concentration of 10% v/v RCM:Oxyrase for Broth (RCM/OB). Solid media cultures used RCM media with 3% agar and Oxyrase for Agar (OA, Oxyrase Inc) per manufacturer's instructions. These solid media cultures were incubated in anaerobic chambers for bacterial growth (BD GasPak containers with sachets). These plates were incubated in anaerobic conditions until utilized. OxyDish specialized plates were also used with solid RCM media to create individual, single plate anaerobic chambers per the manufacturer's instructions (Oxyrase Inc).

### ***C. novyi Freezer Stocks***

3mLs of RCM+10% Oxyrase was inoculated with *C. novyi* and grown anaerobically at 37°C overnight. The resulting solution was spun at 13000rpm for five minutes to pellet vegetative cells and the supernatant was removed. The pellet was resuspended in RCM+10% Oxyrase+50% glycerol v/v as well as the erythromycin selective markers necessary for CRISPR plasmid retention. Resulting freezer stocks were frozen at -80°C.

### **Growth Curve**

Vegetative *C. novyi* cultures were sub-cultured to an OD<sub>600</sub> of 0.1, then allowed to grow for 74-96hrs with 200uL aliquots being harvested at 24 and 72hrs to observe and record OD<sub>600</sub>.

### **Sporulation of *C. novyi*: Atmospheric Chamber**

Sporulation media was adapted from previously published methods<sup>16</sup> and prepared as follows: 0.5g Na<sub>2</sub>HPO<sub>4</sub> (Sigma Aldrich), 3g peptone (Fisher Scientific), 0.05g L-cysteine (Alfa Aesar), 1g maltose (Difco), per 100mL distilled water. The resulting solution was brought to a

pH of 7.5 with NaOH. After aliquoting the media (10 mL) into autoclavable, screwtop, glass jars, dried cooked meat particles (0.5% w/v, Difco) were added. Following autoclaving, the media was degassed for 90 minutes in a sonicating water bath. An aliquot of vegetative *C. novyi* cells was then removed from RCM broth and inoculated into sporulation media. These cells were subsequently grown anaerobically in the sporulation media for a week prior to spore isolation.

### ***Oxygen-fixing Enzyme***

Media was prepared as detailed above for atmospheric chamber growth. Subsequently, the media was autoclaved and aseptically aliquoted prior to the addition of sterile OB (10% v/v, Oxyrase Inc), resulting in sporulation media. Dried cooked meat particles were autoclaved separately and added aseptically to each individual aliquot. An aliquot of vegetative *C. novyi* cells was centrifuged at 2000rpm, and the RCM media was removed. The resulting pellet of cells was inoculated into sporulation media. These cells were also subsequently grown in the sporulation media for a week before isolation.

### **Spore Isolation**

The spore isolation protocol was adapted from a previously published protocol<sup>19</sup> for purifying *C. difficile* spores. Briefly, the entire sporulation sample was centrifuged at 4000rpm in a swinging bucket rotor for 2min at 4°C. The supernatant was removed into Spor-Klenz, and the pellet resuspend in sterile, ice cold distilled water and washed with sterile, ice cold distilled water three times, being pelleted by centrifugated in a fixed angle rotor at 13,000rpm for 5mins each time. The washed spore preparation suspended in distilled water was then incubated at -20°C for at least 48hr to lyse any remaining vegetative cells. Samples were then thawed and centrifuged at 13000rpm for 5min, and the supernatant was removed. The resulting pellet was resuspended in 1ml sterile, ice cold distilled water and further washed in ice cold distilled water

as previously described for a total of five washes. At the conclusion of the washes, the spore preparation in 3mls water was then gently added to the top of a 50% w/v sucrose gradient (10 mL, ACS grade, Research Products International) in a 15ml polypropylene conical tube (Celltreat). The sucrose gradient was then centrifuged in a swinging bucket rotor at 4000rpm for 20min at room temperature. The authors note that better results were achieved when the sucrose gradient was chilled, but not when centrifuged at 4°C (data not shown). Vegetative cells and debris subsequently collect at the interface and distribute throughout the gradient, while the spores form a small, white pellet at the bottom of the tube. After centrifugation, the cell debris and sucrose solution was carefully removed, leaving the spore pellet. This pellet was resuspended into 1mL of sterile, room temperature distilled water and washed through repeated centrifugation at 13000rpm for 2min in a fixed angle rotor for a total of five washes. The final spore preparation was resuspended in 1mL purified distilled water.

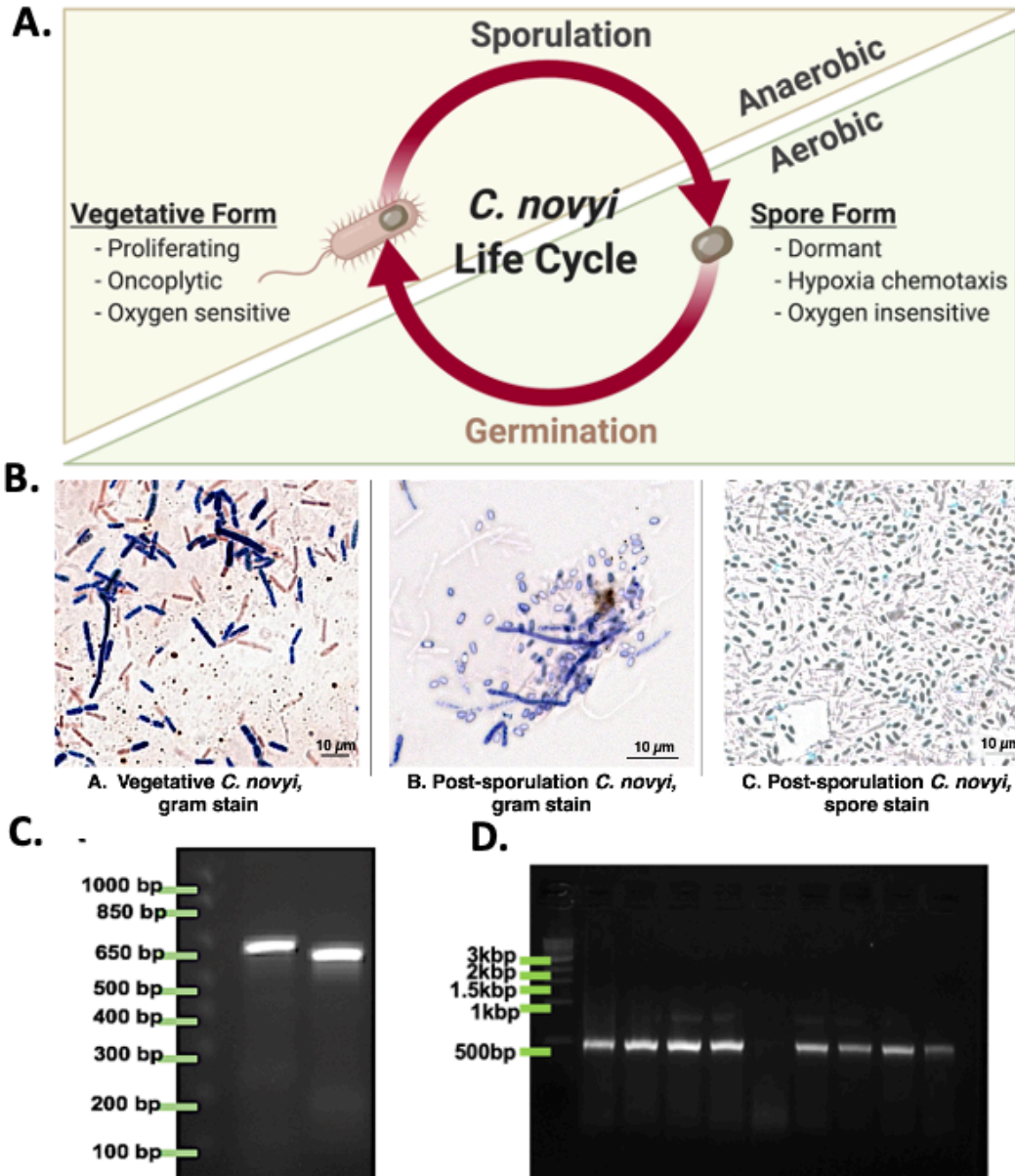


**Figure 2.1.** Demonstrating ability to grow *C.novyi*. A) Schematic representation of *Clostridium novyi* life cycle. B) Brightfield images captured under oil-immersion at 40X. From left to right: a) Gram stain of vegetative *C. novyi*, b) Gram stain of *C. novyi* post –sporulation, c) Malachite green spore stain of post-sporulation *C. novyi*. C) PCR amplicons primers designed with specificity to *C. novyi* 16s rRNA and a-toxin. D) PCR amplification with *C. novyi* a-toxin primers after a-toxin knockout was performed.

## **Spore Activation**

### ***Heat***

After sporulation and isolation, spores were forced to germinate to the vegetative state by heating the culture to 55°C for 20 minutes as previously published<sup>19</sup>.

### ***Tch Additives***

As previously reported for *C. difficile* cultures<sup>19</sup>, a final concentration of 0.1% w/v sterile taurocholate (Tch, Sigma Aldrich) was added to the RCM/OB broth. Subsequently, spores were inoculated into Tch supplemented RCM/OB broth after heat activation.

## **Spore Enumeration**

After spore activation, serial dilutions in sterile water were performed. 10uL of each sterile dilution was spot plated onto RCM agar plates and incubated anaerobically for 48hrs. After 48hrs, the plates were removed from the incubator and the colonies of each serial dilution spot were observed, counted, and recorded. The resulting number of colonies was used to calculate colony forming units (CFUs) per milliliter of media through this standard formula:  
$$\text{CFUs/ml} = (\# \text{colonies} \times \text{dilution factor}) / (\text{volume plated}).$$

## **Alpha-toxin Knock-Out**

A previously published method for *C. novyi* alpha toxin knockout<sup>16</sup> was modified. Briefly, purified spores suspended in water were heated to 70°C for 15min. Samples were then activated by a 20min incubation at 55°C. Solid RCM/agar plates previously degassed for at least 48hours were then inoculated with 100uL of treated spores per plate. Resulting colonies were allowed to grow for 48-72hr on RCM/agar in an anaerobic chamber at 37°C, then picked with a sterile tip to inoculate RCM broth. Liquid cultures were allowed to grow 48-72hr in an anaerobic chamber at

37°C. An aliquot was then harvested and concentrated to undergo colony PCR screening and confirm  $\alpha$ -toxin knock-out.

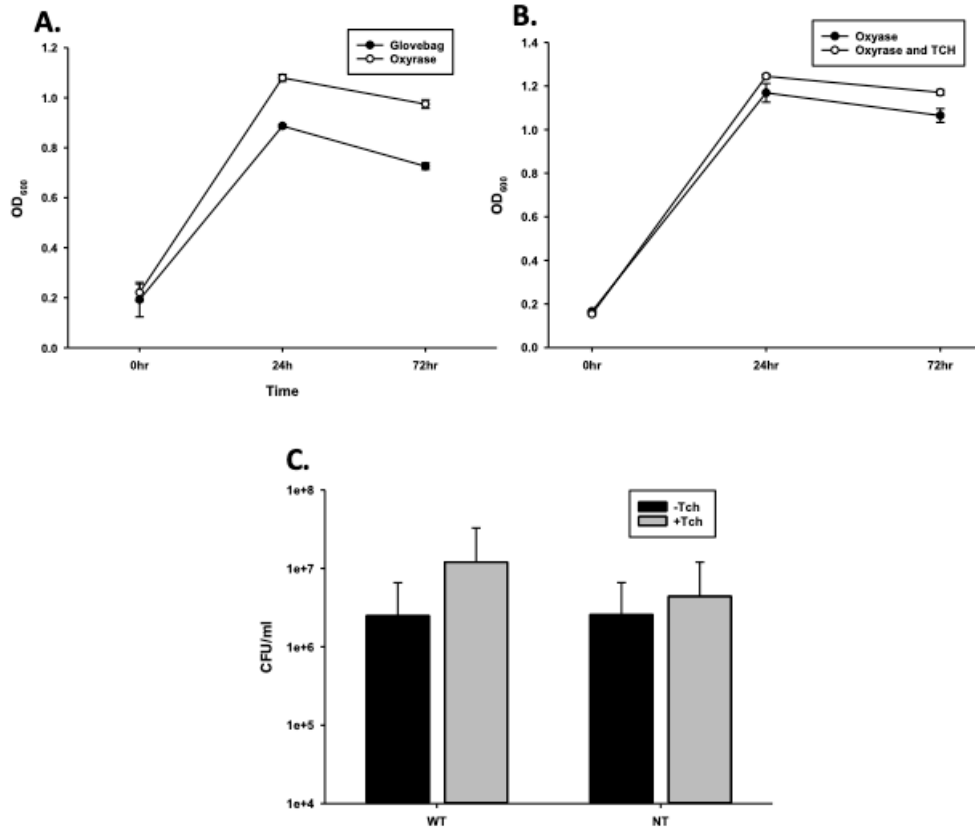


**Figure 2.2.** Comparison of growth techniques. A) Growth curves from observing OD<sub>600</sub> of *Costridium novyi* under glovebag conditions versus with oxyrase enzyme. No statistical difference was found at any time point as determined by a Student's standard t-test (n=3 samples per time point). B) Growth curves from observing OD<sub>600</sub> of *Costridium novyi* under in oxyrase versus oxyrase with the addition of taurocholate. No statistical difference was found at any time point as determined by a Student's standard t-test (n=3 samples per time point). C) Spore enumeration of *Clostridium novyi* wild type and non-toxic strains with and without the addition of taurocholate. No statistical difference was found at any time point as determined by a Holms-Sidak test. (n=3 samples per enumeration).

### Colony PCR Screening

GoTaq Green PCR master mix (Promega) was added to the concentrated aliquot of *C. novyi* cells along with the corresponding forward and reverse primers at a final concentration of 5uM (16s rRNA fwd aagtcgtggctggctattt; 16s rRNA rev ctccaagtgcctctccataag;  $\alpha$ -toxin fwd



gattcaagaggccacagagatag; a-toxin rev gaccacaccttcaaaccactta, IDT DNA) and adequate nuclease free H<sub>2</sub>O (Promega) to bring the final volume to 25uL. Reactions were incubated in a thermocycler according to the following program: 95°C for 5min, (95°C 30sec; 45°C 60sec; 68°C 60sec)x40 cycles, 68°C 5min. Resulting amplicons were loaded into a 1% agarose tris-buffered EDTA gel and separated at 120V for thirty minutes.

### ***C. novyi* Cell Staining**

#### ***Gram Stain***

An aliquot of *Clostridium novyi* liquid culture placed on an un-coated glass microscopy slide (Fisher Sci). The sample was heat fixed, then stained with crystal violet (BD Life Technologies) for 30s, rinsed with distilled water, then soaked in iodine (BD Life Technologies) for a minute. Subsequently, the slide was decolorized with 70% ethanol (BD Life Technologies), and counter stained with safarin red (BD Life Technologies) for a minute. Distilled water was used to rinse excess dye from the slide. The resulting sample was imaged via confocal microscopy (Zeiss Axio Imager M2) under oil immersion at 100x.

#### ***Spore stain***

After sporulation and spore isolation processes had been conducted, a small sample of the resulting solution was washed and resuspended in distilled water. This sample was then heat fixed to an uncoated glass slide for subsequent staining. 0.5% w/v malachite green (VWR) aqueous solution was used to cover the bacterial sample and slides were exposed to a steam bath for five minutes, adding more malachite green as necessary to prevent drying out. After five minutes the slide was rinsed with distilled water and counter stained with safarin red (BD Life Technologies) for a minute and washed again with distilled water. The resulting sample was imaged via confocal microscopy under oil immersion at 100x.

## **Comparison of *C. novyi* to *C. difficile* and *E. coli***

The published *C. novyi* transcriptome<sup>20</sup> was mined to determine the ten highest and lowest expressed genes. These gene sequences were then used to identify putative orthologous genes in both *Escherichia coli* and *Clostridium difficile* through utilization of NCBI BLASTn, UniProt, and GeneID databases. While orthologous sequences for all genes were not located – especially those for the ten least expressed *C. novyi* genes, which are presumably species specific – those that were identified were used to generate a codon adaptation index (CAI) as well as the gene characteristics of GC skew and percent purines (%R) through previously published formulas<sup>21,22</sup>. Putative molecular fraction (% mol) values were mined from previously published gene expression data<sup>23–25</sup> and compared to establish the similarity of *C. novyi* to both *C. difficile* and *E. coli*, more well characterized bacteria species.

## **CRISPR/Cas Plasmid Design**

### ***Cas Enzyme***

pNICKclos1.0 (Addgene #73639), an engineered CRISPR/Cas9 plasmid, was purchased and used for these experiments. This plasmid contained sequences encoding *Streptococcus pyogenes* Cas9nickase protein (5'-NGG-3' protospacer adjacent motif) as well as multiple cloning sites including the *SpeI/NotI* sites for crRNA insertion and *NotI/XhoI* for the gene insert. This plasmid has been used and published to successfully perform CRISPR-mediated gene editing in *Clostridium* species previously<sup>18</sup>. For clarification, figure 2.1B contains a detailed schematic of the cloning cassette inserted into this plasmid backbone.

### ***Gene Insertion Target Selection***

Data was mined from the transcriptome tables produced<sup>20</sup> to identify an appropriate target for gene integration into the spore's coat for ease of identification and assessment. Gene targets

were assessed by the following criteria: 1) integration of the gene insert under the promoter for a surface display protein, 2) avoidance of genes encoding chemotaxis or anaerobic functions, including the operon containing NT01CX2374, NT01CX2375, NT01CX2376, 3) avoidance of any lipases NT01CX0979, NT01CX2047, and NT01CX0630, 4) avoidance of spore genes highly upregulated during tumor infection (21 genes identified<sup>20</sup>). Based on this study's expression goal, four genes (NT01C0401, NT01CX0481, NT01CX1621 and NT01CX1736) were identified as appropriate targets utilizing these criteria.

### ***sgRNA Design***

The primary nucleotide sequence for these four genes was manually analyzed for protospacer adjacent motif (PAM) sequences correlating to the *SpCas9n* contained within pNICKclos1.0. Once candidate sequences were generated, ThermoFisher (<https://apps.thermofisher.com/crispr/index.html>) as well as IDT DNA CRISPR/Cas9 design tools ([https://www.idtdna.com/site/order/designtool/index/CRISPR\\_CUSTOM](https://www.idtdna.com/site/order/designtool/index/CRISPR_CUSTOM)) were used to compare the CRISPR RNA (crRNA) sequence options generated. crRNA sequences were ranked by on-target efficacy, off-target potential (as determined manually via a BLASTn search of the *C. novyi* genome for sequences with high percent identity) and secondary structural concerns (e.g. to avoid internal hairpin formation). Two crRNA sequences were chosen for each gene to be synthesized as gene blocks from Invitrogen. The primary sequence of the crRNAs were synthesized within cloning restriction enzyme sites correlating to the cloning sites present on pNICKclos1.0 (*SpeI* and *NotI*) with an additional unique restriction digest site (*BglII*) included for use in cloning verification. The trans-activating CRISPR RNA (tracrRNA) necessary to recruit *SpCas9n* was included in the backbone immediately to the 3' of the cloning restriction digest sites and was not modified from the original sequence contained within pNICKclos1.0.

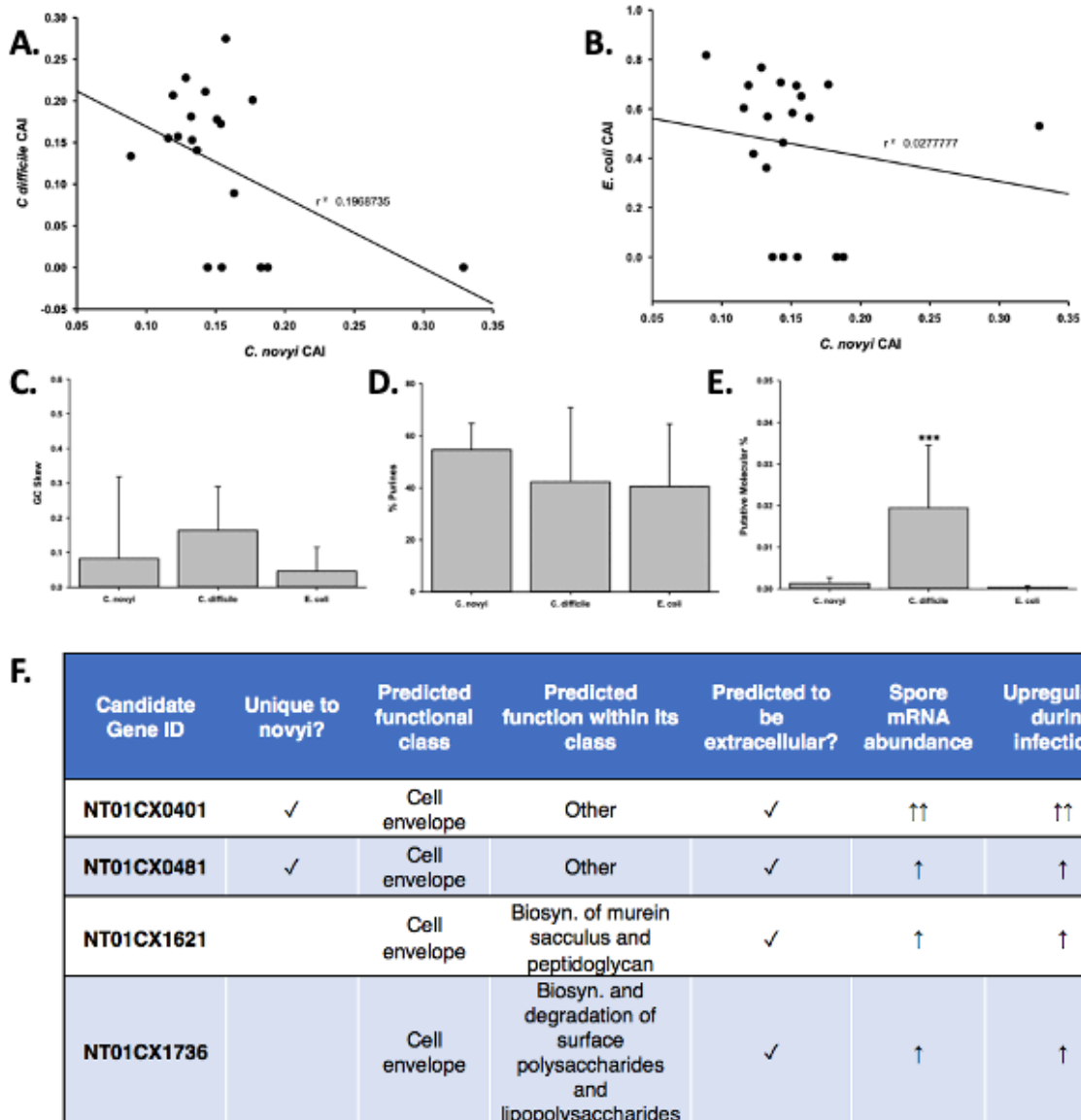


**Figure 2.3.** Designing the plasmid. A and B) The resulting codon adaptation index (CAI) values for orthologous genes in *C. difficile* or *E. coli* were plotted against those of *C. novyi* to ascertain a correlation. C-D) Upon the comparison of the primary sequences of *C. novyi* genes with the orthologs found in *C. difficile* and *E. coli*, the GC skew (C) was determined as was the percent purines for each sequence (D). E) The literature was mined for expression data and the putative molecular percent was obtained for each gene and its ortholog. F) Table indicating the chosen *C. novyi* genes to target CRISPR mediated gene insertion and a few of the important characteristics considered when selecting these targets.

### ***Flanking HDR Arm Design***

The gene sequence 1kbp upstream and 1kbp downstream of the cleavage site determined by the selected crRNA sequenced was used to generate the homologous arms that flank the gene insert. Both arms were contained within unique restriction digest cloning sites (*NotI-KpnI* for the upstream arm and *SacI-XhoI* for the downstream arm) to lend unique flexibility to this CRISPR cassette (Fig. 2.1B). In order to accomplish validation through the construction and cloning of this plasmid, a unique verification restriction digest site, *KpnI*, was included.

### ***Gene Insert***

A simple six amino acid tag was reverse transcribed to account for *C. novyi* codon bias. A Shine-Dalgarno sequence and TATA box were included upstream of the gene insert before the start codon, also translated to account for codon bias. Additionally, an *EcoRV* enzyme site was designed to be present within the HDR template to be used for repair. This restriction digest site would then be incorporated into the genome, indicating gene modification was successful.

### **CRISPR/Cas Plasmid Construction**

#### ***crRNA and HDR Cassette Synthesis***

HDR arms were synthesized to contain an eighteen-nucleotide gene insert between the two flanking arms as a single cassette for ease of cloning. Both the HDR cassette and correlating crRNA sequence were synthesized by GeneArt Gene Services (ThermoFisher Scientific).

#### ***crRNA Insertion***

The resulting oligonucleotide from GeneArt and the pNICKclos1.0 plasmid was digested with *SpeI*-HF and *NotI*-HF (New England Biolabs, Inc) enzymes in CutSmart Buffer (New England Biolabs, Inc) at 37°C for 1hr to generate coordinating sticky-end overhangs. These samples were then run out on a 3% agarose gel at a low voltage, and gel excision was used to

isolate the correct fragments. Subsequently, fragments were purified via the GeneJET Gel Extraction Kit (Thermo Fisher). Purified fragments were then combined with 10uL NEBuilder HiFi DNA Assembly Master Mix (New England Biolabs, Inc) in a 2:1 insert to vector ratio for a total volume of 20uL. This ligation mixture was incubated at 50°C for an hour, then transformed into *E. coli* immediately. NEB 5-alpha Chemically Competent *E.coli* (New England Biolabs, Inc) were transformed via manufacturer's protocol (30min incubation of 2ug plasmid with 25uL of cells for thirty minutes, 90sec heat shock at 42°C, returned to ice for two minutes, then resuspended in 500uL of SOC media, incubated in shaking incubator for 1hr with 100uL plated on ampicillin containing media) with the assembled plasmid. Candidate colonies were grown up in Luria Broth culture supplemented with ampicillin as a selective marker. Transformed plasmid DNA was isolated via GeneJET Plasmid Miniprep kit (Thermo Fisher) and the resulting plasmid DNA was digested with *Bgl*II-HF in CutSmart Buffer at 37°C for 1hr. Digested DNA was run on a 1% agarose gel and analyzed to verify the crRNA sequence had been inserted into pNICKclos1.0. Once crRNA insertion was confirmed, the pNICKclos1.0+sgRNA plasmid was used for HDR cassette insertion.

### ***HDR Cassette Insertion***

The purchased gene cassette from GeneArt and the pNICKclos1.0+sgRNA plasmid were digested with *Not*I-HF and *Xho*I (New England Biolabs, Inc) enzymes in CutSmart Buffer (New England Biolabs, Inc) at 37°C for 3hr to generate coordinating sticky-end overhangs. These samples were then run out on a 3% agarose gel at a low voltage, and the correct fragments were excised from the gel. Excised fragments subsequently underwent gel purification via the GeneJET Gel Extraction Kit (Thermo Fisher). Purified fragments were then ligated using NEBuilder HiFi DNA Assembly Master Mix (New England Biolabs, Inc) in a 2:1 insert to vector

ratio for a total volume of 20uL. This ligation mixture was incubated at 50°C overnight out of direct light. The reassembled, engineered plasmid was then transformed into NEB 5-alpha Chemically Competent *E.coli* (New England Biolabs, Inc) 30min incubation of 2ug plasmid with 25uL of cells for thirty minutes, 90sec heat shock at 42°C, returned to ice for two minutes, then resuspended in 500uL of SOC media, incubated in shaking incubator for 1hr with 100uL plated on ampicillin containing media, with ensuing candidate colonies grown up in Luria Broth cultures with ampicillin and harvested via GeneJET Plasmid Miniprep isolation kit (Thermo Fisher). The resulting plasmid DNA was digested with *KpnI*-HF in CutSmart Buffer at 37°C for 1hr. After incubation, the digestion was run out on a 1% agarose gel and analyzed to verify insertion of the HDR cassette into pNICKclos1.0+sgRNA002. Once HDR cassette insertion was confirmed, the complete pKMD002 plasmid was transformed into NEB 5-alpha Chemically Competent *E. coli* (New England Biolabs, Inc) by the protocol detailed previously and a GeneJET Maxiprep plasmid isolation kit (Thermo Fisher) was used to harvest and purify a stock of plasmid DNA. This purified plasmid DNA was used to transform calcium competent *C. novyi*.

### **Preparation of Calcium Competent *C. novyi***

RCM/OB broth was inoculated with vegetative *C. novyi* and incubated at 37°C in anaerobic conditions overnight. A 30mL of RCM/OB was inoculated to contain a final concentration of 10% v/v of the previous overnight culture. This larger culture was allowed to grow at 37°C in anaerobic conditions overnight to a desired OD<sub>600</sub> of 0.6-0.8. The authors noted that while ODs above this range were largely indifferent, ODs below this range had difficulty surviving the protocol (data not shown). The resulting culture was moved to conicals prechilled at -20°C overnight and centrifuged at 2000rpm and 4°C for 40min. The resulting supernatant was removed, and the pellet was resuspended in 8mL 0.1M CaCl<sub>2</sub> (EMD Millipore) + 10% v/v

Oxyrase for Broth (Oxyrase Inc) prechilled to 4°C. This solution was incubated on ice for thirty minutes, then centrifuged in a swinging bucket rotor at 2000rpm and 4°C for 40min. The supernatant was removed and the pellet was resuspended in 2mL prechilled (4°C) 0.1M CaCl<sub>2</sub>:15% glycerol (Thermo Fisher) + 10% v/v Oxyrase for Broth, then aliquoted into prechilled (-20°C) Eppendorf tubes.

### **Transformation of Calcium Competent *C. novyi***

Calcium competent *C. novyi* cells were allowed to thaw on ice. Subsequently, 5ug of either purified pUC19 control plasmid (New England BioLabs Inc) or the purified pKMD002 plasmid was added to an empty prechilled 15mL tube (4°C). Competent *C. novyi* cells (100uL) were added directly on top of the plasmid DNA in the prechilled tube without vortexing or mixing. The resulting solution of cells and plasmid DNA was incubated on ice for twenty minutes. This mixture was then heat shocked at exactly 42°C for precisely ninety seconds and immediately returned to ice for two minutes. RCM/OB broth was added to each sample, which was then allowed to grow over night at 37°C anaerobically. Note that twenty-four hours of growth is the approximate equivalent to a single life cycle for *C. novyi*, and thus the selective marker was not added until adequate time was allowed for plasmid uptake and expression. After 24hrs, ampicillin (50mg/ml final conc., Fisher Scientific) was added to cells transformed with pUC19 control plasmid while erythromycin (250ug/ml final conc., Sigma Aldrich) was added to cells transformed with pKMD002. Regardless of the antibiotic selective pressure applied, all transformed cells subsequently were allowed to grow anaerobically for twenty-four hours at 37°C. Cells were then plated onto RCM/OA/ampicillin (*C.novyi* transformed with pUC19) or RCM/OA/erythromycin (*C. novyi* transformed with pKMD002) agar plates and grown in



OxyPLUS anaerobic chamber plates for 48hrs. Resulting colonies were counted and used to calculate colony forming units per milliliter media of the successfully transformed *C. novyi*.

### **Verifying Plasmid Transformation**

Candidate colonies resulting from the pKMD002 transformation were picked, designated Candidates A-E, and grown in RCM/OB broth for 48hrs (Fig 2.5A). Selective marker pressure was not maintained beyond 48hrs to facilitate plasmid loss, potentially preventing off-target CRISPR DNA breakage and cell stress that would result in cell death. An aliquot was harvested during the 48hr selective pressure period to determine if the pKMD002 plasmid was indeed present after transformation. This aliquot of *C. novyi* underwent plasmid DNA isolation via GeneJET Plasmid Miniprep kit (Thermo Fisher). PCR utilizing GoTaq Green PCR MasterMix (Promega) and primers specific to the HDR domain of pKMD002 (primers: Internal HDR forward – ttactcagccttaggattacaga, Internal HDR reverse – tcaggtatagttgcaggaatgaa) was done with isolated plasmid as the template, according to the following program: 95°C for 5min, (95°C for 30sec, 45°C for 1min, 72°C for 2min)x40 cycles, and then 72°C for 5min. The resulting amplicons were restriction digested with *EcoRV*-HF (New England BioLabs, Inc) in CutSmart Buffer at 37°C for 1hr, then run out in a 1% agarose gel at 120V. Gels were imaged on an Omega LumG gel imaging system and analyzed to verify the presence of pKMD002.

### **Verifying Genomic Modification**

Aliquots of Candidates A-E were harvested after 48hrs of growth in non-selective media. These samples underwent TRIzol (Zymo Research) genomic DNA isolation according to manufacturer's protocol (Fig 2.5A). Extracted genomic DNA then underwent PCR utilizing primers specific to the HDR domain contained within pKMD002 (see above) that include an *EcoRV* restriction site for verification. PCR was performed using GoTaq Green PCR MasterMix

(Promega) and a thermocycler program as follows: 95°C for 5min, (95°C for 30sec, 45°C for 1min, 72°C for 2min) x40 cycles, 72°C for 5min. The resulting amplicons were digested with the *EcoRV*-HF (New England BioLabs, Inc) in CutSmart Buffer at 37°C for 1hr and run on a 1% agarose gel at 120V. Gels were imaged and analyzed for genomic insertion after exposure to pKMD002 as previously described.

## **Determining Off-Target Effects**

### ***Growth Curves***

RCM/OB cultures were grown for Candidates A-E and sub-cultured to an OD<sub>600</sub> of 0.1, then allowed to grow for 74-96hrs with aliquots being harvested at as previously described to establish growth curves.

### ***Spore Enumeration***

Candidates A-E underwent forced sporulation and germination as detailed previously. Colony forming units were observed and recorded to determine CFU/mls.

### ***Cell Lysis***

PANC-1 cells were grown using Dubelco's Modified Essential Media (DMEM, Caisson Labs) with 10% v/v fetal bovine serum (VWR) and 1% v/v penicillin-streptomycin (Caisson Labs) and 1% v/v fungicide additives (Fungizome Antimycotic, Thermo Fisher). Cells were plated at 100,000 cells per well in a 12-well plate (Corning Costar) and were allowed to attach at 37°C in 5% carbon dioxide overnight. Subsequently, adhered cell cultures were inoculated with *C. novyi* cultures at a concentration of 5000 spores per well. Co-cultures of human and bacterial cells were incubated both aerobically (normal cell culture) and anaerobically (in BD GasPakEZ containers with sachets) for 24hrs. The media was then removed, and wells were rinsed with phosphate buffered saline (Caisson Labs) before fresh media containing purified resazurin

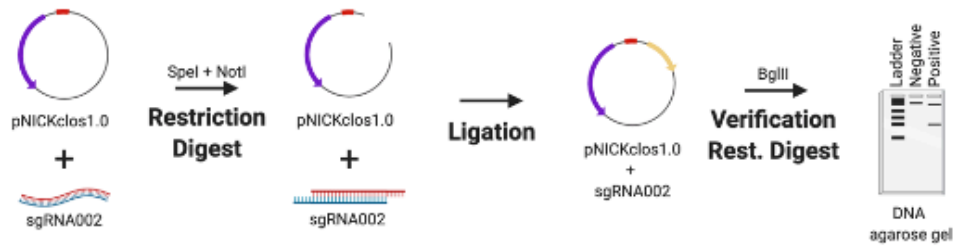
(44uM final conc, Thermo Fisher) was added. Cells were incubated with the cell viability determining enzyme for five hours, and then Abs<sub>570</sub> was observed and recorded.

## Results

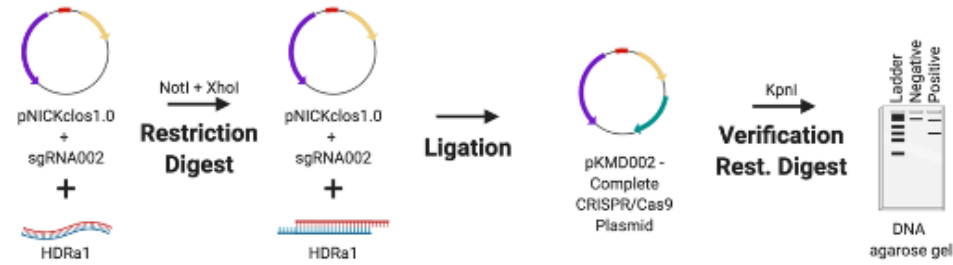
### Establishing Growth of *C. novyi* (Fig 2.1) :*C. novyi* Cell Images

Since *C.novyi* is an ultrasensitive anaerobe when in its vegetative, proliferative state even growing it prior to any manipulation was challenging. Initially, cells were grown in RCM media within a bench top atmospheric chamber (a glovebag). Maintaining an anaerobic atmosphere under these conditions can be challenging; hence, to confirm the growth of vegetative *C. novyi* (ATCC 19402), cells were gram stained. A gram stained sample of vegetative *C. novyi* visually confirmed the presence of gram-variable rod-shaped bacteria. Alternatively, vegetative cells were forced to sporulate as described in the methods, and spores were stained with malachite green. Similarly, to ensure that spores had indeed been isolated, cells were forced to germinate through a modified heat treatment protocol and stained with gram stain (Fig 2.1Bb) as well as a malachite green differential stain. The presence of spores was visually confirmed (Fig 2.1Bc). Although cultures visually appeared and stained as expected for *C.novyi*, 16s rRNA PCR was used to confirm its presence. The *in silico* predicted amplicon sizes for 16s rRNA and  $\alpha$ -toxin were 578bp, and 533bp respectively. Colony cracking and PCR of the anaerobic bacterial cultures resulted in amplicons of the expected length (Fig 2.1C), confirming the presence of *C. novyi* specifically.

### A. I. sgRNA incorporation



### II. HDR and Gene Insert incorporation



### CRISPR Cloning Cassette

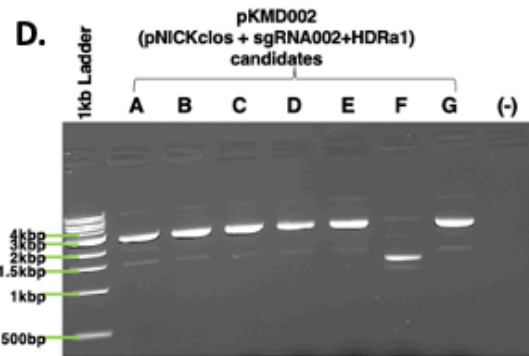
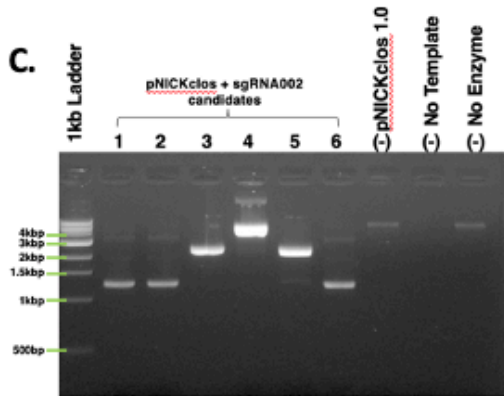
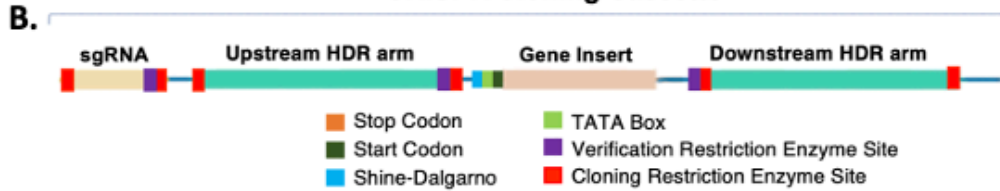


**Figure 2.4.** Building the CRISPR/Cas9n plasmid. A) Schematic representation of stepwise cloning method. B) DNA domain map of CRISPR cloning cassette build and utilized within pNICKclos1.0 to generated plasmid (pKMD002) used in this study. C) Verification restriction digests confirming the insert of sgRNA002 targeting NT01CX0401. Singlet is negative for insertion of desired sgRNA after digest with BglII, doublet indicates positive insertion. D) Verification restriction digests confirming the insert of HDR cassette corresponding sgRNA002 to gene target NT01CX0401. Singlet is negative for insertion of desired sgRNA after digest with KpnI, doublet indicates positive insertion.

## **$\alpha$ -Toxin Removal**

Establishing a Non-Toxic strain of *C. novyi* (*C. novyi* NT) required the removal of a phage DNA plasmid contained within Wild Type *C. novyi*. A modification of the knock-out published heat treatment protocols<sup>16</sup> was performed on sporulated *C. novyi* cells to include an activation step at 50°C. Briefly, PCR with *C. novyi*  $\alpha$ -toxin specific primers was conducted to confirm the absence of a 533bp amplicon that results from  $\alpha$ -toxin phage DNA, thus confirming this protocol adaptation had yielded several *C. novyi-NT* (non-toxic) colonies (Fig 2.1D).

## **Comparison of Growth Techniques (Fig 2.2)**

To probe the efficacy of the oxygen-fixing microbial broth additive Oxyrase for Broth (OB) to create an anaerobic environment capable of sustaining *C. novyi* cells, *C. novyi* vegetative cells were seeded in both a carbon dioxide purged atmospheric chamber (glovebag) and in an aerobic atmosphere with broth containing OB. Aliquots were removed every 24hrs over 72 total hours and OD<sub>600</sub> was observed and recorded (Fig 2.2A).

## **Addition of Tch**

Previous publications describing methods for *C. difficile* have indicated that higher levels of spore germination to vegetative cells can be achieved with the addition of 0.1% taurocholate (tch) to the media<sup>19</sup>. To establish the effect of supplementing the media with tch, as well as begin to probe the efficacy of using already established *Clostridia* protocols with *C. novyi*, growth curves were generated. Purified *C. novyi* spores were forced to germinate through heat activation in RCM/OB media or RCM/OB/Tch media, and resulting cultures were observed by OD<sub>600</sub> for 72hrs (Fig 2.2B). Notably, previous experiments comparing RCM with RCM plus Oxyrase for broth indicated that there was no significant difference in growth due to Oxyrase (Fig 2.1). The resulting growth curves demonstrated no statistical significance when tch was

added to the media. To further corroborate these results, spores were isolated and subsequently forced to germinate, and ensuing spore enumeration was quantified via serially diluted colony forming units on solid RCM/Oxyrase for Agar (OA) media. Again, no statistical difference was observed for either *C. novyi* Wild Type or Non-Toxic strain with the addition of Tch to the media.

### **CRISPR/Cas9n Plasmid Design (Fig 2.3)**

#### ***Comparing C. novyi Genes to C. difficile and E. coli***

In order to select the most suitable targets for insertion into the genome, it was necessary to determine the relationship of gene sequences of *C. novyi* compared to those in the more characterized species, *C. difficile* and *E. coli*. The ten most and ten least expressed genes from the published transcriptome<sup>20</sup> were compared to orthologous sequences found through BLASTn searches in *E. coli* and *C. difficile*. The codon adaptation index (CAI) was then determined through the application of a well-known formula<sup>21,22</sup>, and the resulting CAI were used to create a scatter plot to establish the correlation between *C. novyi* and *C. difficile* as well as *C. novyi* and *E. coli* (Fig 2.3A and 2.3B). Basic characteristics, such as the GC skew (Fig 2.3C), percent purines (%R, Fig 2.3D) of *C. novyi* genes and putative orthologs were determined based on the primary sequence for each gene. Additionally, a putative molecular percentage of total protein expression for the protein encoded by each gene was mined from the literature<sup>23-25</sup> and compared in Figure 2.3E. No significant correlation was found for the comparative analysis of gene sequences, indicating a necessity to manually design and implement experimental methods and gene constructs specific to *C. novyi*.

After mining the published *C. novyi* transcripts and proposed proteome<sup>20</sup>, several genes were chosen as targets within which to insert a foreign gene encoding a six amino acid tag.

Targets were selected ultimately based on the following criteria: 1) integration of the gene insert under the promoter for a surface display protein, 2) avoidance of genes encoding chemotaxis or anaerobic functions, including the operon containing NT01CX2374, NT01CX2375, NT01CX2376, 3) avoidance of lipases NT01CX0979, NT01CX2047, and NT01CX0630, 4) avoidance of spore genes highly upregulated during tumor infection (21 genes identified<sup>20</sup>). Expression of the tag was thus targeted to the surface of the spore coat. Subsequent sgRNA and HDR gene cassettes were designed with these four genes as targets: NT01C0401, NT01CX0481, NT01CX1621 and NT01CX1736 (Fig 2.3F).

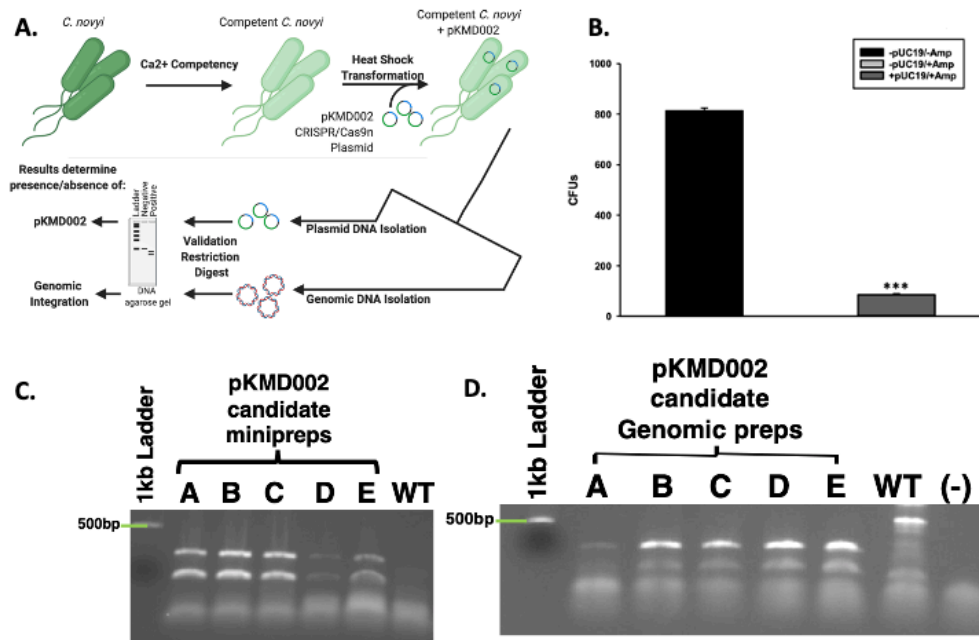


**Figure 2.5.** Calcium competent *C. novyi* transformations A) Schematic representation of experimental flow. B) Resulting CFUs after *C. novyi* cells underwent calcium competent transformation with pUC19. Statistical significance was determined to be  $p < 0.001$  through the application of the Holms-Sidak test ( $n=3$  experiments) C) After calcium competent *C. novyi* were transformed with pKMD002, five candidates (A-E) underwent plasmid isolation, and restriction digest to confirm plasmid present in cultures. Singlet is negative for presence, doublet is positive due to the presence of a *EcoRV* site designed in the insert. D) After calcium competent *C. novyi* were transformed with pKMD002, five candidates (A-E) underwent genomic DNA isolation, and subsequent restriction digestion to confirm plasmid present in cultures. Singlet is negative for genomic insertion, doublet is positive due to the presence of a *EcoRV* site designed within the insert.

### ***Building the CRISPR/Cas9n Plasmid (Fig 2.4)***

The CRISPR cloning cassette (Fig 2.4B) to insert the gene encoding a six amino acid tag was built in the pNICKclos1.0 backbone. To facilitate downstream screening as well as to build a versatile cloning system, several restriction sites were included. Briefly, the *Bg*/III restriction digest site was predicted by *in silico* experiments to indicate successful insertion of the desired sgRNA sequence by resulting in a doublet of 10.1kb and 973bp. If cloning was unsuccessful, *in silico* digestion resulted in a single band of 11kb after digestion. Using this strategy, several candidate plasmids were observed to produce the correctly sized doublet pattern, indicating successful insertion of sgRNA002 into the pNICKclos1.0 backbone. pNICKclos 1.0 with the inserted sgRNA002 was subsequently used to integrate the HDR cassette. Once again, *in silico* modeling indicated successful insertion of the entire HDR and gene insert cassette would be indicated by doublet bands at 8.137kb and 2.967kb after digestion with the validation enzyme *Kpn*I, while unsuccessful cloning would result in a single fragment of 11kb. Using this strategy, *Kpn*I digestion resulted in several candidates, completing the CRISPR/Cas9n plasmid pKMD002.

Earlier attempts to transform *Clostridia* sp.s, or indeed virtually any species other than *E. coli*, have met with extremely low efficiency plasmid uptake. To overcome this challenge, a standard protocol to create calcium competent *E. coli* was modified to include Oxyrase enzymes for use with *C. novyi*. To confirm the validity of this method, prepared competent *C. novyi* were transformed with pUC19. The resulting colonies after transformation were counted and colony forming units per milliliter of PBS was determined (Fig 2.5A). A significant difference was observed for transformations that occurred without ampicillin or pUC19 ( $p < 0.001$ ). Subsequently, calcium competent *C. novyi* cells were transformed with the complete



CRISPR/Cas9 plasmid, pKMD002, and grown under erythromycin selective pressure. No breakthrough colonies were noted. Several colonies grew on erythromycin containing RCM/OA plates after transformation with pKMD002, indicating several candidates for CRISPR/Cas9 gene modification. Upon isolating plasmid DNA from the candidate colonies, PCR was conducted with primers corresponding to the HDR arms and amplicons were validated via restriction digest with *EcoRV*. All five tested candidates contained the pKMD002 plasmid as per the doublet pattern observed (Fig 2.5B). Once the presence of the plasmid was confirmed, genomic DNA was isolated to evaluate if introduction of pKMD002 had conferred a genomic insertion of the cassette encoding the six amino acid tag. Primers correlating to the sequence flanking the site of gene insertion were used with genomic DNA from each candidate as a template (Fig 2.5C). *EcoRV* was used to digest the amplicons, with those candidates positive for gene insertion showing a doublet after *EcoRV* digestion, indicating that the HDR template had been used to repair the DNA damaged by Cas9n. This doublet appeared in all five candidates as predicted and was absent in un-transformed *C. novyi* genomic DNA. Thus, five positive clones were identified after transformation with pKMD002.

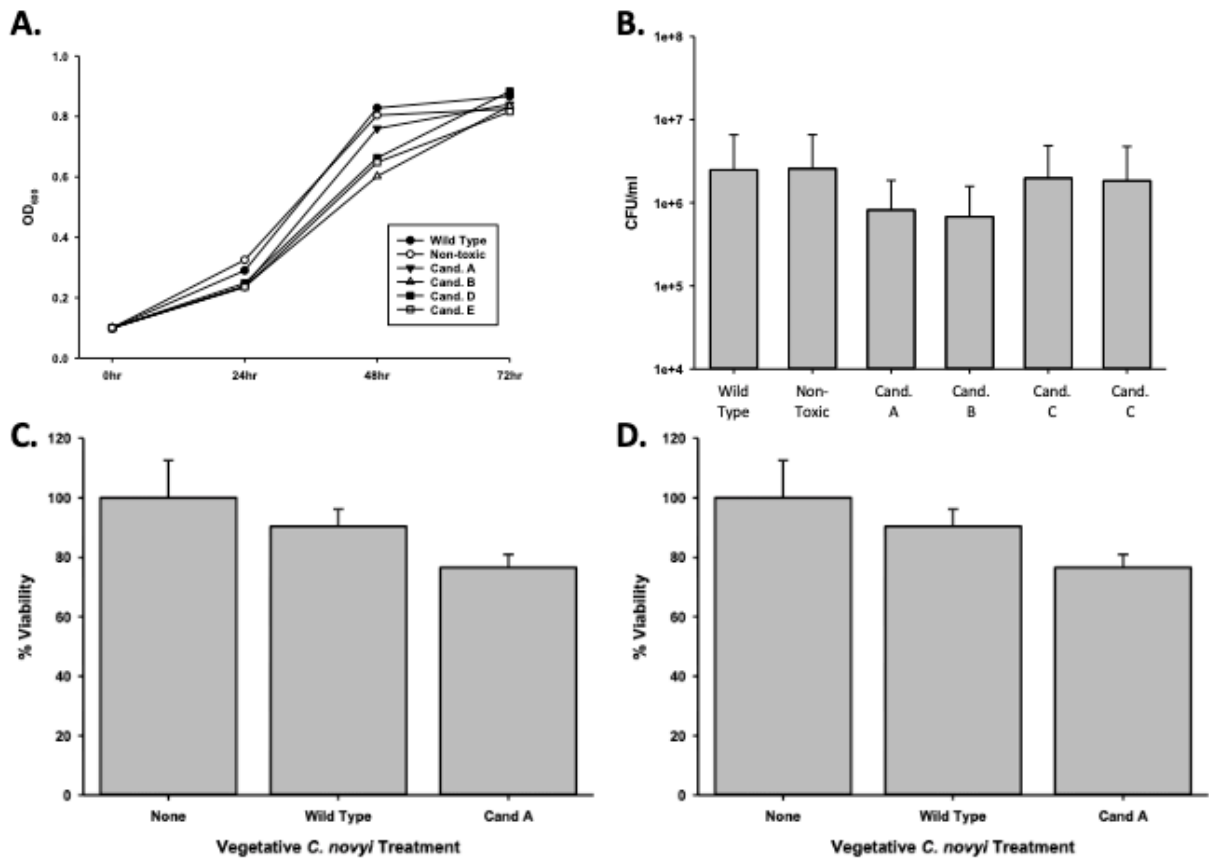


**Figure 2.6.** Determining off-target effects of CRISPR/Cas9 mediated gene editing. A) Growth curves were determined by observing candidates A-E were for 72 hours collecting OD<sub>600</sub> at significant time points. No statistical difference was determined at any time point (n=3 for each time point, Holms-Sidak test, p=0.056). B) Spore enumeration was conducted for genetically modified candidates and compared to non-modified wild-type and non-toxin *C. novyi* strains. No statistical difference was determined at any time point (n=3 for each strain, Holms-Sidak test, p=0.058) C) Cell lysis was determined under both anaerobic and aerobic conditions by applying vegetative *C. novyi* wild-type, non-toxic, candidate a, and non-toxic candidate a to PANC-1 cells. (No statistical significance was determined by Holms-Sidak test n=3 for each group).

Once it was established that genomic integration had occurred, each candidate was characterized to elucidate any physiological manifestation of off target gene modification events. To elicit its oncolytic effect at the most basic level, *C. novyi* must be able to sporulate and germinate as well as to lyse cells. Initially, candidates were evaluated for their ability to traverse their life cycle normally. Candidates were grown in RCM/OB broth for 72hours with aliquots harvested every 24hours. The OD<sub>600</sub> of each of these candidates' samples was observed and

recorded (Fig 2.6A). A Holms-Sidak statistical test found no significant difference between the growth of any of the candidates and the *C. novyi* wild-type or non-toxic cells lines ( $p > 0.05$ ). Each gene insertion candidate was then sporulated and subsequently forced to germinate back to its vegetative form. Each candidate was capable of sporulating and germinating. Additionally, upon germination, serial dilutions were used to determine colony forming units (Fig 2.6B). Again, a Holms-Sidak statistical test found no significant difference between any of the candidates and the *C. novyi* wild-type or non-toxic cells lines ( $p > 0.05$ ). After the life cycle of modified *C. novyi* was established, its ability to lyse cancer cells was determined. To determine if any genes involved in the innate lytic capacity of *C. novyi* had been subjected to off-target gene modification that would lead to loss of function, *C. novyi* vegetative cells and spores were co-cultured with PANC-1 cells both anaerobically and aerobically. Data presented is normalized to the no treatment in corresponding culture conditions (aerobic or anaerobic). No significant lysis occurred in any of the co-cultures when incubated aerobically and no statistical differences were determined between the genetically modified candidate A or wild-type *C. novyi* when cultured anaerobically.

## Discussion

*C. novyi* has quite the potential to become an oncotherapy – perhaps even the ‘holy grail’ oncotherapy not only able to distinguish tumorigenic cells from normal cells but also able to do so through intravenous introduction for both primary solid tumors as well as metastases. However, the development of *C. novyi* as such a treatment is hindered at least in part by a lack of established methods with which to conduct experimentation into what makes this bacterial species so promising. Indeed, while *C. novyi*’s innate ultra-sensitivity to oxygen confers its potential to be developed as a targeted, intravenous therapy, this same characteristic is

intimidating when it comes to formulating and executing experiments. Typically, the growth of anaerobic bacterial species requires expensive and cumbersome atmospheric chambers, such as gloveboxes or glovebags. Furthermore, all experimentation and equipment necessary for downstream experiments (*e.g.* centrifuges, vortexes, heat blocks, etc.) must also conform to these environmental restrictions, fitting inside the confines of these environmental controls. At a fundamental level, this study established the ability to work with *C. novyi* cultures outside of the restraints of a controlled atmosphere with relative ease (Fig 2.2), thus substantially improving both the physical and theoretical flexibility and range of methods than can be used.

Once the physical constraints of working with an anaerobic organism were eased, this study was able to adapt and build upon several other methods to increase efficacy and allow genetic manipulation of *C. novyi*, thereby further reducing the hurdles facing the clinical translation of *C. novyi* (Fig 2.5). One of the primary hurdles encountered is the possibility of sepsis due to off target effects. Through the addition of a 55°C incubation after the published 70°C heat cycle alpha toxin phage DNA, responsible for much of the toxicity associated with *C. novyi*, was able to reliably and efficiently be removed (Fig 2.1D). After presumably increasing the safety of *C. novyi* treatments by knocking out alpha toxin, introducing new, advantageous functions via genetic manipulation became the next challenge to overcome. Previous methods had met with limited success<sup>18,26</sup>. According to the published efficiency rate of the original protocol<sup>16</sup>, the modification performed here conferred an increased efficiency of approximately 10- to 100-fold (data not shown). Hence the development of methods to create and transform chemically competent *C. novyi* were tackled.

The generation of calcium competent *C. novyi* cells, demonstrated here for the first time (Fig 2.5B), would not have been possible without the use of RCM/OB broth to create an

anaerobic environment within the broth itself, allowing *C. novyi* experimentation to occur on the benchtop. Without the ability to substantially increase transformation efficacy by approximately 100-fold and subsequently accomplish plasmid transformation within *C. novyi*, CRISPR gene editing would not have been possible. The ability to overcome low transformation efficiency gives rise to a wide range of potential further experimentation for *C. novyi*, including further attempts at genetic modification. Notably, during the process of methods optimization, it was also established that despite the high percent genetic identity shared with *C. difficile*, not all of the techniques that garner success in that particular strain can be directly applied to *C. novyi* (Fig 2.2B, 2.2C). This study found that though *C. difficile* demonstrates a significant response to the addition of taurocholate to growth media, particularly after germination, *C. novyi* does not. This data, combined with a lack of correlation found in Fig 2.3, may indicate that while *C. novyi* and *C. difficile* are cousins, *C. novyi* has many unique characteristics prohibiting the direct application of data characterizing *C. difficile*. While this study found that simple adaptations of *C. difficile* methods were effective in many cases, these protocols (*i.e.* sucrose gradient spore purification) had more to do with the shared physical characteristics of the two species than the biochemical or genotypic similarities (Fig 2.3A-E).

### **Comparison to Other Bacterial Species and Techniques**

The current study attempted to probe the relevance of methodologies that have been established in other bacterial species, including *C. novyi*'s closely related cousin *C. difficile* and the commonly utilized *E. coli* (Fig 2.3A-E) through a basic characterization of orthologous genes. Much of the current methodology available for *C. novyi* is largely based on the assumption of phenotypic similarity as a result of genotypic similarity to its more well-known cousins such as *C. difficile*. While by no means exhaustive, this study probed differences in the

codon adaption index between three species using the ten most and least expressed genes from a previously published report detailing the transcriptome of *C. novyi*. The data generated in this study failed to establish any correlation between CAIs of *C. novyi*'s ten most and least expressed genes and their corresponding orthologous genes in *C. difficile* or *E. coli*. No statistically significant differences were noted when comparing the GC skew or %R of these genes between the three species via these methods. However, a statistical significance was found for the %mol of the twenty selected genes in *C. difficile* when compared to both *C. novyi* and *E. coli*. Since this data was generated through mining published literature, it should be noted that this significance could be an artifact of the *in vitro* conditions from which this data was obtained. The current study provides a necessary glimpse into species-specific genetic differences that must be accounted for when conducting genetic modification studies such as this. As a result of this analysis, commercially available methods and algorithms based largely on model species such as *E. coli* and *C. difficile* were not solely relied upon to accomplish the generation of CRISPR elements utilized. Manual methods were included to design and verify the validity of the chosen sequences to accomplish CRISPR gene modification. Furthermore, methodology was neither excluded nor included based upon the species it had previously been successfully performed within, instead, an iterative process ensued to establish the best practices with which to accomplish genetic modification of this unique oncolytic species.

### **CRISPR/Cas Gene Modification in *C. novyi***

Traditional CRISPR/Cas9 has been reported to cause increased cell death in *Clostridium* species, likely due to double strand breaks initiated by Cas9. This study was able to overcome this complication through the utilization of Cas9nickase (Cas9n) - a Cas9 with a mutated active site resulting in a single stranded DNA break encoded in the plasmid pNICKClos1.0 (Addgene).

This plasmid had previously been published to accomplish gene modification in other *Clostridium* species, but not *Clostridium novyi* in particular. Thus, it remained an open question whether or not the promoters and basic genetic elements of the plasmid would work in this particular species that has demonstrated several unique characteristics when compared with other members of its genus. While a single stranded DNA nick might limit the efficacy of DNA repair, *C. novyi* experiences an innate molecular bias to homologous domain repair rather than non-homologous end joining<sup>18</sup>. In theory, this bias could overcome - or at least mitigate - any decreased efficiency observed from the use of a Cas9n. When homologous domain repair (HDR) occurs in response to a DNA damage event, a repair template is used that corresponds, or is homologous, to the sequences immediately flanking the breakage site<sup>18</sup>. The same method occurs when the DNA damage occurs synthetically, such as through targeted cleavage accomplished by Cas9n. This study took advantage of this naturally occurring repair pathway to accomplish the genomic insertion of the genetic sequence encoding a simple six amino acid tag. The genetic sequence intended for insertion was prefaced by several novel elements not published in any previous bacterial CRISPR/Cas gene modification schemes: a ribosomal binding Shine-Dalgarno site as well as a TATA box promoter sequence.

While this study identified four potential gene insertion targets with two corresponding crRNA segments for each gene to accomplish the spore coat expression of a six amino acid insert, ultimately only a single target was necessary to accomplish gene editing. Generally, experimental duplicity at the molecular level is necessary with construction the CRISPR plasmids, particularly in the context of naturally high GC content, such as that seen in the *C. novyi* genome. However, surprisingly, no such complications were encountered and a single sgRNA, sgRNA002 was ultimately used for this study. This is very good news for the field

because it should reduce the hesitance to attempt further gene modification studies in this particular species.

### **Off-Target Effects**

Currently, the field of CRISPR gene modification is just beginning to elucidate how the implementation of this particular mechanism differs in prokaryotes from that performed in eukaryotic organisms. There has been some hesitancy when attempting CRISPR gene modification in prokaryotes due to the presence of a naturally occurring CRISPR system as an equivalent of the adaptive immune system<sup>26</sup>. This study represents one of the first to begin to probe the efficacy of such a gene modification system in a non-model bacteria. These results indicate that no measurable physiological off-target gene modification events occurred when the life cycle and lytic capacity was tested. However, it is important to note that this study was limited in that we cannot ensure expression in the spore coat based on the assays performed. Additionally, this study is further limited by the application of vegetative cells to a monolayer cell culture when it has been well detailed that these conditions are unlikely to replicate those that are conducive for lysis *in vivo*. Yet, these studies undeniably provide necessary insights into the potential for genetically modifying oncolytic bacteria to generate better suited characteristics for clinical translation.

### **Conclusion**

As a unique oncolytic species, *C. novyi* has the potential to provide significant benefits to the current chemotherapeutic regimens; however, a lack of tools has hindered progress in this direction. This study described the development and modification of several key steps forward in the methodology necessary for further experimentation and commercialization of *C. novyi*. Given the exponential expansion in the applications of CRISPR/Cas mediated genomic



engineering in eukaryotes to address disease states of all kinds, it is surprising that this modification has yet to gain the same level of popularity in prokaryotes. Much of the recent literature has suggested a hesitancy to attempt CRISPR-mediated gene modification in bacterial species due to the presence of endogenous CRISPR systems<sup>26-28</sup>. It is thought that any synthetic, targeted attempts to accomplish gene editing will combine synergistically to ultimately result in wide spread off-target modifications at best, and at worst systemic cell death<sup>26-28</sup>. However, as the data contained within this study demonstrates, due to the expansion of CRISPR technology, there are now ways to design an effective, selective CRISPR system despite the presence of endogenous mechanisms. In fact, we believe quite the opposite – that the presence of an endogenous CRISPR mechanism increases the on-target efficacy while decreasing the off-target capacity in ways not seen in eukaryotes.

Furthermore, much of the challenges initially encountered in applying CRISPR gene editing to bacteria can be addressed through the ever expanding CRISPR toolkit. New alliterations on this type of genomic customization have been rapidly discovered and herald the dawn of a new era in harnessing the power of single-celled organisms. In particular, this study utilized the capacity of a Cas9 enzyme modified to create a single stranded break instead of the canonical double stranded DNA break to overcome the noted propensity that double stranded DNA breaks cause wide-spread cell death in bacteria, particularly in *Clostridial* species<sup>18</sup>. Special attention was taken in this study to select an originating species for the sequence corresponding to a Cas9 enzyme with a PAM sequence different from that noted for enzymes isolated from *Clostridia*, conferring an added layer of target specificity to this study. The generation the system with which to conduct CRISPR/Cas9 gene modification contained within this report had to be applied manually due to a lack of fundamental knowledge, conferring a

level of attention to detail that has been advantageously phased out with the development of commercial eukaryotic systems. It is our hope that this study will serve as inspiration leading to the generation of similar capacities in prokaryotic systems, particularly those of the oncolytic bacteria poised to become the next generation of oncotherapeutics.

### **Acknowledgments**

The authors would like to acknowledge the use of Biorender.com for the creation of several figures contained within this publication. The authors also acknowledge funding support from the Center for Diagnostic and Therapeutic Strategies in Pancreatic Cancer at North Dakota State University. A special thanks to the NDSU Agriculture Department's Advanced Imaging Microscopy laboratory, specifically Pawel Borowitz and Jordan Flaten.

### **Author Contributions**

Conceptualization: KMD, AEB.; writing—original draft preparation: KMD, AEB; review and editing: KMD, AEB; data generation: KMD, RIJ, PRJ, TJW, RJ; figure creation and editing: KMD, AEB, PRJ; supervision: AEB, SM, JK; supplies: AEB, SM, JK.

### **Funding**

This research was funded in part by a pilot project award to AEB from NIH COBRE award 1P20 GM109024 (SM) and by a NDSU Graduate School Dissertation Fellowship to KMD.

### **Conflicts of Interest**

The authors declare no conflicts of interest. The funders had no role in the design of this publication; in the collection, analyses, or interpretation of data; in the writing of the manuscript, or in the decision to publish the results.

## References

- (1) McKeown, S. R. Defining Normoxia, Physoxia and Hypoxia in Tumours—Implications for Treatment Response. *Br. J. Radiol.* **2014**, *87* (1035). <https://doi.org/10.1259/bjr.20130676>.
- (2) Minchinton, A. I.; Tannock, I. F. Drug Penetration in Solid Tumours. *Nat. Rev. Cancer* **2006**, *6* (8), 583–592. <https://doi.org/10.1038/nrc1893>.
- (3) Finger, E. C.; Giaccia, A. J. Hypoxia, Inflammation, and the Tumor Microenvironment in Metastatic Disease. *Cancer Metastasis Rev.* **2010**, *29* (2), 285–293. <https://doi.org/10.1007/s10555-010-9224-5>.
- (4) Boedtkjer, E.; Pedersen, S. F. The Acidic Tumor Microenvironment as a Driver of Cancer. *Annu. Rev. Physiol.* **2020**, *82* (1), 103–126. <https://doi.org/10.1146/annurev-physiol-021119-034627>.
- (5) Gonzalez, H.; Hagerling, C.; Werb, Z. Roles of the Immune System in Cancer: From Tumor Initiation to Metastatic Progression. *Genes Dev.* **2018**, *32* (19–20), 1267–1284. <https://doi.org/10.1101/gad.314617.118>.
- (6) Miller, K. D.; Nogueira, L.; Mariotto, A. B.; Rowland, J. H.; Yabroff, K. R.; Alfano, C. M.; Jemal, A.; Kramer, J. L.; Siegel, R. L. Cancer Treatment and Survivorship Statistics, 2019. *CA. Cancer J. Clin.* **2019**, *69* (5), 363–385. <https://doi.org/10.3322/caac.21565>.
- (7) Redmond, K. M.; Wilson, T. R.; Johnston, P. G.; Longley, D. B. Resistance Mechanisms to Cancer Chemotherapy. *Front. Biosci. J. Virtual Libr.* **2008**, *13*, 5138–5154. <https://doi.org/10.2741/3070>.
- (8) Mansoori, B.; Mohammadi, A.; Davudian, S.; Shirjang, S.; Baradaran, B. The Different Mechanisms of Cancer Drug Resistance: A Brief Review. *Adv. Pharm. Bull.* **2017**, *7* (3), 339–348. <https://doi.org/10.15171/apb.2017.041>.
- (9) Wei, M. Q.; Mengesha, A.; Good, D.; Anné, J. Bacterial Targeted Tumour Therapy-Dawn of a New Era. *Cancer Lett.* **2008**, *259* (1), 16–27. <https://doi.org/10.1016/j.canlet.2007.10.034>.
- (10) Diaz, L. A.; Cheong, I.; Foss, C. A.; Zhang, X.; Peters, B. A.; Agrawal, N.; Bettegowda, C.; Karim, B.; Liu, G.; Khan, K.; Huang, X.; Kohli, M.; Dang, L. H.; Hwang, P.; Vogelstein, A.; Garrett-Mayer, E.; Kobrin, B.; Pomper, M.; Zhou, S.; Kinzler, K. W.; Vogelstein, B.; Huso, D. L. Pharmacologic and Toxicologic Evaluation of C. Novyi-NT Spores. *Toxicol. Sci.* **2005**, *88* (2), 562–575. <https://doi.org/10.1093/toxsci/kfi316>.
- (11) Wang, Y.; Guo, W.; Wu, X.; Zhang, Y.; Mannion, C.; Brouchkov, A.; Man, Y.-G.; Chen, T. Oncolytic Bacteria and Their Potential Role in Bacterium-Mediated Tumour Therapy: A Conceptual Analysis. *J. Cancer* **2019**, *10* (19), 4442–4454. <https://doi.org/10.7150/jca.35648>.

- (12) Chien, T.; Doshi, A.; Danino, T. Advances in Bacterial Cancer Therapies. *Curr. Opin. Syst. Biol.* **2017**, *5*, 1–8.
- (13) Safety Study of Intratumoral Injection of Clostridium Novyi-NT Spores to Treat Patients With Solid Tumors That Have Not Responded to Standard Therapies - Full Text View - ClinicalTrials.gov <https://clinicaltrials.gov/ct2/show/NCT01924689> (accessed Apr 24, 2019).
- (14) BioMed Valley Discoveries, Inc. *Phase I Safety Study of Intratumoral Injection of Clostridium Novyi-NT Spores in Patients With Treatment-Refractory Solid Tumor Malignancies*; Clinical trial registration NCT01924689; clinicaltrials.gov, 2019.
- (15) Staedtke, V.; Roberts, N. J.; Bai, R.-Y.; Zhou, S. Clostridium Novyi-NT in Cancer Therapy. *Genes Dis.* **2016**, *3* (2), 144–152. <https://doi.org/10.1016/j.gendis.2016.01.003>.
- (16) Dang, L. H.; Bettegowda, C.; Huso, D. L.; Kinzler, K. W.; Vogelstein, B. Combination Bacteriolytic Therapy for the Treatment of Experimental Tumors. *Proc. Natl. Acad. Sci. U. S. A.* **2001**, *98* (26), 15155–15160. <https://doi.org/10.1073/pnas.251543698>.
- (17) Staedtke, V.; Bai, R.-Y.; Sun, W.; Huang, J.; Kibler, K. K.; Tyler, B. M.; Gallia, G. L.; Kinzler, K.; Vogelstein, B.; Zhou, S.; Riggins, G. J. Clostridium Novyi-NT Can Cause Regression of Orthotopically Implanted Glioblastomas in Rats. *Oncotarget* **2015**, *6* (8), 5536–5546.
- (18) Joseph, R. C.; Kim, N. M.; Sandoval, N. R. Recent Developments of the Synthetic Biology Toolkit for Clostridium. *Front. Microbiol.* **2018**, *9*. <https://doi.org/10.3389/fmicb.2018.00154>.
- (19) Edwards, A. N.; McBride, S. M. Isolating and Purifying Clostridium Difficile Spores. *Methods Mol. Biol. Clifton NJ* **2016**, *1476*, 117–128. [https://doi.org/10.1007/978-1-4939-6361-4\\_9](https://doi.org/10.1007/978-1-4939-6361-4_9).
- (20) Bettegowda, C.; Huang, X.; Lin, J.; Cheong, I.; Kohli, M.; Szabo, S.; Zhang, X.; Diaz, L.; Velculescu, V.; Parmigiani, G.; Kinzler, K.; Vogelstein, B.; Zhou, S. The Genome and Transcriptomes of the Anti-Tumor Agent Clostridium Novyi-NT. *Nat. Biotechnol.* **2007**, *24*, 1573–1580. <https://doi.org/10.1038/nbt1256>.
- (21) Musto, H.; Romero, H.; Zavala, A. Translational Selection Is Operative for Synonymous Codon Usage in Clostridium Perfringens and Clostridium Acetobutylicum. *Microbiology* **2003**, *149* (4), 855–863. <https://doi.org/10.1099/mic.0.26063-0>.
- (22) Sharp, P. M.; Li, W. H. The Codon Adaptation Index--a Measure of Directional Synonymous Codon Usage Bias, and Its Potential Applications. *Nucleic Acids Res.* **1987**, *15* (3), 1281–1295.
- (23) Ishihama, Y.; Schmidt, T.; Rappsilber, J.; Mann, M.; Hartl, F. U.; Kerner, M. J.; Frishman, D. Protein Abundance Profiling of the Escherichia Coli Cytosol. *BMC Genomics* **2008**, *9*, 102. <https://doi.org/10.1186/1471-2164-9-102>.

- (24) Janoir, C.; Denève, C.; Bouttier, S.; Barbut, F.; Hoys, S.; Caleechum, L.; Chapetón-Montes, D.; Pereira, F. C.; Henriques, A. O.; Collignon, A.; Monot, M.; Dupuy, B. Adaptive Strategies and Pathogenesis of *Clostridium Difficile* from in Vivo Transcriptomics. *Infect. Immun.* **2013**, *81* (10), 3757–3769. <https://doi.org/10.1128/IAI.00515-13>.
- (25) Permpoonpattana, P.; Phetcharaburanin, J.; Mikelson, A.; Dembek, M.; Tan, S.; Brisson, M.-C.; Ragione, R. L.; Brisson, A. R.; Fairweather, N.; Hong, H. A.; Cutting, S. M. Functional Characterization of *Clostridium Difficile* Spore Coat Proteins. *J. Bacteriol.* **2013**, *195* (7), 1492–1503. <https://doi.org/10.1128/JB.02104-12>.
- (26) Cho, S.; Shin, J.; Cho, B.-K. Applications of CRISPR/Cas System to Bacterial Metabolic Engineering. *Int. J. Mol. Sci.* **2018**, *19* (4). <https://doi.org/10.3390/ijms19041089>.
- (27) Barrangou, R. The Roles of CRISPR–Cas Systems in Adaptive Immunity and Beyond. *Curr. Opin. Immunol.* **2015**, *32*, 36–41. <https://doi.org/10.1016/j.coi.2014.12.008>.
- (28) Bikard, D.; Jiang, W.; Samai, P.; Hochschild, A.; Zhang, F.; Marraffini, L. A. Programmable Repression and Activation of Bacterial Gene Expression Using an Engineered CRISPR-Cas System. *Nucleic Acids Res.* **2013**, *41* (15), 7429–7437. <https://doi.org/10.1093/nar/gkt520>.

## CHAPTER 3: PROBING CLINICAL RELEVANCE: ESTABLISHING THE EFFICACY OF *C. NOVYI* AGAINST A PANEL OF 2D CULTURED PANCREATIC CANCER

### CELLS<sup>3</sup>

#### Abstract

Pancreatic cancer presents a unique challenge for the development of effective oncotherapies. The tumor microenvironment (TME) of this type of tumor typically contains a dense desmoplastic barrier composed of aberrant extracellular matrix proteins, as well as an acidic, hypoxic and necrotic core. Additionally, the immune system surrounding this type of tumor has often been suppressed by the TME. Hence, choosing the correct model of the tumor microenvironment within which to test a potential anti-cancer therapy is a critical experimental design decision. While the typical solid tumor contains a complex microenvironment including both phenotypic and genotypic heterogeneity, the methods used to model this disease state often do not reflect this complexity. This simplistic approach may have contributed to stagnant five-year survival rates experienced over the past four decades. Oncolytic bacteria, a class of bacteria with the innate ability to seek and destroy solid tumors has been revived from historical anecdotes in an attempt to overcome these challenges. Regardless of the promise of oncolytic bacteria, accurate assessment of the potential requires choosing the proper tumor model. This study explores the impact of cancer cell lines co-cultured with Wild-Type *C. novyi* to establish the efficacy of this oncolytic bacteria in a monolayer culture.

---

<sup>3</sup> The material in this chapter was co-authored by Dailey, K.M.; Jacobson, R.I.; Kim, J.; Mallik, S.; Brooks, A.E. Dailey, K. M. had primary responsibility for designing all experiments, collecting all data, analyzing all data, and generating subsequent figures and tables. Dailey, K. M. was the primary developer of the conclusions that are advanced here. Dailey K.M. also drafted and revised all versions of this chapter. Brooks, A. E. served as proofreader and checked the math in the statistical analysis conducted by Dailey, K. M

## Introduction

Only around five percent of patients diagnosed with a pancreatic tumor survive the next five years – a staggering statistic that has not changed in four decades<sup>1,2</sup>. This stagnant statistic stands in stark contrast to the significantly improved outlooks for most other major cancer types<sup>1,2</sup>. In large part, the difficulty in treating this particular type of solid tumor is due to several challenging aspects of the tumor microenvironment (TME). While these characteristics are commonly found in other solid tumors, they are considered almost ubiquitous for pancreatic tumors, presenting unique and inescapable challenges for developing effective oncotherapies. The TME of a pancreatic tumor is typically characterized by a dense abnormal extracellular matrix forming a desmoplastic barrier<sup>3,4</sup>. This dense structure not only limits the number of patients who are candidates for surgical tumor removal, but also inhibits the diffusion of traditional chemotherapeutics into the center of the tumor<sup>3</sup>. Furthermore, the center of solid tumors is very distant from any blood vessels, and thus distant from the delivery of oxygen or nutrients as well as the removal of toxic metabolic byproducts. This distance from blood vessels ultimately results in a highly acidic, necrotic tumor core that continues to confound current oncotherapeutics<sup>5</sup>, and predisposing the tumor to a high rate of metastasis. In fact, pancreatic cancer has a metastases rate of about 80%, ranking in the top five most metastatic cancer types<sup>1</sup>. This characteristic is particularly concerning as most tumors and thus the cells that constitute the tumor have developed an ability to evade the immune system through various mechanisms of suppression<sup>6</sup>.

This acidic, immunosuppressive, necrotic microenvironment presents a level of complexity, including both phenotypic and genotypic heterogeneity, that is rarely recapitulated in the methods used to model solid tumors, which can be relatively simplistic. Traditionally,

establishing the efficacy of a novel therapeutic in a pre-clinical trial occurs through the use of monolayer cellular culture. However, over the past decade, an increasing amount of literature has begun to establish how important it is for an *in vitro* tumor model to accurately capture the three dimensional growth that occurs *in vivo*<sup>7,8</sup>, calling into question the value of such pre-clinical experimentation . In fact, while all novel cancer therapeutics must demonstrate anti-tumor activity quite thoroughly in pre-clinical experimentation, only about five percent of therapeutics that enter clinical trials successfully achieve clinical translation<sup>9</sup>. It is therefore entirely possible that clinical translation for many novel treatments has been confounded or at least complicated by weighing results generated in monolayer tissue culture too greatly.

In order to address the challenges facing current oncotherapies, several treatments from historical anecdotes are being reconsidered – especially with the advent of new technologies such as CRISPR/Cas gene editing. Among these therapies is a class of bacteria termed oncolytic bacteria for their innate ability to seek out the complex, harsh microenvironment contained in the center of solid tumors. As opposed to current therapeutic options that rely on the enhanced permeability and retention (EPR) effect for drug delivery to the tumor margins and passive diffusion of the therapeutic from the margins to the tumor core<sup>10,11</sup>, oncolytic bacteria have an innate, yet poorly understood, ability to navigate through the bloodstream to actively sense, locate and mobilize to the center of the tumor and subsequently destroy the tumor from the inside out<sup>12,13</sup>. One of these oncolytic bacterial species, *Clostridium novyi*, has shown a great deal of potential as an anti-cancer therapeutic. There is at least one current clinical study probing the efficacy of an attenuated, non-toxic form as an intratumorally injected therapy<sup>14</sup> and pre-clinical studies have alluded to the potential to develop *C. novyi* to be delivered intravenously<sup>15</sup>. Given the potential for intravenous delivery, and thus potential efficacy against both the primary tumor



as well as any metastases, methods and techniques to evaluate this novel therapeutic must be developed. Paramount among these methods is the appropriate *in vitro* tumor model for initial evaluation.

Several monolayer pancreatic cancer cell lines have been developed in order to test the potential of novel therapeutics. For the purposes of this study, both the most commonly utilized human-originated cell lines and a murine pancreatic cancer cell line have been included. While the human cell lines have very clear – though limited – clinical relevance, the murine KPC cell line is used to generate pancreatic tumors in immunocompetent mice to give rise to a disease model that includes the immune system<sup>16</sup>. Characteristics of the original tissue sample have been included in Table 3.1 for reference, and Table 3.2 contains the genotypic information for the four most commonly mutated genes in tumorigenic pancreatic cells. A more thorough review of these characteristics and other pancreatic cancer lines can be found elsewhere in the literature<sup>9,17</sup> and lies beyond the scope of this study. Nevertheless, a summation of the phenotypical characteristics of these cell lines as correlated to their clinical tumorigenicity can be found in Figure 3.1. In the current study, the five most common pancreatic cancer cell lines (original references for cell line discovery: BxPC-3<sup>18</sup>, HPAF-II<sup>19</sup>, KPC<sup>20</sup>, MIA PaCa-2<sup>21</sup>, PANC-1<sup>22</sup>) were co-cultured with Wild-Type *C. novyi* as well as the attenuated, Non-Toxic *C. novyi* strain to establish the efficacy of this oncolytic bacteria in a monolayer culture.

**Table 3.1.** Characteristics of the original tissue sample for each pancreatic cancer cell line.

<b>Cell Line</b>	<b>Age</b>	<b>Gender</b>	<b>Derivation</b>	<b>Metastasis</b>	<b>Clinical Prognosis</b>	<b>Original Reference</b>
<b>BxPC-3</b>	61	F	Primary Tumor	Yes	Poor	18
<b>HPAF-II</b>	44	N	Ascites	Yes	Well	19
<b>KPC</b>	n.a.	n.a.	Ductal Adenocarcinoma Model	Yes	n.a.	20
<b>MIA PaCa-2</b>	65	M	Primary Tumor	Unknown	Poor	21
<b>PANC-1</b>	56	F	Primary Tumor	Yes	Poor	22

**Table 3.2.** Genotypic information regarding the four most commonly mutated genes in tumorigenic pancreatic cancer cell lines. (WT – wild type, HD – homologous deletion).

<b>Cell Line</b>	<b>KRAS</b>	<b>Tp53</b>	<b>CDK2a/p16</b>	<b>SMAD4/DPC4</b>	<b>Original Reference</b>
<b>BxPC-3</b>	WT	220 Cys	WT/HD	HD	17, 18
<b>HPAF-II</b>	12 Asp	151 Ser	Several deletion mutations	WT	17, 19
<b>KPC</b>	12 Asp	172 His	WT	WT	20
<b>MIA PaCa-2</b>	12 Cys	248 Try	HD	WT	17, 21
<b>PANC-1</b>	12 Asp	245 Ser	HD	WT	17, 22

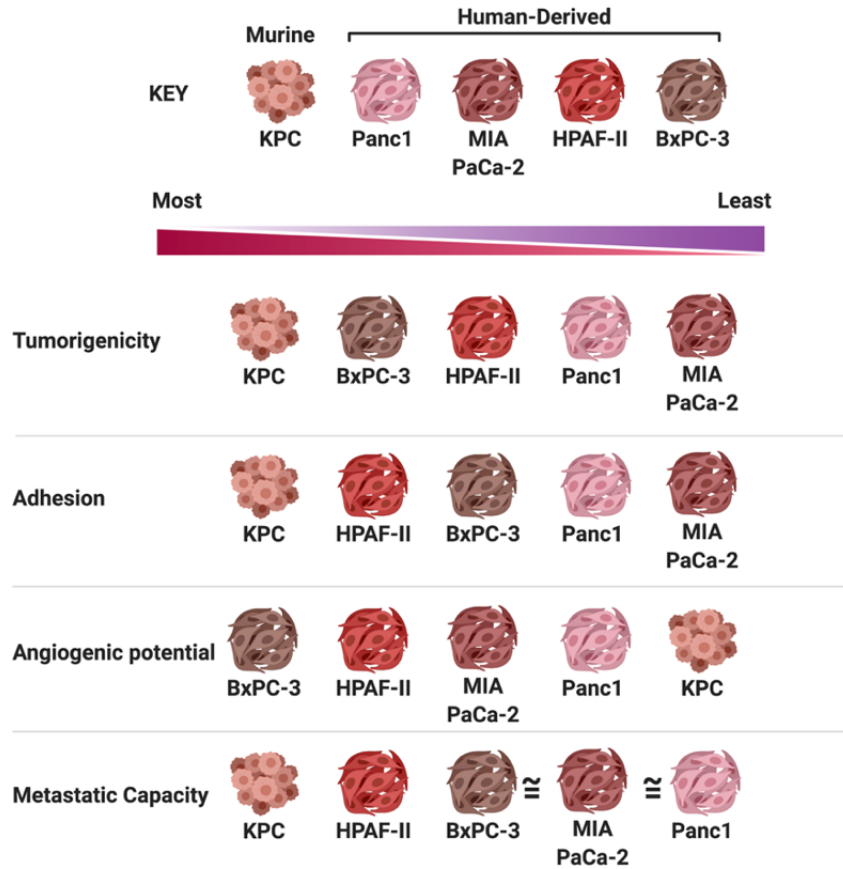


**Figure 3.1.** Pictorial summation of phenotypical characteristics of pancreatic cancer cell lines as correlated to clinical tumorigenicity.

## Materials and Methods

### Tissue Cell Culture

BxPC-3 cells (ATCC CRL-1687) were grown in RPMI media (VWR) with 10% fetal bovine serum (FBS) and 1% penicillin-streptomycin-fugizone (PSF, Caisson Labs). HPAF-II cells (ATCC CRL-1997) were cultured in Eagle's Minimum Essential Media (EMEM, VWR) completed with 10% FBS and 1% PSF. KPC cells, a murine pancreatic cancer cell line, was acquired from MD Anderson via Dr. Jiha Kim. These cells were grown in complete RPMI media (10% FBS, 1% PSF). Mia PaCa-2 cells (ATCC CRL 1420) were cultured in complete DMEM (10% FBS, 1% PSF) with an additional 2.5% horse serum (VWR). PANC-1 cells (ATCC CRL-

1469) were grown using Dubelco's Modified Essential Media (DMEM, Caisson Labs) with 10% FBS (VWR) and 1% v/v PSF (Caisson Labs). Cells were grown at 37°C in 5% carbon dioxide with media changed no less than every three days or when cultures reached confluency to be split.

### **Bacterial Culture**

Wild-type *Clostridium novyi* was purchased from ATCC (19402) and grown under anaerobic conditions in reinforced clostridial media (RCM, BD Difco) supplemented with the oxygen fixing enzyme Oxyrase for Broth (Oxyrase, Inc). Resulting cultures were quantified by serial dilution and enumerated on solid media containing Oxyrase for Agar (Oxyrase, Inc) as per manufacturer's instructions to accomplish quantification through calculating the CFUs/ml mathematically (Eq.1). The Non-Toxic *C. novyi* cell line was generated through the removal of the  $\alpha$ -toxin phage DNA plasmid through membrane permeabilization at 70°C for twenty minutes as previously published<sup>23</sup>. Sporulation of *C. novyi* and RGD modified *C. novyi* spores was accomplished according to a previously published protocol<sup>15</sup>. Briefly, a specialized media replicating conditions that would force sporulation naturally was prepared and sterilized. Vegetative cells were inoculated into this media and allowed to sporulate for seven days. Subsequent purification occurred via a protocol previously for the isolation of *C. difficile* spores<sup>24</sup>.

$$\text{CFUs/ml} = (\# \text{colonies} \times \text{dilution factor}) / (\text{volume plated}) \quad (1)$$

### **Lysis Assay**

Pancreatic cancer cells were plated at 100,000 cells per well in a 12-well plate (Corning Costar) and allowed to attach at 37°C in 5% carbon dioxide overnight. The resulting samples were inoculated with *C. novyi* cultures at a concentration of 5000 cells or spores per well as

determined by spore enumeration. Co-cultures of human and bacterial cells were incubated both anaerobically in BD GasPakEZ containers with oxygen-fixing sachets (BD), and aerobically, as described above, for 24hrs. After incubation, the media containing *C. novyi* cells or spores was removed and the wells were rinsed twice with phosphate buffered saline (Caisson Labs). Fresh media, including purified resazurin (44uM, Thermo Fisher), appropriate to the pancreatic cancer cell line in that well was added to each well. The resulting samples were then incubated with resazurin containing media for five hours, then Abs<sub>570</sub> was observed and recorded.

## **Results**

### **BxPC-3**

No statistical significance was found when BxPC-3 cells were treated with either vegetative or sporulated *C. novyi*, regardless of the incubation conditions.

### **HPAF-II**

A significant difference was observed when HPAF-II cells were treated with vegetative Wild-Type *C. novyi* in aerobic conditions ( $p < 0.001$ ). No statistical significance was observed for any other treatment or condition for HPAF-II cells.

### **MIA PaCa-2**

While no significance was determined when vegetative *C. novyi* cells were applied to MIA PaCa-2 cells in aerobic conditions, under anaerobic conditions, the application of wild-type *C. novyi* cells did garner statistical significance ( $p < 0.05$ ). Treatment of MIA PaCa-2 cells with the Non-Toxic *C. novyi* counterpart in anaerobic conditions was not significant. The application of sporulated *C. novyi* did not elicit a statistically significant result regardless of the culture conditions.

## **PANC-1**

No statistical significance was noted for any co-cultures of *C. novyi* with PANC-1 cells for any growth conditions.

## **KPC**

Under anaerobic conditions, a co-culture of the murine KPC cells and wild-type vegetative *C. novyi* cells was determined to have significance ( $p < 0.05$ ), however treatment in the same conditions with vegetative Non-Toxic *C. novyi* did not establish the same significance. No co-cultures of sporulated *C. novyi* with KPC cells established significance.

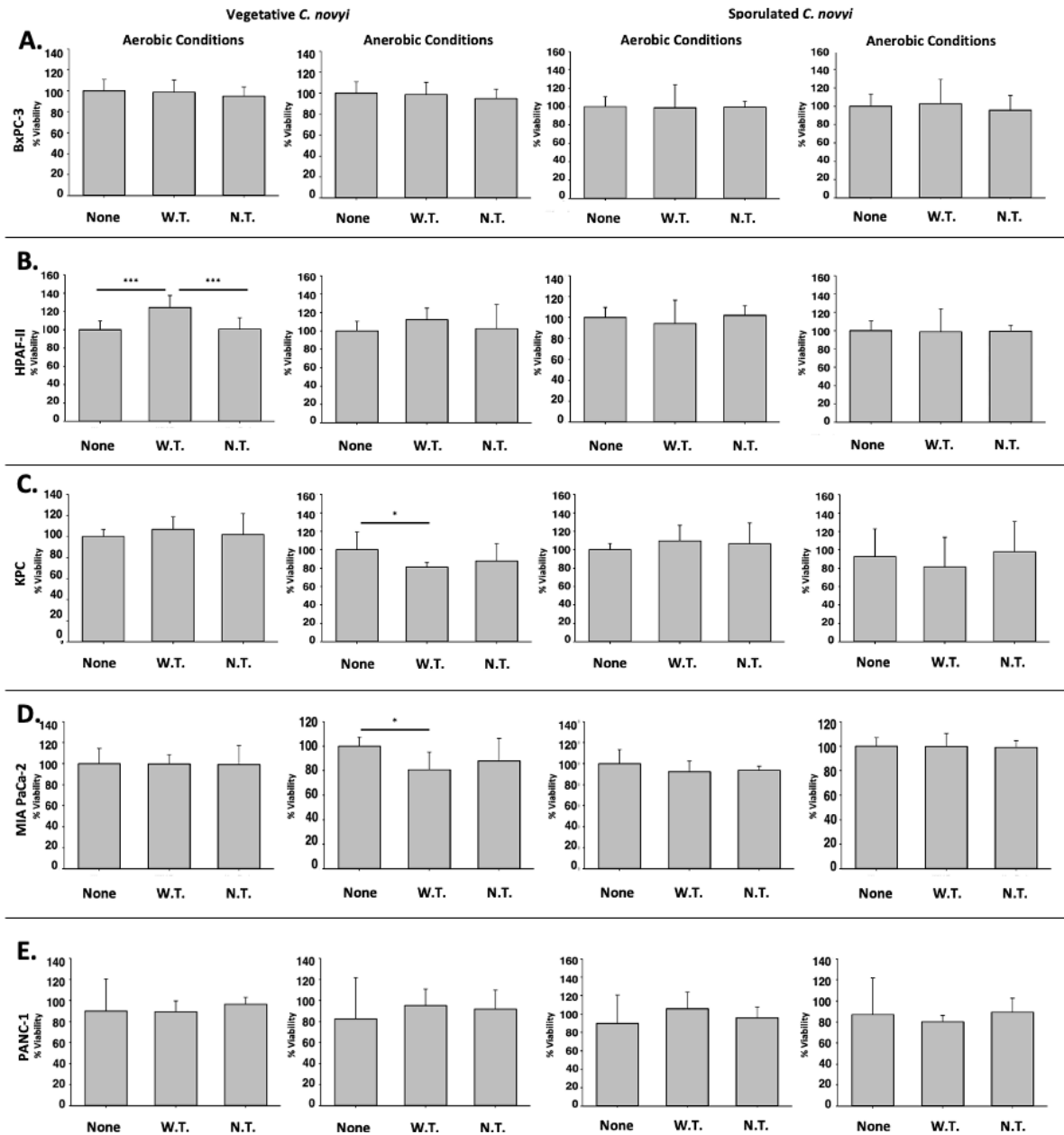


**Figure 3.2.** Lytic capacity of wild-type and non-toxic *C. novyi*. *C. novyi* vegetative or sporulated cells (5000/well) were added to cultures of pancreatic cancer cell lines A) BxPC-3, B) HPAF-II, C) KPC, D) MIA PaCa-2, and E) PANC-1 to assess the lytic capacity in anaerobic and aerobic conditions

## Discussion and Conclusions

Choosing the correct tumor microenvironment model with which to test a novel oncotherapeutic is a critical experimental design decision. Simple monolayer, or 2D, cell culture

is a common starting point for testing chemotherapeutics and is not without its benefits. However, monolayer culture has its limitations, including the lack of several tumor microenvironment characteristics – particularly those that characterize solid-state tumors. The decision of which model to employ is perhaps even more important when oncolytic bacteria are deployed as an oncotherapy where the entire system is composed of biological elements. Oncolytic bacteria have an innate ability to target and destroy solid tumors, but the biochemical mechanisms detailing how this process occurs have not yet been elucidated. These results of the current study demonstrate that this tumor destruction capacity, perhaps unsurprisingly, likely is triggered by an aspect of the 3D tumor microenvironment that is not found in monolayer cultures, regardless of the phenotypic or genotypic background of the cell line.

Here, we have shown that the oncolytic bacterial, *Clostridium novyi*, is not well served by testing upon 2D culture. This is perhaps unsurprising given that the aspects of a solid tumor that recruit *C. novyi* are related to the hypoxia and acidity found at the center. *C. novyi* is already in clinical trials as a potent oncolytic treatment when directly injected into a tumor, granting an interesting perspective upon the results of this study. Had these results been published before those of the intra-tumoral injections, it is possible that the development of *C. novyi* as any sort of an oncotherapy would never have occurred. However, intriguingly, this study did hint at a trend for *C. novyi* treatment to be least efficacious in cell lines that are known to overexpress cyclooxygenase-2 (COX-2). BxPC-3 is reported to have the highest level of COX-2 expression among the five cell lines tested by this study<sup>17</sup>. COX-2 (also known as PTGS2) is classified as a proangiogenic molecule commonly found to be over expressed in highly metastatic cancers such as pancreatic cancers<sup>25</sup>. COX-2 is thought to elicit angiogenesis through the conversion of arachidonic acid into molecules with bioactivity (e.g. prostaglandin E2). This study raises the



question of if this overexpression is enough to inhibit *C. novyi* lytic capacity in a monolayer culture, would it also effect this oncotherapy in a more complex environment. Presumably, a 3D tumor microenvironment would be much more hypoxic and acidic than a monolayer, but it is possible that pro-angiogenic molecules either directly or indirectly through subsequent angiogenesis inhibit - or create inhibitory environments - for *C. novyi* to accomplish tumor lysis.

Furthermore, this study represents the first published direct comparison of wild type *C. novyi* and its non-toxic counterpart, only differing by the loss of a non-genomic phage DNA plasmid. Though this toxin removal is necessary to overcome the potentially deadly systemic toxicity wild-type *C. novyi* has been linked to<sup>15,23</sup>, it seems as though the loss of this a-toxin also may reduce the overall lytic capacity comparatively. These results, however, should remain within the context of a monolayer environment and not be applied too generously as the intra-tumoral injections of *C. novyi* NT have demonstrated substantial anti-tumor activity<sup>14,26,27</sup>, as has a pre-clinical attempt in intravenously injected *C. novyi* NT<sup>15</sup>.

### **Acknowledgments**

The authors would like to acknowledge the use of Biorender.com for the creation of several figures contained within this publication. The authors also acknowledge funding support. The authors acknowledge the support of their colleagues in the Cell and Molecular Biology program as well as the Pharmaceutical Sciences Department at NDSU throughout this research.

### **Author Contributions**

Conceptualization: KMD, AEB.; writing—original draft preparation: KMD, AEB; review and editing: KMD, AEB; data generation: KMD, RIJ; figure creation and editing KMD, AEB; supervision: AEB, SM, JK; supplies: AEB, SM, JK.

## Funding

This research was funded in part by a pilot project award to AEB from the NIH Center for Diagnostic and Therapeutic Strategies in Pancreatic Cancer at North Dakota State University, COBRE award 1P20 GM109024 (SM) and by a NDSU Graduate School Dissertation Fellowship to KMD.

## Conflicts of Interest

The authors declare no conflict of interest. The funders had no role in the design of this publication; in the collection, analyses, or interpretation of data; in the writing of the manuscript, or in the decision to publish the results.

## References

- (1) Ilic, M.; Ilic, I. Epidemiology of Pancreatic Cancer. *World J. Gastroenterol.* **2016**, *22* (44), 9694–9705. <https://doi.org/10.3748/wjg.v22.i44.9694>.
- (2) Key Statistics for Pancreatic Cancer <https://www.cancer.org/cancer/pancreatic-cancer/about/key-statistics.html> (accessed Apr 23, 2019).
- (3) Farrow, B.; Albo, D.; Berger, D. H. The Role of the Tumor Microenvironment in the Progression of Pancreatic Cancer. *J. Surg. Res.* **2008**, *149* (2), 319–328. <https://doi.org/10.1016/j.jss.2007.12.757>.
- (4) Spear, S.; Candido, J. B.; McDermott, J. R.; Ghirelli, C.; Maniati, E.; Beers, S. A.; Balkwill, F. R.; Kocher, H. M.; Capasso, M. Discrepancies in the Tumor Microenvironment of Spontaneous and Orthotopic Murine Models of Pancreatic Cancer Uncover a New Immunostimulatory Phenotype for B Cells. *Front. Immunol.* **2019**, *10*. <https://doi.org/10.3389/fimmu.2019.00542>.
- (5) Finger, E. C.; Giaccia, A. J. Hypoxia, Inflammation, and the Tumor Microenvironment in Metastatic Disease. *Cancer Metastasis Rev.* **2010**, *29* (2), 285–293. <https://doi.org/10.1007/s10555-010-9224-5>.
- (6) Binnewies, M.; Roberts, E. W.; Kersten, K.; Chan, V.; Fearon, D. F.; Merad, M.; Coussens, L. M.; Gaborilovich, D. I.; Ostrand-Rosenberg, S.; Hedrick, C. C.; Vonderheide, R. H.; Pittet, M. J.; Jain, R. K.; Zou, W.; Howcroft, T. K.; Woodhouse, E. C.; Weinberg, R. A.; Krummel, M. F. Understanding the Tumor Immune Microenvironment (TIME) for Effective Therapy. *Nat. Med.* **2018**, *24* (5), 541–550. <https://doi.org/10.1038/s41591-018-0014-x>.

- (7) Myungjin Lee, J.; Mhaweche-Faucegla, P.; Lee, N.; Cristina Parsanian, L.; Gail Lin, Y.; Andrew Gayther, S.; Lawrenson, K. A Three-Dimensional Microenvironment Alters Protein Expression and Chemosensitivity of Epithelial Ovarian Cancer Cells in Vitro. *Lab. Invest.* **2013**, *93* (5), 528–542. <https://doi.org/10.1038/labinvest.2013.41>.
- (8) Boghaert, E. R.; Lu, X.; Hessler, P. E.; McGonigal, T. P.; Oleksijew, A.; Mitten, M. J.; Foster-Duke, K.; Hickson, J. A.; Santo, V. E.; Brito, C.; Uziel, T.; Vaidya, K. S. The Volume of Three-Dimensional Cultures of Cancer Cells InVitro Influences Transcriptional Profile Differences and Similarities with Monolayer Cultures and Xenografted Tumors. *Neoplasia N. Y. N* **2017**, *19* (9), 695–706. <https://doi.org/10.1016/j.neo.2017.06.004>.
- (9) Hickman, J. A.; Graeser, R.; de Hoogt, R.; Vidic, S.; Brito, C.; Gutekunst, M.; van der Kuip, H.; IMI PREDECT Consortium. Three-Dimensional Models of Cancer for Pharmacology and Cancer Cell Biology: Capturing Tumor Complexity in Vitro/Ex Vivo. *Biotechnol. J.* **2014**, *9* (9), 1115–1128. <https://doi.org/10.1002/biot.201300492>.
- (10) Fang, J.; Nakamura, H.; Maeda, H. The EPR Effect: Unique Features of Tumor Blood Vessels for Drug Delivery, Factors Involved, and Limitations and Augmentation of the Effect. *Adv. Drug Deliv. Rev.* **2011**, *63* (3), 136–151. <https://doi.org/10.1016/j.addr.2010.04.009>.
- (11) Tran, S.; DeGiovanni, P.-J.; Piel, B.; Rai, P. Cancer Nanomedicine: A Review of Recent Success in Drug Delivery. *Clin. Transl. Med.* **2017**, *6* (1), 44. <https://doi.org/10.1186/s40169-017-0175-0>.
- (12) Wei, M. Q.; Mengesha, A.; Good, D.; Anné, J. Bacterial Targeted Tumour Therapy-Dawn of a New Era. *Cancer Lett.* **2008**, *259* (1), 16–27. <https://doi.org/10.1016/j.canlet.2007.10.034>.
- (13) Rius-Rocabert, S.; Llinares Pinel, F.; Pozuelo, M. J.; García, A.; Nistal-Villan, E. Oncolytic Bacteria: Past, Present and Future. *FEMS Microbiol. Lett.* **2019**, *366* (12). <https://doi.org/10.1093/femsle/fnz136>.
- (14) Safety Study of Intratumoral Injection of Clostridium Novyi-NT Spores to Treat Patients With Solid Tumors That Have Not Responded to Standard Therapies - Full Text View - ClinicalTrials.gov <https://clinicaltrials.gov/ct2/show/NCT01924689> (accessed Apr 24, 2019).
- (15) Diaz, L. A.; Cheong, I.; Foss, C. A.; Zhang, X.; Peters, B. A.; Agrawal, N.; Bettegowda, C.; Karim, B.; Liu, G.; Khan, K.; Huang, X.; Kohli, M.; Dang, L. H.; Hwang, P.; Vogelstein, A.; Garrett-Mayer, E.; Kobrin, B.; Pomper, M.; Zhou, S.; Kinzler, K. W.; Vogelstein, B.; Huso, D. L. Pharmacologic and Toxicologic Evaluation of C. Novyi-NT Spores. *Toxicol. Sci.* **2005**, *88* (2), 562–575. <https://doi.org/10.1093/toxsci/kfi316>.
- (16) Chulpanova, D. S.; Kitaeva, K. V.; Rutland, C. S.; Rizvanov, A. A.; Solovyeva, V. V. Mouse Tumor Models for Advanced Cancer Immunotherapy. *Int. J. Mol. Sci.* **2020**, *21* (11). <https://doi.org/10.3390/ijms21114118>.

- (17) Deer, E. L.; Gonzalez-Hernandez, J.; Coursen, J. D.; Shea, J. E.; Ngatia, J.; Scaife, C. L.; Firpo, M. A.; Mulvihill, S. J. Phenotype and Genotype of Pancreatic Cancer Cell Lines. *Pancreas* **2010**, *39* (4), 425–435. <https://doi.org/10.1097/MPA.0b013e3181c15963>.
- (18) Tan, M. H.; Nowak, N. J.; Loor, R.; Ochi, H.; Sandberg, A. A.; Lopez, C.; Pickren, J. W.; Berjian, R.; Douglass, H. O.; Chu, T. M. Characterization of a New Primary Human Pancreatic Tumor Line. *Cancer Invest.* **1986**, *4* (1), 15–23. <https://doi.org/10.3109/07357908609039823>.
- (19) Metzgar, R. S.; Gaillard, M. T.; Levine, S. J.; Tuck, F. L.; Bossen, E. H.; Borowitz, M. J. Antigens of Human Pancreatic Adenocarcinoma Cells Defined by Murine Monoclonal Antibodies. *Cancer Res.* **1982**, *42* (2), 601–608.
- (20) KPC Cell Line (C57/BL6 genetic background) <https://ximbio.com/reagent/153474/kpc-cell-line-c57bl6-genetic-background> (accessed Oct 2, 2020).
- (21) Yunis, A. A.; Arimura, G. K.; Russin, D. J. Human Pancreatic Carcinoma (MIA PaCa-2) in Continuous Culture: Sensitivity to Asparaginase. *Int. J. Cancer* **1977**, *19* (1), 128–135. <https://doi.org/10.1002/ijc.2910190118>.
- (22) Establishment of a continuous tumor-cell line (PANC-1) from a human carcinoma of the exocrine pancreas - Lieber - 1975 - International Journal of Cancer - Wiley Online Library <https://onlinelibrary-wiley-com.ezproxy.lib.ndsu.nodak.edu/doi/abs/10.1002/ijc.2910150505> (accessed Oct 2, 2020).
- (23) Dang, L. H.; Bettegowda, C.; Huso, D. L.; Kinzler, K. W.; Vogelstein, B. Combination Bacteriolytic Therapy for the Treatment of Experimental Tumors. *Proc. Natl. Acad. Sci. U. S. A.* **2001**, *98* (26), 15155–15160. <https://doi.org/10.1073/pnas.251543698>.
- (24) Edwards, A. N.; McBride, S. M. Isolating and Purifying Clostridium Difficile Spores. *Methods Mol. Biol. Clifton NJ* **2016**, *1476*, 117–128. [https://doi.org/10.1007/978-1-4939-6361-4\\_9](https://doi.org/10.1007/978-1-4939-6361-4_9).
- (25) Chu, J.; Lloyd, F. L.; Trifan, O. C.; Knapp, B.; Rizzo, M. T. Potential Involvement of the Cyclooxygenase-2 Pathway in the Regulation of Tumor-Associated Angiogenesis and Growth in Pancreatic Cancer. *Mol. Cancer Ther.* **2003**, *2* (1), 1–7.
- (26) BioMed Valley Discoveries, Inc. *Phase I Safety Study of Intratumoral Injection of Clostridium Novyi-NT Spores in Patients With Treatment-Refractory Solid Tumor Malignancies*; Clinical trial registration NCT01924689; [clinicaltrials.gov](https://clinicaltrials.gov), 2019.
- (27) Pembrolizumab With Intratumoral Injection of Clostridium Novyi-NT - Full Text View - ClinicalTrials.gov <https://clinicaltrials.gov/ct2/show/NCT03435952> (accessed Aug 24, 2020).

## CHAPTER 4: EFFICACY OF RGD-MODIFIED CLOSTRIDIUM NOVI-NT AS AN INTRAVENOUS THERAPY FOR PANCREATIC CANCER<sup>4</sup>

### Abstract

The capacity of oncolytic bacteria to mitigate solid tumors can be found in anecdotal stories dating back thousands of years<sup>1</sup>. In particular, *Clostridium novyi*, has demonstrated a selective efficacy against solid tumors largely due to the microenvironment contained within the dense tumor cores. The core of a solid tumor is typically hypoxic, acidic, and necrotic - impeding the penetration of current therapeutics. However, in contrast, *C. novyi* is drawn to the tumor and once there, can both lyse and proliferate in the local microenvironment. Unfortunately, even after mitigating the toxicity of the bacteria by knocking out the alpha toxin, the spores were quickly and naturally cleared by the immune system without septic incidence but also without accomplishing significant tumor localization. Intra-tumoral injections of *C. novyi* NT spores have demonstrated great promise with a recently published phase II clinical trial reporting efficacy as a refractory solid tumor therapy<sup>2-4</sup>. However, not all tumors are accessible to direct injection, hence developing alternative forms of delivery is necessary. *C. novyi* NT could be designed to overcome this limitation via intravenous delivery. This study utilized CRISPR/Cas9 to modify the genome of *C. novyi* to encode the tumor targeting peptide, RGD. The RGD sequence was successfully targeted for expression within the promoter region of a spore coat protein. Expression of the RGD peptide on the outer spore coat of *C. novyi* was hypothesized to

---

<sup>4</sup> The material in this chapter was co-authored Dailey, K. M.; Pullan, J.E.; Shreffler, J.W.; Delgado, A.; Jacobson, R.I.; Johnson, P. R.; Orr, M.; Kim, J.; Mallik, S.; Brooks, A. E. Dailey, K. M. had primary responsibility for designing all experiments, collecting all data, analyzing all data, and generating subsequent figures and tables. Dailey, K. M. was the primary developer of the conclusions that are advanced here. Dailey K.M. also drafted and revised all versions of this chapter. Brooks, A. E. served as proofreader and checked the math in the statistical analysis conducted by Dailey, K. M

increase the tumor localization of *C. novyi* upon intravenous introduction based on the natural binding of RGD with the  $\alpha v \beta 3$  integrin, which is commonly overexpressed on the epithelial tissue surrounding a tumor.

## **Introduction**

Pancreatic cancer accounts for seven percent of all cancer morbidities in the United States, yet pancreatic cancer diagnoses only account for three percent of all cancers diagnosed. After decades of research the 5-year relative survival rate for most major forms of cancer (*e.g.* breast, colon, melanoma, etc.) has seen major improvements lending patients an 85-90% chance of surviving the next five years<sup>5,6</sup>. Pancreatic cancer, however, despite experiencing the same scientific advancements, has a relative survival rate of a scant 10%, with little improvement in more than forty years, a mere one percent increase seen for 2019<sup>7</sup>. This one percent survival rate increase was the result of an investment totaling more than \$178 million specifically granted for pancreatic cancer research by the National Cancer Institute alone<sup>8</sup>. While substantial studies characterizing tumors have led to impressive novel therapeutics, these glaring statistics and lack of clinical progress beg for the exploration of alternative strategies.

Anecdotes indicating the capacity of oncolytic bacteria to mitigate solid tumors can be found dating back to ancient Mesopotamia<sup>1</sup>. In contrast to current therapeutics, oncolytic bacteria are attracted to the same characteristics of solid tumors that typically confound traditional drug delivery efforts: poor vascularity, high acidity, hypoxia and dense desmoplasia<sup>9-12</sup>. Oncolytic bacteria have a natural capacity to detect and navigate subtle cytokine, pH, and oxygen gradients. This class of bacteria have demonstrated an ability to localize specifically to solid tumors from the bloodstream using this innate, ultra-sensitive chemotaxis<sup>13,14</sup>. Once localized to the tumor center, the bacteria then colonize the center and not only lyse the tumor from its core but also

simultaneously activate the immune system at the margins. Oncolytic bacteria accomplish this localization through an active, motile mechanism and are therefore not limited by the enhanced permeability and retention (EPR) effect. Additionally, the initial dose of oncolytic bacteria introduced does not limit the tumor lytic capacity as these bacteria can actively proliferate in the environment at the center of the tumor.

One bacterial species, *Clostridium novyi*, is unique within the oncolytic bacterial classification in part because of its strict, obligate micro-anaerobicity. *C. novyi* is also a sporulating bacteria with an innate motility due to a flagellated membrane. The lifecycle of *C. novyi* consists of two distinct phases: the active, lytic and proliferation capable vegetative stage, and the largely dormant but still motile spore phase. Importantly, the vegetative cells of *C. novyi* cannot survive in virtually any level of oxygen while the spores are unperturbed in oxygenated environments. Though the spores will survive in oxygenated environments such as the blood stream, germination from spores to vegetative cells cannot occur until an adequately hypoxic environment is achieved. The culmination of these characteristics leads to the potential to modify *C. novyi* spores for tumor specific therapeutic delivery through intravenous injection. While this bacterial species has been known to cause tissue necrosis, recognized as gas gangrene clinically, initial studies were able to remove the phage plasmid encoding  $\alpha$ -toxin thereby mitigating sepsis and creating a non-toxic strain known as *C. novyi* NT<sup>15</sup>. This attenuated form of *C. novyi* has not demonstrated any significant decrease in the other characteristics that make *C. novyi* such a potent oncolytic.

Early studies probing the toxicity of *C. novyi* NT spores determined spores are cleared naturally by the immune system without septic incidence within 24 hours of exposure<sup>16</sup>. Intertumoral injections of *C. novyi* NT spores have demonstrated great promise in both pre-

clinical studies and recently in a phase II clinical trial as a therapy for refractory solid tumors<sup>2-4</sup>. However, access to all tumors is not physically possible, and intravenous delivery of *C. novyi* NT could be developed to overcome this administration limitation. In theory, intravenous delivery of spores could allow for localization to not only the primary tumor but also to any metastases in a single treatment due to natural proliferative cycles. *C. novyi* NT oncotherapy targets physical characteristics that are shared by nearly every solid tumor and small malignant islands<sup>11,12</sup>. Therefore, it is reasonable to predict that this therapy would have efficacy against a solid tumor regardless of its tissue origin, location, or stage.

Since *C. novyi* NT seeks out a hypoxic, acidic and necrotic environment within which to proliferate and thus lyse, it may prove to be effective, perhaps even more effective, against even the latest stages of solid tumors that have evaded detection. Previous studies have indicated that while tumor colonization was incredibly specific with *C. novyi* NT spores incapable of colonizing several other *in vivo* models of hypoxia, rapid clearance by the immune system poses significant delivery challenges<sup>16</sup>. Indeed, an initial study of intravenous delivery established that less than 1% of the initial dose was capable of localizing to and colonizing a subcutaneously injected tumor<sup>16</sup>. However, despite this low delivery, more than 95% of the mice were found to have significant tumor mitigation<sup>16</sup>. In order to develop an intravenously capable *C. novyi* NT oncotherapy, this study utilized CRISPR/Cas9 to modify the genome of *C. novyi* to encode the tumor targeting peptide, RGD. Furthermore, the RGD sequence was targeted to expression under a spore coat protein promoter. The integrin,  $\alpha v \beta 3$ , that binds to RGD is commonly overexpressed on the epithelial tissue surrounding a tumor. In this study we probe the efficacy of the incorporation of this tumor targeting peptide to increase the localization of *C. novyi* NT in a murine pancreatic tumor model.



## Materials and Methods

### Generation and Preparation of RGD-Modified *C. novyi* Spores

#### *Bacterial Culture*

*Clostridium novyi* was purchased from ATCC (19402) and grown up anaerobically in reinforced clostridial media (RCM, BD Difco) supplemented with the oxygen fixing enzyme Oxyrase for Broth (Oxyrase, Inc). Sporulation of *C. novyi* and RGD modified *C. novyi* spores was accomplished according to a previously published protocol<sup>16</sup>. Briefly, a specialized media replicating conditions that would force sporulation naturally was prepared and sterilized. Vegetative cells were inoculated into this media and allowed to sporulate for seven days. Subsequent purification occurred via a protocol previously for the isolation of *C. difficile* spores<sup>17</sup>. Resulting spores were quantified by serial dilution and enumerated on solid media containing oxyrase for agar as per manufacturer's instructions to normalize the concentration through calculating the CFUs/ml mathematically (*see* Eq.1).

#### *CRISPR Plasmid Construction*

A plasmid containing a Cas9nickase enzyme, previously published to have successfully cleaved DNA in *Clostridial* species<sup>18</sup>, was utilized to modify the genome of *C. novyi* cells (pKMD002). To generate pKMD002, the sgRNA contained within the commercial pNICKclos1.0 plasmid, which contained the Cas9nickase enzyme, was removed through restriction digest using *SpeI* and *NotI*, replacing it with a sgRNA sequence that correlated with the putative<sup>19</sup> *C. novyi* spore coat protein encoding gene NT01CX0401. The sequences of pNICKClos1.0 containing homologous recombination domains were also exchanged via restriction digest (*NotI* and *XhoI*) with 1kb sequences corresponding to both upstream and downstream genomic sites targeted by the NT01CX0401 sgRNA. Within these two HDR arms,

the genetic sequence for RGD was cloned. This insertion sequence also contained a start codon, Shine-Dalgarno sequences, and TATA box as well as a flexible GGA linker to allow for some molecular rotation of the RGD peptide (Fig 4.1A). All of these sequences were modified to account for species specific codon bias (Fig 4.1B). Additionally, an *EcoRV* restriction digest site was inserted into the HDR sequences to allow for verification of a successful genomic insertion.

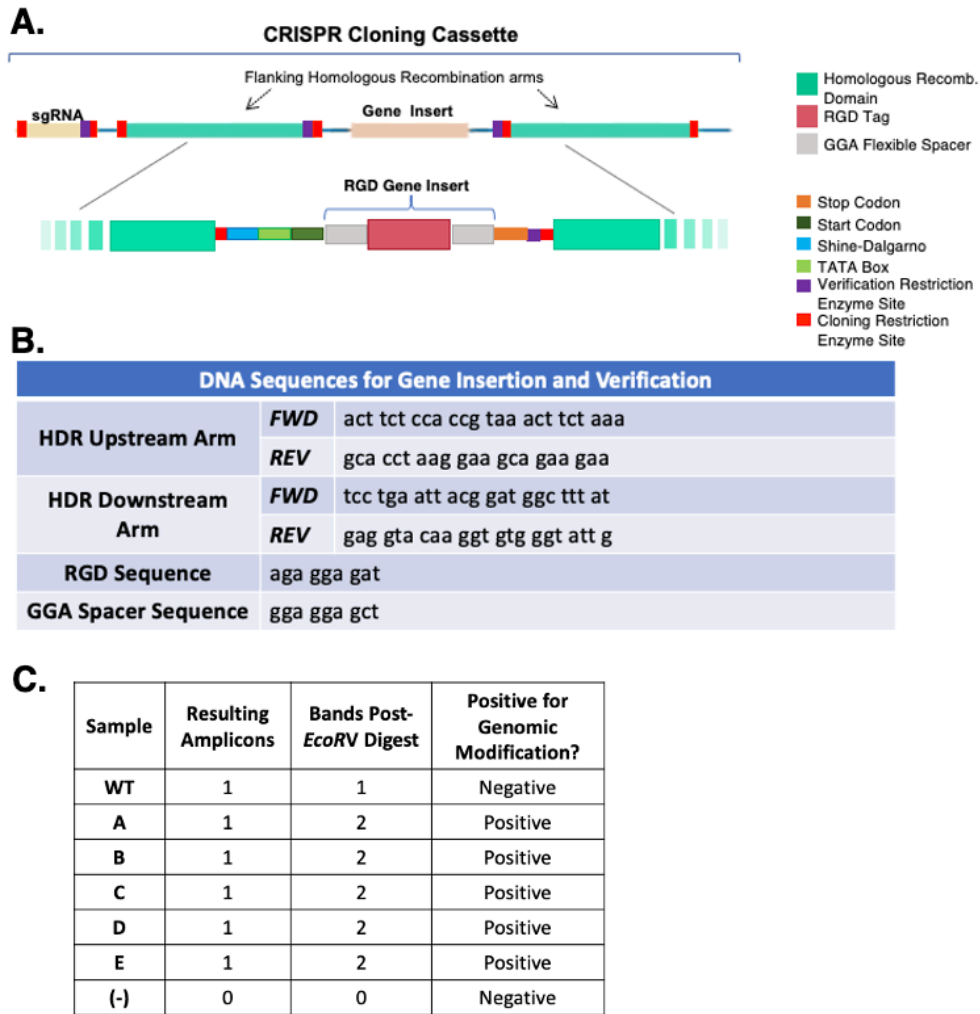


**Figure 4.1.** CRISPR-mediated genomic insertion of RGD peptide encoding gene. A) Schematic representation of the CRISPR cloning cassette utilized in pKMD002 for gene insertion. B) DNA sequences relevant to the cloning and confirmation of the pKMD002 plasmid. C) The results of CRISPR/Cas9n mediated genomic insertion of the RGD peptide into *C. novyi* candidates A-E and controls.

### ***Transformation***

Calcium competent *C. novyi* cells were created by modifying a standard protocol for *E. coli*<sup>20</sup> to include Oxyrase for Broth at 10% in all calcium chloride solutions. Resulting *C. novyi* cells were then transformed with 5ug of purified pKMD002 plasmid DNA via heat shock. After 24hrs, the resulting bacteria cultures were exposed to the selective marker, erythromycin (250ug/ml final conc., Sigma Aldrich), for twenty-four hours at 37°C anaerobically. Cells were then plated onto solid media containing reinforced clostridial media (RCM, BD Difco) with 10% Oxyrase for Agar (Oxyrase Inc.), erythromycin (250ug/ml) and 3% agar (Sigma-Aldrich) and grown in OxyPLUS anaerobic chamber plates (Oxyrase, Inc) for 48hrs. Candidate colonies were then picked from the agar plates and grown up in RCM broth containing 10% Oxyrase for Broth.

### ***Genomic Insertion Confirmation***

Resulting candidate spore cultures underwent TRIzol (Zymo Research) genomic DNA isolation according to the manufacturer's protocol. The resulting genomic DNA then underwent PCR utilizing primers specific to the HDR domain (forward – ttactcagccttaggatttacaga, reverse – tcaggtatagttgcaggaatgaa) contained within pKMD002 which included the *EcoRV* restriction site as designed for verification. GoTaq Green PCR MasterMix (Promega) and nuclease free water (Promega) was used to perform PCR. The thermocycler program was as follows: 95°C for 5min, (95°C for 30sec, 50°C for 1min, 68°C for 2min) x40 cycles, and then 68°C for 5min. The resulting oligonucleotides were then digested with *EcoRV*-HF enzyme (New England BioLabs, Inc) in CutSmart Buffer at 37°C for 1hr. After digestion, samples were run out a 1% agarose gel at 120V, then imaged and analyzed to verify if genomic insertion had occurred after transformation with pKMD002.

### ***Alpha Toxin Removal***

A previously published method<sup>15</sup> was modified to include an activation step consisting of a 20min incubation at 55°C after the membrane permeabilization incubation at 70°C. PCR screening was then conducted with primers (forward gattcaagaggccacagagatag; reverse gaccaccttcaaaccactta) from the published method corresponding to *C. novyi*  $\alpha$ -toxin in order to confirm  $\alpha$ -toxin knock-out.

### **Characterization of RGD-modified *C. novyi* Spores**

#### ***Adhesion Assay***

Circular borosilicate glass cover slips (Fisher Scientific) were treated with air plasma (corona) treatment (Enercon Compak 2000 Corona Treater Model LM4045-06). Resulting cover slips were then placed into the center of a well of a 6-well plate (Celltreat) for further experimentation. Purified  $\alpha_v\beta_3$  integrin (100uL of 10ug/mL carrier-free, human recombinant protein, R&D Systems Bio-Techne 3050-AV) was placed in the center of the corona-treated cover slips. The authors note that it is important for subsequent steps that the slide covers be in the center of the wells and not touching the sides. The protein carrier solution (1x phosphate buffered saline, VWR) was allowed to evaporate at 4°C for 48hr, thus allowing deposition and subsequent adhesion of  $\alpha_v\beta_3$  integrin to the cover slip. Once the carrier solution had evaporated, 100uL of purified *C. novyi* spores normalized via spore enumeration to 1,000 spores/uL were applied. The 6-well plates were then returned to 4°C to again evaporate the carrier solution (1x PBS), thus facilitating the adherence of the *C. novyi* spores to the surface. Slides were then washed with 1x PBS to remove any excess unadhered spores. 1% v/v crystal violet (CV) was then applied to the center of the coverslips to dye the remaining spores adhered to the integrin coated surface. CV stain was allowed to incubate for 3hrs at room temperature. Excess CV stain

was removed by three washes using 10% v/v acetic acid incubated on the cover slip for 10min while shaking on an orbital shaker at 150rpm. The resulting run off of acetic acid and crystal violet dye was removed to a 96 well plate and the absorbance at 590nm was observed and recorded. After all the washes, coverslips with adhered, CV dyed spores were then placed on slides for microscopy imaging. Brightfield confocal scanning microscopy images were obtained for each slide (Zeiss Axio Observer Z1 LSM 700). Quantification of blue/violet pixels on each slide was determined using Fiji open source image processing suite<sup>21</sup> on captured images at 4x magnification covering the center fifty percent of each slide cover. The image was separated into color channels, the area selected and the corrected total cell blue/violet color (CTCC) was determined using the internal density and the area and mean blue violet color. A one-way ANOVA test was performed to ascertain statistical significance.

$$\text{CTCC} = \text{Integrated Density} - (\text{Area} * \text{Mean}) \quad (2)$$

### ***Transmission Electron Imaging***

Specimens for transmission electron microscopy were fixed in 2.5% v/v glutaraldehyde in a 0.1 M sodium phosphate buffer, pH 7.35 (Tousimis Research Corporation, Rockville MD) for at least two hours at 4°C. Specimens were rinsed twice in sodium phosphate buffer and then placed in 2% osmium tetroxide in buffer for two hours at room temperature. Following buffer rinse, water rinse, and dehydration in a graded acetone series, samples were embedded in Epon-Araldite-DDSA with DMP-30 accelerator and sectioned at 60-80 nm thickness on a RMC MT XL ultramicrotome (Boeckeler Instruments, Tucson AZ). Sections on copper grids were stained with lead citrate for two minutes and dried before being observed and photographed on a JEOL JEM-100CX II electron microscope (JEOL Inc., Peabody MA).

## **Immunocompetent Mouse Model Establishment**

Wild type C57 black 6 mice were used in this pilot study. KPC5504 pancreatic tumor cells (MD Anderson) were injected as described below to create a tumor. Alternatively, one cohort of mice underwent a mock surgery, in which sterile phosphate buffered saline (1x PBS) was injected in lieu of cells. Mice were randomly assigned to treatment groups, with both male and female mice utilized (Table 4.1).

### ***Xenographic Tumor Implantation Surgery***

Mice were anesthetized by isoflurane (3% in 1 L/min 100% oxygen for induction, 2% in 1 L/min 100% oxygen for maintenance), and a lack of pedal reflex was obtained in order to assess anesthetic depth. Eye gel (Hanna Pharmaceutical Artificial Tears Ophthalmic Ointment) was applied to both eyes. Surgeries were performed on a sterile benchtop, and the animal was laid on a heating pad covered by a sterile drape to maintain body temperature and prevent hypothermia for the duration of the surgery. The fur of approximately a square inch surrounding the incision site on the left flank was removed by shaving. Betadine solution was then applied with sterile gauze in a circular fashion starting at the surgical incision site and rotating outward. The spleen of the mouse was visualized, and the abdomen of the mouse was then opened using sterile surgical scissors to create a 1cm incision in the medial upper abdomen, just over the location of the spleen. KPC5504 cells ( $10^5$ ) were suspended in 25uL of sterile saline and loaded into a sterile syringe (28-gauge needle on a 0.5mL insulin syringe) for the tumor implantation cohort. For the mock tumor implantation cohort, 25uL of sterile PBS was loaded into a sterile syringe (28-gauge needle on a 0.5mL insulin syringe). The peritoneum was gently grasped with forceps and a small incision was made just over the spleen (~1cm). The spleen was grasped gently with sterile forceps, exteriorizing it along with the pancreas, and a small portion of the

intestine. While holding the spleen vertically, the dark line indicative of the pancreatic vein running down the pancreas was located as a landmark for injection. The needle of the syringe was pre-loaded with either KPC cells or PBS and then inserted parallel to the pancreatic vein, then the solution was slowly injected so that a small bubble appeared in the pancreas. The needle was then gently removed from the pancreas, and forceps were used to manipulate around either side of the opening in the peritoneum and gently return the organ into the peritoneal cavity. Subsequently, the peritoneum and skin were sutured in layers (Ethicon/Ethilon chromic gut, 5-0, 1.5 metric, 687G or Ethicon/Ethilon, nylon suture/black monofilament, 5-0, 1.0 metric, 698H). Neosporin and subsequently tissue glue were placed over the incision to prevent infection and reopening of the incision. The mouse was given buprenorphine (0.1mg/kg) subcutaneously for pain control. Mice were returned to micro-isolator housing after they had recovered normal posture and were walking around the cage freely/normally. Mice were then singly housed after surgery to help prevent suture disruption and monitored twice a day. Injected cells were allowed to develop into a tumor for 14 days following implantation, with tumor progression being monitored daily by visualization and palpating the area every 3-5days.

### ***Tail Vein Treatment***

Both mice bearing tumors and non-tumor bearing mice (those injected with sterile saline) underwent treatment with purified *Clostridium novyi* NT spores. Regardless of their tumor status, all cohorts underwent one of three treatments: 1) tail vein injections of 200uL sterile 1x PBS, 2) tail vein injections of  $10^5$  in 200uL sterile 1x PBS *Clostridium novyi* NT spores (WT-NT), and 3) tail vein injections of  $10^5$  in 200uL sterile 1x PBS RGD-modified *Clostridium novyi* NT spores. A table detailing the cohort specificities has been included for clarity (Table 4.1). All treatments were administered by a single tail vein injection (200uL) 14 days post-surgery. Mice were

anesthetized with isoflurane as previously described prior to tail vein injections. As a method to prevent sepsis, which is a rare complication following IV injection with bacteria, mice were given an injection (26-gauge needle on a 0.5mL syringe) of 200uL 37°C sterile saline subcutaneously (SC) immediately following injection of *C. novyi* NT spores. Mice received additional 200uL SC injections of sterile saline every 4hrs for a total of 1.2mL of saline per mouse.

### ***Euthanasia***

Twenty-four hours following treatment with spores (or PBS in the control group), mice were euthanized by isoflurane gas (5% in 2L/min 100% oxygen) and cervical dislocation. The spleen, pancreas and associated tumor (the tumor was often inextricable from the pancreas), liver, kidney, lung, heart and brain were then aseptically harvested with half of each organ being flash frozen in liquid nitrogen to undergo PCR for the presence of *C. novyi* NT spores and the other half being submerged in 10% neutral buffered formalin (NBF) to undergo histological processing. Before being halved, the pancreases and associated tumor tissue were weighed to establish the mass.

### **Characterization of RGD-modified *C. novyi* Spores *In Vivo***

#### ***Homogenization of Murine Tissues***

To homogenize harvested organs, a liquid nitrogen physical pulverization method was modified<sup>22</sup>. A brass hose connector and coordinating cap were sterilized and chilled in liquid nitrogen. This hardware was then used to create a pulverization chamber in which the tissue and liquid nitrogen could be placed. A snugly fit zinc-platted carriage bolt that corresponded to the hose connector was used as a piston that when tapped with a hammer pulverized the tissue. The resulting pulverized tissue was removed and placed in tubes that contained 0.5mm silica



homogenization beads (BeadBug, Sigma Aldrich). Tubes were vortexed for 20min or until the tissue was sufficiently homogenized. This solution was then pelleted at 12,000rpm for 5min and the resulting supernatant was removed to another tube. Genomic DNA was then isolated via manufacturer's protocol for TRIzol (Zymo Research, Inc.).

### ***Biodistribution of C. novyi NT Spores***

The harvested genomic DNA underwent PCR with primers specific to 16s rRNA (Forward aagtcgtggctggctattt; Reverse ctccaagtcctctccataag) characteristic of *C. novyi* to determine the presence or absence of spores in the organs harvested. Each genomic preparation (5uL) was loaded as the template with GoTaq Green PCR MasterMix (Promega), nuclease free water (Promega), and 10uM final concentration of primers. The thermocycler program was as follows: 95°C for 5min, (95°C for 30sec, 50°C for 1min, 68°C for 2min)x40 cycles, and then extension at 68°C for 5min. Resulting amplicons were run on a 1% agarose gel at 130V and imaged.

### ***Bacterial Burden Quantification***

The genomic DNA for samples that resulted in an amplicon after PCR were quantified to obtain the concentration (ng/uL) and quality (260/280) of the extracted sample. The resulting quantifications were used to calculate a corrected concentration that accounted for samples with low quality (Eq 3). The corrected concentration (ng/uL) was then used to normalize all samples to 19ng per reaction. Subsequent PCR occurred with 16s rRNA primers using the same thermocycler program and gel procedure as detailed previously. The resulting amplicons were quantified using Fiji software to create an intensity plot for each band on the gel and then quantifying the area contained within the peak that corresponded to the 16s rRNA band. This area was then normalized to allow for comparison between multiple gels by utilizing the known

quantification of the 3kb band contained in the 1kb molecular ladder (TriDye 1kb Ladder, Promega) to convert the area value to nanograms of DNA contained in the amplicon.

$$\text{Corrected ng/uL} = (\text{ng/uL}) \times (260/280) \quad (3)$$

## Results

### RGD Peptide Encoding Gene Genomic Insertion Confirmation

Transformation of calcium competent *C. novyi* with the CRISPR plasmid pKMD002 (Fig 4.1A) resulted in the growth of more than thirty colonies on selective media plates. Five candidates were selected for genomic DNA isolation and subsequent 16s rRNA PCR amplification. The resulting PCR amplicons were digested with *EcoRV* to establish the successful insertion of RGD-peptide encoding gene into the *C. novyi* genome. All five candidates indicated the presence of two bands after restriction digestion, indicating that all five were positive for genomic insertion (Fig 4.1B).

### Characterization of RGD-Modified *C. novyi* Spores

#### *Adhesion Assay*

To demonstrate the protein expression, physical availability, and functionality of the genetically inserted RGD gene an adhesion assay was created based on the known RGD integrin  $\alpha_v\beta_3$  binding interaction. An  $\alpha_v\beta_3$  coated surface was created and inoculated with RGD-modified *C. novyi* spores (Fig 4.2). Excess spores were washed away, and remaining spores were stained with crystal violet. The excess crystal violet was quantified via absorbance at 590nm, with a lack of signal indirectly indicating the quantity of spores that had remained dyed by CV on the integrin coated surface (Fig 4.3A). Candidate A demonstrated a fold change significantly greater than that of both un-modified *C. novyi* spores (used as a control) as well as the other candidates probed. Alternatively, to directly quantify the spores remaining on the integrin coated

surface, 40X scanning confocal microscopy images were obtained after crystal violet staining. The blue/violet pixels contained within these images were then counted via Fiji (64-bit), the open source image processing packet<sup>21</sup>. The resulting quantification from this method corroborates the data generated from measuring the excess CV run off and confirms that Candidate A demonstrates a higher rate of adhesion by the presence of more remaining spores on the surface (Fig 4.3A and 4.3B).

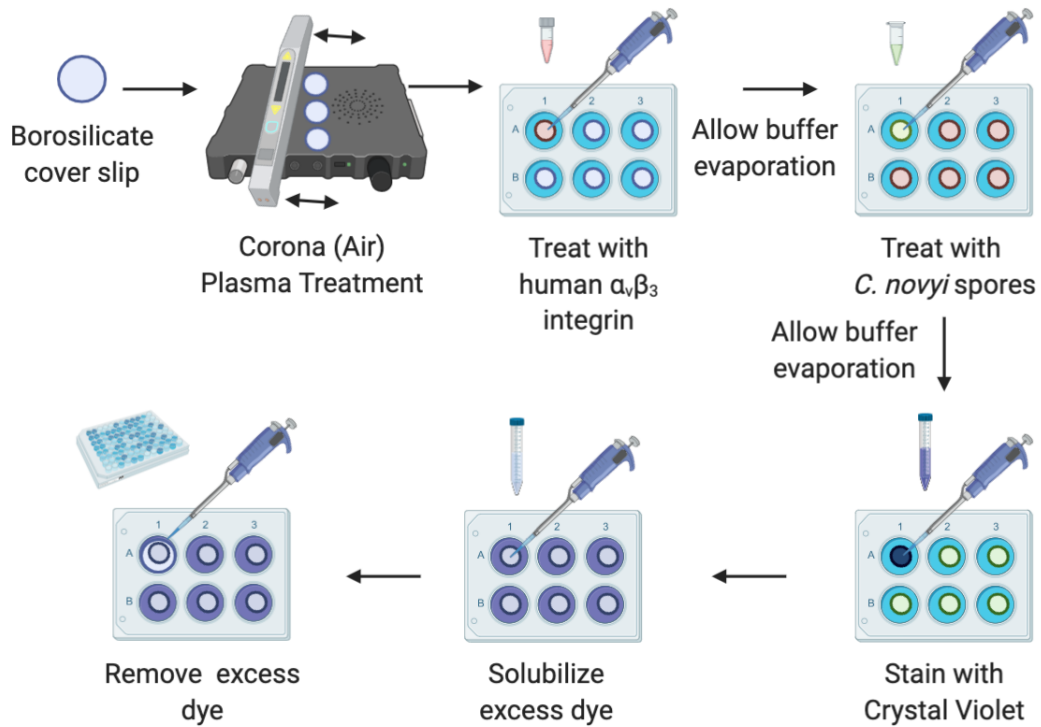


**Figure 4.2.** Pictural description of the  $\alpha_v\beta_3$  adhesion assay methodology.

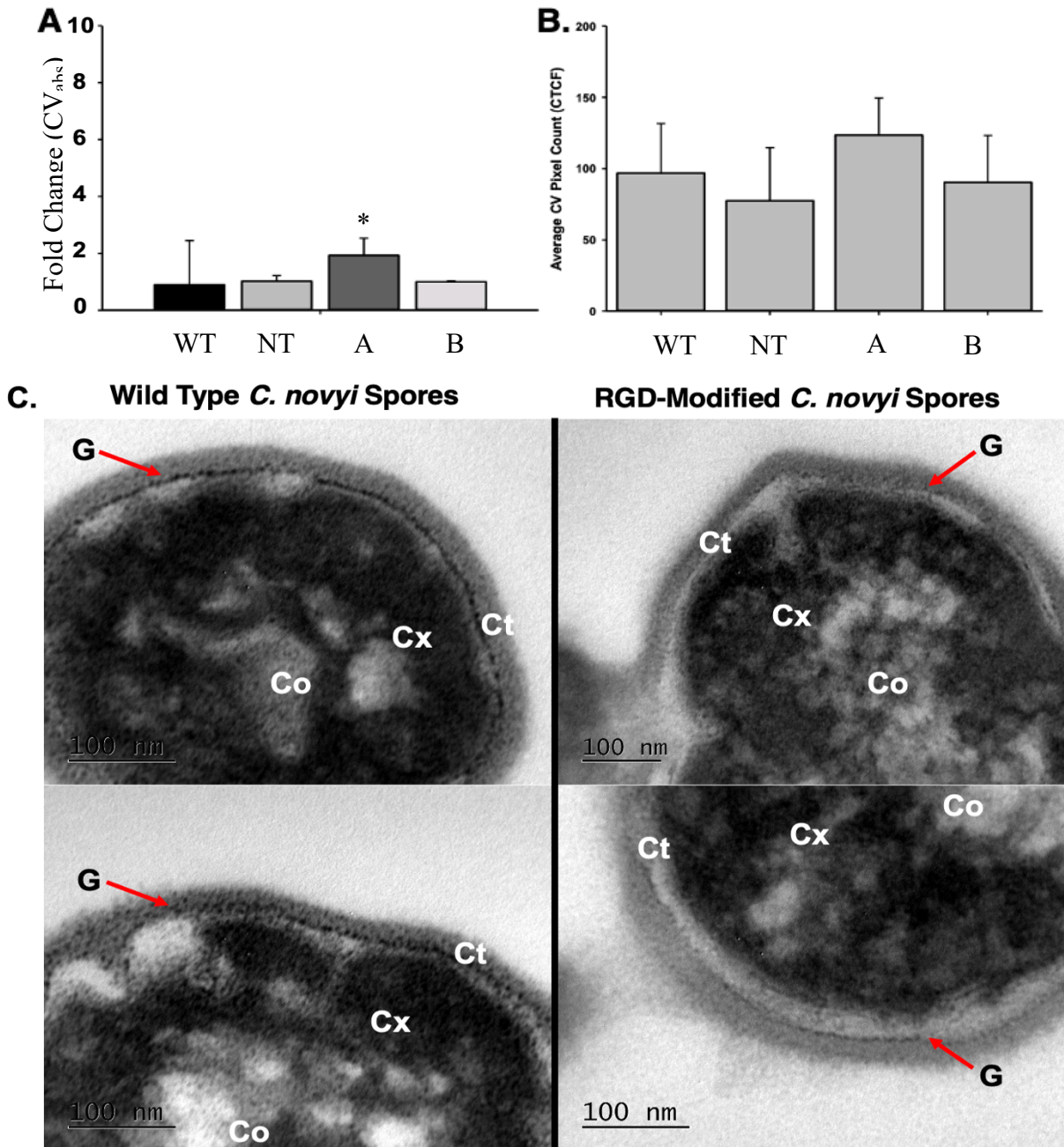


**Figure 4.3.** Physical characterization of the inserted RGD peptide A) Fold change observed in crystal violet (CV) absorbance at a wavelength of 570 for wild type (WT), non-toxic (NT) *C. novyi* as well as the putative RGD-modified candidates ( A and B) after exposure to the  $\alpha_v\beta_3$  coated surface of the adhesion assay. B) Average CV pixel count for candidates A and B as well as wild-type (WT) and non-toxic (NT) *C. novyi* that remain on the  $\alpha_v\beta_3$  coated surface. C) Transmission electron microscopy images of wild type and RGD-modified candidate A *C. novyi* spores. (Co – core, Cx- cortex, Ct – coat, G – granular layer).

### ***Transmission Electron Microscopy***

In order to further probe the expression and functionality of the RGD peptide, spores were isolated and purified for transmission electron microscopy. Typically, spores generated from *C. novyi* vegetative cells are surrounded by a complex spore coat consisting of multiple layers. The outermost layer of the spore consists of a sacculus, then an amorphous shell with intertwined honeycomb layers composed of an amorphous region interleaved with parasporal layers<sup>23</sup>. Frequently, this ‘honeycomb’ layer has an attachment to the spore coat, which consists of 3-6 layers: undercoat, cortex, germ cell wall, and the spore core. Several landmarks associated with normal spore coat architecture, which had been previously published<sup>23</sup>, were observed in images of modified spores. Some layers of the spore architecture were notably absent through this method of preparation; however, others remained. The dark, dense core (Co) and surrounding cortex (Cx) layers were observable, as was the gray layer just outside the cortex indicating the characteristic 5-7 layer coat (Ct) containing the dark staining granular (G) paracrystalline layer. The germ cell wall that distinguished the spore core (Co) from the cortex (Cx) cannot be observed because ultrathin sections were not obtained for this study. Furthermore, the method of isolation utilized in this study, which would be synonymous to that used for clinical spore preparation, does not result in an intact amorphous layer. When compared to previously published TEM images for unmodified *C. novyi* spores<sup>23</sup>, the RGD-modified spores showed an observable, disrupted paracrystalline layer as indicated by G on the images. However, it should be noted that due to the complexity of the many layers of the spore coat, which exact layer the RGD peptide was subsequently incorporated is not indicated by the methods of this study. Representative images are included in Figure 4.3C, with all resulting images contained within the supplementary data for this text.

## *In Vivo* Modeling of Intravenously Injected *C. novyi* Spores

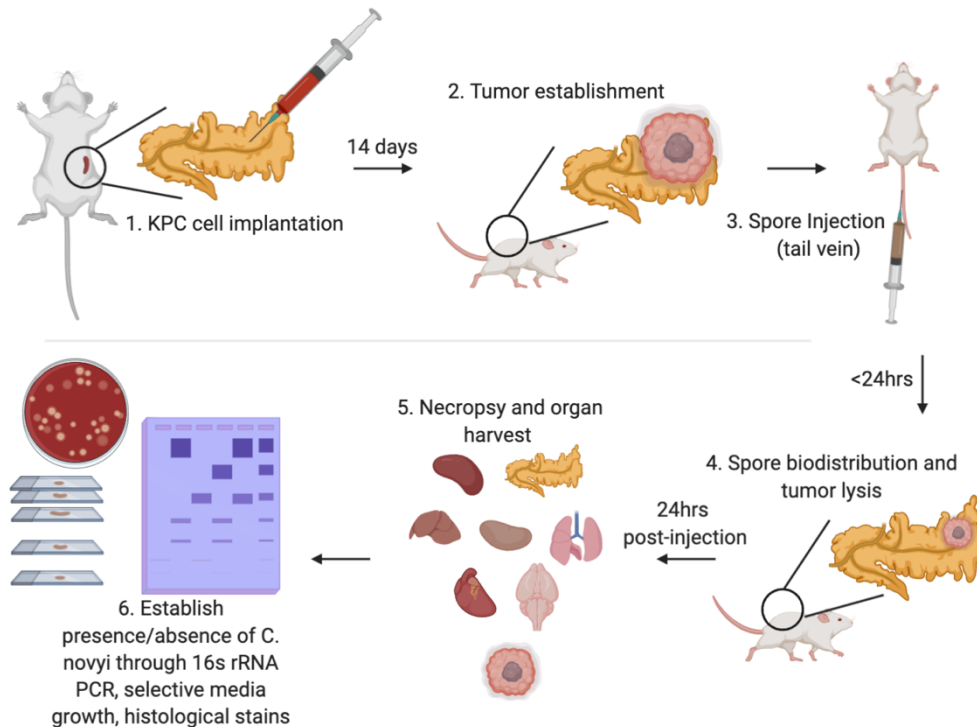


**Figure 4.4.** Pictorial representation of the surgical procedure utilized to produce the orthotopic pancreatic tumor model in C57/B16 immunocompetent mice.

Once both the genetic and physical insertion of RGD had been confirmed, the physiological effect of this modification was characterized in an immunocompetent C56/BI6 murine model. Half of the mice (n=9) underwent a pancreatic tumor implantation surgery with KPC 5504 cells, while the other half (n=10) underwent a mock surgery that implanted PBS instead of tumorigenic cells. After tumors developed for two weeks, tail vein injections of *C. novyi* NT spores, RGD-modified *C. novyi* NT spores, or PBS were given to each mouse (n=3 each cohort) to simulate intravenous injection of spores as an oncotherapy (Fig 4.4). The murine cohort breakdown has been included in Table 4.1 for clarity. No adverse events occurred at any point in this study, no blood clots, fever or other signs of distress including sepsis were observed for any of the mice. The composition of each cohort is included in Table 4.1 for clarity.

### ***Pancreas Percent Mass***

The weights of murine pancreases were observed after sacrifice to probe the efficacy of RGD-modified *C. novyi* NT to lead to tumor necrosis. All three tumor implanted cohorts had pancreases with notably a higher percentages of the corresponding mouse's overall mass, indicating that tumors did indeed form after implantation. Surprisingly, the tumor-containing pancreases from mice injected with spores demonstrated a higher percent mass than the pancreas and associated tumor tissue of the cohort that received PBS treatment (Fig 4.5A). Furthermore, the pancreas percent mass for the cohort injected with RGD-modified spores was observed to be less than that of the non-modified spore injected cohort (WT Spores > RGD-modified spores>PBS). Representative blood smears stained with the spore differential stain malachite green from each cohort have also been including in Figure 4.5B. The presence of *C. novyi* was not demonstrated in any of the smears harvested from every mouse.

**Table 4.1.** Representative table of the number and sex of mice in each cohort.

<b>Tumor Implantation</b>	<b>Tail Vein Injection</b>	<b>Male</b>	<b>Female</b>	<b>Total</b>
<b>Mock (PBS)</b>	PBS	2	1	3
	WT	2	1	3
	RGD-mod	1	2	3
<b>KPC</b>	PBS	3	1	4
	WT	2	1	3
	RGD-mod	2	1	3

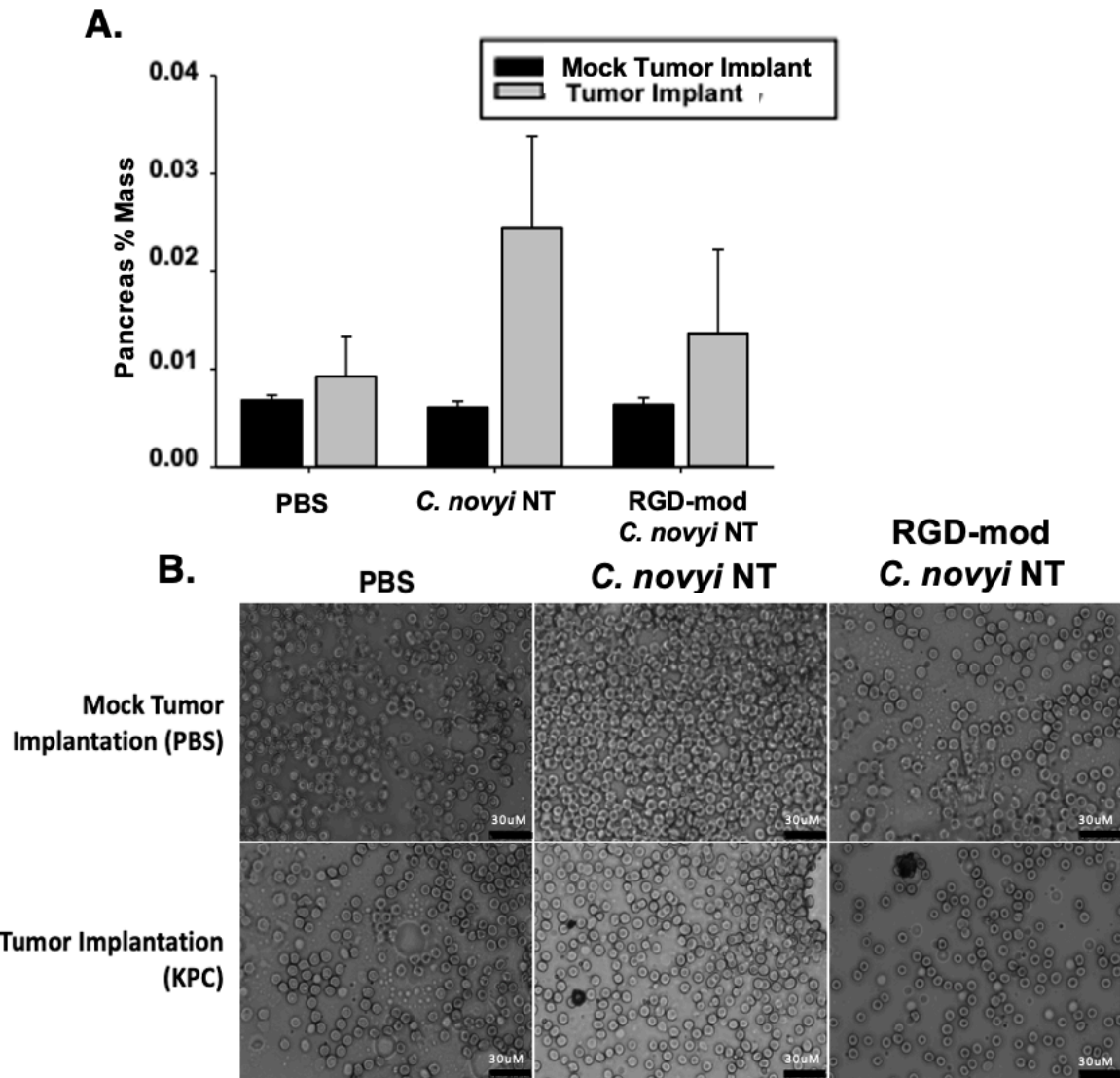


**Figure 4.5.** The effect of RGD-modified *C. novyi* spores intravenously injected in an *in vivo* orthotopic tumor model. A) The average percent weight of tumors harvested from murine models. C) Phase contrast confocal microscopy images of representative blood smears from each cohort. Scale bar in bottom right is 30uM.

### ***Biodistribution of C. novyi NT Spores***

Homogenized tissues harvested post-injection underwent genomic isolation and subsequent PCR with primers designed to be specific to the 16s rRNA of *C. novyi*. For the cohort of mice that underwent mock tumor implantation and PBS tail vein injection only one amplicon was observed in the lung of a single mouse, likely due to cross contamination in the euthanasia



chamber as neither of the other two mice in this cohort demonstrated any presence of *C. novyi* in any tissue (Table 4.2). When wild type *C. novyi* NT spores were injected into control mice without a tumor (*i.e.* mock implantation with PBS), amplicons were observed in the liver and kidney of one mouse, and the spleen and pancreas for another from the three mice within this cohort. The third mouse on this cohort did not have any amplicons present after PCR was conducted. Analogously, 24hrs after injection, RGD-modified *C. novyi* NT spores were detected in the spleen, pancreas, kidney, lung, heart and brain of two control mice with no tumors (*i.e.* mock implantation with PBS). Not surprisingly, in mice implanted with tumors and subsequently injected with PBS *C. novyi* NT was not detected in any mice in the cohort. The presence of wild type *C. novyi* NT spores was indicated in the spleen, pancreas and associated tumor tissue, kidney, and lung of two of the three mice in the cohort after tail vein injection. Similarly, in tumor containing mice that received RGD-modified *C. novyi* NT spores, spores were discovered in two of four harvested spleens, all four pancreases and associated tumor tissue, in half of the harvested lungs, three quarters of harvested hearts and half of the harvested brains (Table 4.2). It should be noted that the tumor contained within the pancreas could not be visualized for one of the mice within this cohort.

### ***Bacterial Burden Quantification***

In order to establish the bacterial burden of organs that had previously indicated the presence of spores via *C. novyi* 16S rRNA PCR, the genomic DNA isolates underwent normalization and additional 16s rRNA PCR analysis. The total bacterial burden for each mouse was quantified (Fig 4.6A), with the nanograms of amplified DNA being notably higher for mice inoculated with RGD-modified spores than those injected with unmodified spores. When the nanograms per amplicon were quantified per organ, the bacterial burden was found to be higher

for mice exposed to RGD-modified *C. novyi* NT spores in almost every organ except the lungs of tumor containing mice (Fig 4.6B and 4.6C). Importantly, a larger quantity of *C. novyi* DNA was indicated in the pancreas and tumor associated tissue of the tumor implant cohort that received RGD-modified *C. novyi* NT spore injections (Fig 4.6C).

**Table 4.2.** Biodistribution of *C. novyi* spores after IV injection. Primers designed specifically for 16s rRNA of *C. novyi* were used to conduct PCR to determine the biodistribution of spores twenty-four hours after injection. Each ‘+’ indicates the presence of an amplicon representing the presence of *C. novyi* in a single animal.

Tumor Implantation	Tail Vein Injection	Isolated Tissue							
		Spleen	Pancreas	Pancreatic Tumor	Liver	Kidney	Lung	Heart	Brain
Mock (PBS)	PBS			n.a.			+		
	WT	+	+	n.a.	+	+			
	RGD-mod	+	++	n.a.		++	++	+	++
KPC	PBS								
	WT	+	++	+		++	+		
	RGD-mod	++	++++	+			++	+++	++

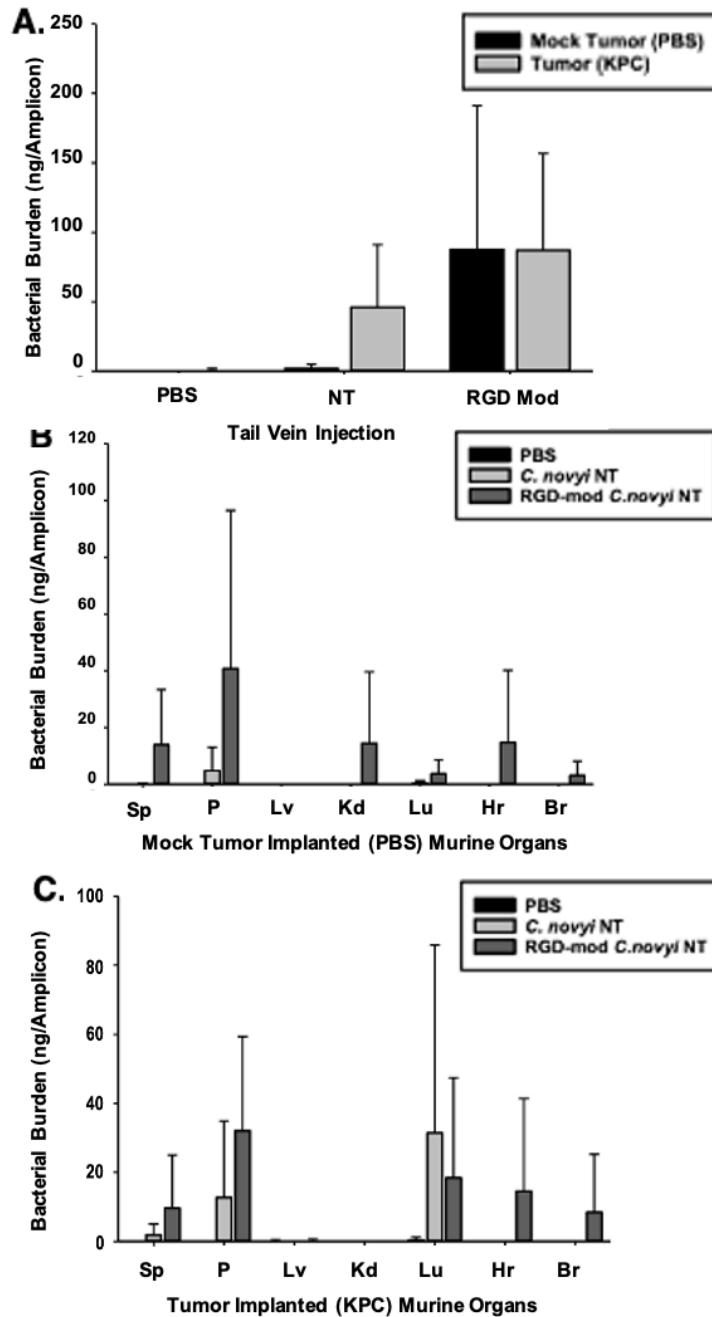


**Figure 4.6.** Quantifying *C. novyi* spores after IV injection. After tissue harvest and homogenization, bacterial burden was assessed for tissues that indicated a presence of *C. novyi*. 16s rRNA PCR was conducted with the template concentration normalized across tissues. A) The combined bioburden of all major organs within each cohort (WT – wild type *C. novyi* spore tail vein injection, RGD-mod - RGD-modified *C. novyi* tail vein injection) and Each major organ within a cohort when B) mock tumor implantation surgery occurred versus when C) tumor implantation with KPC cells was conducted. (Sp – spleen, P – pancreas, P&Pt – pancreas and pancreatic tumor, Lv- liver, Kd- kidney, Lu – lung, Hr – heart, Br – brain.)

## Discussion

Oncolytic bacteria, and in particular *Clostridium novyi* with its characteristic biphasic life cycle that requires unique environmental conditions, demonstrate great promise for treating solid tumors, particularly in those cancers that current therapeutics have demonstrated limited efficacy. While clinical trials are currently underway to advance direct intra-tumoral injections of *C. novyi* NT spores, pre-clinical trials probing the efficacy of this same bacteria delivered intravenously demonstrated a very high clearance rate that would limit widespread translation. This study attempted to overcome this pitfall using CRISPR-mediated genetic engineering (Fig 4.1) to create a stable genetic construct that allowed *C. novyi* to accomplish a higher rate of tumor localization and colonization in a pancreatic tumor model.

### Characterization of RGD-modified *C. novyi* Spores

Determining the presence and functional ability of the RGD expressed peptide to bind with the  $\alpha_v\beta_3$  integrin, which is over-expressed on pancreatic tumor cells, was very challenging as many of the traditional immunochemistry techniques are not available due to a lack of RGD antibodies. Furthermore, there was nothing in the published literature that detailed the presence of  $\alpha_v\beta_3$  integrin or RGD analog expression in bacteria of any species nonetheless spores. Hence, in order to evaluate the physical presence and functionality of the RGD-encoding sequence that was genetically inserted into the *C. novyi* genome, a novel adhesion assay to assess the interaction between RGD and its integrin binding partner was created, marrying the fields of a general bacterial adhesion assays and what has been published describing the interaction in adhesion assays between human RGD and  $\alpha_v\beta_3$  (Fig 4.2A). Importantly, before treating the integrin coated surface with *C. novyi* spores, x-ray photoelectron spectroscopy (XPS) (Sup Table 4.3) confirmed the presence of integrin on the borosilicate surface. While this assay was able to

functionally show that the modified *C. novyi* spores showed preferential adhesion to the integrin coated surface (Fig 4.2B and 4.2C), it was unable to directly demonstrate the expression of the RGD peptide on the spore surface.

Previously, an elegant study was done by Plomp et al<sup>20</sup> to examine the architecture of the spore coat using TEM, potentially allowing a more direct visualization of the integrity of the spore coat after the insertion of the RGD peptide. The spore coat of *C. novyi* is characterized by several layers, including from outer most to inner most: sacculus, amorphous shell, and honeycomb layers. Within the honeycomb layer there can be 3-6 layers consisting of an undercoat, cortex, germ cell wall, and the spore core. Several landmarks detailing spore coat architecture that had been previously published<sup>23</sup> were successfully observed in the current study (Fig 4.2E). The dark, dense core (Co) and surrounding cortex (Cx) layers were observable, as was the gray layer just outside the cortex indicating the characteristic 5-7 layer coat (Ct) containing the dark staining granular (G) paracrystalline layer. Certain spore coat layers (*i.e.*, an intact amorphous layer and the germ cell wall) were not observable due to both the method of isolation, which was selected to be both scalable and compatible for clinical spore preparation, as well as the TEM sample preparation.

While it is impossible to draw direct comparisons between TEM images due to the difference of angles used to slice the spores and variabilities in the instrumentation, the images generated of RGD-modified spores indicate a disorder in the paracrystalline layer, the target of RGD expression, when compared to both the wild-type *C. novyi* spores imaged in this study as well as in previous publications<sup>23</sup>. This study notably utilized a different method of preparation and thus the sacculus layer and germ cell wall from previously published images are absent. A sucrose gradient was chosen as the method of isolation in order to mitigate any toxicity that

might remain from reagents used to isolate *C. novyi* spores. The loss of the sacculus layer through this isolation technique - being the commercially applicable and least toxic method- was anticipated and thus the method of genomic insertion of the RGD peptide targeted the honeycomb layers for expression instead. However, the core (Co), cortex (Cx) and other coat layers (Ct), as well as the dark granular layer (G) of the outer edge of the cortex can be seen. The dark granular layer (G) that represents the paracrystalline layer has been previously published to be near the sacculus that this method of isolation removed, and thus this layer is much closer to the edge of the spores in our images. Yet, these images seem to indicate a fundamental difference in the spore coat architecture with a disrupted protein coat organization that seems correlated with the genetic incorporation of the RGD-encoding gene (note that all images are included as supplementary information).

### ***In Vivo* Biodistribution of Intravenously Injected *C. novyi* Spores**

This study was designed to establish the biodistribution of modified spores, and thus data indicating the potential lysis of tumors was a surprising fortuitous discovery. Tail vein injection was used as the route of administration as this is the most clinically relevant to establish the migration of RGD modified *C. novyi* NT spores from the blood stream into a solid pancreatic tumor in an intact immune system (Fig 4.3A). The percent mass the pancreas constitutes for mice that underwent tumor implantation is larger than that of the mice that underwent mock tumor implantation despite the tail vein treatment administered (Fig 4.3C). However, both cohorts with pancreatic tumors and *C. novyi* NT spore injections had a greater percent mass than the those that had PBS tail vein injections administered. This is quite intriguing and could represent bacterial abscess formation or immune cell recruitment and fluid retention due to inflammation from successful *C. novyi* NT colonization, as is corroborated by the bacterial burden data gathered in

Figure 4.4A. One of the primary benefits of using oncolytic bacteria may be the combination of tumor cell lysis and immune cell activation<sup>1,15</sup>. Furthermore, the reduction in percent mass upon administration of RGD-modified *C. novyi* NT spores when compared to the non-modified spores may represent increased tumor lysis based on increased localization of spores and subsequent earlier colonization as indicated by the bacterial burden established in Figure 4.4. It is possible that this increased bacterial burden could not only represent successful bacterial localization and colonization but also the beginnings of proliferation occurring within the tumor microenvironment. The previous study detailing tumor mitigation accomplished by intravenously delivered *C. novyi* NT spores did not observe significant tumor mitigation until 2-3 days post introduction<sup>16</sup>, with full tumor lysis occurring at the earliest at 12 days post injection. The current study only allowed for a 24hrs post injection time point so as to capture the biodistribution of the spores, which had been reportedly cleared in less than 24hrs in other similar models<sup>15,16</sup>.

The intravenous delivery of *C. novyi* NT spores to a tumor has occurred once before in the literature<sup>16</sup>. While this landmark study provided a substantial foundation for the current study, it is critical to note that there are several crucial differences between this study and the work of Diaz *et al*. First, the tumors implanted by Diaz *et al* were generated by subcutaneous injection of CT26 cells into the flanks of BALB/c mice to probe the pharmacologic and toxicological characteristics of intravenous *C. novyi* NT spore treatment. Conversely, we chose a rigorous, orthotopic, pancreatic tumor model to establish the biodistribution of RGD-modified *C. novyi* NT spores. It is crucial to draw two main comparisons between the two studies detailing intravenous delivery of spores: 1) BALB/c mice have a notably higher rate of clearance than the immunocompetent C57/BI6 mice used in our study as well as a Th2 biased immune system<sup>24</sup>, and 2) CT26 cells originate from a murine colon carcinoma and were used to create a non-

organoid tumor, while our study used a murine pancreatic carcinoma cell line KPC5504 to generate tumors within the pancreas. The second significant difference is that the Diaz study introduced 15,000,000,000 unmodified *C. novyi* NT spores via tail vein injection at their highest dosage, and they demonstrated substantial tumor mitigation when less than a relative 1% of the total spore dosage reached the tumor after rapid clearance of the majority of the spores within 24 hours. After a single hour, Diaz *et al* indicated that more than 80% of the relative initial injection had been cleared from the blood stream and could not be located anywhere in the mouse as indicated by <sup>125</sup>I-labeled spores. In the current study, 100,000 unlabeled spores were injected via tail vein injection in a strain of mouse with an intact immune system. Even at this significantly lower dosing, the modified *C. novyi* NT spores were able to localize to the tumor and showed preliminary indications of tumor mitigation as well. This dose was determined to be in line with the dosages currently undergoing clinical trials for intratumoral injection<sup>2-4</sup> as well as to avoid any potential for blood clotting caused by the addition of an RGD-peptide to the spore coat.

To further probe the efficacy of the *C. novyi* spores with an RGD modified spore coat, the burden of bacteria was quantified by PCR using primers specific for *C. novyi* 16s rRNA in normalized samples of genomic DNA. Quantification was only performed using genomic DNA from tissue samples that had previously indicated the presence of *C. novyi* (Table 4.1 and Fig 4.4). When the ng/amplicon calculated based on the densitometry of the PCR is extrapolated to represent a relative percent of the average total *C. novyi* DNA remaining in mice dosed with RGD-modified spores (86.65ng from Fig 4.4A), it was found that a relative 41% (35.34ng from Fig 4.4C) of the remaining bacterial load was successfully localized from the blood stream into the pancreas and associated tumor tissue (which could often not be clearly dissected away from the normal pancreatic tissue). When the same methods are applied to the data generated to



quantify the bacterial burden of non-modified *C. novyi*, 29% of the total bacterial burden was localized to the pancreas and associated tumor tissue. However, it should be noted that almost twice as much overall *C. novyi* DNA was found to be present in animals that received the RGD-modified spores over those that received wild-type spores. When this difference is accounted for, Only a relative 14% of wild-type spores accomplished translocation to the pancreas and pancreatic tumor. Thus, through these calculations, the RGD modification resulted in not only twice the bioburden of spores throughout organs after twenty-four hours, but also an almost 30% increase in relative tumor localization to the pancreas and tumor.

It should be noted that while the presence of 16s rRNA is specific to *Clostridium novyi*, and thus adequate to demonstrate biodistribution of the bacterial species in general, it does not indicate whether the injected spores have (1) germinated to the vegetative phase, (2) remained as spores, or (3) died . Furthermore, the mouse model studies reported here represent a pilot study to demonstrate the potential of pursuing such a path for the development of an intravenously capable *C. novyi* oncotherapeutic. Thus, additional animals would need to be examined in a statistically powered cohort design to determine the spore load in the pancreas and tumor; nonetheless, the RGD modification seems to have conferred not only significant increase in the overall bioburden after 24 hours, an indication of increased circulation, but also an increase in tumor localization when compared to previous studies.

### **Conclusions**

This study is among the first to probe the efficacy of CRISPR gene modification in harnessing the vast potential for bacterial pharmaceutical applications. Several species of bacteria, including *C. novyi* have demonstrated an innate ability to not only accomplish selective targeting of the microenvironment contained within a solid tumor, but also the colonization and

eradication of the tumor to its margins. Upon reaching the tumor margins, oncolytic bacterial therapy continues to demonstrate efficacy in actively recruiting and reactivating the immune system to accomplish both the eradication of the tumor margins as well as the bacterial abscess now contained within them. Recent technological advances (*e.g.* CRISPR) have made it possible to pursue the design and development of genetically modified forms of these oncolytic bacteria in order to confer further advantages while honing of their innate tumor eradication abilities. However, a large knowledge gap still remains surrounding the basic biochemical methods through which they detect and accomplish localization to the hypoxic core of a solid tumor, and only a skeletal knowledge has been obtained detailing how tumor lysis is accomplished. Furthermore, the methodology with which to establish the efficacy of these treatments remains to be fully developed. The use of a biologically living therapeutic overcomes many of the hurdles of current oncotherapeutics, including no longer being limited by the initial dosage since oncolytic bacteria can proliferate upon successfully colonizing the tumor. However, this ability to multiply confounds many of the modern pharmacological methods commonly used to determine efficacy.

While there are several hurdles yet to overcome in order to accomplish the clinical translation of intravenously delivered *C. novyi* NT spores as an oncotherapy, the potential of this therapy should not be ignored. Challenges will include developing the necessary methodology to produce spores that are consistent in composition across multiple batches as well as scaling up to large batch production. Patient and physician consent may also prove to be a challenge as injecting bacteria into a patient's veins is far from intuitive in terms of treatment for any disease state. Nevertheless, this study demonstrates two things; first, that oncolytic bacteria and in particular *Clostridium novyi* NT can be genetically modified to accentuate their innate tumor

mitigation, and second, that RGD modification of *C. novyi* NT can successfully localize to a tumor with a much smaller dose than previously used in published studies. We believe this study clearly demonstrates that there is great potential in applying CRISPR/Cas genetic engineering techniques in the quest for a better oncotherapeutic, particularly in the face of such a potent threat as pancreatic cancer.

### Supplementary Figures

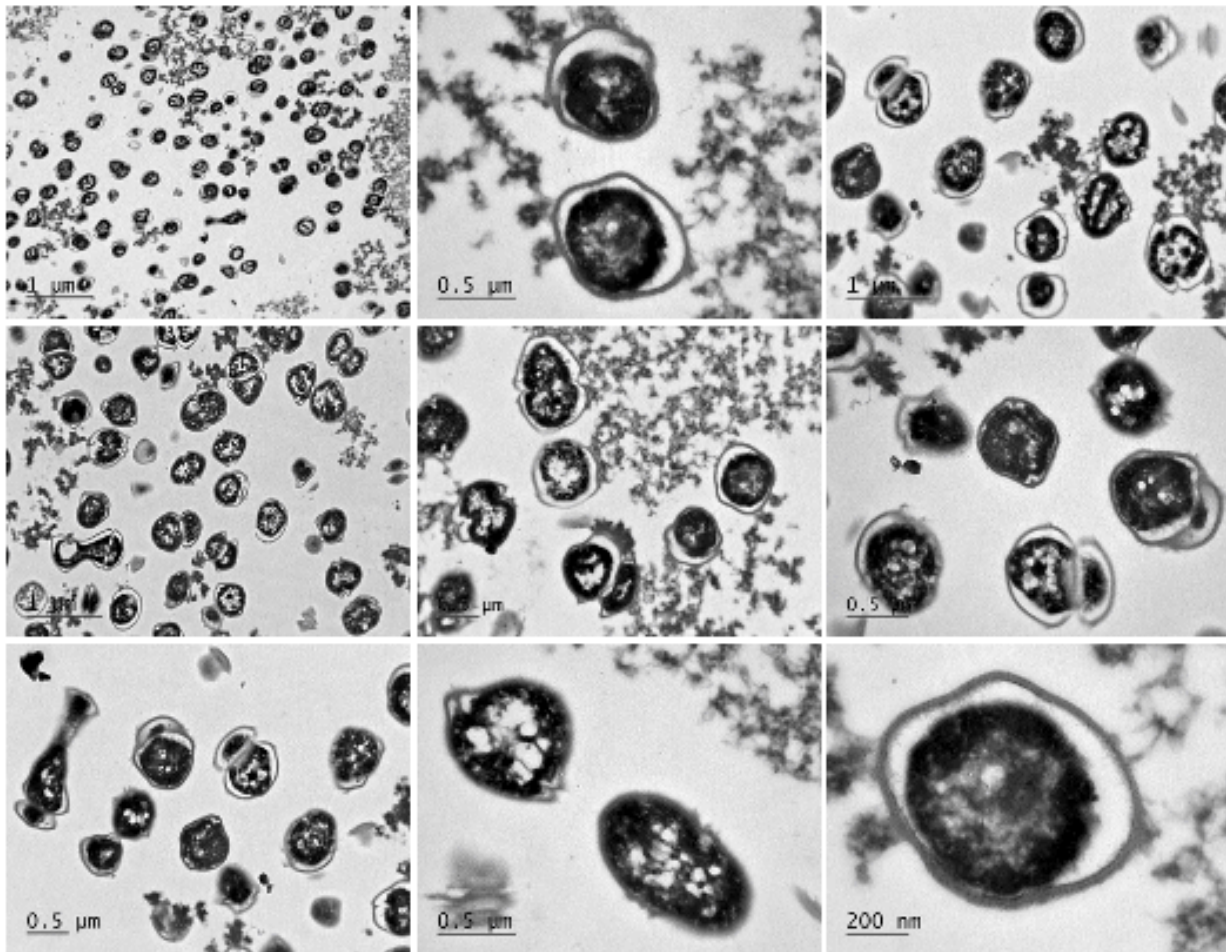


**Figure 4.7.** TEM images of unmodified *C. novyi* NT spores.

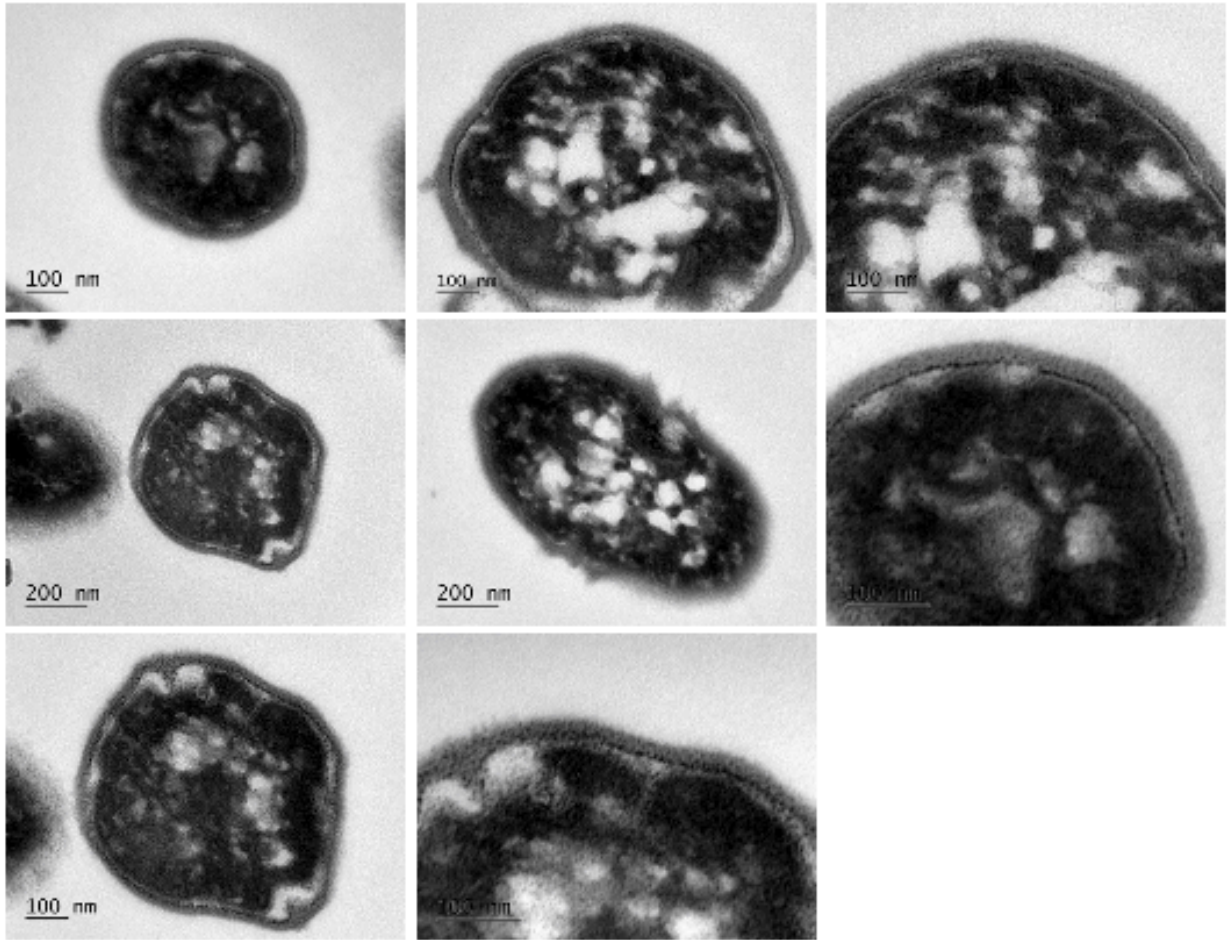


**Figure 4.7.** TEM images of unmodified *C. novyi* NT spores (continued).

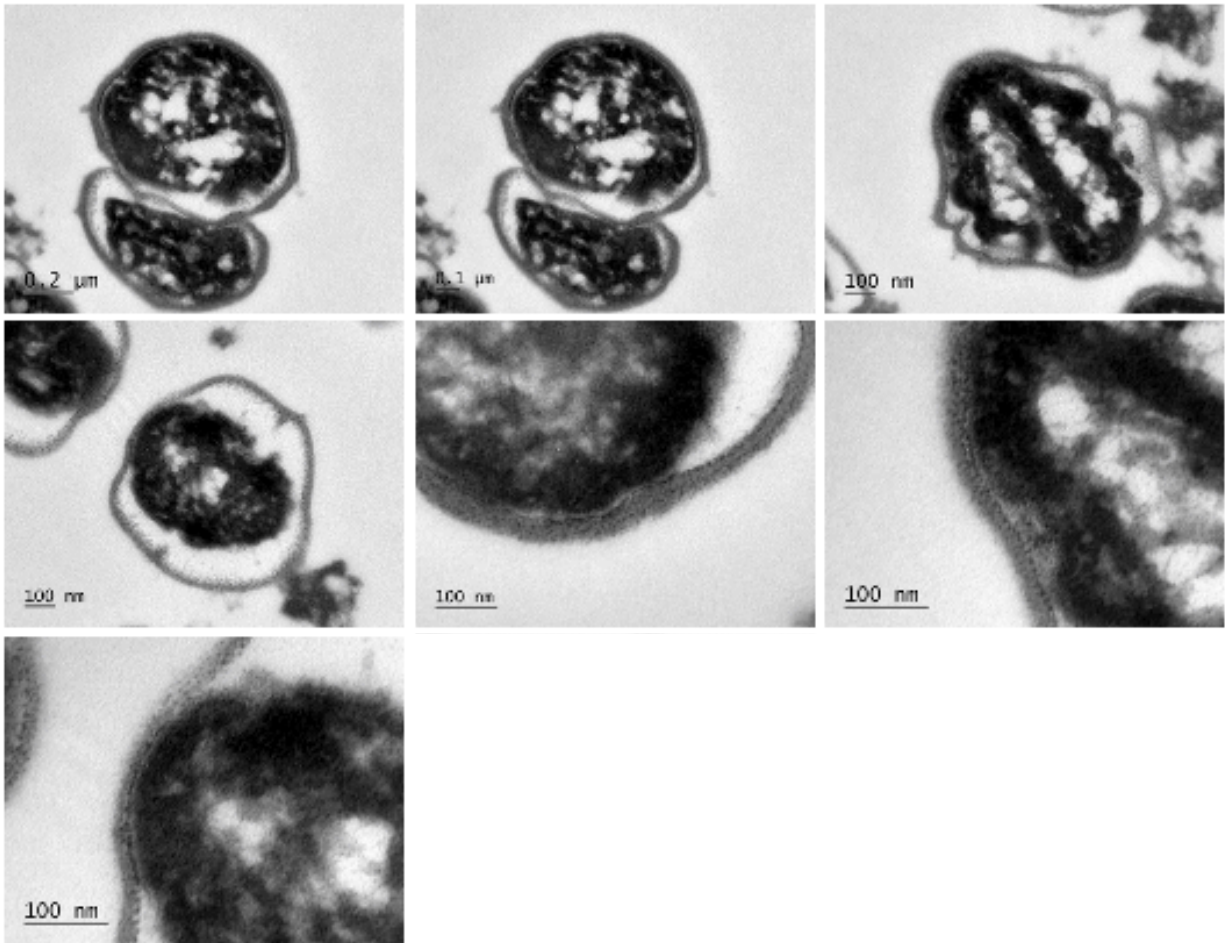


**Figure 4.7.** TEM images of unmodified *C. novyi* NT spores (continued).



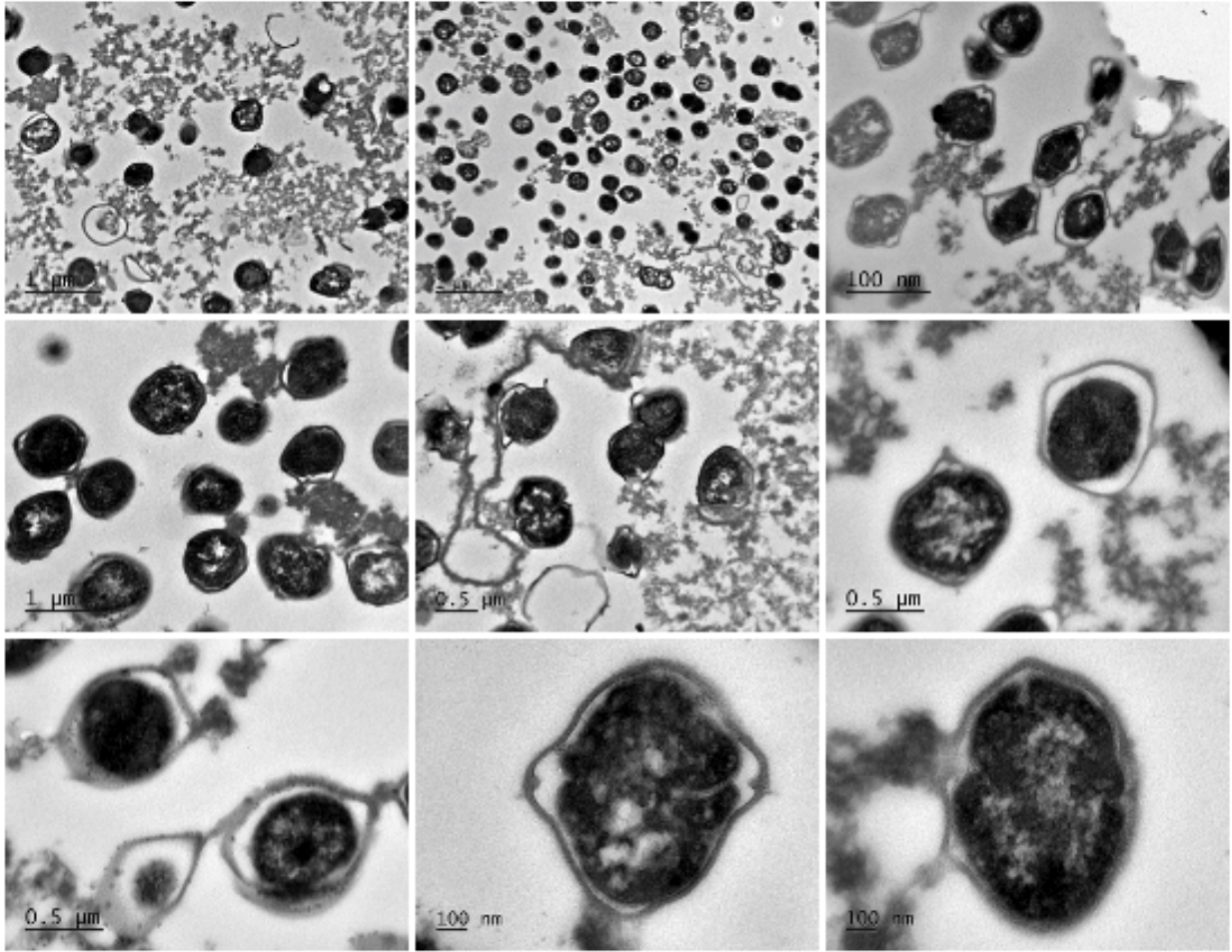


**Figure 4.8.** TEM images of RGD-modified *C. novyi* NT spores.

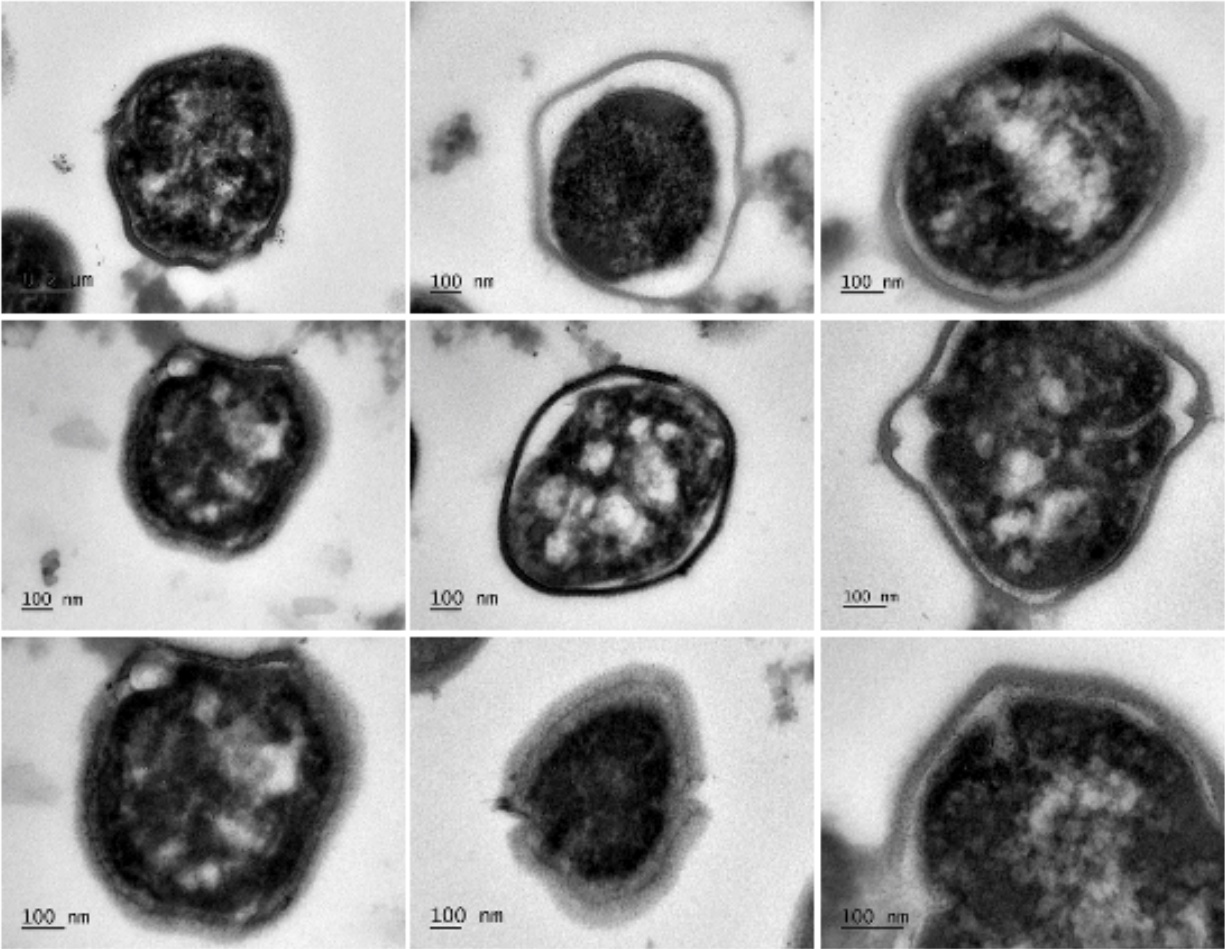


**Figure 4.8.** TEM images of RGD-modified *C. novyi* NT spores (continued).

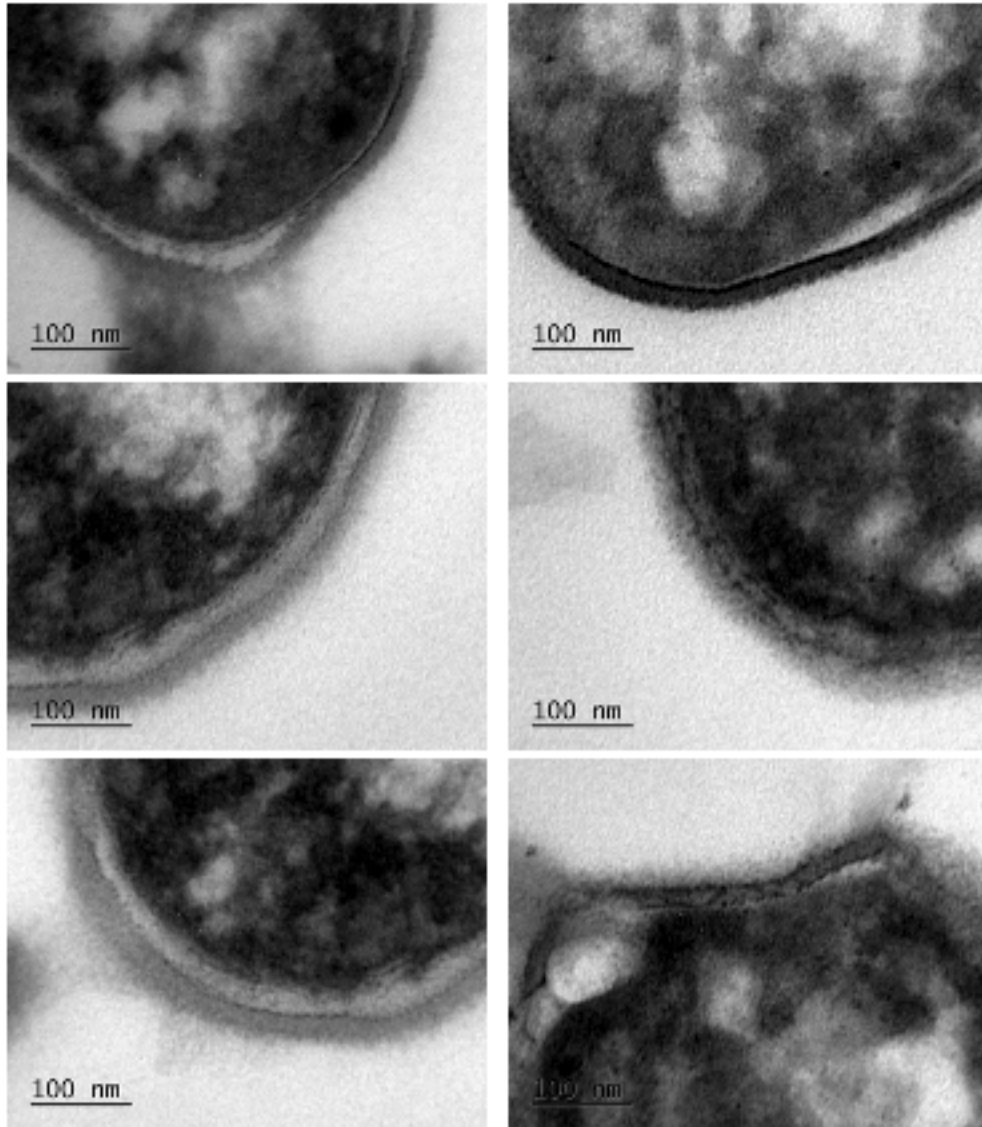


**Figure 4.8.** TEM images of RGD-modified *C. novyi* NT spores (continued).



**Table 4.3.** Assessing the  $\alpha_v\beta_3$  coated surface designed for an adhesion assay. X-ray photoelectron spectroscopy was conducted to assess the elements present on a borosilicate sild cover after corona plasma treatment and subsequent coating with integrin. Adequate presence of integrin was determined when silicate was no longer detectable and nitrogen content had reached its maximum.

<b>Atomic %</b>						
<b>Element</b>	<b>No Treatment</b>	<b>Plasma Treatment</b>	<b>PBS</b>	<b>5ug/mL <math>\alpha_v\beta_3</math></b>	<b>10ug/mL <math>\alpha_v\beta_3</math></b>	<b>20ug/mL <math>\alpha_v\beta_3</math></b>
<b>O</b>	57.96	64.05	55.4	34.76	44.78	38.33
<b>C</b>	9.81	3.54	12.68	25.37	25.34	8.09
<b>Si</b>	23.2	25.08	18.67	1.69	0	0
<b>P</b>			2.53	4.15	8.07	5.82
<b>N</b>				5.34	7.02	7.22
<b>Cl</b>			14.63	14.63	3.75	5.05
<b>K</b>	2.5	2.3	1.92	1.28	1.84	1.7
<b>Na</b>	3.95	3.25	8.14	12.78	9.2	33.79

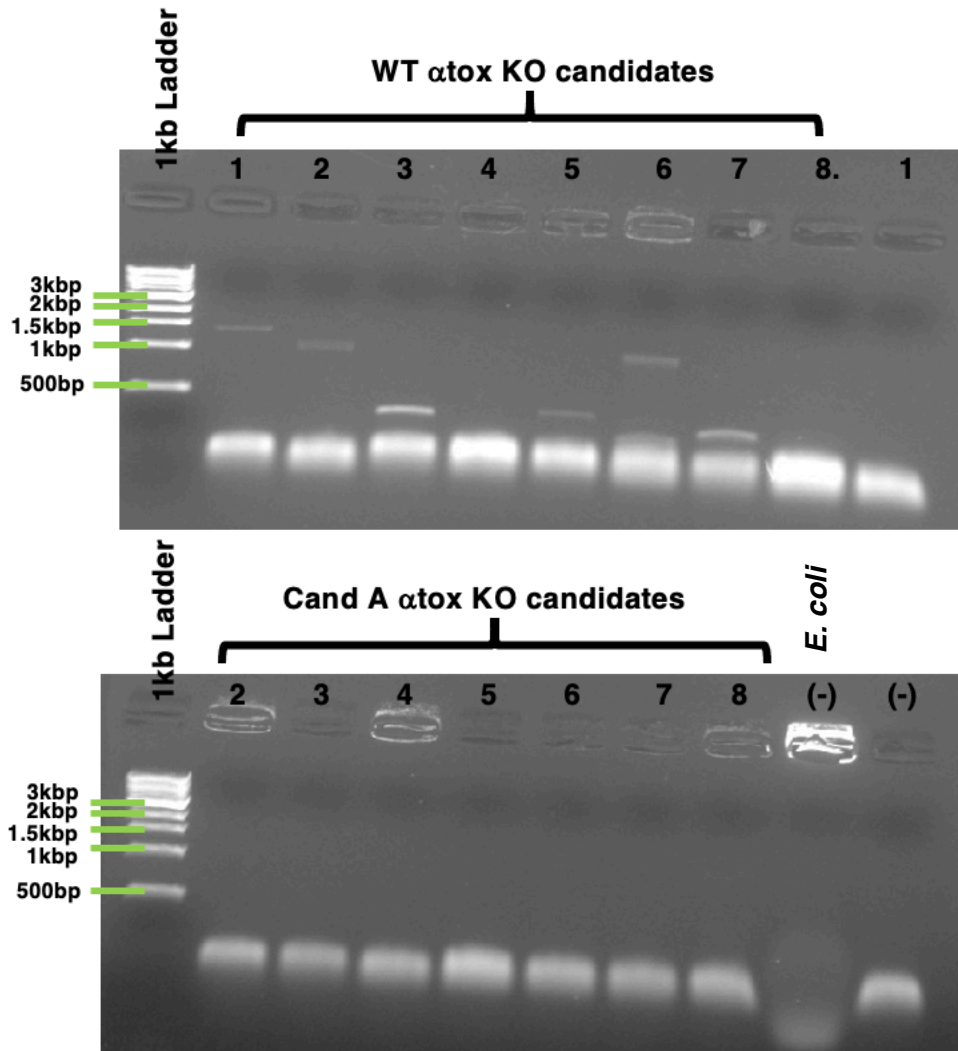


**Figure 4.9.** Generation of a non-toxic RGD-modified *C. novyi* spore. In order to accomplish *in vivo* introduction without substantial toxicity, the  $\alpha$ -toxin encoded phage DNA had to be knocked out in *C. novyi* that had already undergone successful genetic modification with RGD-encoding DNA. Upon knockout, PCR was conducted with primers specific to the  $\alpha$ -toxin so that a lack of a band around 500bp represents  $\alpha$ -toxin removal.

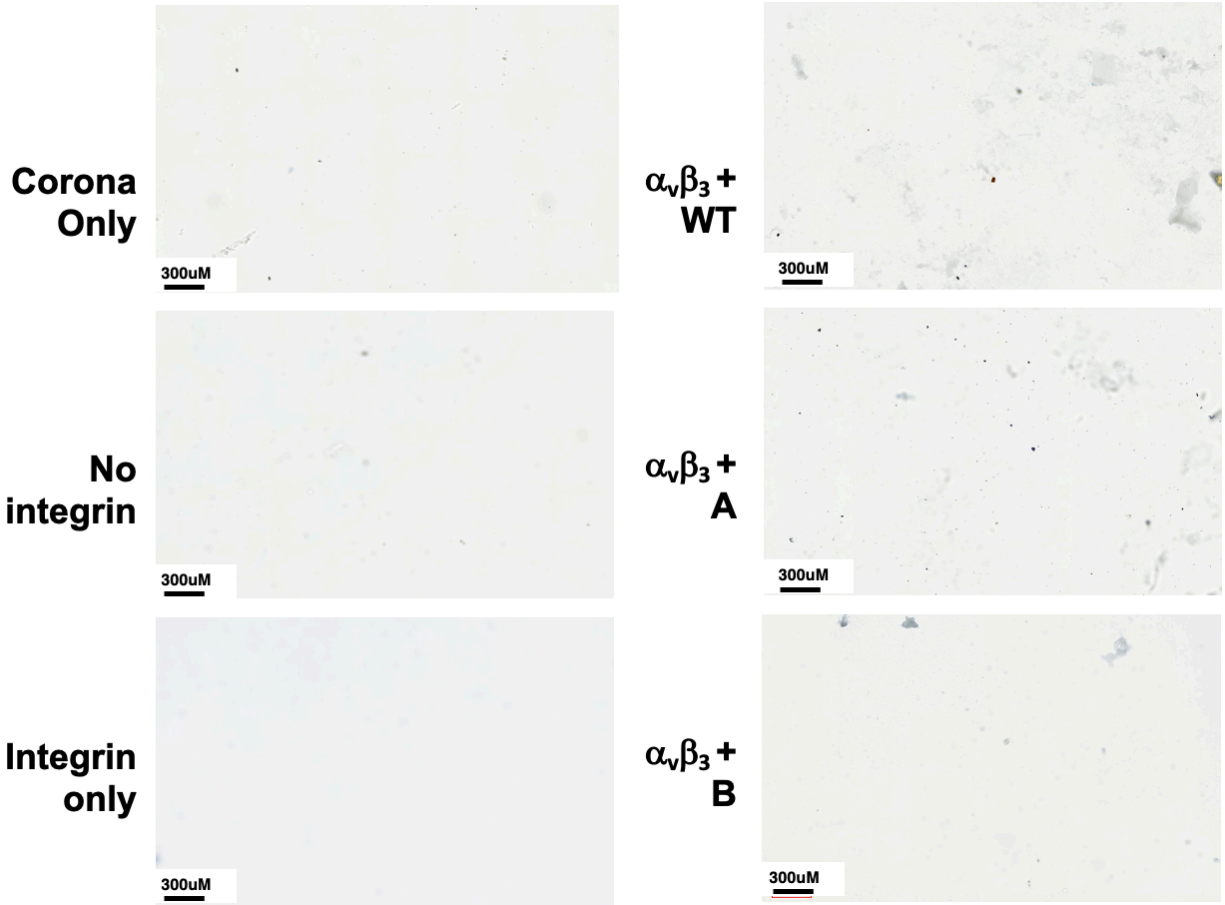


**Figure 4.10.** Representative images used to generate the CV pixel count quantification of the adhesion assay.

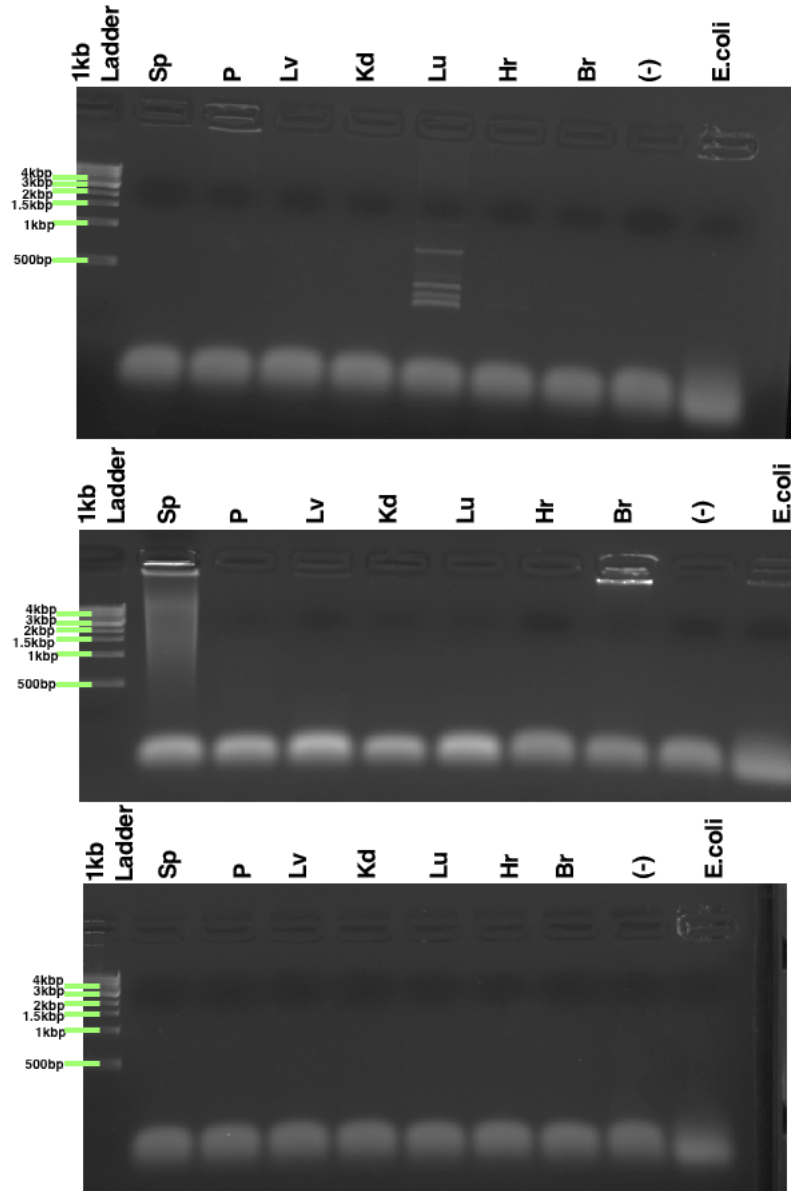


**Figure 4.11.** 16s rRNA PCR amplicons used to establish the biodistribution for the mock tumor (PBS) implant cohort treated with PBS via tail vein injection. (Sp – spleen, P – pancreas, Lv- liver, Kd- kidney, Lu- lung, Hr- heart, Br- brain, (-) no template control, *E. coli* DNA control)

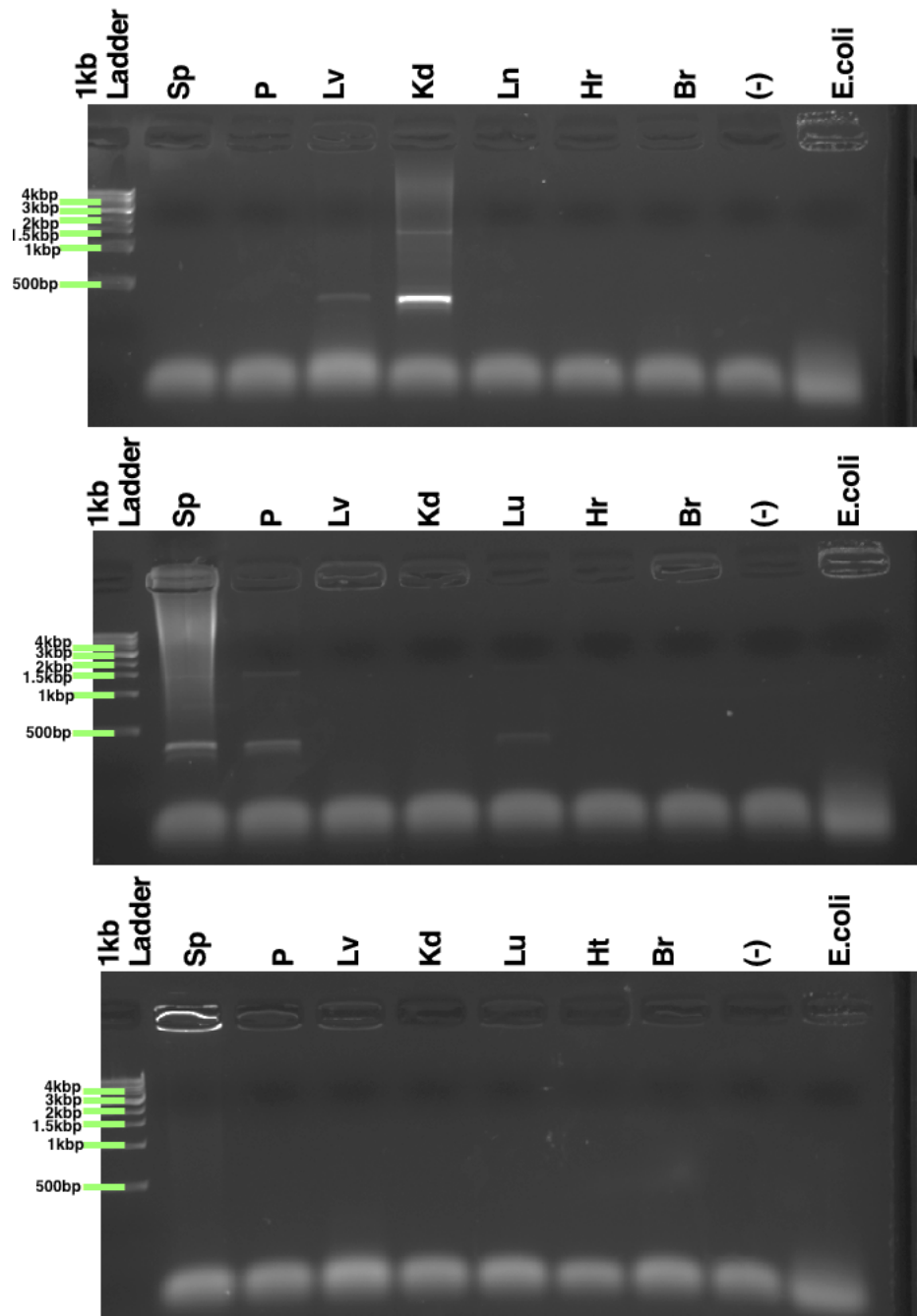


**Figure 4.12.** 16s rRNA PCR amplicons used to establish the biodistribution for the mock tumor (PBS) implant cohort treated with *C. novyi* NT spores (100,000) via tail vein injection. (Sp – spleen, P – pancreas, Lv- liver, Kd- kidney, Lu- lung, Ht- heart, Br- brain, (-) no template control, *E. coli* DNA control)

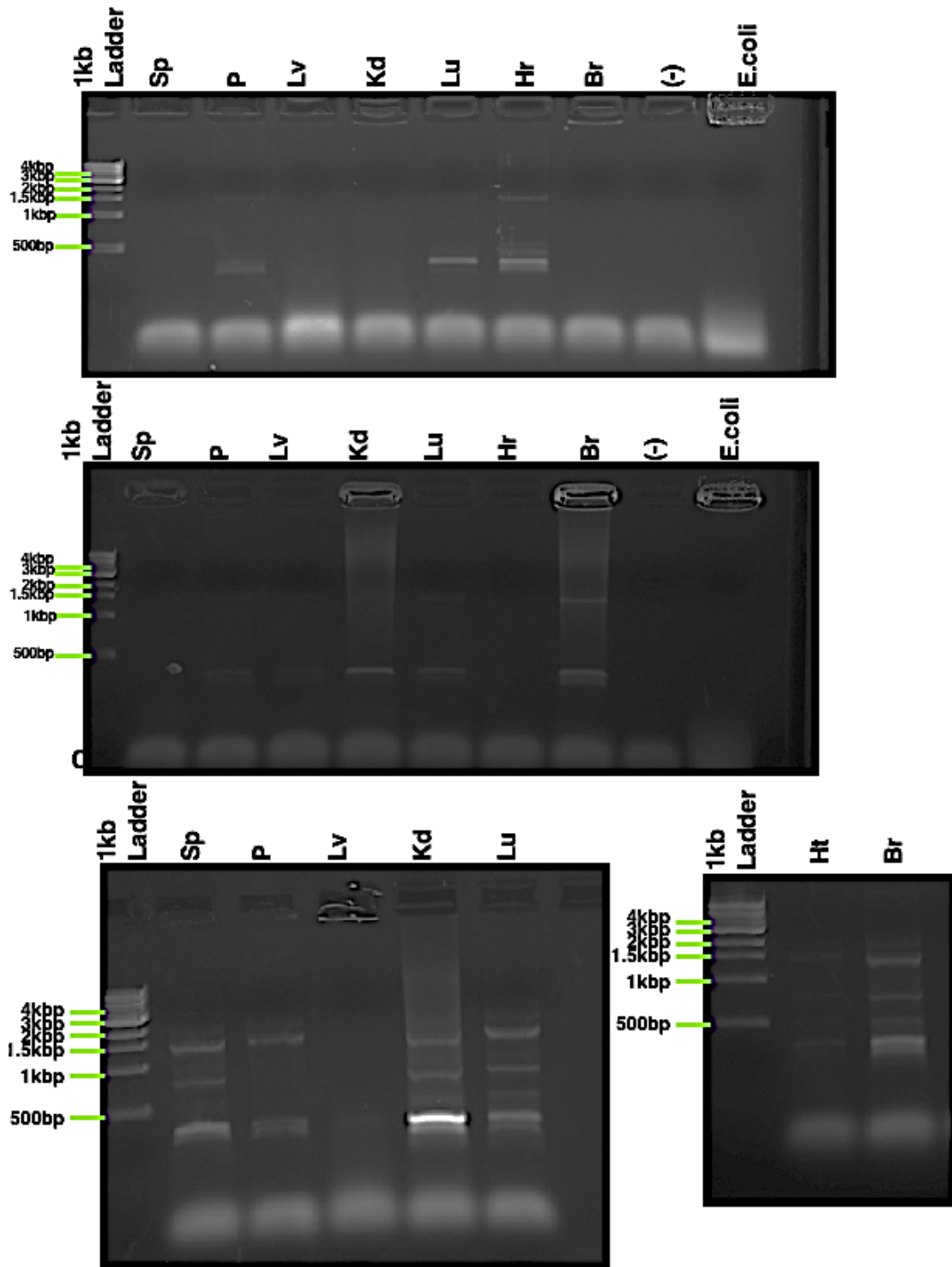


**Figure 4.13.** 16s rRNA PCR amplicons used to establish the biodistribution for the mock tumor (PBS) implant cohort treated with RGD-modified *C. novyi* NT spores (100,000) via tail vein injection. (Sp – spleen, P – pancreas, Lv- liver, Kd- kidney, Lu- lung, Ht- heart, Br- brain, (-) no template control, *E. coli* DNA control)

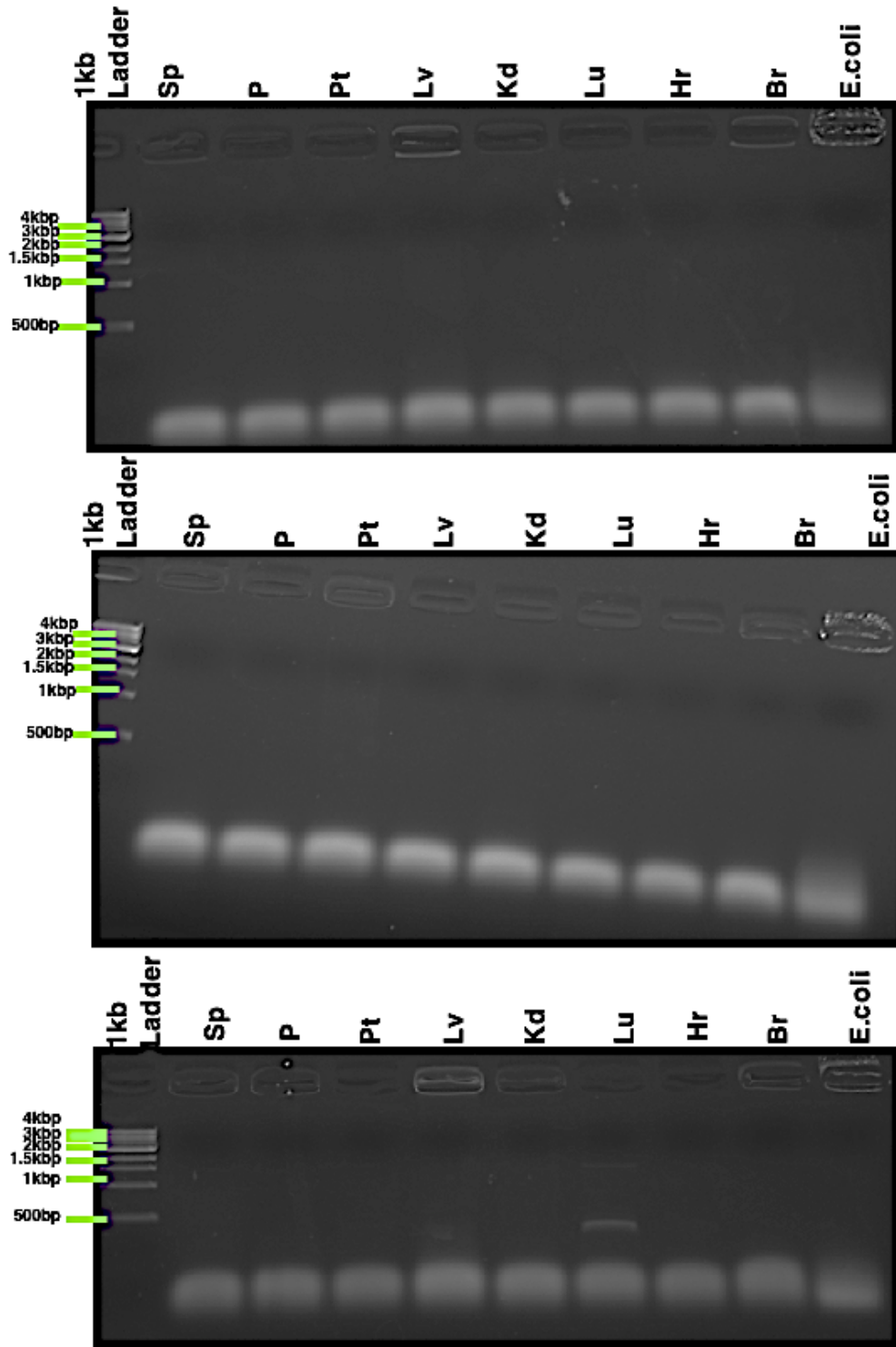


**Figure 4.14.** 16s rRNA PCR amplicons used to establish the biodistribution for the tumor (KPC) implant cohort treated with PBS via tail vein injection. (Sp – spleen, P – pancreas, Pt – pancreatic tumor, Lv- liver, Kd- kidney, Lu- lung, Hr- heart, Br- brain, (-) no template control, *E. coli* DNA control).

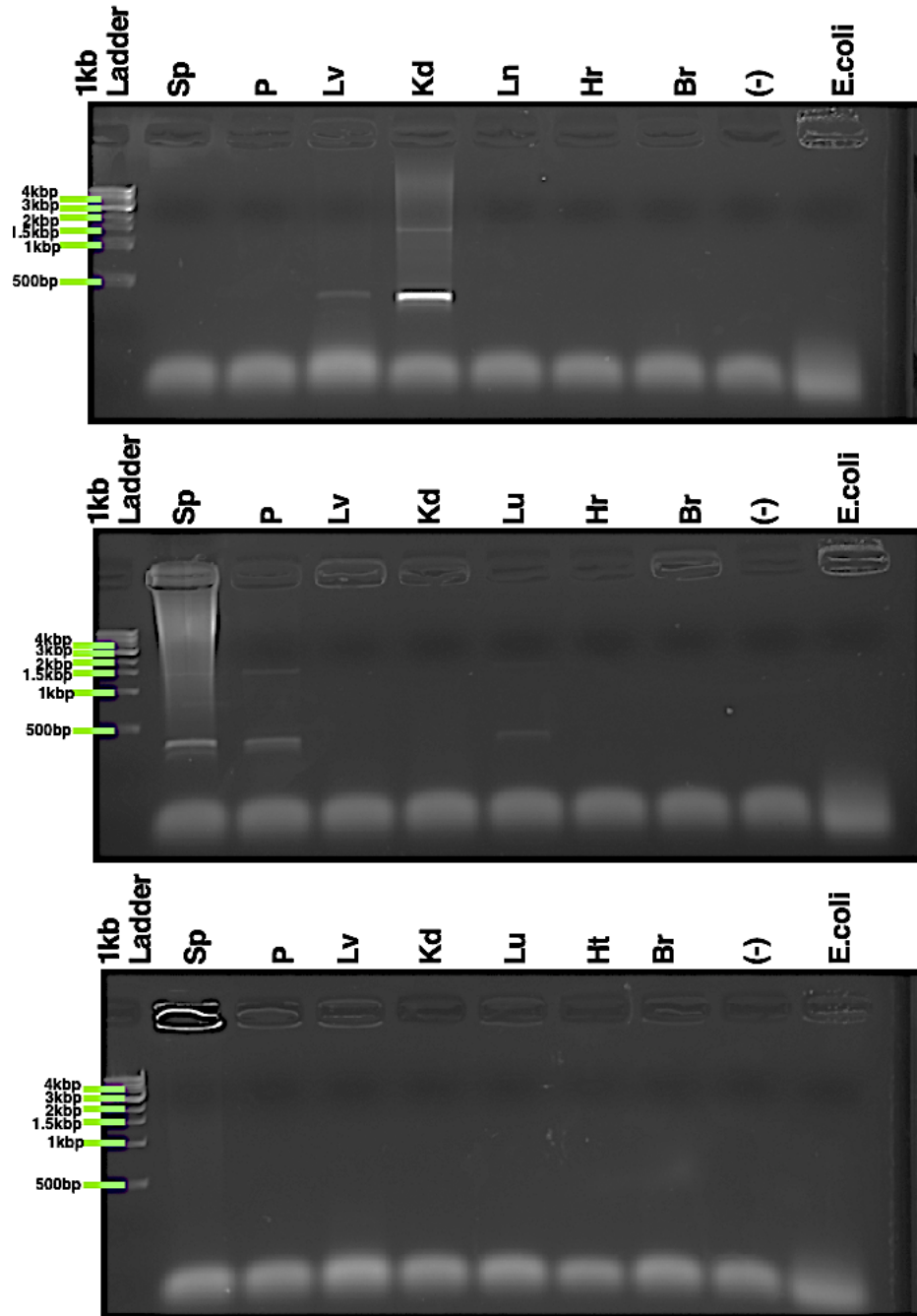


**Figure 4.15.** 16s rRNA PCR amplicons used to establish the biodistribution for the tumor (KPC) implant cohort treated with *C. novyi* NT spores (100,000) via tail vein injection. (Sp – spleen, P – pancreas, Pt – pancreatic tumor, Lv- liver, Kd- kidney, Lu- lung, Ht- heart, Br- brain, (-) no template control, E. coli DNA control).



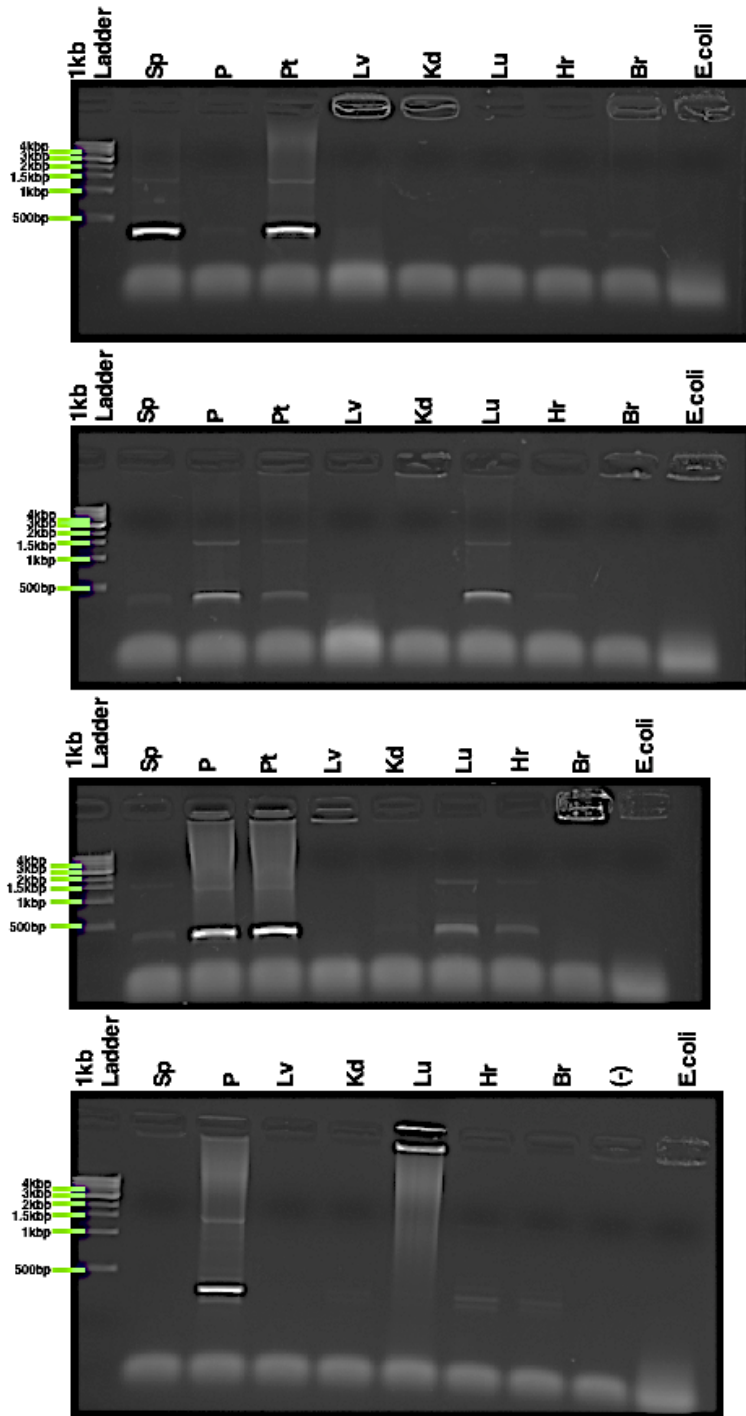


**Figure 4.16.** 16s rRNA PCR amplicons used to establish the biodistribution for the tumor (KPC) implant cohort treated with RGD-modified *C. novyi* NT spores (100,000) via tail vein injection. (Sp – spleen, P – pancreas, Pt – pancreatic tumor, Lv- liver, Kd- kidney, Lu- lung, Hr- heart, Br- brain, (-) no template control, *E. coli* DNA control).

**Table 4.4.** Key to the samples run in Supplementary Figures 4.17.

Sample	Tumor Implant	Tail Vein Injection	Tissue
2	KPC	WT	Pancreas
3	KPC	WT	Spleen
26	KPC	RGD-Mod	Spleen
27	KPC	RGD-Mod	Pancreas
28	KPC	RGD-Mod	Pancreatic Tumor
31	KPC	RGD-Mod	Lung
32	KPC	RGD-Mod	Heart
37	KPC	PBS	Liver
<i>E. coli</i>	n.a.	n.a.	n.a.
39	KPC	PBS	Lung
42	KPC	RGD-Mod	Spleen
43	KPC	RGD-Mod	Pancreas
44	KPC	RGD-Mod	Pancreatic Tumor
45	KPC	RGD-Mod	Liver
47	KPC	RGD-Mod	Lung
50	KPC	RGD-Mod	Spleen
52	KPC	RGD-Mod	Pancreatic Tumor
<i>E. coli</i>	n.a.	n.a.	n.a.
59	KPC	WT	Pancreas
60	KPC	WT	Pancreatic Tumor
63	KPC	WT	Lung
66	KPC	RGD-Mod	Pancreas
69	KPC	RGD-Mod	Lung
70	KPC	RGD-Mod	Heart
71	KPC	RGD-Mod	Brain
74	PBS	RGD-Mod	Kidney
<i>E. coli</i>	n.a.	n.a.	n.a.
75	PBS	RGD-Mod	Spleen
76	PBS	RGD-Mod	Pancreas
77	PBS	RGD-Mod	Liver
78	PBS	RGD-Mod	Kidney
80	PBS	RGD-Mod	Heart
81	PBS	RGD-Mod	Brain
82	PBS	RGD-Mod	Spleen
83	PBS	RGD-Mod	Pancreas
<i>E. coli</i>	n.a.	n.a.	n.a.
85	PBS	RGD-Mod	Kidney
86	PBS	RGD-Mod	Lung
87	PBS	RGD-Mod	Heart
88	PBS	RGD-Mod	Brain
89	KPC	WT	Spleen
90	KPC	WT	Pancreas
96	PBS	PBS	Spleen
103	PBS	RGD-Mod	Spleen
<i>E. coli</i>	n.a.	n.a.	n.a.

**Table 4.4.** Key to the samples run in Supplementary Figure 4.17 (continued).

Sample	Tumor Implant	Tail Vein Injection	Tissue
104	PBS	RGD-Mod	Pancreas
107	PBS	RGD-Mod	Lung
108	PBS	RGD-Mod	Heart
117	PBS	WT	Spleen
118	PBS	WT	Pancreas
121	PBS	WT	Lung
128	PBS	PBS	Lung
<i>E. coli</i>	n.a.	n.a.	n.a.
132	PBS	RGD-Mod	Liver
135	PBS	RGD-Mod	Kidney
140	PBS	RGD-Mod	Blood
141	PBS	RGD-Mod	Urine
<i>E. coli</i>	n.a.	n.a.	n.a.

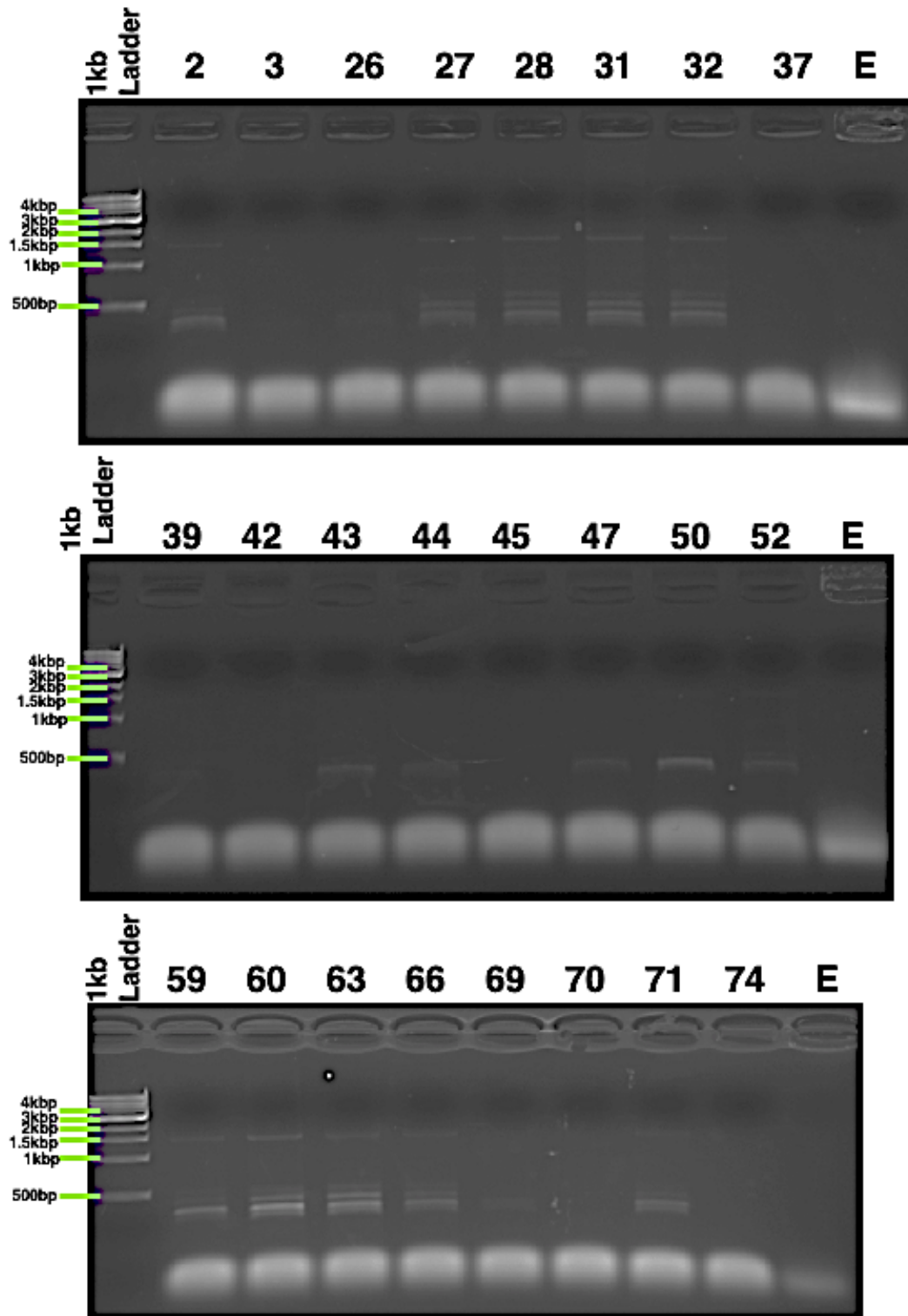


**Figure 4.17.** 16s rRNA PCR amplicons from normalized genomic DNA isolates used to establish the bacterial burden in ng/amplicon in Figure 4.6. A sample legend can be found in Sup. Table 4.4.

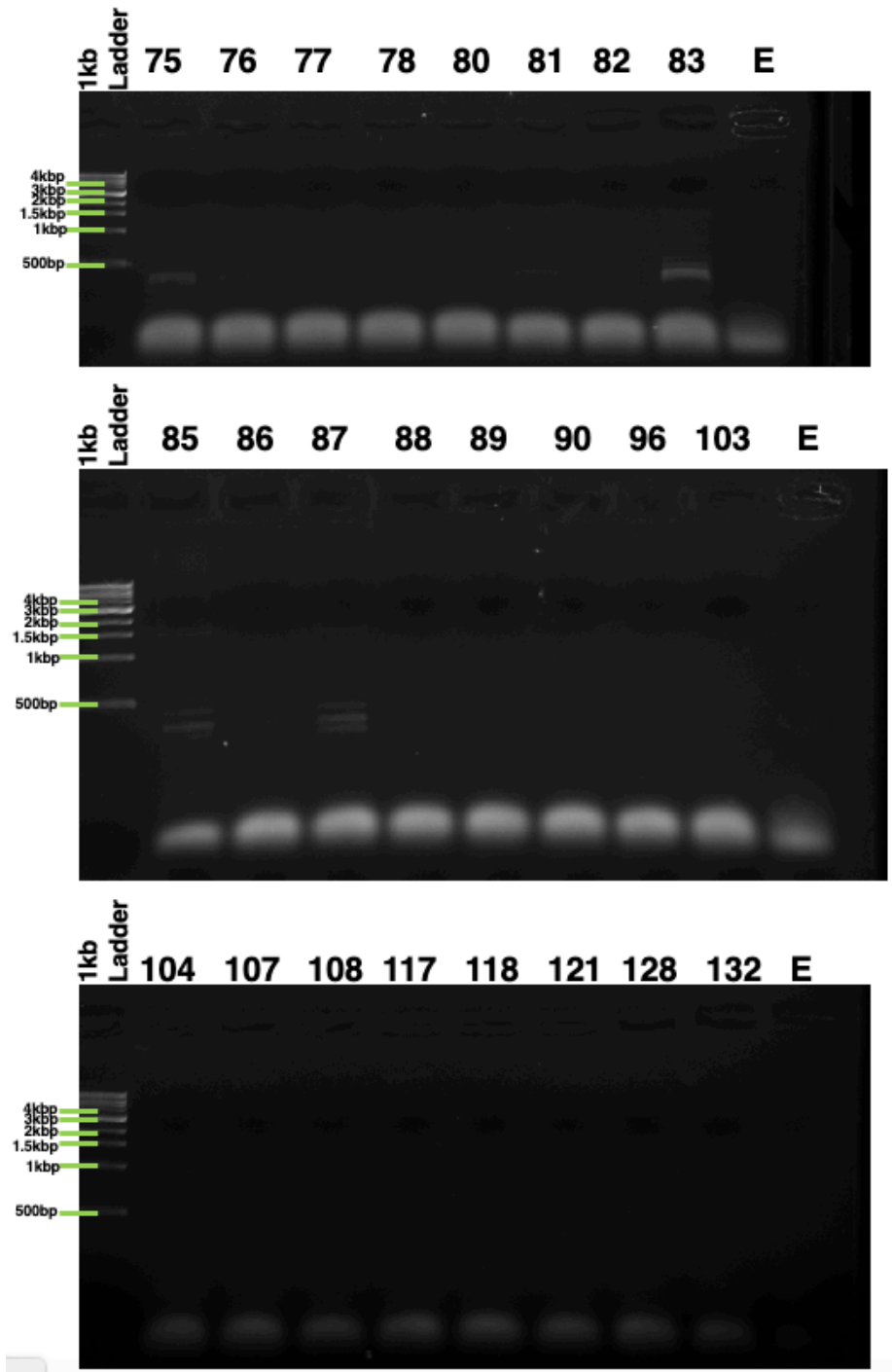


**Figure 4.17.** 16s rRNA PCR amplicons from normalized genomic DNA isolates used to establish the bacterial burden in ng/amplicon in Figure 4.6 (continued). A sample legend can be found in Sup. Table 4.4.

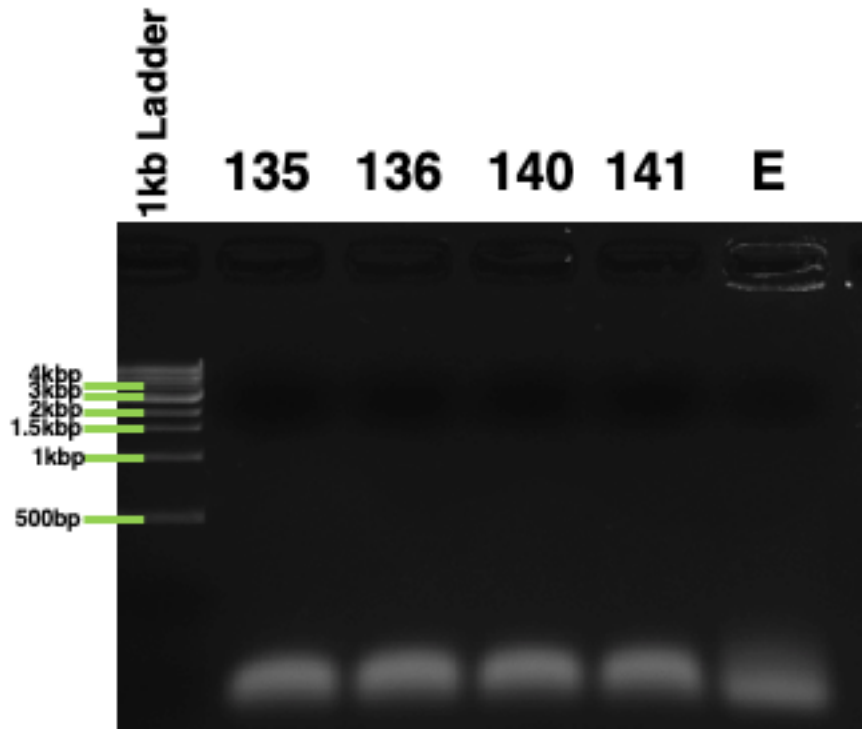


**Figure 4.17.** Resulting 16s rRNA PCR amplicons from normalized genomic DNA isolates used to establish the bacterial burden in ng/amplicon in Figure 4.6 (continued) A sample legend can be found in Sup. Table 4.4.

### References

- (1) Wei, M. Q.; Mengesha, A.; Good, D.; Anné, J. Bacterial Targeted Tumour Therapy-Dawn of a New Era. *Cancer Lett.* **2008**, *259* (1), 16–27.  
<https://doi.org/10.1016/j.canlet.2007.10.034>.
- (2) Safety Study of Intratumoral Injection of Clostridium Novyi-NT Spores to Treat Patients With Solid Tumors That Have Not Responded to Standard Therapies - Full Text View - ClinicalTrials.gov <https://clinicaltrials.gov/ct2/show/NCT01924689> (accessed Apr 24, 2019).
- (3) BioMed Valley Discoveries, Inc. *Phase I Safety Study of Intratumoral Injection of Clostridium Novyi-NT Spores in Patients With Treatment-Refractory Solid Tumor Malignancies*; Clinical trial registration NCT01924689; clinicaltrials.gov, 2019.
- (4) Janku, F.; Zhang, H. H.; Pezeshki, A. M.; Goel, S.; Murthy, R.; Wang-Gillam, A.; Shepard, D. R.; Helgason, T.; Masters, T.; Hong, D. S.; Piha-Paul, S. A.; Karp, D. D.; Klang, M.; Huang, S. Y.; Sakamuri, D.; Raina, A.; Torrisi, J.; Solomon, S. B.; Weissfeld, A.; Trevino, E.; DeCrescenzo, G. A.; Collins, A.; Miller, M.; Salstrom, J. L.; Korn, R.; Zhang, L.; Saha, S.; Leontovich, A. A.; Tung, D.; Kreider, B.; Varterasian, M.; Khazaie,

- K.; Gounder, M. M. Intratumoral Injection of Clostridium Novyi-NT Spores in Patients with Treatment-Refractory Advanced Solid Tumors. *Clin. Cancer Res.* **2020**. <https://doi.org/10.1158/1078-0432.CCR-20-2065>.
- (5) Ilic, M.; Ilic, I. Epidemiology of Pancreatic Cancer. *World J. Gastroenterol.* **2016**, *22* (44), 9694–9705. <https://doi.org/10.3748/wjg.v22.i44.9694>.
- (6) Saad, A. M.; Turk, T.; Al-Husseini, M. J.; Abdel-Rahman, O. Trends in Pancreatic Adenocarcinoma Incidence and Mortality in the United States in the Last Four Decades; a SEER-Based Study. *BMC Cancer* **2018**, *18*. <https://doi.org/10.1186/s12885-018-4610-4>.
- (7) Cancer of the Pancreas - Cancer Stat Facts <https://seer.cancer.gov/statfacts/html/pancreas.html> (accessed May 6, 2019).
- (8) 2018 NCI Budget Fact Book - Research Funding - National Cancer Institute <https://www.cancer.gov/about-nci/budget/fact-book/data/research-funding> (accessed Oct 22, 2020).
- (9) Binnewies, M.; Roberts, E. W.; Kersten, K.; Chan, V.; Fearon, D. F.; Merad, M.; Coussens, L. M.; Gaborilovich, D. I.; Ostrand-Rosenberg, S.; Hedrick, C. C.; Vonderheide, R. H.; Pittet, M. J.; Jain, R. K.; Zou, W.; Howcroft, T. K.; Woodhouse, E. C.; Weinberg, R. A.; Krummel, M. F. Understanding the Tumor Immune Microenvironment (TIME) for Effective Therapy. *Nat. Med.* **2018**, *24* (5), 541–550. <https://doi.org/10.1038/s41591-018-0014-x>.
- (10) Boedtkjer, E.; Pedersen, S. F. The Acidic Tumor Microenvironment as a Driver of Cancer. *Annu. Rev. Physiol.* **2020**, *82* (1), 103–126. <https://doi.org/10.1146/annurev-physiol-021119-034627>.
- (11) Finger, E. C.; Giaccia, A. J. Hypoxia, Inflammation, and the Tumor Microenvironment in Metastatic Disease. *Cancer Metastasis Rev.* **2010**, *29* (2), 285–293. <https://doi.org/10.1007/s10555-010-9224-5>.
- (12) McKeown, S. R. Defining Normoxia, Physoxia and Hypoxia in Tumours—Implications for Treatment Response. *Br. J. Radiol.* **2014**, *87* (1035). <https://doi.org/10.1259/bjr.20130676>.
- (13) Rius-Rocabert, S.; Llinares Pinel, F.; Pozuelo, M. J.; García, A.; Nistal-Villan, E. Oncolytic Bacteria: Past, Present and Future. *FEMS Microbiol. Lett.* **2019**, *366* (12). <https://doi.org/10.1093/femsle/fnz136>.
- (14) Wang, Y.; Guo, W.; Wu, X.; Zhang, Y.; Mannion, C.; Brouchkov, A.; Man, Y.-G.; Chen, T. Oncolytic Bacteria and Their Potential Role in Bacterium-Mediated Tumour Therapy: A Conceptual Analysis. *J. Cancer* **2019**, *10* (19), 4442–4454. <https://doi.org/10.7150/jca.35648>.

- (15) Dang, L. H.; Bettgowda, C.; Huso, D. L.; Kinzler, K. W.; Vogelstein, B. Combination Bacteriolytic Therapy for the Treatment of Experimental Tumors. *Proc. Natl. Acad. Sci. U. S. A.* **2001**, *98* (26), 15155–15160. <https://doi.org/10.1073/pnas.251543698>.
- (16) Diaz, L. A.; Cheong, I.; Foss, C. A.; Zhang, X.; Peters, B. A.; Agrawal, N.; Bettgowda, C.; Karim, B.; Liu, G.; Khan, K.; Huang, X.; Kohli, M.; Dang, L. H.; Hwang, P.; Vogelstein, A.; Garrett-Mayer, E.; Kobrin, B.; Pomper, M.; Zhou, S.; Kinzler, K. W.; Vogelstein, B.; Huso, D. L. Pharmacologic and Toxicologic Evaluation of C. Novyi-NT Spores. *Toxicol. Sci.* **2005**, *88* (2), 562–575. <https://doi.org/10.1093/toxsci/kfi316>.
- (17) Edwards, A. N.; McBride, S. M. Isolating and Purifying Clostridium Difficile Spores. *Methods Mol. Biol. Clifton NJ* **2016**, *1476*, 117–128. [https://doi.org/10.1007/978-1-4939-6361-4\\_9](https://doi.org/10.1007/978-1-4939-6361-4_9).
- (18) Joseph, R. C.; Kim, N. M.; Sandoval, N. R. Recent Developments of the Synthetic Biology Toolkit for Clostridium. *Front. Microbiol.* **2018**, *9*. <https://doi.org/10.3389/fmicb.2018.00154>.
- (19) Bettgowda, C.; Huang, X.; Lin, J.; Cheong, I.; Kohli, M.; A Szabo, S.; Zhang, X.; Diaz, L.; Velculescu, V.; Parmigiani, G.; W Kinzler, K.; Vogelstein, B.; Zhou, S. The Genome and Transcriptomes of the Anti-Tumor Agent Clostridium Novyi-NT. *Nat. Biotechnol.* **2007**, *24*, 1573–1580. <https://doi.org/10.1038/nbt1256>.
- (20) Behle, A. Preparation of Chemically Competent Cells. **2018**. <https://doi.org/10.17504/protocols.io.n8mdhu6>.
- (21) Schindelin, J.; Arganda-Carreras, I.; Frise, E.; Kaynig, V.; Longair, M.; Pietzsch, T.; Preibisch, S.; Rueden, C.; Saalfeld, S.; Schmid, B.; Tinevez, J.-Y.; White, D. J.; Hartenstein, V.; Eliceiri, K.; Tomancak, P.; Cardona, A. Fiji: An Open-Source Platform for Biological-Image Analysis. *Nat. Methods* **2012**, *9* (7), 676–682. <https://doi.org/10.1038/nmeth.2019>.
- (22) Hasan, R.; Schaner, K.; Schroeder, M.; Wohlers, A.; Shreffler, J.; Schaper, C.; Subramanian, H.; Brooks, A. Extended Release Combination Antibiotic Therapy from a Bone Void Filling Putty for Treatment of Osteomyelitis. *Pharmaceutics* **2019**, *11* (11). <https://doi.org/10.3390/pharmaceutics11110592>.
- (23) Plomp, M.; McCaffery, J. M.; Cheong, I.; Huang, X.; Bettgowda, C.; Kinzler, K. W.; Zhou, S.; Vogelstein, B.; Malkin, A. J. Spore Coat Architecture of Clostridium Novyi NT Spores. *J. Bacteriol.* **2007**, *189* (17), 6457–6468. <https://doi.org/10.1128/JB.00757-07>.
- (24) Shreffler, J. W.; Pullan, J. E.; Dailey, K. M.; Mallik, S.; Brooks, A. E. Overcoming Hurdles in Nanoparticle Clinical Translation: The Influence of Experimental Design and Surface Modification. *Int. J. Mol. Sci.* **2019**, *20* (23). <https://doi.org/10.3390/ijms20236056>.



## CHAPTER 5: CONCLUSION

By 2030, pancreatic cancer diagnoses are projected to increase by over 50%, bringing the number of patients from 14 million to a staggering 21 million cases worldwide<sup>1</sup>, resulting in rising mortality projections. Despite significantly increased survival rates in other major forms of cancer, minimal gains have been made in pancreatic cancer therapeutics<sup>1</sup>. Limited progress in the face of this alarming trend demands a new perspective, even a paradigm shift, in the field of pancreatic cancer therapeutics. Solid tumors present a unique set of challenges for traditional drug delivery and are an intrinsic promoter of tumor development and metastases<sup>2</sup>. The underlying basis of these challenges lies - at least partially - in the tumor microenvironment (TME). The TME of a solid tumor is characterized by aberrant vascularization and abnormal extracellular matrix structures such as desmoplasia, which combine to cause a build-up of metabolic byproducts culminating in hypoxic and acidic gradients intimately connected with the tumor core<sup>3</sup>. Ultimately, dysfunctional lymphatics and irregularly composed extracellular matrixes (ECM) hamper passive, intratumoral diffusion, vastly limiting the bioavailability and efficacy of intravenously delivered (IV) therapeutics<sup>3</sup>. However, these same aspects of the TME that are barriers for traditional chemotherapeutics allow oncolytic bacteria to migrate to and colonize the center of a solid tumor - ultimately resulting in the lysis of tumorigenic cells. While oncolytic bacteria are not a new discovery<sup>4</sup>, they are reemerging on the therapeutic landscape. Using the natural chemotactic responses of oncolytic bacteria provides an opportunity to harness the inherent active targeting and translocation of a biological system to exploit the TME. This is a stark contrast to more traditional approaches that attack the cancer at the proliferating, normally oxygenated tumor margins.

The oncolytic bacteria *Clostridium novyi* has demonstrated exquisite sensitivity to hypoxia much beyond its cousins *C. difficile* and *C. botulinum*, and has recently shown promise in preclinical and early stage clinical trials of direct intratumoral injection<sup>5</sup>. Upon intratumoral injection of *C. novyi* spores, >90% curative rate has been observed in a murine tumor model<sup>6</sup>; however, not all solid tumors are accessible for direct injection. Initial challenges posed by off-target sepsis encountered with *C. novyi* treatment have been largely mitigated by the ability to create a non-toxic strain (*C. novyi*-NT)<sup>6</sup>. The toxin responsible for *C. novyi* toxicity,  $\alpha$ -toxin, has been removed from attenuated bacteria via common cell membrane permeabilization<sup>7</sup>. However, there are still improvements to be made as *C. novyi* is quickly cleared from the blood stream by the mononuclear phagocyte system (MPS) before it has a chance to reach the primary tumor site<sup>6</sup>. Previous efforts geared toward IV delivery of *C. novyi* spores have led to only a 25-30% cure rate with <1% of injected spores reaching the tumor<sup>6</sup>. The majority of injected spores were rapidly cleared to the liver and the spleen by the MPS without adverse side effects<sup>6</sup>. These observations lead to this thesis's hypothesis: an attenuated oncolytic bacterial spore, *Clostridium novyi*-NT, genetically engineered to express an RGD peptide in its spore coat will adhere specifically to the  $\alpha\beta 3$  integrin overexpressed<sup>8</sup> on cancerous pancreatic tumor cells.

This dissertation work has successfully used CRISPR/Cas9 to insert the genetic sequence encoding an RGD peptide into *C. novyi* for the first time as detailed in Chapter 2. To accomplish this new CRISPR application, the ten most and least expressed genes<sup>1</sup> in *C. novyi* were compared to those of the much more well characterized species *C. difficile* and *E. coli*, leading to a critical understanding of *C. novyi*'s codon bias. For the first time, the codon adaptation index, a number that describes the species specific codon biasing, was generated for *C. novyi* genes and compared to more well characterized species. The comparison of these genes between the three species

indicated that the methods commonly used to experiment with *C. difficile* and *E. coli* would not be adequate for application to *C. novyi*. Thus, new methods were developed. The utilization of the oxygen fixing enzyme Oxyrase allowed for a much greater range of methodologies to be attempted with no indicated effects compromising the innate characteristics of *C. novyi*. Due to this newfound ability to leave the confines of a benchtop atmospheric chamber, this thesis was able to not only generate calcium competent *C. novyi* bacteria in order to address the previous challenge of low transformation rates but also to successfully accomplish the introduction of a CRISPR/Cas9n plasmid. Upon confirmation that the transformation had indeed resulted in the introduction of this plasmid into *C. novyi* cells, a genomic DNA isolation and validating restriction digests confirmed that this plasmid had indeed inserted its RGD encoded sequence into a targeted genomic location.

The RGD peptide was selected for this study both due to the body of literature detailing its functionality and its relatively small molecular size making the genetic insertion a a proof of concept model. The sub-hypothesis tested by this work was that the incorporation of the genetic sequence encoding an RGD peptide would act as a potent tumor targeting system, allowing the bacteria to remain in circulation longer and increasing the bioburden of the tumor. At least one candidate indicated a stronger affinity for an  $\alpha_v\beta_3$  integrin coated surface. Characterization efforts detailed in Chapter 2 have demonstrated no statistical difference in the candidate's life cycle compared to unmodified *C. novyi* spores, indirectly suggesting no off-target genetic effects. RGD-modified *C. novyi* NT spores demonstrated lytic capacity against pancreatic cancer cells similar to their wild type counterparts. Additionally, for the first time, wild type and non-toxic strains of *C. novyi* were directly compared through a co-culture with a panel of several pancreatic cancer cell lines. These co-culture experiments had two major findings. First, they

overwhelmingly demonstrated that mono-layer cell culture is not a sensitive enough model system to test the lytic capacity of *C. novyi*, regardless of the form (vegetative vs sporulated). Second, these studies, however, did demonstrate that the expression of the COX-2 enzyme has a strong effect on the lytic capacity of *C. novyi* vegetative cells. The limitations this enzyme and the potential angiogenic implications of COX-2 will have a significant impact on the clinical translation and context within which this therapy eventually may be applied.

The physical and functional characterization conducted in Chapter 3 indicate genomic incorporation has successfully resulted in the expression of an RGD peptide contained within the spore coat without ablating the necessary natural tumor localization and destruction characteristics. To probe the functional capacity of the integrated RGD peptide, the development of more novel methods was necessary. An integrin coated surface was designed utilizing the well-characterized bond between the RGD peptide and the  $\alpha_v\beta_3$  integrin. The number of spores that adhered to this surface were measured through utilization of the crystal violet stain. These studies indicated at least one of the genetically modified *C. novyi* candidate cell lines did adhere in a larger quantity than the wild type, non-toxic as well as other candidates. TEM images further corroborated the physical expression of the RGD peptide by indicating a disruption of the polysaccharide layer in the modified candidate A.

Once the physical presence and functionality of the RGD peptide in the spore coat of *C. novyi* were confirmed, the biodistribution of a non-toxic, RGD modified *C. novyi* spore was assessed as a targeted, IV injectable dosage form in an immunocompetent mouse model. The study detailed in Chapter 4 represents a critical step, intravenous injection in an immunocompetent orthotopic tumor model, in the progression of this modified *C. novyi*. While these results are only from a pilot study, they demonstrate quite clearly the potential of both this

specific modification of *C. novyi* NT as an oncotherapeutic as well as the potential of genetic engineering to accomplish the translation and application of oncolytic bacterial in general. Upon calculating a relative percent tumor localization it was determined that while 14% of wild type spore accomplished pancreatic and pancreatic tumor localization, 41% of the RGD-modified spores were found to be localized the pancreas and associated tumor tissue representing an almost 30% increase. Furthermore, the addition of the RGD peptide to the *C. novyi* spore coat lead to approximately twice the total bacterial burden twenty-four hours after administration. The culmination of this data supports the hypothesis this dissertation work set out to test.

In order to strengthen the data demonstrated within this study, additional animals should be examined in a statistically powered cohort design to determine the spore load in the pancreas and tumor as well as to determine the over all percentage of initial dose. Furthermore, a more accurate quantification of the biodistribution with a higher level of data integrity could be obtained through utilization of radiographically labeled spores as without this data it is very difficult to make comparisons with published literature. Establishing the biodistribution through the use of gamma scintillation would allow for a direct analysis of the clearance rate of modified spores versus unmodified spores. RGD-modified spores could be applied in the cremaster model for determining immune cell recruitment to gain a more direct measure of the immunogenicity of the modified spores versus wild-type spores. This model uses the immune priveleged environment of the testes as a blank canvas to measure which immune cells are recruited by the introduction of a novel therapeutic.

Perhaps the most convincing argument made by the work within this dissertation is that CRISPR gene modification can be used to customize bacteria, most notably oncolytic bacteria. The advent of this novel technique capable of accomplishing genetic engineering with relative

ease, speed, and affordability has revolutionized the landscape of eukaryotic disease research. It is only a matter of time until this transformation spreads into the prokaryotic realm. Indeed, examples of bacterial genome engineering are beginning to emerge in the landscape of biofuel and bioremediation. Harnessing the power of bacteria for pharmaceutical applications is a natural evolution of this process, and this study serves to establish a premise for future studies. To directly build upon the work presented here, studies could be proposed to incorporate other tumor targeting moieties such as folate, LRP, or transferrin, all of which have recently demonstrated efficacy in the world of nanoparticle targeting. Incorporation of other molecules could also be attempted, e.g. spider silk, chitosan, or PEGylation, in order to further extend the half-life of spores in the blood stream, thus allowing a longer time frame within which spores are able to localize to the tumor. Furthermore, the exceptionally specific tumor localization capacity could be developed beyond a therapeutic into a potent tumor detection system through the incorporation of a radiolabeled molecule into the spore coat. Should the lytic capacity prove to impede the development of such an application, the publication of the entire transcriptome makes it possible to use CRISPR and/or CRISPRi to accomplish the knock-out of the enzymes responsible for lysis. Several ‘ghost’ cells are currently in development for other oncolytic bacteria where the ‘shells’ or membranes with trans-membrane and membrane associated proteins remain intact, but the contents of the cell, which allow for proliferation and independent action, have been removed. If a lyophilized form of the anti-tumorigenic spores could be developed, this could be developed into a potent probiotic to be distributed to those predisposed to the development of tumors, whether due to genetic or environmental conditions.

This dissertation began with the hypothesis that an attenuated oncolytic bacterial spore, *Clostridium novyi*-NT, genetically engineered to express an RGD peptide in its spore coat will

adhere specifically to the  $\alpha_v\beta_3$  integrin overexpressed on cancerous pancreatic tumor cells. While the data generated in efforts to test this hypothesis may not have established a strong specific adhesion to the  $\alpha_v\beta_3$  integrin thus conferring tumor localization, an extension in the circulatory time of RGD-modified spores is one potential explanation for the increased over all *C. novyi* bacterial burden observed for both mice with mock tumor implantations as well as tumors. This observation may be further supported with more mice and a longer time frame to more strongly and directly support the hypothesis. However, a secondary hypothesis has long been considered that was supported by the data generated in the pursuit of this doctorate degree. The  $\alpha_v\beta_3$  integrin is expressed in varying levels in most epithelial cells, including those that line blood vessels. The secondary hypothesis proposed that the presence of these integrins may serve to temporarily bind to the RGD peptide contained in the spore coat while they are still within the blood vessel, thus serving to slow the shearing force of spores within the blood stream. While further data could be gathered to corroborate this hypothesis, the data demonstrates that the incorporation of a RGD-peptide into the spore coat of *C. novyi* via CRIPSR/Cas9 gene editing was not only successful, but also changed the biodistribution and resulting bacterial burden in a tumor-bearing immunocompetent mouse models.

### References

- (1) Pancreatic cancer statistics <https://www.wcrf.org/dietandcancer/cancer-trends/pancreatic-cancer-statistics>.
- (2) Whatcott CJ, et al. Desmoplasia and chemoresistance in pancreatic cancer. In: Grippo PJ, Munshi HG, editors. Pancreatic Cancer and Tumor Microenvironment. Trivandrum (India): Transworld Research Network; **2012**. Chapter 8.
- (3) Minchinton, et. al. Drug Penetration in Solid Tumours. Nat. Rev. Cancer **2006**, 6 (8), 583–592.
- (4) Wei, M. et al. Bacterial Targeted Tumour Therapy-Dawn of a New Era. Cancer Lett. **2008**, 259 (1), 16–27. <https://doi.org/10.1016/j.canlet.2007.10.034>.

- (5) Safety Study of Intratumoral Injection of *Clostridium Novyi*-NT Spores to Treat Patients With Solid Tumors That Have Not Responded to Standard Therapies - ClinicalTrials.gov
- (6) Diaz, L. A. et al. Pharmacologic and Toxicologic Evaluation of *C. Novyi*-NT Spores. *Toxicol. Sci. Off. J. Soc. Toxicol.* **2005**, 88 (2), 562–575. <https://doi.org/10.1093/toxsci/kfi316>.
- (7) Staedtke, V.; et al. *Clostridium Novyi*-NT in Cancer Therapy. *Genes Dis.* **2016**, 3 (2), 144–152. <https://doi.org/10.1016/j.gendis.2016.01.003>.
- (8) Danhier, F.; et al. RGD-Based Strategies to Target Alpha(v)beta(3) Integrin in Cancer Therapy and Diagnosis. *Mol. Pharm.* **2012**, 9 (11), 2961–2973.



## **APPENDIX A: CLONING SEQUENCES FOR SPORE COAT GENE INSERTION IN *C.***

### ***NOVYI***

In order to insert an genetic sequence encoding an RGD peptide into the genome of *C. novyi*, target genes were identified by mining the published literature using the following criteria: 1) integration of the gene insert under the promoter for a surface display protein, 2) avoidance of genes encoding chemotaxis or anerobic functions, including the operon containing NT01CX2374, NT01CX2375, NT01CX2376, 3) avoidance of lipases NT01CX0979, NT01CX2047, and NT01CX0630, 4) avoidance of spore genes highly upregulated during tumor infection (21 genes identified<sup>18</sup>). Four genes (NT01C0401, NT01CX0481, NT01CX1621 and NT01CX1736) were identified as appropriate targets for this study's expression goal utilizing these criteria.

**Table A.1.** Gene sequences of insertion target. Sequences of the four genes identified as targets for spore coat protein insertion. sgRNA sequences are within brackets (targets [1] and {2}) and underlined and bold.

<u>Gene ID</u>	<u>Sequence</u>	<u>Genome Loci (5'-3')</u>
NT01CX0401	ttatattgctccatttgaactcctctacaaccaatcaaattgaataactctgatctgcataacttttccttggaa atctctctgcaccttattatccttaataggacctcaaatactgtcttctctgaaattattctcttaactgttttac ttttctctgcttcttaggtgcatttttgaagagggtgaagatcaactattccatcttaagtcctcccaatagcta tcattttccatgtaccatctacaatagatttattgtttacatagaatggccccagttccacacaggagctgcata tatgcttttggcttactttcc{ <b><u>atatcagtggtatatacctat</u></b> }tgaaaatgcaccttttctctgctgctgtgag gtcctgctgatcttgatgttgagtaattacatctgcaccttcatctaatagtgctttgcctgcttcttttttcagga tcataccaagtgttagtccacttaacttttactacagccttaggattfacagatcaactcctaatgtaaaagcatttatt ccttaactactctggcatttcgtgctgctacataccaatcattgcttttagtcttactcctgcaactataact gatagatactgcttcatatatttccaaaataattgataagttgcagccactttattctgcaaatgcataaatt taactctggatgactttggatgatttaacattccattaagaaaacc <b><u>aaagctgttccaattatta</u></b> cttaccat ccttgatcaatcactttcaactgtgtttgaactcagcatctcttcttactgattcctgaattacggatggcttat tccaagttcttttcaatactttctcttgatcatgagaatagtccaaccaccatccactggccaacataca aaaatccaacttaatgtcttataacttaatttttccctattttcactactattggtgcttactattccacatccagt taataatgttctatagtaaaaactaaaataataataggatctcttttca	2096139 – 2095021
NT01CX0481	actgattctgattgaatgtttctcctctattgagatgctgcaatttaattgtcttttctttaaactctca <b><u>ggataat</u></b> <b><u>acaatactacc</u></b> aaggcttgagttatttgattcaagaacccaattctctttagtaaaactaaaaggagctga cgccactactcttccattttctataagatttaacgaacatctataatfaaatagattctcatggccattgcgaataa acaatcaacgattaagcttccatctgattaaacttagcattgattggattaatgatactgatcc{ <b><u>tttgaatat</u></b> <b><u>cacctaatt</u></b> }atttagtactttgtagtcttcttttcttattcattaattttgctaataccgctagaggtccaaaact atattttgattaactttaggcacattttatcttttaggctattattagaagagttctggttctttgtataccacagccctg aaataaaaaataaatgaaattagcataagcgttaataattcttttca	2168120 – 2167590
NT01CX1621	ttaaaagatacgtctatttctctacggttaaaattatttgaataaaatattatataccaaaataatgcaataattacta taaccaacataagtagctaggtataaaaagattatcttaaac{ <b><u>faatgtagaagaagatatag</u></b> }tagggat aagtcataagtttagttataccttttcttttaaaactagtttccgacactagtgttttacctaatggcctatagaaag tttggtagtcaaatcagcttattataagattatataattcattattatagtaagtgac{ <b><u>atcctcttttaaggtac</u></b> <b><u>ag</u></b> }gaacattattgttttaccagaccaaaagaatttaattggtctatactgattgtaaaagttttaattctatattgct ttatatagaggaaactggttttggaaatagcaaaagttcattatcttagccatataaaaaacataggtatcatttta tcgtaaaactgattcattacaactcaataagaactctattgctttgttaaacatagcaactaagcatctccagcctt ttagtaaaactgatttaccacctacatactgcattagattcaggaattgttttgaataattcctatagtagaaag aaatttagaatctaactgtgcccactagttatttctattttgaggatccaagaattccattagataattctacttta gattttttaaattcatagtttcttaccattcattagaataagcagctttacctataatgcttaaatcataagccgaag tatagtgatcggaaattccactatctaatccattaggtgtcacaatgagatatttttaactcagttgtttactttgtca ttcatcttttagcaaaagttttagtatttctctacattatcagctatcatagaggctatgctattagctgaatgaaga agaagtcctttcattgcatcatcagcactcattgatctccaactttaaagtttctttaaaggaaagaacgcaaaagtat attctggttgttaatagaacctcagtatatgtaagcatatcagtaggtttttgtttcagctagtaatagagctgttaa aagtttagttgcttctgctgatacattggagatgcatcagcatttttagcatataaactccactgttttagcatcaat tacaatagcagatttaccactatatttggctcactaaattatcagcaaatgctgtgtgtaaaaatgaaagaaatag aatgtttagtaataaagttgaaattttacgtctca	825486 – 824155
NT01CX1736	tatgagtgacaaaatgttttaaagttttcaaaaaataggtgtttttattgcaggaattttgtgtttttcagcttat tttttagcgtttagattaaatcatgttgaatggcaagttctaaagttcaaaaatttctatatactgtggatactaaa gaaaaaaaggtgcttattctttgacaccaattggggaactaataacactaaaaaagtttggatatttagataag tataatgcaaaaactacattttttaaagttggaacatggatagataaacatccagaagaaccaaagaaatttttaa agaggtcatgaaatggaatcactctaatagtcagcggattttactttaatatctgaaagtagaatgattgagga aatagctgctactgatgcaaaatataaaaacttctaggaaggatagtaaggttttagatttcc{ <b><u>ttcaggttcttat</u></b> <b><u>aatgaaa</u></b> }aagcagttaaagtagctgaaaatactaatctttttgatacaatgggatgttgacagtatagattgga ggaaagaggggagacatagagtataatagatgaaatgaaatgtaatccgggatctattatattttcacgata atgcaaaagtatacaccagataatttagtgaataattggggaattacaaaagggaag{ <b><u>gatacaagtttgaactat</u></b> <b><u>a</u></b> }tcggatcttataataaagaaatattcatattgataaactggtgtcaaaaatfaaatta	942795 – 943565

**Table A.2.** Sequences of designed sgRNA. Sequences of the four sgRNA sequences designed to targets [1] and {2} in Sup Table 1. These sequences include necessary restriction digest sequences for cloning as well as additional nucleotides to allow for digestion. **Bold underlined sequence** – *SpeI* cloning site, **bold text** crRNA sequence, **bold underlined** italics – *Bg/III* verification site, ***bold italics*** – *NotI* cloning site. Codon bias for *Clostridium novyi* is accounted for in every synthetic sequence.

Gene Target	sgRNA sequence	ID
{NT01CX0401}	gcgcagtctgctttatacggatgataat <b><u>actagta</u></b> ataggatata <b><u>aacactgata</u></b> gttttagagctagaat agcaaggcaccgagtcggtgcttttt <b><u>agatctg</u></b> <b><i>cgcccgct</i></b> ggtcttaaggcgattcaaccaagcgc	CnovNT_0401_ sgRNA001_KD
[NT01CX0401]	Gcgcagtctgctttatacggatgataat <b><u>actagtg</u></b> taata <b><u>aattggaacaagctt</u></b> gttttagagctagaat agcaaggcaccgagtcggtgcttttt <b><u>agatctg</u></b> <b><i>cgcccgct</i></b> ggtcttaaggcgattcaaccaagcgc	CnovNT_0401_ sgRNA002_KD
{NT01CX0481}	gcgcagtctgctttatacggatgataat <b><u>actagtt</u></b> ta <b><u>aatttagtgata</u></b> ttt <b><u>caag</u></b> gttttagagctagaata gcaaggcaccgagtcggtgcttttt <b><u>agatctg</u></b> <b><i>cgcccgct</i></b> ggtcttaaggcgattcaaccaagcgc	CnovNT_0481_ sgRNA003_KD
[NT01CX0481]	gcgcagtctgctttatacggatgataat <b><u>actagtg</u></b> gataata <b><u>tacaata</u></b> tact <b><u>cca</u></b> gttttagagctagaat agcaaggcaccgagtcggtgcttttt <b><u>agatctg</u></b> <b><i>cgcccgct</i></b> ggtcttaaggcgattcaaccaagcgc	CnovNT_0481_ sgRNA004_KD
{NT01CX1621}	gcgcagtctgctttatacggatgataat <b><u>actagta</u></b> cagg <b><u>accaa</u></b> aga <b><u>aattt</u></b> taagtttagagctagaat agcaaggcaccgagtcggtgcttttt <b><u>agatctg</u></b> <b><i>cgcccgct</i></b> ggtcttaaggcgattcaaccaagcgc	CnovNT_1621_ sgRNA005_KD
[NT01CX1621]	gcgcagtctgctttatacggatgataat <b><u>actagtg</u></b> ataat <b><u>atctttt</u></b> ata <b><u>acct</u></b> gttttagagctagaatag caaggcaccgagtcggtgcttttt <b><u>agatctg</u></b> <b><i>cgcccgct</i></b> ggtcttaaggcgattcaaccaagcgc	CnovNT_1621_ sgRNA006_KD
{NT01CX1736}	gcgcagtctgctttatacggatgataat <b><u>actagta</u></b> taca <b><u>agttt</u></b> g <b><u>taact</u></b> atatgttttagagctagaata gcaaggcaccgagtcggtgcttttt <b><u>agatctg</u></b> <b><i>cgcccgct</i></b> ggtcttaaggcgattcaaccaagcgc	CnovNT_1736_ sgRNA007_KD
[NT01CX1736]	gcgcagtctgctttatacggatgataat <b><u>actagtt</u></b> ttt <b><u>cattata</u></b> aga <b><u>acctga</u></b> gttttagagctagaata gcaaggcaccgagtcggtgcttttt <b><u>agatctg</u></b> <b><i>cgcccgct</i></b> ggtcttaaggcgattcaaccaagcgc	CnovNT_1736_ sgRNA008_KD

Naming system = Species\_genelocation\_purposeandnumber\_creatorinitials







## APPENDIX C: CLONING SCHEMATIC FOR INSERTION GENE

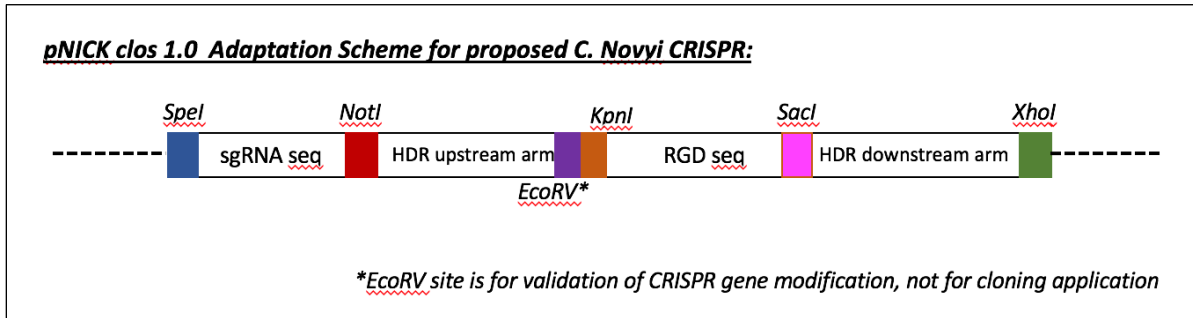


**Figure C.1.** Schematic representation of cloning scheme. Schematic map of the cloning elements incorporated to generate a CRISPR/Cas plasmid for gene insertion in *C. novyi*. Restriction digest enzyme cleavage sites: *SpeI*, *NotI*, *XhoI*, *KpnI*, *SacI* and *EcoRI*, *BglII*, *Clal*; sgRNA= single guide ribonucleic acid; HDR = homologous domain repair

## APPENDIX D: EXPECTED RESULTS OF RESTRICTION DIGESTS IN THE GENERATION OF CRISPR PLASMIDS

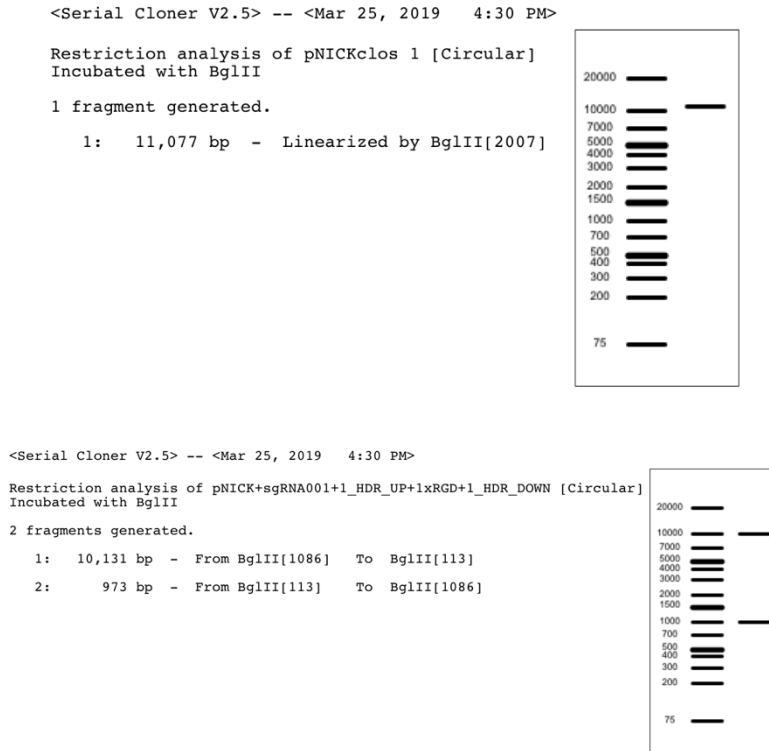


**Figure D.1.** Verification of insertion of desired sgRNA *BglII* digest. Insertion of desired sgRNA can be determined by *BglII* restriction digest. A digest with *BglII* of candidate plasmids will result in either 1) a single 11kb band, which would confirm that insertion did not occur, or 2) two bands at 10.1kb and 973bp, which would confirm that insertion took place.

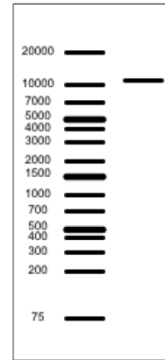


<Serial Cloner V2.5> -- <Mar 25, 2019 5:38 PM>

Restriction analysis of pNICKclos 1 [Circular]  
Incubated with KpnI

1 fragment generated.

1: 11,077 bp - Linearized by KpnI[4072]



<Serial Cloner V2.5> -- <Mar 25, 2019 5:39 PM>

Restriction analysis of pNICK+sgRNA001+1\_HDR\_UP+1xRGD+1\_HDR\_DOWN [Circular]  
Incubated with KpnI

2 fragments generated.

1: 8,137 bp - From KpnI[4099] To KpnI[1132]

2: 2,967 bp - From KpnI[1132] To KpnI[4099]

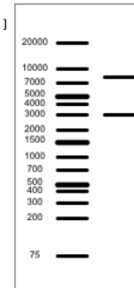


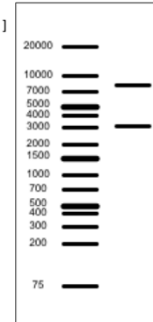
**Figure D.2.** Verification of insertion of desired HDR *KpnI* digest. Desired HDR can be determined by *KpnI* restriction digest. A digest of candidate plasmids with *KpnI* will result in either 1) a single 11kb band, which would indicate that insertion did not occur, or 2) two bands at 8.14kb and 3.0kb, confirming that insertion took place.

<Serial Cloner V2.5> -- <Mar 25, 2019 5:40 PM>

Restriction analysis of pNICKclos 1 [Backup 2019-03-25 17\_23\_46\_5:23 PM] [Circular]  
Incubated with SacI

2 fragments generated.

1: 7,993 bp - From SacI[9350] To SacI[6260]  
2: 3,090 bp - From SacI[6260] To SacI[9350]



<Serial Cloner V2.5> -- <Mar 25, 2019 5:42 PM>

Restriction analysis of pNICKclos+sgRNA001+HDR1xrgdcasette [Backup 2019-03-25 17\_35\_53\_5:35 PM] [Circular]  
Incubated with SacI

3 fragments generated.

1: 5,095 bp - From SacI[1186] To SacI[6281]  
2: 3,090 bp - From SacI[6281] To SacI[9371]  
3: 2,919 bp - From SacI[9371] To SacI[1186]

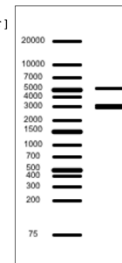


**Figure D.3.** Verification of insertion of desired HDR by alternative *SacI* digest. The desired HDR can be determined by *SacI* restriction digest. Digesting candidate plasmids with *SacI* will result in either 1) the presence of bands at 8.0kb and 3.1kb, which will indicate a negative plasmid or 2) the presence of three bands at 5.1kb, 3.1kb and 2.9kb, confirming a positive on a 3% agarose gel.

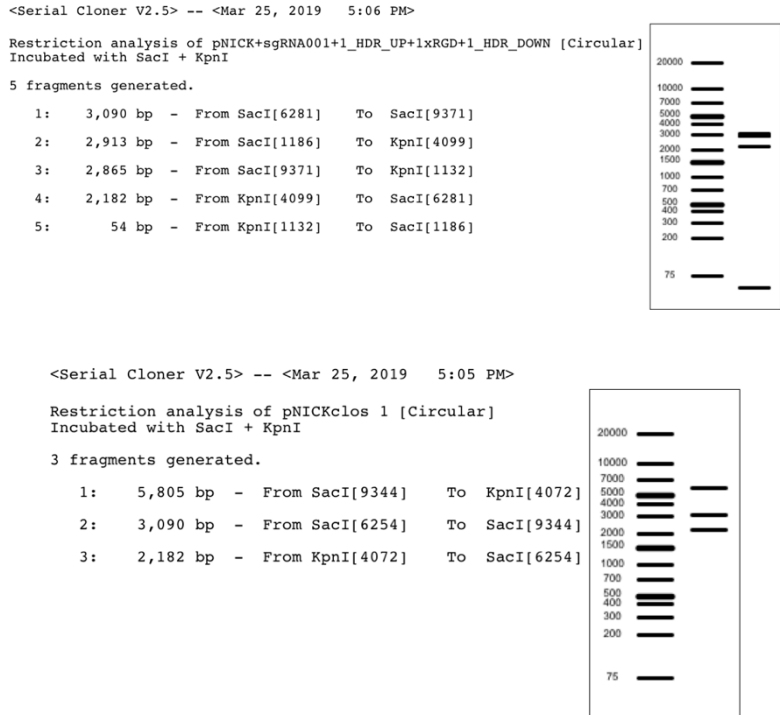


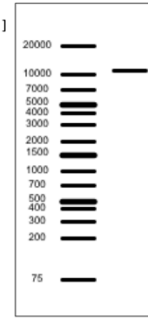
**Figure D.4.** Verification of insertion of desired RGD by *SacI* and *KpnI* digest. Insertion of a single RGD sequence can be determined by a double digest with *SacI* and *KpnI*. A digest with both *SacI* and *KpnI* of candidate plasmids will result in either 1) confirmation of negative result for desired sequence by the presence of 2 visible bands at 3.0kb, 2.2kb, and 54bp, or 2) confirmation of positive clone for desired cloning event will generate three bands at 5.8kb, 3.1kb, and 2.2kb.

<Serial Cloner V2.5> -- <Mar 25, 2019 5:09 PM>

Restriction analysis of pNICK+sgRNA001+1\_HDR\_UP+1xRGD+1\_HDR\_DOWN [Circular]  
Incubated with ClaI

1 fragment generated.

1: 11,104 bp - Linearized by ClaI[10222]



<Serial Cloner V2.5> -- <Mar 25, 2019 5:09 PM>

Restriction analysis of pNICK+sgRNA001+1\_HDR\_UP+3xRGD+1\_HDR\_DOWN [Circular]  
Incubated with ClaI

2 fragments generated.

1: 9,042 bp - From ClaI[1222] To ClaI[10264]

2: 2,104 bp - From ClaI[10264] To ClaI[1222]

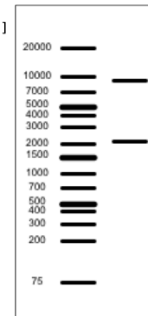


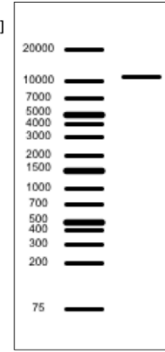
**Figure D.5.** Verification of insertion of desired 3xRGD by *ClaI* digest. Insertion of the single RGD sequence can be distinguished from the insertion of the 3xRGD repeat by a digest with *ClaI*. A digest with *ClaI* of candidate plasmids will result in either 1) the presence of a single band at 11.1kb indicating a clone with 1xRGD, or 2) two bands at 9.0kb and 2.1kb, indicating the presence of 3xRGD.

<Serial Cloner V2.5> -- <Mar 25, 2019 5:17 PM>

Restriction analysis of pNICK+sgRNA001+1\_HDR\_UP+1xRGD+1\_HDR\_DOWN [Circular]  
Incubated with BamHI

1 fragment generated.

1: 11,104 bp - Linearized by BamHI[5703]



<Serial Cloner V2.5> -- <Mar 25, 2019 5:17 PM>

Restriction analysis of pNICK+sgRNA001+1\_HDR\_UP+9xRGD+1\_HDR\_DOWN [Circular]  
Incubated with BamHI

2 fragments generated.

1: 6,731 bp - From BamHI[5853] To BamHI[1330]

2: 4,523 bp - From BamHI[1330] To BamHI[5853]

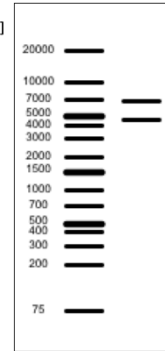


**Figure D.6.** Verification of insertion of desired 9xRGD by *Bam*HI digest. The insertion of the single RGD sequence can be distinguished from the insertion of the 9x RGD repeat by a digest with BamHI. A digest with BamHI of candidate plasmids will result in either 1) a single band at 11.1kb for 1xRGD, or 2) two bands at 6.7kb and 4.5kb indicating the insertion of 9xRGD.

APPENDIX E: GENE SEQUENCES USED TO COMPARE *C. NOVYI*, *E. COLI*, AND *C.*

*DIFFICILE*

**Table E.1.** Ten most expressed genes in *C. novyi*. Genes that were considered the most expressed *C. novyi* genes from previously published data were utilized to draw comparisons with *E. coli* and *C. difficile*.

Most Expressed Genes	Gene ID	Putative Function	Sequence	Genome Loci
1	NT01CX 1134	Ribosomal protein L15, rplO	aatgaaactcatgaattaagacgtcgaaggttcaagaagctcctaaaagagttggtagag gaaacggttctggattaggtaaaactgcaggaaaaggtcataaaggacaaaacgctagatcag gcggtggtgtagaccaggttgaaggtggtcaaatgcctttatacagaagattacctaagaga ggttcactaataatfcgctaaagaatatgtagaagtgaacgtaagcagattaaatctcgaag acggaaactgaagttaccacagaagtattaaaagcaaatggtgtaacagtaaaagtaagatgg agttaaaactaggaaacggcactttagaaaagaagtaactatcaaagcaactaaattactaa gggtgctgtagaaaaatagataatccatagggggaaaagcagaggtgatata	244373- 244813
2	NT01CX 1120	Ribosomal protein L22, rplV	agctagagctatagcaaaatgtaagaatgtctccaagaaaagtagagttgttctgacttagt agaggtaaaaatgtaagcgaagcttttctatattaaaatatactccaaaggatgcggtactgta gttttaaaagtttaaaacagctgtagtaaatgcagaaaataattcaacttagatgtaataaaltat atattgcagaagcatatgcaaaccaaggccaacattaaagagattaaaccacgtgcacaag gtagagcatattcaataatgaaaagaactagtcacggttacactagtagttaaagaaaagagcata	238788- 239123
3	NT01CX 1117	Ribosomal protein L23, rplW	aatgttaaacagttacgatttaataagaagacctgtaataactgaaaaagcatgctgctatggc agatagacaatacacctttatagtagatatactgctgacaaaactcaaatcaaaaagcagttg aaaaagttcgggtgtaaaagttgaagaagttagaactcaagatttgacggaaaagttaaaag agttggagttcacgttgaaagagatctgactacaaaaagcaatggttaagctaacagaagat agcaaaactattgaattctttgaaggaatgta	237225- 237515
4	NT01CX 1116	Ribosomal protein L4/L1 family, rplD	aatgcctacagtagattatataatagaaggtcaaaaagttggagattacaattagctgaaact gtattcgcagtagaagttaatgaagatgttttacatcaagttgtagttgcacaactgcaataaaa gacaaggaatcaatcagctaaaacaagagctgaggtttctggaggtggaaaaaaacctggga gacaaaaaggaactggttagagcaagacaaggttctattagagctccacaatggatacaggtg gtgtagtttctgctccaaagccaagagactataaaatgtctattcacaatcaatgagaagattg ctatgaaatcagcgttaactgcaaaagttaatgaaaatgaattagtagtcttgaagtttagaatta gatgcacaaaaactaaggaatggttaaatgattaatgctttcgaaggtaaaaaaccaatc gtagtaccagaaaagtaacgaagttatctataaatcagtaagaaatatagaaggtgcaactgtagt accagtaacaatataaacgtttatgatattaaaacacgataaatttatcatacaaaaaggaagca gtatctaagattgaggaggtgatgcata	236605- 237225
5	NT01CX 1127	Ribosomal protein L5, rplE	gatgagtagactacaggaataatacaataaagaagtaataaccggctcttatggagaagttcggga tataaaaatataatgcaagttccaaaactagagaaaatagttgtaacatgggtgtggagaagc taaagataactctaaagtttagaatcagcaattgctgacctacaacaattacaggacaaaaacc agtaataacaagagcaaaagaaatctgtagtaactttaaatacagacaaaacatgcctattggtg taaagttacactaagaaaagacatgatggttgaattgacagataaattaatgaatcgcgttacca agagttagagacttttagaggagttcagtaagtctttgacggttagaggaaactatgcttttagga atfaaagaacaatcatattcccagaatcgaatatgacaaaatagataaagtaagaggtatgga tataatattgttactcgaagactgacgaagaagcaagagaattgcttagatattcttggaaatg ccgtttgctcaata	241503- 242042

**Table E.1.** Ten most expressed genes in *C. novyi* (continued). Genes that were considered the most expressed *C. novyi* genes from previously published data were utilized to draw comparisons with *E. coli* and *C. difficile*.

Most Expressed Genes	Gene ID	Putative Function	Sequence	Genome Loci
6	NT01CX 1113	Translation elongation factor Tu	aatggcaagacaaaagtgtgaagaataagccacacgtaaatataggaacaataggtcacgt agaccacggtaaaacaacaacacagcagcaatcacaatgacacttgcaaaagcaggtggag cagaagtacaaaactacgaagatattgataaagcaccagaagaaaaagaaggaggaatcaca atcaatacatcacacgtagaatatgaaacagaaaacagacactatgcacacgttgactgccag gacacgcagactatgtaagaacatgatcacaggagcagcacaatggacggagctatcttag ttgatcagcagcagatgttccaatgccacaacaagagaacacatcctattagcatcaagagt aggagttaaccacatagtagtattcttaacaaagcagaccaagtagatgatccagaattactag aattagtagaaatggaagtaagagaattattaagcgaatacggattgacggagacgaatgtcc agtagtagtaggatcagcattaaaagcaatcgaagaagggatgaccaatgcatccttagactta atgaaagctgtagatgaatataatccaactccagaagagcaacagatcaaccattcttaagcc tgtagaagatgtattacaattacaggaaagggaacagttgcaacaggaaaggtgaaagagg agtactacagtaggagatgaagtacaaatcgtaggaaatgaaagaaagaatcggaaagaca caatcacaggagtagaaatgttcagaagatgttagatgaagcaatggctggagataacatcgg agcattattaagaggtagtacaagagacgaaatcgaagaggtcaagtactagcaaaaccag gttcagtaaacctcacaataaattcgtaggtcaagtcttactgattaaaagaaagaaaggtgga agacacactccattcttaacggatacagaccacaattctactcagaacaacagacgtaacagg atcaatcgtttaccagaaggagtagaaatggtaatgccaagagacatatagacatgaacgta gaatfaatcacaccagtagcaatggaaaacaacctaagattcgctatcagagaaggtggaaga acagtaggttcaggagttgtactagcatagttgaata	233984- 235165
7	NT01CX 1104	Ribosomal protein L1, rplA	tatggcaaaaatgggtaagaatattcagagagcatcaagctaatgataaaaactttatatac acctctgaagctatagatcttactttaaacaacagcaaaagcctaattcgtgaaactatcgaactt tctataaagacttgggtgatccaagacatgcagatcaacaagttagaggagcagtagtacttct catggaacaggttaagaaagttagattttagtattgtaaggagataaggctaaaagaagcag aagctgcaggagcagattatgtaggagcagaagaatacttagacaaaatcacaagaaagaaact ggtttgatttcagcgtagttgtgcaactccagatatgatggagtagtaggtagattaggtagag tattaggacctaaaggatattgcttaacccaataatcaggaacagttacattttagtagcaaaa gcaatagctgacatcaaagctggtaaaagttgaatagattagataaaaacagctatcattcacgtt ccaataggaaagaatctttggagaagaaaattagctgaaaactacaatgttttaaggaagct atagftaaagtaaacagctgcagctaaaggacaatacataaatcattaagcatatcaagcaca atgggaccaggagtaaaaatcaatccagcaaaaagtttagctta	220981- 221679
8	NT01CX 2322	Electron transfer flavoprotein, alpha subunit, efa	attattgtagcttttgattgtgctattaatctgggattattttgtaagtccaactaatccaagat cagcaacttcatgattgcagcatctgcatctttataatagcagatgatgtaatacactgcttgcattc cagctaaagttggtgattgctcctgaaataccgcaagcagatgatatttttaggtcttacagtttacca gtttgtcaactgtgattgctgatctatccagccgtatctgtagctgctctgacatcgtcacaact ccaccgaatacgtcagcaagttctgttagtttagcgaagtttcttcttccaactcctcaccacc tgctacgattactcagcttccaagatcagcaactcttagctattttaacaactctttaacagtt actttaaacttcagcatctaatttaactgcaacttttctgatttagctgcatctactcttgatcgtct gctgctaattgtcgaaaacaccaggtctfacagttgacatttggtctgtttctgtacacatgatt gtgccaattaagttccaccgaatgctgcttgcattaataagtgacctgttctctcagatctca atgatgtacaatctgctgttaaacaggtgttaactagctgcaactctaggtcctaactcttctct atgaagctagctcctatgaataagattctggtttcttctgfttaactacaactcacttagtgt aagcaccagttgtgattgtctaatcttctatctcagcatatagaactttgtagctcctgctgctca ataattcttgcacaactttcagattttatttccaagtaaaaactcaggttaattctacgtttaaattgctg caatttctactcttccaagtaattctaaagctacttttgaattctccatcttctgtctcgaata cccaaacgccttgaatctgctatattca	1520720 - 1521727
9	NT01CX 1103	Ribosomal protein L11, rplK	tatggcaaaaaagtagtaggaatgattaaactcaactccagcaggaaggaactccagca ccaccagttggaccagcattaggacaacacgggtgaaatatttgctttctgtaaggaatacaat gctaaaacagcaaatcaagcaggaatgactattccagttataatctgtatatacaagatagatctt cagcttctttaaagactcctccagcagcagtttaataaaaaagcagctggattagacagtggtg ttcaggtgaacaaaacagactaaagtaggaaagattactaaagctcaataaaaagaaattgctg aaactaagatgccagactaaacgctggatcagttgaaagcgtatgagcatgatagcaggaa ctgctagaagtaggtattacagtagaagaata	220502- 220927

**Table E.1.** Ten most expressed genes in *C. novyi* (continued). Genes that were considered the most expressed *C. novyi* genes from previously published data were utilized to draw comparisons with *E. coli* and *C. difficile*.

<b>Most Expressed Genes</b>	<b>Gene ID</b>	<b>Putative Function</b>	<b>Sequence</b>	<b>Genome Loci</b>
10	NT01CX 1115	Ribosomal protein L3, rplC	aatgaaaaagctataataggaagaaaattggaatgactcaaatttcgatgaaaatggaaaag ttatcccagttacagttgtagaagcaggtccatgtcgttctctaaaagaaaactgaagaaaaag atggatataatgcaatacaagtaggattgaaagatattagagaaaaattagctaacaacctaag aaaggacacttgcaaaagctggtgtatctttaaagagaatgtagagaatttagattagaaaat attgatgaatatgaagtggaaactgaataaaaagctgacgttttgcagcaggagataaagttgat gtaactggagtttcaaaaggttaaggattccaagggaacaaftaaagatggaaactccacagag gacctatggctcacggttctaataaccacagagctgttgatcaatgggagcagcatctgatcca tcaagaacatttaagaacaaaaaatgccaggacacatgggaaacaaaaatcaactatcttaa acatagaagttgtaagtaatggctgacaaaacgftctttaaataaaaggtggaataaccaggac caataaaggctacgttgaattaaagatacagtaaaagctta	235950- 236579



**Table E.2.** Ten least expressed genes in *C. novyi*. Genes that were considered the least expressed *C. novyi* genes from previously published data were utilized to draw comparisons with *E. coli* and *C. difficile*.

Least Expressed Genes	Gene ID	Putative Function	Sequence	Genome Loci
1	NT01CX 0324	Hypothetical protein	aatgcttctggaatcattgtgccataatcaccatctttcctaacaatataacacctattatgaatatt ataacacaataaattataaagaatttataaagaatcatttctataatattttaatatataatttaattggtt attatattgtatttta	2009297 - 2009461
2	NT01CX 2307	ferrous iron transport protein B	tttatacctaagcaaatatttataataagtgattaaacatacacacaacaatagctattgacagttgga attaatgctgcaagtgctgtccattgttactttcagctctctttttatgtccataatgtagcacaag gccaatgaagaagtgtaaatatcataacatttagtcagtaagataagccaaccattgttataatata tccttttaattgattcctaaactcctcaaatctatcatagAACCTGTGACAAGTATGACATTAATAATAGG TACTACTATTCATTTGCTGGTATTCCTAAAATAAATGCTAAGAGAATAAACCATCAAGTCCCATTAATTT TGCAAAAGGATTTAAGAAATTTGCTACATGAGATAATACTAAATTCCTATAGTAACATCTAAAT CCATATTAACTCCTGCGGGGCTGCTATTGCAACTGCCCTCCTAAAACAATATAGTCTATCTATTA TAGATGTGTATAAATTTACTACTTTTGGTTTCTGTAAGTGGTAATCTAAAGTAAACCTAGATGGTAT ACCTTTAGTAGGGTTTAGACAGAATATGAAACGAATAGTGAATAAATCCTCAAGTACCAT ATTGTAATGACAACTGGAATTGCACTGTATGCTACTATTCTCTACAATAAGAACAGATG ATATAGCAAGTAGTGTGAAATCTACCATACAAGGCATAAAATATTAGTAAATTTGCAATTAACCTT TCTCTGGTGATCAATTAATCTGCACCCTATAACTCCCGCTGCATTACAACCAATCCCATACATAGT AAGACACTGTTTCCATGTGCGCAAGCTTTTTAAATAGATGCTAAATTAATGCTACTCTGGAAAGT ATCCCAATCTCAAGCAATGTAATAGTGGAAAGATATAGCCATTGGAGTAACATAACTGATATA CCCACCAAGTGTCTATAAAGACCTAATACTATTACCCATAAAGCCACTTTGGTGCAATTTATTCGT AACCAACTAGTAAGTACCCCTCAAAATTAATAAAGCTTTGATAGAAGTCCGATGGATAATTGCTC CAGTTAAGGTTATCAAAAAGTAATGCCAGTATAGCTATCATTATTGGAATCCAATATCTAGATGT ATATACTGTCAATTTTCTATCCCTGTCATTTATCTTGTCTATAATTACACAGGCTTTATTACATCTCAAC TCTTTATATGTTCTGTGTATATACTCTTATGTTTCTTATCTATATTTTAGTAAFTCACATCTCTTTAA TATTTCTTCTATTTCTCACTAATCTTTAAATAAGATGATTATAGTGCATCCATCAATAAGTCTT AAAGCTATCCATCTTGATTTATCTTTGGAATCTTTTGTATTATGTTTCTATGTACTACTATAGATCAA TTTCTCCTTATACACTACTCTTCAAGGTTTACTGTAACCTTATTAGATACAACTTTATATACAGCACTTTTAA TTCTCTATAACCAATGCCACTCTGCTGCTGCTATAACAACCTGGTATCCAAGTCACTTTGTAATCTATT GAGTCTATTAATTTTTTCTTTCCTCATCTATAAATTTACACATAACACAACCTTATCTGTAAGCTCC ATTATTGATAAAGTAAATTTCTTCAAGACAAGTGGCATCCGCAACTACAACAGTGACATCAG GATCTCCAAGCAATAAATCTCTTCAACTCTCTCTGAGATGTTGCAAAAAGTGAATATGTTCC TGGTAAATCAACTAATACATATTACTAGATTAACCTAAATTTCTCTCTGCAATGACAACCTTTTCCA GGCAATTTCCCGTATGTGATGAATCTGTAAGTGAAGTGAAGTGAAGTGAAGTGAAGTGAAGTGAAGT CCCCTAAAAGTACTACATACTGCTCTCTTTCTTCTACTTATAGATGCTCTAAAAGTACTACTGGA GTTGACTTATAAGTAAAGTCCCA	1502758 - 1504878
3	NT01CX 2204	Mg chelataase-related protein	ttcaaggattcactggaacaagcataaaattgctaggatattccacagcccactggctctacttat tttataactctgtcttcaaggggtgccttaaaactctagggttttcttaaaattctagtatttcatctaa aaataatactccattatgagctaatgaaattcaccaggcatttagcttattccacctcaactaatgaa acctgagatgcagtagatgtggacttcaaaaggctttcatatatacaatcattattatctttaaattatt agataactataaatcttagtaactctaatgcttctcataacttaactctggaagtatagttggaattctt ftagctatcattgtcttccacatcctgggggaccaacaataagtatattgtgctctccagcagctgcta cctctatagctctttacagcttcttggcctagtacatctgaaaaatccaatattctttaaatttttatt ttctcaatttatatggaataagatctctatattaaagaattcaataactgacttaagtgttcaaatggg aaaactttgcatcatttacgaagcacattcattgcatatccataggcactataaagttgataatcc atttctattgcatctattataataggtagatgcctcttatttttaattcacctaaaagagatagttctcc tataataaaaaattctcaacattgtcacatttattctgattgctagctaaatfatagctatagctataggt agatctaatagtgaacctctttttaaatacagctggtgctaaatattgtattctctcattggaatcc aatccagaattattattgcagctctactcttctttgattctttaaagcaatatacaggaattcctact atataaatgccgtagtccattgaaatattctattctacattataatagttccattattctctgtaaaag agctgattttattttgtaacca	1398532 - 1399575
4	NT01CX 1812	Hypothetical protein	Tatgataagtgggataaaaatggttatattgcaataaaaaagaatcttctatattattaggaggtttta aaaagatatagaaatataactactattacaataatatttcatagtata	1020881 - 1021003

**Table E.2.** Ten least expressed genes in *C. novyi* (continued). Genes that were considered the least expressed *C. novyi* genes from previously published data were utilized to draw comparisons with *E. coli* and *C. difficile*.

Least Expressed Genes	Gene ID	Putative Function	Sequence	Genome Loci
5	NT01CX 1354	Hypothetical protein	tatgattactcataatTTTTCTCCTTCTATATTTAAAGAAGCTTTATATTAGTATCCACAAAACAATAAA aacTTTAGAGGAAAATATAGAAAAGAAAATACAAAATTGTACATATGATAATAAATTGTTATGTA	503413- 503556
6	NT01CX 1718	RNA polymerase sigma factor	ctaaaacctcccatatctTTGTGTTAACTATACATTACATCAATGTTAATAAAAGTTGAGAAATTTAG accatgctgaagatagTAAAGACTAAATATATCTGGATAAACTCCAAGTTCTTTTATAGAATAGACA gtgagaaaagTTTTATAGAGTTGAAATATTTACTATAGAGGGTATATTTACCTGTTTATAGTCAATTA attctagcttgcatttgataagaagTGGAGTTTACTACTTTACAACATATAAGATTAGAATCCTCTTAAA ggTtATGAATTTGCTAGAAGTAAAATCACAACTTTATCAAGAGGTTAAGAATAAAGTTTATGG cattagTGGCATAAGATTTAAATAAAGATTCTCTGTGTTAGATTGGTAACCTGTAGACAACCAATTTATA TAAAGGATCTAGGAGTGCATCATAAGATAAGATGGATTAGAATGTTTTATTTATCATATAAGGTT TtATGAAGTATATACAAGAGAAAGGTTTATTAATCTCCA	926256- 926801
7	NT01CX 0939	Resolvase	tcaaggatataataataaaataatattTTTTTACTCTAACAGCTCTAATTAAGCACTCTACTATA catgtaattcttcaacatatagtaactattacttctaatagattagTGCATGATCTATTGTCTCTTTGTA tatttttaggtctacctctTAAATCCTGGTTTGTGTTTGAATAGCCTTCCAGCTGTGACGTTCTATTAT TgtattacgtccattctgcaactgccaagaagTtaagaattgaacaaaaaaggataaaaaaataa gcctaataaaaaggctataggtagca	60986- 61306
8	NT01CX 2035	Hypothetical	atcaatattcctccttaggtttaaatattgctgatgatttttaaggataaaaaaataatagttata tagataatcttacctaataataaaaaattatactTTTAAATCTATTTAAATATAGAATTAATAATTTAGGA actacattacagTtaaaatgTTAATAATAAAAATAGATCGTAATAATCCGTAGATAAGAAAACTACT atgtataagaccataaaatataaccagttatagcggcattttcagagccatacaaaaacatttaagtcaatt Ttaagtttgaattatataatctctgcattttgtatataatactttgtagtttaacataacaagtttgg ggaaaatacctttaggcttaggttcaggcatagatttaatagttttttagaaggataactttaacttat aaatataatataaattattttcgttaagttactttaaagttaagggtaaaggaatataaaaaataaa aaaaaatgcaataatacaaatca	1230290 - 1230823
9	NT01CX 0110	Hypothetical	ctggccatacatgaattatgcaccaagacatttctatctgatacaaaaatcgtatgccagcttctactt caaaagtatacttttacaggcttatttaatafttctacatttattctacttactcagtaacttttccTgaata tagaattacccttatctctacttttaaactcctctctaccctctctctattaccagaatggatgt gtttctgtgtttttatttcttccgctatataataatgtactatttattagtttcatgtacaatatattttga cttttttaaccttttctccgfttctattcgtat	1769182 - 1769517
10	NT01CX 1998	Hypothetical	ctcaactgtttatatcaaaagactaaactacaaaatgttttaaagtggttaaatgttgatagtataaataat gtgatcctattccagTtaaaaatcTaaatggaaaagtaattttacagatggacatacaagagcatttgc tatgtataaaatgggtattgaaaatattaaggtatattgggatgaagatgagcttactggagagcata Tgaaaattgtgtgattggtgfactaaggatggtataaaaagtatatcacatctagaccaaaagattatt agtaatgatgagatgagatcttatggatgaaagatgcaggaaaatgcaagggggttagaagatt gataaattgcattgcactgaaaagaaaatgggataaaattttagttagaaatgaatatggatatatg gagattgaaaaaaatgggttattca	1197425 - 1197868

**Table E.3.** *E. coli* genes that were considered orthologs to the most expressed *C. novyi* genes from previously published data utilized to draw comparisons with *C. novyi* and *C. difficile*.

Most Expressed Genes	Putative Function	Sequence
1	Ribosomal protein L15, rplO	atgctgttaaataactctgtctccggccgaaggtctcaaaaagcgggtaaacgcctgggtcgtggtatcggtctggcctcggtaaaaccggtggctgtgtgcacaaaaggtcagaagtctcgttctggcgggtgctgacgtcgcggttcgagggtggtcagatccctctgaccgtcgtctccgaaattcggctcactctcgtaaagcagcgattacagccgaaattcgtctgtctgacctggctaaagtagaagcgggtgtgtagacctgaacacgctgaaagcggctaacattatcggatccagatcgaagttcgcgaaagtgtactgtggcgaagtaacgactccgtaactgtctgtggcctgctgttactaaaggcctcgtgctgctatcgaagctgtggcggtaaaatcgaggataa
2	Ribosomal protein L22, rplV	atggaaactatcgctaaacatcgccatgctcgttctctgctcagaaggtcgcctgtgtgctgacctgattcgcgtaagaaagtgtcgcaggctctggatatttgacctacaccaacaagaagcggctgtactgtcagaaggttctggaatctgccattgctaacgctgaacacaacgatggcgtgacattgacgtatgaaagtacgaaaatttcgtagacgaagcccgagatgaagcgattatgccgctgcaaaaaggtcgtgagatcgcacatcgaagcgcaccagccacatcactgtggtgtgtccgatcgtga
3	Ribosomal protein L23, rplW	atgattcgtgaagaacgtctgtgaaggtcgtcgtgcaccgcacgtttctgaaaaagcgtctactcgatggaaaaatccaacacctgactcaaaagttgctaaagacgcgacaaaagcagaatcaaaagctgctgtgcagaaactgttgaagtcgaagtcgaagtcgttaacacctgtgtagttaaagggaaagttaaactgcacggacagcgtatcggctcgtcgtgacgactggaaaaagcttacgtcacctgaaagaagccagaaactggactcgtggcggcgtgagtaa
4	Ribosomal protein L4/L1 family, rplD	atggaattagttatgaaagacgcgcagagcgcgctgactgttccgaaactaccttcggctcgtgattcaacgaagcgtggtaccagggtgtgttcttatgcagctgctcgtcagggactcgtgctcagaagactcgtgctgaagtaactggtccgtaaaaaaccgtgctgcca gaaagcaccggcctgctcgttctgttctatcaagagcccgatcggcgttctggtgctgacatctgtcgtcgtccgagaccacagtcacaaaagttaacaagaagatgtaccggcgcgctgaaaaatcctcgtccgaactggtacgtcaggatcgtctatcgtgtcgtcagagttctctgtagaagcggcaaaactaagctcgtggcagcaaaactgaaagacatggctctggaagatgtgctgatcaccgggtgagctggacgaaaactgttctgctcgcgcgaacctgcacaaggtgacgtacgcgatgcaactggtatcgaccgggttagctgatcgccttgacaaaagtcgtaatgactcgtgatcgttaagcaagttgaggagatgctggcatga
5	Ribosomal protein L5, rplE	atggcgaactcgcattactacaagacgaagtagttaaaaaactcatgactgagtttaactacaattctgcatgcaagtcctccggctc gagaagatcacctgaactgggtgtgtggaagcgtcgtgacaaaaactcgtggataacgcagcagcagacctggcagcaatctc cgtcaaaaaccgctgatcaccaaaagcagcaaatctgttgcaggctcaaaaactcagggctatccgatcggctgtaaaactctg cgtggcgaacgcgatgtggggtcttctgagcgcctgatcactatgctgtacctcgtatccgtaactccggtgctcgtccgtaagctcttcg acgctcgtggtaactacagcatgggtgtccgtgagcagatcatctccagaatcgaactacgataaagtcgaccgcttcgtgtgttgat attaccattaccactcgcgaaatcgcagagaagggcgcctcgtcgtgctgcttctgactccgctccgcaagtaa
6	Translation elongation factor Tu	gtgtctaagaaaaattgaaactgacaaaaccgcagttaacgttgactatcgccacgttgaccaggtgtaaaactactgaccgtc gcaatcaccctgactggctaaaactacggcgtgctcgtgcaatcaccagatcagataacgcgccggaagaaaaagctcgtggtat caccatcaaacctctcacgttgaaatcagacccccgaccgtcactacgcacacgtagactgcccgggacgcccactatgttaaaaa catgatcaccggctgctcagatggagcgcgatcctgtagtctgctgactgacggcccgatccgagactcgtgagcacatct gctgggtcgtcaggtagggcttccgtacatcctggttctgaacaaatcgacatggttgatgacgaagagctgctggaactggtgaaa tggagttcgtgaacttctgtcagtagtactccgggcgacgactcagatcgtcgtgttctgctcgtgaaagcgtggaagggcgc gcagagtggaagcgaaaatcctggaactggctgctcctgattctatattccgaaacagagcgtgcgattgacaagcgttctctgct gccgacgaagacgtattctccatctccggctggtgtaaccgtgtgtaccggctgtagaacgcggtaicacaaagtgtggaagaattga aatcgttggtatcaaaagactcagaagctactgtagcgtgtaaatgttccgcaaaactggtgacgaagggcgtgctggtgagaac gtaggtgtctgctcgtggtatcaaacgtgaagaatcgaacgtggtcaggtactggttaagccgggcaccatcaagccgacaccaag ttcgaatcgaaggtgacattctgtccaaagatgaagcggcctcactccttctcaaaagcactcgcagttctactccgactactac tgactgactggtaccatcgaactccggaagcgtagagatggtaatcggggcgacaacatcaaaatggtgttaccctgatccacc gatcgcgatggacgacggctcgtttcgcaatccgtgaagggcggcgtaccgttggcggggcgtgtgtgtaaaagtctgggctaa
7	Ribosomal protein L1, rplA	atggctaaactgaccaagcgcgtgttaccggagaaagttagtgcaccaaacagtagacatcaacgaagctatcgactgctga aagactggcactgctaaattcgtagaagcgtggacgtagctgtaacctggcctcagcgtcgtgaaatctgaccagaactgactggtg tcaactgtactccgcagcggctactggcgttccgtcgtgtagccgtatctaccaaaggtgcaaacgctgaagctgctaaagctgcaggc gcagaactgtaggtatgaaagtctggctgaccagatcaagaagcgaatgaaactttgactgtgtattgcttccggatgcaatgctc gctgttggccagctggcggcgttctggtcgcggcctgatgccaaaccgaaagtgggtactgtaacaccgaacgttctgctgaagc ggttaaaacgctaaagctggcaggttctgtaccgtaacgacaaaaacggcatcaccacaccacctggtaaagtggactttgacgct gacaaactgaaagaaactggaagctcgtggtgctgctgcaaaaagcaaaaccgactcaggcgaagggcgtgtacatcaagaaggt tagcatcaccaccatgggtgacaggtgtgagttgaccaggtggcctgagcgttctgtaaaactaa

**Table E.3.** *E. coli* Genes that were considered orthologs to the most expressed *C. novyi* genes from previously published data utilized to draw comparisons with *C. novyi* and *C. difficile* (continued).

Most Expressed Genes	Putative Function	Sequence
8	Electron transfer flavo-protein, alpha subunit, etfA	atgagtcgaattaaacagcgtctgggtctttagcagataatctgaacgttatgctgaactgtttggcggcgtcagcaatggggccaacaggtgta tgccattgtacaaaataccgaccaggcgcaggtatgccttatggtccaaaatgtctttatgttcttgcgcaaaacgacgcgctgcaacgca ctgaaaattacgccgaaagcattgctgccctgctgaaagataaacaccccctatggtgctgtggccgcgacgaaacgtggtaaacgctgg cagcacggtaagtgtgcaactgaatggcggcgtggaacgatgccacggcgtggatattgctgatggtcacatttgcgccgaacaccgg atgtatggcgggtagcgttcgctcaggaaaagatcaacagcccgtgctgatcattacccttgcaccgggtgfcaggaaccgtgaccagt gatacctctcatcagtgcccgacagaaacggtacctatgttgcctccgctcatgaaattctctgctgcgcaacgccgtgagccgcaagcagc gtggacctgagcaaaacgaaacgtggttggcgtcggctgctgactggcggcgcagggatgacctaaaaatggtccacgaactggcggcg gtgctgaatgctgaagtcggctgttcacgtccaattgccgaaggcgagaactggatggagcgtgaacgttatatcgggtgtctccggcgtgttc tgaatccgatctctacgtgacgtgggatctccggcagatccagcatatggttggcggcaacggcgcaaaagtgattgtcccatcaata aagataaaaatgcgcaatctcaactatgccgactcggctgtggtggcgatactcaaaagtcgtccctgacctgattagccagttgagccgc taa
9	Ribosomal protein L11, rplK	atggctaagaaagtacaagcctatgtcaagctgcaggtgcagctggtatggtaaccggagtcgccagtaggtccggctctgggtcagcag ggcgtaaacatcatggaattctgcaaaagcgtcaacgcaaaaactgattccatcgaaaaaggtctccgattccggtagaatcaccgtttacgc tgaccgttcttcaacttctgttaccagacccccgccggcagcagttctgctgaaaaaagcggctggtatcaagtctggttccggaagccgaaca aagacaaaagtggtgtaaaattcccgctcagctgcaggaatcgccgacgacaaagctgccgacatgactggtgcccacattgaagcgat gactcgtccatcgaaggtactgcacgttccatgggctggtatgtaggactaa
10	Ribosomal protein L3, rplC	atgattggttagtcggtaaaaaagtggtatgaccgtatcttcacagaagacggcgttctatcccagtaaccgtaatcgaagtgaagcaaac cgcgttactcaggttaaaagacctggcctaacgatggctaccgtgctatfcaggtgaccaccgggtgctaaaaaagtaaccgtgtgaccaagcctg aagctggccacttcgctaaagctggcgtagaagctggcgtggtctgtgggaaltccgctggctgaaggcgaagatgactgtaggtcaga gcattagcgttgaactgttctgacgttaaaaaagttgacgttaactggcacctctaaaggtaaagtttcgaggtaccgttaagcgtggaact tccgtaccaggacgtactcaggttaactcctgtctcaccgcgttccgggtctatcggtcagaaccagactccggcgaaggtgtcaaaag caagaaaatggcaggtcaggtgtaacgaacgtgtaaccgtcagagccttgacgtatgacgcttgacgtgagcgcgcaacctgctgctggt aaaggtgctgtcccgggtgcaaccggtagcactgatcgttaaccagctggaaagcgtaa



**Table E.4.** *E. coli* orthologs for the ten most expressed genes in *C. novyi* (continued). *E. coli* genes that were considered orthologs to the least expressed *C. novyi* genes from previously published data utilized to draw comparisons with *C. novyi* and *C. difficile*.

Most Expressed Genes	Putative Function	Sequence
4	NT01CX1812 Hypothetical protein	No BLAST results for nucleotide or peptide
5	NT01CX1354 Hypothetical protein	No BLAST results for nucleotide or peptide
6	NT01CX1718 RNA polymerase sigma factor	No BLAST results for nucleotide or peptide
7	Resolvase	accctgctgagcgtggcggaaatggaacgcgatatgattgtggaacgcaccaggaaggcaaaatgttgcgcgcaaaaacaacc gaactftcgcgaaggccgcccgaagcgaccattaccccgaaaaacccatgctgatgaactgctgaccagggcaaaagctataa agaagtggaaagcgattaccggcttagccgagcaccctgtttcgctaa
8	NT01CX2035 Hypothetical	No BLAST results for nucleotide or peptide
9	NT01CX0110 hypothetical	ggctatgcgTTTTTgaaccggcaccgcatgaacagcgataaagtgatgtatggcggcaaaagtattgatgtgagcgtctgccggc gagcaacttaacagcccgtgaaactgaactggaaactgaccagcgattgggataactataacattagctgggataaccgcctgtaa
10	NT01CX1998 hypothetical	atgagcggcagccaggtgaaacgcattgcaaaagatatgaaagcgaacggctataacgggatgaaccgggtggatgtggcgattgt gaacggcaaaatgattattattgatggccatcatcgcgcggaagcggcgcgcaaaagcgggcattaaaaacattccgggtgtaa

**Table E.5.** *C. difficile* orthologs for the ten most expressed genes in *C. novyi*. *C. Difficile* genes that were considered orthologs to the most expressed *C. novyi* genes from previously published data utilized to draw comparisons with *C. novyi* and *E. coli*.

Most Expressed Genes	Putative Function	Sequence
1	Ribosomal protein L15, rplO	atgaagttacatgagttaaaacctgctgaaggtgcagtaagagcctaagagaagattaggtagaggtactgccaactggacaaggt aaaactgcaggacgtggacaaaaaggtcaatggtctcgttctgggtggagtaagagtaggattfgaaggtggacaaatgcc actagctagaagactcctaagagaggtttcaatacattttaagaaagtttacacagaagtaagtgtgaagtttaaacagattg aaaatggaacagaaataactgcagaattataaaactactataaaactataagcaaaataggttaagacggaattaaaacttaggt gaagtaatttagaagaagcttaactgttaaaagctctaatttacagctcagctcaagaaaaatagaaaaagctggtggaaa agcagagttagtataa
2	Ribosomal protein L22, rplV	atggaagcaaaagctactgctaatacgtactgctgtatcaccaagaaaagcagccaaatgtgacctgttagaggaaagaat gtfgatgaagcattagcaatattaagttactccaagaggagcagcttcaataatagctaaggtgtgaaatcagctaaagctaac gcagaaaacatcacgaaatggatactgaaaaatataatagcatcaatagttgctaatacaggccaacaatgaagagattca tgcttagagctatgggtcgtgcaactacaataagaaaaagaaacttctcatatagaggtgtgttaagaaaaaaaataa
3	Ribosomal protein L23, rplW	atgactaatccacatgatgtaataaagaccaggtgtaactgagcagactatgctgaaatgggtgaaaaaaaatacactttgtt gtggctaaagatgcgaacaaaactgaaataaaaaagcagtagaaaaagtattcggagttagttgataaagtaaaactttaa actacgatggaaaagttaaaagaatgggtgaactcaaggaagaacatcaagctttaagaaagcagtagttaaattaaactgctg atagtaaaagaataagaattctccaaggaatgtag
4	Ribosomal protein L4/L1 family, rplD	atgccaaaataaattgactaaatgttagtggacaaaacgttggagaaatagaattatcagattctatatttggcgtagaagttaatg gacatgttttatacgaagttgtaaaaaatcaattagcaataaagagacaaggaactcaactgctgtaaaaactagagcagaagttaga gggtggcgaagaaaaccttggaaacaaaaggaacaggtagagcaagcaaggttctacaagatctgacaatgggtaggtg gaggagttgctttgcactaaaccaagaagctacaataatatacattacttaagaaggttaagaagattagctatgaagagttctta tctcaaaagtcaaaaatagtgaaattatagttatagatgcaftaaacatggatgctcctaagactaaagaatttgcataaattaaa caataaaatgctgtaaaaagcttttagttatagctgcaaaaaacgataacgttaataaaatcagctagaatataagaaggtg ttcaactgcattagttactatgaatgtatgatataataaaatacattcattataataactacagatgctgttaaaaagttgga ggaggtgtacgcataa
5	Ribosomal protein L5, rplE	atggctctagattacaagaaaaatcatgaagaaggtgctcctgctttaatggagaaatttgatatacaaaaacgtaattggagat acctaagttaaataaattagttataactgggtataggtgacgctagagaaaaatccaaaaggattgaaaaagccgttgaagaa ttagaatgatacaggacaaaagcctgttataactaaagctagaataatctgttgcactcaaattaagagaaggaatgccaat aggaaacaaaagttacattaagagctgcaaaaatgttctactcatggacaaattagtttcttaccagaaggttagagacttta gaggagttaacctaattgctttgatgtagaggaaattatgcttttaggagttaaagaacaattatattccctgaaatagaatga taaaatagataaagtaaggaatggatataatattgtactacgcaaaaactgacgaagaagctcgtgaattataaaattatta ggaatgccatttctaagtaa
6	Translation elongation factor Tu	atggctaagctaaatcgaagaacaaaacctcatgtaatatagggacaataggacacgtagaccacggtaaaactacatta acagcagcaataacaaaacattatagcagatatcaattaggagaagcagtagatttcgcaaacatagataaaagctccagaa gaaagagaaagaggaatcacaatatcaacagcacacgtttagatgaaacaccaaatagacactatgcacacgttgactgcc aggacatgctgactacgttaagaacatgataacaggagcagcacaatggcggagcaatattagttgttcagcaacagatgg accaatgccacaacaagagagcatatactattatcaagacaagttggagtagcatatatagtatttcaacaaatgtgacat ggtagatgatgaagagttattagagttagatggaagtaagagatttataacagaatatttcccaggagatgacactc caatagtaagaggtcagcattaatggcattagaagatccaaagcagagtgaggagataagatagtagaattattcagcaaaa tagatgagtatataccagctccagagagagatacagataaaaccttctaatgccagtagagacgtattctcaatcacaggaag aggaaacgttgcaacaggaaggtggaagaggagtactaaaagtacaagacgaagtagaattagtaggattaacagaagca ccaagaaaagttagtaacaggagtagagatgttcagaaaattattagaccaagcacaagcaggggataatattaggagcatt attaagaggagtacaagaacgagatagaagaggacaagtactagcaaaagactggatcagtaaaagccacacacaaaagttt acagcagaagtatatgacttaaaaaagaaggggtggaagacatacaccattctttgatgatatagaccacaattctatttcag aacaacagacgtaacaggagcttgaagttaccagaaggaatagagatgtaatgctggagataacgtaacaatggaagtag acttaaaactcaatagttgtagaagaggattaaagattctcaataagagaaggtggaagaacagtagcttcaggagttgtgct acaataatagagtaa

**Table E.5.** *C. difficile* orthologs for the ten most expressed genes in *C. novyi* (continued). *C. Difficile* genes that were considered orthologs to the most expressed *C. novyi* genes from previously published data utilized to draw comparisons with *C. novyi* and *E. coli*.

Most Expressed Genes	Putative Function	Sequence
7	Ribosomal protein L1, rplA	atggctaaaaaggtataaagatatgcaggtgcattacaaaaagtagatagaactaaatttatgatcatcagaagcattaacatt agttfcagatatagctggagctaaatftgatgagacagtagaagcacacattaaatagggttgactcaagacatgctgaccaac aagtaagagggtcagttgtattacctatggaactggtaaaacaaaaagagttttagtttgcctaaagggtgaaaaagctaaagaa gctgaacaagctggctgactttgtaggagctgaaagaattagttcaaaaaatacaagggtgaaaactggttgactttgatatagta gttgctactccagatatgatgggtgtagtaggtagattagtagtagtattaggacctaaagggttaagtccaaccctaaatcagg aacagttacatttgatgtagctaaagctatagatgaaataaaagctggtaaaagtgaatacagattagacaaaactaacataataca cgtccagtaggaaaaatgatcattggtgggaaaaataaactgaaaactttactgcattaatggatgctataataaaagctaaacc agctgctgctaaaggacaatattaaagaagtataacagtagcttctcaatggacctggagttaaataaacccgcaagacag ctgaataa
8	Electron transfer flavoprotein, alpha subunit, etfA	atgaatgatataaaagatttaagttctataaaaactgatggatattgcagaacaaagagaaggaaaaatagctccagtagttata gaattattaggagaaggaaagaaatagctaaagaagtagatgcagaactttgtgcaatattattaggaaaaagatgttgatggatt agctaaagaattaactctttggagctgacaaagtattgttcagatgatgctcttttagaaaaatatacaactgatcatatacaa aagtaataaaagatgcaatagatgaaataaaaccgaaataatgctttcggagcaactcatataggtagagacttagcacctag aatagctcaagagttggaactggattaacagctgactgtactaagttagaatagaccagaagataaagaaaaaaacaaact cgtccagcattggtggaacataatggctacaatcatttgcacaacctagacctcaaatgctacagtttagacctggtgttatg gataaagctgaaaaagacgaacaagaactggtgaagttagcattagactacaaaataactcaagatgataaagaactact gttttagaaacagftaaactaagaagatttagtatctctacagatgcaaatgttagtatacaggtggtctaggattaggtggac cagaaggattgaaatgcttaagaatagctgacaaataggtggagtagtggctctctcgtgctgctgttgatgctggatgga tagaccattctaccaagtaggtcaaacaggaactactgttaaaccaacctatatactgtggttatatcaggagcaatacaaa catttagcaggtatgcaatcatcagattcataattgctataaacaacccagcagctccaattttagaatcgtgactatgga gtagttggagacttacatgaaatgtccaatgcttatagaaaaatagatagcgttgatgattatagaagctataaaaagcttaa
9	Ribosomal protein L11, rplK	atggctaaaaaagttataggcaaaataaaatacaaatctcagcaggaaaggctactccagcggccaccagttggaccagcatta ggacaacatggtgtaataataatgggattcacaagaatftaatgctaaaactgcagatcaagctggaatgataataaccagttgtt ataactgtatatcaagatagatcattcagttttatacaaaaactccaccagctgcagtttaattaaaaaagcattaaactaaatc aggttctggagaaccaacaagaaaaagttgctaaaatgacttcagctcaagtaagaaatagctgaataaagatgcctga ctaaatgctgcatcagtagaagctctatgagtagatagctggtactgctagaagcatgggtgttgaatcgaagactaa
10	Ribosomal protein L3, rplC	atgaaaggatattaggcaaaaaagttgtagtactcaaatctactgataaaggtagttatctgtaacagctgttgaagca ggcctatggtcgttactcaataaaaaacagttgataaagatggatacaatgctatacaaataggtttgaagatgctaaagaaaa agctttaaacaacctaataaaagacatttagctgctgctaatgttttaagaacattfaaaagaatttagagtagtctgtagaa ggatacacagtaggacaagaataaaagctgatgtattgaaagcaggtgcaaaaatagatgttactggaataaagtaaggttaag ggattccaaggtccaataaaaagacatggacaagtagaggtcctgaaactcacggttctagataccacagaagaccaggttc aatgggagctgttctaccaggtagtagtattaaaaacaaaaaattagctggacatattgggaagcgtaaaggttaacagttcaa aacttagaggtgttaagtagatgctgacaagaaccttatttagttaaaggagctataccaggagctaaagggttcagtagtaact ataaaagaagctataaaggtttcaata



**Table E.6.** *C. difficile* orthologs for the ten least expressed genes in *C. novyi*. *C. difficile* genes that were considered orthologs to the least expressed *C. novyi* genes from previously published data utilized to draw comparisons with *C. novyi* and *E. coli*.

Most Expressed Genes	Putative Function	Sequence
1	NT01CX0324 Hypothetical protein	No BLAST results for nucleotide or peptide
2	Ferrous iron transport protein B	<p>gtgattaatgtagcattattagaaacccaaatgttgtaaaactactgttttaatctacttacaggttcaaatcaatatgtaggtactggcctgggttactatagaaaaaaagaaggattcttgaaaaagagataaagggtgtcattacctggatataatgcaatggatactttcacaatgaagaaagggttctaaatcatattagaaaaatgaagatgtgatgtaaatgtaagtgtgctc taattatcaagaacaccttacttaacaactcaacttaagcaatcaaacagcctatagttatattgcttaatatgttagacattgcag aatctaaaggagttaatatagatgccccaaaaaataagtgaaagactggagtaattgtttccaattatagcaaaaaagaaaa atggtgtgataggatagaagaagagattaggagctacgcaaaaaactttatatacagaaaaactttggaagtgaaca gaaacataaaaaaattagaatcattttcaagatgtacaaaaactacatatacagaaaaaactctatcagtgataagatag acaatatagcttgaacctatattagcacaatccaatattttgggtgattgtcctcttattaaatcactttgactggctggag gtccactacaaggggattgctagcttataagggcttatttctgcacctgttagtgatattctaacctagccccatgggt taaactactatagttgatggaataatggagggtgtggtggtactttaccattctcccttaataattacattattcttggatatcg ttgttgaagatagtgatacatgtcaagaacagcatttttaattgataaagttatgagaagggtgtctatctgttaaaactttt atacctatagttatgggatggtgcttctccagctataatggcaactagaacattggaaagcgaagaaagatagaagagtt acagctctattgaccactatgactgtgagcaaaagctacatataatgcaactattgttagctatattcttccacataatgctg ctftagtaactacatcactgtattggtgggtatagttatggcaattgtagtgcaattcttaataaaacagccttaaaacaga ggctgaaccatttataatagaattaccagaatatagaatccctactatagatgcacttataaaaaacttggaaataatcaaaag gttcttgataagagttgtactgtcattgttgcattgtcagctgtaattggggactttctcaattcaatgttttggatatacagaag atataaatgtaagcttctgctacttaggtcatattatctcctatattcaaaccttggtttgatgattggagaactcagtt gctattttaagtgcttggagcaaaaatacgtagtaaaacttttaataatactataggtaatcaactgttcttaccaca atatttaattggagttactgcataatccttgcatttactgcttataaactccatgataagctgcaacttgcacttgaaaaaaga atatggcaataaaatgatgtttacatcatttgcatacaatttatactagcatgataatggcctttatagttaaaagataggtgga gtactattatgggtaattcaataatagaagctttgataggtggaataattatagcttgcacttattctgtttaaataaactca aacagaaagggcaaaatgtctgtagtggttctattgtctggatgccaagtgcaattcttgcactaaagtaggagcaaatct ggtatgccatataaaagaagattgtaaaaaatattaaataataataa</p>
3	Mg chelatase-related protein	<p>atgggaaacatagttgtcataggaagtgtaaacatggacatggtatgttctgtagataaaagaccagaaaaaggagaaca gtattaggtaatagtttttacatcacctggaggaaaaagggtcaatcaagctatctcagcttcaaacaggagcaaatgtaa aaatgatcatgcataggggaagatggccttaggagagggttaataagaaatttagaacgaataaagttgattatagcttag tatccagaaataatcacaagaatgctgtgtgctgttataacattatgtgaaatgataatagattgtgtgtaccagggacta atgagctagatagatagaatataaaagaatgaagaagagataaagaatgcagatagattgtctacaattagagattc cattaaaaacaataaattatgtagtgaatttctgtttgaaaataggattagggttttataaatcagcaccagcagtaaaactaa atgaaagataataagaaaaagtaacttacttaacccaatgaacatgaatataagatagttttgacacaaatgaaggatag aagaagtataaaaaatatacaataaacttgaataacagaaggaataatggagctagattttatgatggtgaggaatc aagcatgtatctgtataagttgatgttcaagataccacagagcaggagatacatattaatggagcattggcagtggtctata acagaaggcgaatattatatacagcagtagaatatgcagtagtagtatcaggtcttctgtaactaaactaggtgcacaatct ggtatgccatataaaagaagattgtaaaaaatattaaataataataa</p>
4	NT01CX1812 Hypothetical protein	No BLAST results for nucleotide or peptide
5	NT01CX1354 Hypothetical protein	No BLAST results for nucleotide or peptide

**Table E.6.** *C. difficile* orthologs for the ten least expressed genes in *C. novyi* (continued). *C. difficile* genes that were considered orthologs to the least expressed *C. novyi* genes from previously published data utilized to draw comparisons with *C. novyi* and *E. coli*.

Most Expressed Genes	Putative Function	Sequence
6	NT01CX1718 RNA polymerase sigma factor	gtgaaaataaatcgaataaaaaagagttaaaaaggttactgctaagacattaatagaaaaaggaaaaagcaaggctctgacacttgcagagataatggaagcttttccggagactgaacttgataaggatcaagtagaaaatcttatgagactttaggaaattgggaatagaaataacagaacaaaaactataaagctgatagattttcgggtgctgatgacgatttaagtataggccacttagatgaagatgcagaggcaattcacatgatgactcttctcaatagaaatagaactgtggatttatcttaccaaaagggataagtatagatgacctgtaagaatgtacttaaaagaaataggaaaaatcctctacttaaacacatgaagaagtgaatttctag aaggatgcacgaaggtgatgagatagcaaaacaaagggttagtgaagcaaaccttaagactagttgtaagtatagcaaaaag atgtaggaagaggatgcttttctggatttaatacaagagggaatttaggtcttataaaagcagtcgaaaaatttgactatacaa aaggatataagtttagtacttatgcaacatggtggataagacaagctataacacgtgctattgcagaccaagctagaactataag aataccagttcatatggtagagactataaataagctaataagatcaagacaactctcaagaaactggaagagatcctaaa accagaagaaatgcaaaagaaatggaatgacagaagataaaagtaagagaaataatgaaaatgctcaagacctgtgtct ttagaaaccaataggagaagaagaatagccatttaggtgactttatccagatgatgctccagccccagcagagc agcagcattcttttaaaagaacaaatagaagatgacttggttcattaatgatagagaacaaaagtattaaagcttagatt tggcttgaggatgtagagccagaactcttaggaagttggaagagtttgatgtaactagagagagaataagacagatag aagcaaaagcactaagaaaactaagacatccaagtagatcaaaaaacttagagatttttagactaa
7	Resolvase	atgataatattggggattgaccaggtatagccatagttggatggtataattgaatacaaaaatagcaagtttaagcaatcga ttatggagcagttacaacacctgcccatatgaatatatcgagaagattggaacttgtgataaaggaattgatacaatagtaaa gaaftacaatataatgaagttggaatggaagaattattcttaacaagaatgtaaaaacagctataacagttgcacaagctagagg tgttactatgcttgcattgctcataatgggaagcctgtatatgaatacactccactcaagtaaaaacaggtgtgattggatagg gagagcagataaggcacaagttcaacagatggttaactcatttttaagtctaaaaaaagttccaaaaccagatgatgttgcagat gctttagctgtgctatttccatgctcattcaaaaactgaaaaaacttaagaatataaggtgtaagatgtagat
8	NT01CX2035 hypothetical	No BLAST results for nucleotide or peptide
9	NT01CX0110 hypothetical	No BLAST results for nucleotide or peptide
10	NT01CX1998 hypothetical	No BLAST results for nucleotide or peptide

**APPENDIX F: PUTATIVE CODON BIAS UTILIZED TO TRANSLATE SEQUENCES  
FOR *C. NOVYI* CLONING**

**Table F.1.** Putative codon bias for *C. novyi*. Codon bias was probed using the genes selected for insertion. SerialCloner software was used to accomplish the annotation of the gene sequence's open reading frame into amino acids.

<i>Clostridium novyi</i> Codon Adaption Index								
Amino Acid	<i>C. novyi</i> Codon	Fraction in <i>E. coli</i>	Fraction in Human	Amino Acid	<i>C. novyi</i> Codon	Fraction in <i>E. coli</i>	Fraction in Human	
<b>A</b>	GCA	0.23	0.23	<b>N</b>	AAT	0.49	0.46	
	GCT	0.18	0.26		AAC	0.51	0.54	
	GCG	0.33	0.11	<b>P</b>	CCT	0.18	0.28	
<b>C</b>	TGT	0.46	0.45		CCG	0.49	0.11	
	<b>D</b>	GAT	0.63		0.46	CCC	0.13	0.33
GAC		0.37	0.54	CCA	0.2	0.27		
<b>E</b>	GAA	0.68	0.42	<b>Q</b>	CCA	0.34	0.25	
<b>F</b>	TTT	0.58	0.45		CAG	0.66	0.75	
	TTC	0.42	0.55	<b>R</b>	AGA	0.07	0.2	
<b>G</b>	GGT	0.35	0.16		<b>S</b>	TCA	0.14	0.15
	GGA	0.13	0.25			AGT	0.16	0.15
<b>H</b>	CAT	0.57	0.41	TCC		0.15	0.22	
	CAC	0.43	0.59	TCT		0.17	0.18	
<b>I</b>	ATT	0.49	0.36	<b>T</b>	ACA	0.17	0.28	
	ATC	0.39	0.48		ACT	0.19	0.24	
	ATA	0.11	0.16	<b>V</b>	GTA	0.17	0.11	
<b>K</b>	AAA	0.74	0.42		GTT	0.28	0.18	
	AAG	0.26	0.58		GTG	0.35	0.47	
<b>L</b>	TTA	0.14	0.07	<b>W</b>	TGG	1	1	
	CTA	0.04	0.07		<b>Y</b>	TAT	0.59	0.43
	TTG	0.13	0.13	TAC		0.41	0.57	
	CTT	0.12	0.13	<b>Stop</b>	TGA	0.3	0.52	
<b>M</b>	ATG	1	1		TAA	0.61	0.28	
					TAG	0.09	0.2	